Microalgal Growth and Lipid Production: Trends, Multiple Regression Models, and Validation in a Photobioreactor

Aimee Slajer Guha Roy

DPhil in Engineering Science

Lady Margaret Hall
University of Oxford

Abstract

Algae are a promising new source of oil for biodiesel. They are aquatic organisms that do not require cropland, and they can produce many useful side-products for bioenergy, aquaculture, and nutraceutical production. To be cost-effective, algae need high and reliable oil productivities; however, there is still a great deal to learn about the effects of culturing conditions on algae growth rates and lipid production. These culturing conditions include light intensity, gas flow, use of CO_2, and culture volume. An extensive database of published research on algae growth rates and lipid contents under a wide variety of environmental conditions was prepared. By graphing data from 116 publications on 132 microalgae species, several key trends were identified relating to culturing parameters and algae biomass and lipid production. In addition, data from 131 publications on 128 microalgae species were graphed to look at presence of flagella, nutrient limitation, lipid productivity, and productivity tradeoffs. Moreover, cell size information was gathered for 146 species. The interactions between culture variables are complex, so it is difficult to quantify the degree to which each culture variable affects algae growth rates and lipid production. Therefore, several multivariate analyses were performed to generate a set of general and simple predictive models to assess specific growth rates, maximum lipid contents, and volumetric lipid productivities. These models were used to determine which culture parameters were significant predictors of algae growth rates and lipid production, and the contribution of each environmental parameter was quantified. In addition to models for algae in general, genera specific models were prepared for *Chlorella*, *Isochrysis*, *Nannochloropsis*, *Phaeodactylum*, and *Tetraselmis*. These models show high predictive capabilities, and they greatly extend the range of species-specific multiple regression models available. Furthermore, one *Tetraselmis* model was validated using *Tetraselmis impellucida* growth experiments in a large novel photobioreactor.

Acknowledgements

I dedicate this work to my mother, Barbara Slajer, who gave me constant support and laughter during my studies. She always pushed me to explore the world, and I would not have completed this without her. I also want to thank the rest of my family for supporting me during long hours of research work.

In addition, I would like to thank my supervisor, Professor Robert Field, and Dr. Alex Lubansky for providing their comments on this thesis and for their encouragement during my thesis. I would also like to thank Pharima Pongpairoj and Kat Glover for helping me with one of my growth experiments. Furthermore, I would like to thank Garry Axe for all of his smiling technical expertise and Dr. Igor Dyson for sharing equipment and providing support. In addition, Sarah Rodgers and Carolyn helped with autoclaving. Moreover, John Mooney and Sukarni Wheeler consistently made the department a more welcoming place.

I would also like to thank the United States National Science Foundation for partially funding this research. This research was also supported by a University of Oxford John Fell Fund Award, which funded the building of the photobioreactor.

Please Note:

This material is based upon work supported under a United States National Science Foundation Graduate Research Fellowship. Any opinions, findings, conclusions or recommendations expressed in this publication are those of the author and do not necessarily reflect the views of the National Science Foundation.

Abbreviations

Abbreviation	Term
ACCase	acetyl CoA carboxylase
AFDW	ash free dry weight
ASP	Aquatic Species Program
ASW	artificial saltwater
CO_3^{2-}	carbonate ion
CO_2	carbon dioxide
DHA	docosahexaenoic acid
DI	deionized water
dw	dry weight
EPA	eicosapentaenoic acid
HCO_3^-	bicarbonate ion
LCA	life cycle analysis
LED	light emitting diode
O_2	oxygen
PBR	photobioreactor
UV	ultraviolet
US DOE	United States Department of Energy

Variables

Abbreviation	Variable	Unit
a	specific area available for mass transfer	m^{-1}
C_{CO2L}^{*}	CO_2 concentration in culture medium adjacent to bubble and in equilibrium with partial pressure on the gas side	mol L^{-1}
C_{CO2}	CO_2 concentration in the bulk culture medium	mol L^{-1}
$\%CO_2$	% CO_2 added to gas supply by volume	%
$C_{L/W}$	ratio of average cell length/average cell width	--
CW_{Min}	minimum cell width	µm
d	days	d
D	container depth	m
E	einsteins	E
GFR	gas flow rate	L L^{-1} min^{-1}
ha	hectare	ha
k_L	liquid-phase mass transfer coefficient	min^{-1}
LI	light intensity	µE m^{-2} s^{-1}
IS	illumination schedule	hr
MLC	maximum lipid content	% dw
m	maintenance requirement for cells	--
m	meters	m
N	number of cases used to generate a model	--
N_{CO2}	molar flux of CO_2 at the gas-liquid interface	mol L^{-1}
N_t	biomass concentration at time = t	g L^{-1}
P	product concentration	mol L^{-1}
pH_{Avg}	average pH	--
Q_A	areal biomass productivity	g m^{-2} d^{-1}
Q_V	volumetric biomass productivity	g L^{-1} d^{-1}
µ or SGR	specific growth rate	d^{-1}
s	seconds	s
S	substrate concentration	mol L^{-1}
Salinity	salinity	ppt
t	time in days	d
t_d	doubling time	d
Temp	temperature	°C
VLP	volumetric lipid productivity	mg L^{-1} d^{-1}
Vol	culture volume	mL
W	watts	W
X	biomass concentration	g L^{-1}
Y	yield coefficient	--

Table of Contents

List of Figures

Table of Tables

Chapter 1. Introduction

1.1. Background

In recent years, biofuel research has been stimulated by increased energy needs, petroleum supply constrictions, and concerns over fuel security. Furthermore, biofuels offer the promise of near carbon neutrality, whereas global fuel production and vehicle emissions currently account for almost 25% of energy-related greenhouse gas emissions [1]. Biodiesel is a biofuel that can be used in place of traditional petroleum diesel. It is biodegradable and nontoxic, so it is preferred for use in sensitive habitats. In addition, biodiesel is renewable and has fewer carbon monoxide, particulate matter, and sulphur oxide emissions than traditional diesel. Furthermore, biodiesel can increase employment in rural areas, and it can be transported within current fossil fuel infrastructure.

Most biodiesel production begins with pure vegetable oil, but algae are a promising new oil source. This is significant because a major limit to biodiesel production is feedstock availability, since traditional plant sources, like soybean, rapeseed, and palm, require vast energy and land resources. In the UK, rapeseed is currently the most productive biodiesel crop. In 2004, the UK's petroleum transport requirements were 37.6×10^6 tons, so, assuming a rapeseed yield of 1.5 t ha^{-1}, 26×10^6 ha would be needed to displace all fossil fuels [2]. This is larger than the UK's 18.4×10^6 ha agricultural land area [2], so traditional biofuels will not be sufficient to replace all of the UK's petroleum needs domestically. Chisti [3] calculated the percentages of United States (US) existing crop area required to produce enough biodiesel to meet half of the US's existing transport fuel needs, and he estimated that soybeans would require 326% of existing crop area, while microalgae would only require 2.5% depending upon the assumed microalgal oil content. Chisti [3] also calculated rapeseed and palm oil at 122% and 24% of existing US crop area respectively. Chisti's microalgae oil calculations have been suggested as overly optimistic [4]. Even so, *Nannochloropsis* cultures in Tuscany with a calculated 20 t ha^{-1} of oil

production would perform 20 times better than sunflower or rapeseed and 3.5 times better than tropical palm [4].

In addition, algae can be cultivated on non-arable land using seawater or wastewater. Algae have several other advantages as well. Algal cells from which oil has been extracted leave a residue suitable for animal feed or for anaerobic digestion, which can produce energy to offset the oil extraction process. Additionally, algal residues from some species could provide sources of other high-value products, such as pigments or nutritional supplements. Yet another advantage of algae biodiesel is the large number of countries that have the potential for large-scale algae production. These benefits notwithstanding, to date, algae grown in mass culture have produced lipid yields 10-20 times lower than theoretical yields [5], so additional research is needed to maximize algal lipid productivity in large-scale cultures.

Algae lipid contents can be maximised by varying growth conditions [4]. However, significant limitations must be overcome before large-scale algae biodiesel production is feasible; these include selecting and learning to grow highly productive lipid producing algae; maintaining selected species in outdoor culture; researching more large-scale microalgae growth; and decreasing the high energy inputs required for water pumping, CO_2 transfer, culture mixing, and harvesting/dewatering the algal biomass [4].

1.2. Thesis Structure

This thesis begins with a literature review in Chapter 2. First, background is provided on concepts important to algal growth, including photosynthesis and growth calculations. Then, algae mass production systems are discussed with details on the advantages of open and closed PBR designs and illumination type. Next, current commercial algae production is covered for a variety of products with discussion of combining algae production with wastewater treatment. Afterwards, algae biodiesel is discussed. This includes clarifying algae oil types, summarizing production from oil extraction to transesterification, meeting

quality standards, and noting economic and environmental considerations. Methods to alter algae oil concentrations and compositions are also noted. Chapter 2 concludes with a list of the objectives of this thesis.

Industrial scale production can be enhanced by gaining a better understanding of how culture variables affect specific growth rates (SGRs) and maximum lipid contents (MLCs). Chapter 3 discusses in detail the effects of culture variables on algae SGRs and MLCs. This chapter combines data from 116 publications on 132 microalgae species. Major trends are clarified for the following variables: culture volume, temperature, light intensity, light source, illumination schedule, reactor type, gas flow rate, and CO_2 supplementation level. Furthermore, the need to standardise data reporting is highlighted.

There are a wide variety of microalgae species, and they span a broad range of sizes, excel under numerous culture conditions, and have an assortment of lipid contents. Species choice is important for large-scale culturing. Chapter 4 graphically combines data from 131 publications on 128 microalgae species to describe a wide variety of microalgae characteristics. These include cell sizes and groupings, and cell lengths are provided for 146 microalgae species. Moreover, lipid contents are examined for marine and freshwater algae, for each algae Class, and to see the effects of nutrient limitation. Lipid productivities and lipid contents are also considered, and flagellate algae are discussed. Key trends are identified.

Several multivariate analyses were performed to quantify the impacts of various environmental parameters on algae SGRs, MLCs and lipid productivities. These models were prepared using data from 53 publications on 81 species. They identify variables that should be concentrated on during algae facility design, biomass life cycle analyses, and carbon capture estimations. Chapter 5 also includes a discussion of current algae models. Furthermore, the theory behind multiple regression is discussed along with the necessary

data pre-screening required and the validation checks performed on the models. Chapter 5 concludes with a summary of the key parameters identified and future work possibilities.

The general algae models developed in Chapter 5 are important to provide non-species specific results. However, the models may be more accurate if genera specific results are included. Considering this, multiple regression analyses were produced for *Chlorella*, *Nannochloropsis*, *Isochrysis*, *Phaeodactylum*, and *Tetraselmis* in Chapter 6. Several models were produced to predict SGRs, MLCs, and volumetric lipid productivities (VLPs), and these models were compared with published models.

Alongside database and modelling work, numerous growth experiments were performed using *Tetraselmis impellucida*. First, trial experiments were performed because the department had not previously grown algae. Chapter 7 describes these small-scale bottle experiments, which include comparing several light sources at various light intensities and assessing mixing methods. In addition, modifications were made to improve the bottle experiment setup, and sterilization procedures were tested for use in larger experiments.

A 230 L PBR was built for scaled-up experiments. Chapter 8 begins by describing theory behind CO_2 addition, oxygen (O_2) removal, and shear stress in a PBR. Reactor setup planning and construction are detailed. Next, mixing patterns and bubbling effects are noted for several tubing arrangements. The PBR hydrodynamics were characterized for freshwater with and without baffles and compared to saltwater hydrodynamics with baffles. This work aided choice of reactor setup for PBR growth trials.

In Chapter 9, the results of *Tetraselmis* growth experiments in the PBR were used to validate a *Tetraselmis* multiple regression model beyond statistical validation. Cell settling and a significant lag phase were problems identified during growth, so potential methods of overcoming them were noted. Overall results are summarized in Chapter 10.

Chapter 2. Literature Review

Algae are plants that exist in an astounding array of species and types. Many species are useful for industrial production as detailed in Section 2.2.3. This chapter contains a lot of background information useful to those new to algae growth. Those with a background in this area may wish to skip to Section 2.4, which discusses several ways to affect algae lipid contents and compositions. Several of the necessary requirements for algae growth are identified in Section 2.1, and industrial production systems are discussed in Section 2.2. Next, Section 2.3 summarizes algae oil extraction and biodiesel production methods.

2.1. Algae Growth Basics

Algae growth rates depend on nutrients, temperature, pH, and light. Varying these parameters can greatly affect both growth rates and cell composition.

2.1.1. Photosynthesis Reaction

Algal cells produce the glucose needed for cellular growth via photosynthesis, as defined below, which clearly illustrates the main energetic requirements for growth.

$$6\ CO_2 + 6\ H_2O + \text{light energy} \leftrightarrow C_6H_{12}O_6 + 6\ O_2$$

Algal cells are grown in a nutrient solution of salts, mainly nitrogen and phosphorous; silica is added for diatom culturing. Many algae also require vitamin B12, either from bacteria or supplemented in the media. A wide variety of media recipes are used depending on the species and culturing facility. In addition, algal cells require proper temperatures and controlled pH. Continual removal of O_2 is also essential to decrease photorespiration rates and reduce photooxidative damage [6].

Photosynthesis is driven by energy from light. As light travels through water, it is attenuated. This occurs as water absorbs the lower energy, longer, red wavelengths. Also, although dissolved salts do not generally absorb light, dissolved organic matter strongly absorbs the higher energy, shorter, blue wavelengths of light. In addition, both water molecules and suspended particulates scatter light. Scattering is greatest for short

wavelengths, and it increases light absorption as the light bounces around the reactor. Algal light requirements vary depending upon the species in question. Species that generally grow in the upper oceanic zones require more light than those that grow in deeper zones. In general, however, phytoplankton can grow in water to a depth that receives 1% of surface irradiance [7].

2.1.2. Importance of Temperature

The culture temperature must be controlled because cells produce heat during respiration, and the light source also generates heat. If solar illumination is used, it is especially important to cool the algal colony during the daytime to prevent overheating. Horizontal tubular PBRs, for example, can increase in temperature by as much as 20 °C within a day unless a temperature control system is used [8]. In addition, maintaining lower temperatures within the reactor reduces biomass loss due to respiration. Temperature control is commonly accomplished by water spraying due to its low cost; however, more precise temperature control can be obtained using internal heat exchangers. This method also avoids the considerable consumption of water that occurs with water spray cooling. When determining the temperature controls necessary, it is important to note that the system may change as the culture grows because the heat transfer coefficient of a dense microbial broth can differ significantly from that of an uninoculated medium.

Along with cell growth rate, temperature can also affect the cells' composition, with their oil compositions of specific concern. At low temperatures, lipids begin to solidify, which affects the structure of the cell membranes. By changing the degree of saturation of the fatty acids, cells can maintain viability at lower temperatures. For example, most lipids in cyanobacterial cells are in their membranes, and increased lipid desaturation at lower temperatures maintains the fluidity of the membranes [9]. When *Dunaliella salina* cultures are moved from 30 °C to 12 °C, they acclimate by increasing phospholipid fatty

acid unsaturation, and they show approximately 20% increases in glycolipids, phospholipids, and protein [10]. In a study on the diatom *Skeletonema costatum*, growth at low temperatures has also been shown to increase production of the fatty acid eicosapentaenoic acid (EPA) [11]. These studies suggest that growing algal cells at lower temperatures may increase lipid contents but may also cause changes in the cellular lipid composition so that more polyunsaturated fatty acids are formed, which could necessitate hydrogenation to increase the lipid's suitability for biodiesel production. Also, most algal species undergo growth rate reductions when grown under low temperature conditions, so an algae biodiesel production system that employs low temperature as a stress condition to increase lipid production would require multiple stages, wherein algal cells would be grown under optimal growth conditions and then transferred to another reactor where the cells would experience conditions that would induce lipid accumulation.

A final important temperature consideration is that temperature fluctuations within a PBR need to be limited to maintain a consistent biochemical composition within the oil product. This is especially important for large-scale cultures. Olofsson et al [12] showed the importance of accounting for seasonal variation in *Nannochloropsis oculata* lipid accumulation when grown outdoors. The effects of temperature on algae growth rates and productivity are discussed further in Section 3.4.

2.1.3. Microbial Growth Calculations

There are many ways to estimate or measure algae growth as detailed in Chapter 3. One of the most commonly used calculations is specific growth rate (SGR). A culture's SGR depends both on cell concentration and how well cultures achieve their potential for growth. The SGR, μ or K', of an algal culture is calculated using Equation 1 as follows:

(1) $$\mu = \frac{\ln\left(\frac{N_2}{N_1}\right)}{(t_2 - t_1)}$$ where N_2 is the biomass at t_2; N_1 is the biomass at t_1 or the inoculation concentration

Equation 1 can be used during the exponential phase of growth. Algal growth can also be calculated using the same growth equations for microbial growth, which account for effects caused by the supply of chemical resources and temperature. However, an additional factor must be considered for algal growth kinetics, and that is the supply of photons for photosynthesis. As cell density increases, the number of photons available to individual cells decreases, which should decrease their SGRs.

Algae growth is also commonly reported as reactor yields or productivities. Reactor yield considers mass produced per volume, while reactor productivity considers yield per unit time. However, the growth conditions that produce maximal yields are generally not the same as those that produce maximal productivities [6]. Yield can be calculated as the amount of biomass produced over the amount of substrate consumed, as shown in Equation 2. In heterotrophic growth, the substrate is generally taken as the carbon source or O_2. When considering photosynthetic growth, the substrate is taken to be CO_2.

(2) $Y = \frac{\Delta X}{-\Delta S} = \frac{\Delta P}{-\Delta S}$ where Y is the yield coefficient; S is the substrate concentration; P is the product concentration

As cells grow they consume energy, either from the substrate provided if grown heterotrophically or from glucose produced by photosynthesis if grown autotrophically. This energy is used for two purposes. First, it is used to maintain the cells by preserving correct pH and osmotic balance, synthesizing replacements for decayed cell components, and performing other vital functions. Second, the energy is used to produce more biomass. As a result, the reaction above can be clarified as follows in Equation 3:

(3) $\frac{dS}{dt} = \frac{\frac{dX}{dt}}{XY_G} + mX$ where X is the biomass concentration; m is the maintenance requirement; Y_G is the maximum growth yield coefficient

Several models of microbial growth dynamics have been developed based upon changes in substrate concentration. When using these models, it is important to note that, although they often predict an instantaneous change to the SGR from a change in substrate

concentration, this does not generally occur. Instead, the response involves a lag phase, which occurs as the cells adjust to factors within the reactor, such as changes in pH or in substrate type or concentration. In continuous cultures, the lag phase generally is not an issue after reactor setup. However, the lag phase can have significant impacts in batch or semi-continuous cultures. The lag phase is just one of a microbial culture's five typical growth phases. These phases are shown in Figure 1.

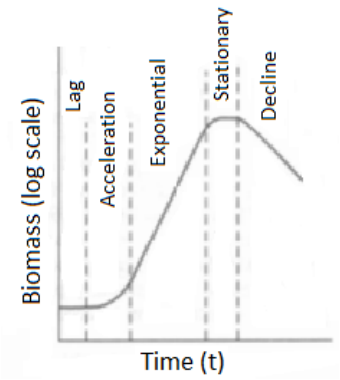

Figure 1. Microbial growth curve in a batch reactor
Typical growth phases in a microbial culture modified from Coulson and Richardson [13].

To grow algal cells for biodiesel, one goal is to keep the cells in the exponential growth phase as much as possible, so biomass is increased quickly. When μ is high, as it is during the exponential growth phase, m is relatively insignificant. However, when μ is comparable with m, as it is during the stationary phase, a lot of the energy that is consumed is used to maintain cells. Exponential microbial cell growth in a batch reactor is often calculated by Malthus' law, which is shown in Equation 4.

(4) $$\frac{dX}{dt} = \mu \times X$$

This law is often integrated with limits of time t = 0 and t = t to give Equation 5 [13].

(5) $$X = X_0 \times e^{\mu t}$$ where X_0 and X are the initial and final biomass concentrations respectively

In this case, the doubling time or t_d for the biomass is shown in Equation 6.

(6) $$t_d = \frac{\ln 2}{\mu}$$

2.2. Algal Mass Production Systems

Several species of algae are currently produced commercially for nutritional supplements or for pigments used in food and cosmetic industries. Most of these cultures are grown in open air systems, such as race tracks and open ponds as shown in Figure 2. These systems are kept shallow to increase percent light penetration. During *Pleurochrysis carterae* growth in an outdoor 0.16 m deep raceway pond, light penetration decreased steadily with increasing depth until 0.08 m depth, where the light penetration was less than 0.5 MJ m^{-2} d^{-1} [14]. Open ponds are mixed by either paddlewheel or wind. They are cheap to build because they generally consist of concrete or compacted clay lined with plastic. These simple construction and mixing requirements lead Life Cycle Analysis (LCA) estimates of open pond energy consumption and greenhouse gas emissions to be lower than for PBRs [15].

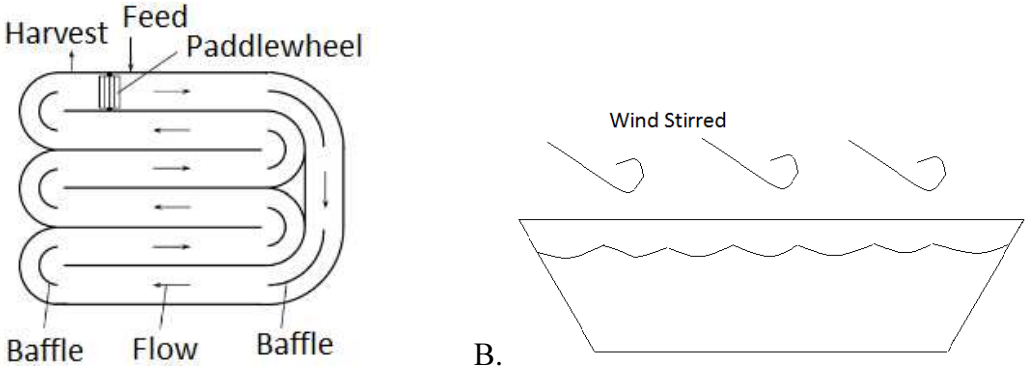

A. B.

Figure 2. Most common open reactor designs
Figure 2A shows a raceway pond aerial view [3]. Figure 2B shows a shallow open pond side view.

However, open air cultivation is only possible for the relatively few species that survive extreme conditions. For other species, open ponds are unstable ecosystems with frequent changes in the culture population and community [4]. Also, these systems undergo extensive water loss, are difficult to keep well-mixed, and must be periodically cleaned and reseeded to keep invasive species from taking over. Although it will increase costs, raceway ponds may also be covered to reduce contamination and decrease sunlight during periods of high irradiance. In addition, the costs of collecting the algae are very

high due to the vast amount of liquid and comparatively low concentration of algae present. Open ponds confer biomass productivities of 60-100 mg L^{-1} d^{-1} with total concentrations up to 1000 mg L^{-1} [16]. Cost analyses performed as part of the US Department of Energy's (DOE's) Aquatic Species Program (ASP) indicated that, due to the low cost requirements, open ponds are the most likely option for fuel production [17]. However, open ponds are also limited by geographic conditions. Algae open ponds in the US desert received ample sunlight but low night temperatures hampered growth [17].

Growth in closed PBRs is currently more costly than growth in open reactors, but it increases productivity because greater control is allowed over aeration, temperature, and sterility. Open and closed systems are compared in Table 1.

Table 1. Comparison of open and closed reactor systems

Parameter	Open pond	Closed system
Contamination risk	Extremely High	Low
Space required	High	Low
Water losses	Extremely High	Almost none
CO_2–losses	High	Almost none
Biomass quality	Not susceptible	Susceptible
Variability as to cultivatable species	Cultivation possibilities are restricted to a few algal varieties	High, nearly all microalgal varieties may be cultivated
Flexibility of production	Change of production between the possible varieties nearly impossible	Change of production without any problem
Reproducibility of production parameters	Dependant on exterior conditions	Possible within certain problems
Standardization	Not possible	Possible
Weather dependence	Absolute, production impossible during rain	Insignificant, because closed configurations allow production also during bad weather
Period until net production is reached after start or interruptions	Long, approximately 6–8 weeks	Relatively short, approximately 2–4 weeks
Biomass concentration during production	Low, approximately 0.1–0.2 g L^{-1}	High, approximately 2–8 g L^{-1}
Efficiency of treatment processes	Low, time consuming, large volume flows due to low concentrations	High, short time, relatively small volume flows

Advantages and disadvantages of open and closed PBRs as summarized by Pulz [18].

2.2.1. Types of Photobioreactors

Several types of closed reactor systems, as shown in Figure 3, are currently used. Due to this wide variety of designs, relatively few LCAs have been performed on PBRs; however, they have been estimated to consume up to 90% more energy than open ponds [15]. This higher operating energy is largely due to pumping media, especially through narrow tubes [15]. Even with this higher energy requirement and higher capital costs,

PBRs can produce cheaper biomass in certain cases, due in part to reduced dewatering costs because the cultures are more concentrated [19].

One of the cheapest and easiest to scale-up PBR systems is based on large, aerated transparent plastic bags; these also have the advantage of being sterile at start-up. However, plastic bags tend to be light-limited, require indoor storage to regulate temperature, and have mixing problems that can lead to culture crashes [20]. Even so, plastic bags are often used to grow inoculation cultures for larger reactor vessels.

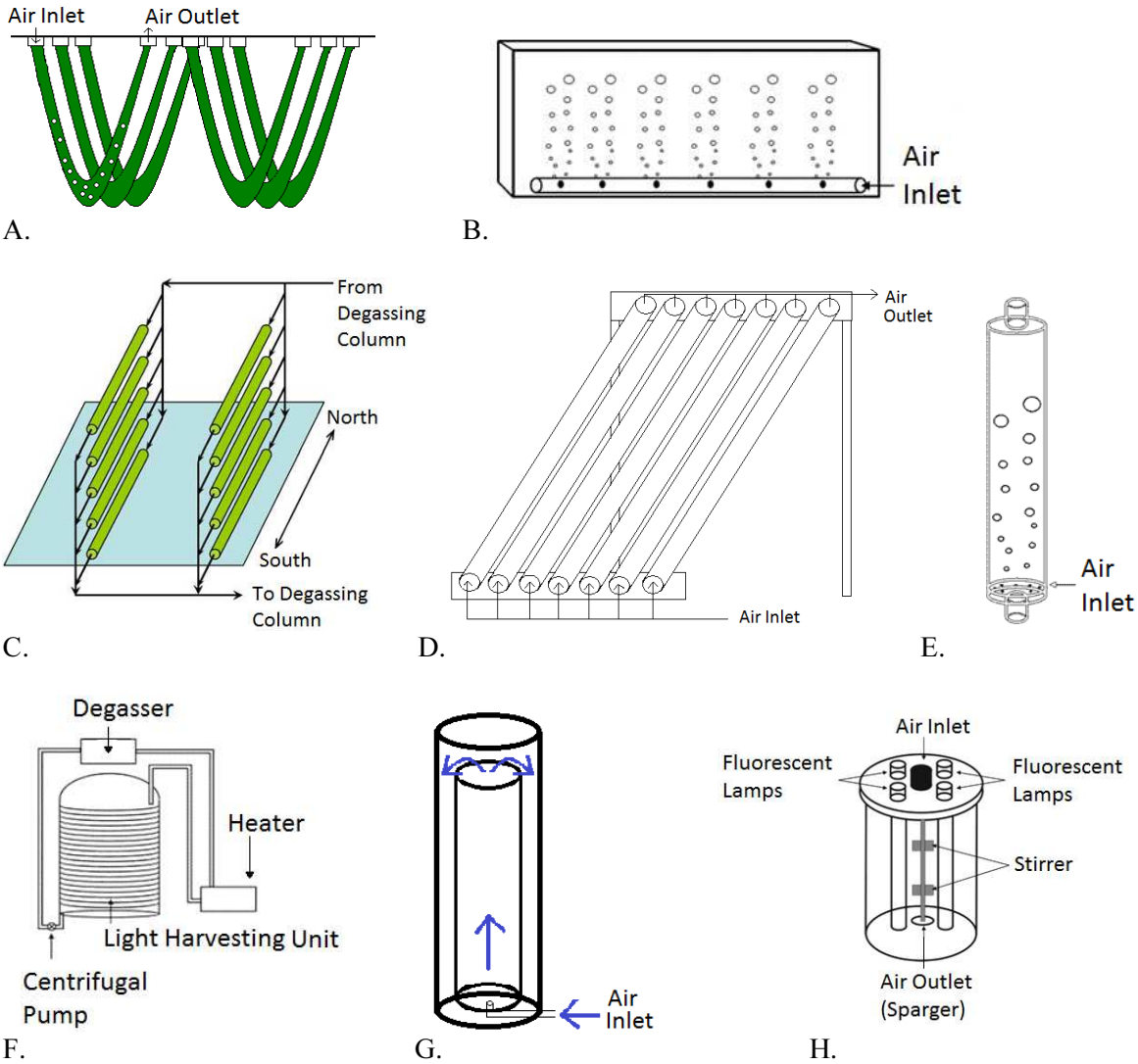

Figure 3. Several common closed reactor designs

Figure 3A: Plastic bag reactors. B: Flat plate reactor [8]. C: Horizontal tubular reactor [3]. D: Inclined tubular reactor. E: Bubble column [8]. F: Helical tubular [8]. G: Concentric Tube Airlift reactor. H: Fermenter type reactor [8].

Another PBR is the tubular PBR, which is a very common reactor design with many variations. Tubular PBRs are well-mixed and generally have a small diameter to decrease the light path across the reactor. One popular tubular PBR is the Biocoil, which uses thin (usually 2-4 cm) plastic tubing wound in a helix, coupled with a gas exchange tower and a heat exchanger, and driven by a centrifugal pump. It allows uniform mixing and easy scale-up, but it does not perform well for all algae species because some algae are either too likely to stick to the tubing or too delicate to survive the centrifugal pump used to drive the Biocoil [8], [20]. Unlike other tubular PBRs, Biocoils are composed of tubing coiled vertically. This gives the Biocoil design the advantages of a high surface area-to-volume ratio and the ability to grow large volumes in a small land area [8]. Other tubular PBRs are formed from straight glass or transparent plastic tubes and are wider (generally <10 cm) in diameter; tube length is limited by pumping and need for gas exchange.

Horizontal tubular PBRs may be laid out flat in fields or stacked vertically in a fence-type arrangement to decrease the land area used, and the ground may be coloured white to increase reflectance onto the tubes [3]. Tubular PBRs may also be inclined to catch more sunlight. The directionality of a tubular PBR is very important when setting it up to catch maximal sunlight, as discussed further in Section 2.2.2. A major drawback of most tubular PBRs is that, due to the narrowness of the tubes, an inordinately large number of tubes would be required to reach culture volumes of 5,000-10,000 L, which would be required for industrial scale production [8]. This large number of tubes would, if laid horizontally or inclined, require an extremely large land area. To reduce the required land area, the tubular diameter can be increased, but this would require the tubular PBRs to be extremely well mixed to prevent light limitation [21]. However, tubular PBRs have highly directional flow axially with little radial flow. Tubular PBRs have culture velocities below 0.5 m s^{-1}, which is far below levels that would damage cells [22]. Also, tubular PBRs can

suffer from poor temperature control, cells sticking to tube walls, and reduced O_2/CO_2 transfer with resulting pH increases [21]. In summary, tubular PBRs are expensive to build, difficult to maintain, and generally only valid for medium-scale production [22].

Flat-plate PBRs are also well-mixed and very thin (2-4 cm) reactors [20]. Flat-plate reactors can obtain high biomass productivities, and they require less land area because they are arranged vertically. Another advantage over horizontal tubular PBRs is that flat-plate PBRs have an open-gas area that prevents oxygen build-up from occurring. Meanwhile, horizontal tubular PBRs, unless specific precautions are taken, are susceptible to O_2 build-up that limits algal cell growth; this issue is discussed further in the gas exchange section below. The short light path that occurs in a flat-plate PBR gives it a uniform light distribution. Some flat-plate reactors are constructed with alveolar plates for increased productivity. Alveolar plates are pre-constructed, strong, clear plastic sheets with internal channels that can be used to direct culture flow. Alveolar reactors risk O_2 build-up due to the high rate of photosynthetic activity achieved in the small reactors [8].

Another common reactor type is the bubble-column reactor, which is mixed by rising bubbles from compressed air injected into the reactor bottom. This bubbling creates a highly chaotic flow regime with greater radial movement than in tubular PBRs [22]. These reactors have a large aspect ratio because they are much taller than they are wide. This increased height may increase CO_2 solubility, and the resulting increased volume leads to increased areal productivity. This effect continues up to a column height of 5 m, but considerations of transparent material strength and wind speed reduce the maximum height to 4 m [22]. A closely related reactor design is the airlift reactor, in which airflow is directed such that flow through the reactor is organized. Airlift and bubble-column reactors are both vertical-column PBRs with a diameter up to 0.19 m and are reported to produce biomass concentrations and SGRs similar to tubular PBRs, which are much more

narrow [21]. When the culture becomes very dense, airlift reactors perform better than bubble columns because the directed media flow pattern in the airlift reactor regularly moves the cells from dark to light zones [23].

Stirred tank or fermenter-type reactors have a simple design that has been widely used in the chemical industry for many years, and, therefore, much knowledge has been accumulated on scaling them up efficiently. These reactors have a low surface area-to-volume ratio, which makes efficient light distribution difficult. As a result, these systems are often illuminated internally, which provides more control over the system than when using sunlight. However, with typical productivities of 30-50 mg L^{-1} d^{-1}, biomass productivity has tended to be low in fermenter-type reactors [8].

In addition to the designs discussed above, bioreactors can use immobilization techniques to retain enzymes or cells within the reactor. Rossignol et al [24] compared a bioreactor with free algal cells and an external membrane to one where the cells were immobilized in agar. They grew *Haslea ostrearia* and measured the effects of dilution rate and nitrogen concentrations on its production of the pigment marennine. The free cell bioreactor used background lighting, while the immobilized cell bioreactor's agar layer was wrapped around a tube containing optical fibres. In this study, the free cell bioreactor produced a higher concentration of marennine, which likely resulted from decreased mass transfer of nutrients and gases through the agar to the immobilized cells [24].

Many teams have compared bioreactor designs to maximize algal growth. Sánchez Mirón et al [25] looked at the growth of *Phaeodactylum tricornutum* in three kinds of externally illuminated vertical bioreactors and found that narrow-bore horizontal PBRs produced more biomass by volume but areal productivity was greater using larger-diameter PBRs. Other work showed areal productivity more than doubling as tube diameter increased [22]. Another team working with PBRs tried a variety of designs to

increase cell doubling and O_2 production rates, and, after several trials, they identified four key issues to increasing PBR productivity. These issues include internal sparging to increase light utilization, semicontinuous ultrafiltration to remove secondary metabolites and provide fresh medium, increasing light intensities present in the PBR, and designing the PBR to have the shortest light path possible [26].

In addition, the reactor design to be used must be chosen based on the algae type intended for growth. Many species grow well in bubble columns and airlift reactors. However, airlift reactors are unacceptable for fragile species, such as *Dunaliella*, which are damaged when the culture flows over the baffle into the downcomer region. Moheimani compared the growth of three coccolithophore algae species *Pleurochrysis carterae*, *Emiliania huxleyi*, and *Gephyrocapsa oceanica*, in several different reactor types including glass flasks, stirred plastic carboy, concentric tube internal airlift, flat plate, vertical helical tubular (Biocoil design), and outdoor raceway pond with paddle wheel. He performed the experiments at scales from 100 mL to 37 L and found that some designs inhibited growth. In raceway ponds, *G. oceanica* cultures failed to establish, and *E. huxleyi* cultures grew but crashed due to massive contamination by ciliates, amoeba and competing microalgae [14]. In the Biocoil design, *G. oceanica* and *E. huxleyi* cells were too damaged to grow, and *P. carterae* cells declined from the inoculation of $1.5x10^5$ cells mL^{-1} to $2.3x10^4$ cells mL^{-1} for 28 days before beginning to increase to a maximum cell concentration of $1.3x10^5$ cells mL^{-1} [14]. When cells grown in the Biocoil reactor were examined, they showed significant loss of coccoliths and clumping. *G. oceanica* and *E. huxleyi* cells also failed to grow in the concentric tube internal airlift reactor, and *P. carterae* had reduced growth in the airlift reactor compared to other reactor types. Since the Biocoil reactor design is often paired with an internal airlift pump section for degasification, it is reasonable that algae species that do not grow well in airlift reactors would also perform poorly in Biocoil reactors.

Moreover, the best reactor designs may be combinations of ideas. By combining the directed mixing of an airlift reactor with a flat-panel design, very dense cultures are possible in which cell shading produces dark zones even though the reactor depth is small. In a 30 mm flat-plate airlift PBR, a light:dark volume proportion of 1:10 is optimal [23]. Using airlift flow direction in a 15 mm flat-plate PBR, biomass productivities of 2.64 g L^{-1} d^{-1} were achieved for *Chlorella vulgaris* [23]. Another combination that has been tested is to use an internally illuminated wide tank for degassing and growth combined with a small coiled unit to provide mixing and an enhanced light zone [27]. In addition, algae growth and wastewater treatment may be combined as discussed in Section 2.2.3.2; this process has been tested by combining membrane bioreactors with photobioreactors.

2.2.2. Solar versus Artificial Illumination in Photobioreactors

One of the most important considerations during reactor design is the type of light to be used in the reactor. Solar light has been commonly researched because it is cheaper than artificial illumination. However, it depends greatly on the solar radiance received in the location being studied. In addition, solar light causes variability in the chemical constituents of the product algae over time due to seasonal changes in light supply [28]. Artificial illumination provides much greater control over the chemical composition of the algae, but it has increased energy costs and a corresponding reduction in CO_2 mitigation.

Bioreactors illuminated by sunlight have a day/night regimen, whereby algal mass grows in the daylight due to photosynthesis and shrinks at night due to respiration. The amount of algal mass lost to respiration varies depending upon reactor conditions. However, the amount of biomass lost to respiration can be up to 25% of that produced during the day [3].

The effects of solar irradiation can differ due to the reactor type used. Due to their inherent sparging, bubble columns and airlift reactors have high gas holdups with many

and large bubbles. Horizontal tubular PBRs, on the other hand, have relatively few and relatively small bubbles along the upper portion of the tubes. These bubbles can aid light transmission. Gas bubbles tend to enhance internal irradiance when sun is low on the horizon and reduce it near solar noon [22]. For optimal bubble column performance, a balance must be struck between using the highest aeration rates consistent with the alga's shear tolerance and not producing high gas holdups that reduce light transmission [22].

When using solar radiation, reactor orientation and latitude have a large effect on both the amount of light received throughout the year and the distribution over a day. Sierra et al [29] found that a flat-panel PBR oriented East/West received similar radiation to a horizontal PBR, with radiance ranging from 13 MJ m^{-2} d^{-1} in winter to 29 MJ m^{-2} d^{-1} in summer for the flat-panel East/West PBR and 11 MJ m^{-2} d^{-1} in winter to 30 MJ m^{-2} d^{-1} in summer for the horizontal PBR. However, the annual variation for the flat-panel North/South PBR showed a reverse trend with 26 MJ m^{-2} d^{-1} in winter and 16 MJ m^{-2} d^{-1} in summer [29]. On the other hand, the distribution of light during a day is completely different for a flat-plate East/West PBR than it is for a horizontal PBR. The East/West oriented flat-plate PBR catches the maximum amount of sunlight near sunrise and sunset, while the horizontal PBR and North/South oriented PBR both receive the maximum sunlight around noon. Other PBR systems have been developed to tilt automatically to follow the sun.

Overall, Sierra et al [29] found that the flat-plate East/West PBR was the best stationary PBR option, as it had the best annual light distribution with increased light in winter, when photolimitation is common, and decreased light in summer, when photoinhibition occurs, along with catching 5% more light annually than the horizontal PBR. However, the latitude of the location of concern also has a great effect on choice of reactor orientation. At latitudes above 35°N, the East/West flat-panel orientation captures

more solar radiation than the North/South oriented flat-panel, with the effect increasing as distance from the equator increases. The reverse effect is also true below 35°N, with the extra amount of solar radiation captured by a North/South flat-panel over an East/West flat-panel increasing as distance from the equator decreases. Furthermore, the type of sunlight gathered by vertical PBRs, such as flat-plate PBRs, is mostly disperse radiation, which has been reported to be more photosynthetically efficient than the direct radiation obtained by horizontal and tilt PBRs.

Seasonal changes also affect light intensities received by other reactor types. A vertical bubble column receives lower average irradiance in summer, when the sun is highest, than in winter when more direct radiation hits more of the reactor's surface [22]. Seasonal variation also occurs in horizontal tubular reactors but not as strongly [22].

Changes in solar radiation, such as reduced or increased light due to seasonal changes, also cause changes in algae compositions. Increased light has been shown to increase saturated and monounsaturated fatty acid contents in *Nannochloropsis* sp [4]. Light intensity changes have also been shown to alter fatty acid compositions in *Isochrysis* sp and *Nannochloropsis oculata* as determined by growth at four light intensities [30]. Growth under high light intensities caused a decrease in the ratio of total unsaturated to saturated fatty acids for both species [30]. When six marine diatoms were grown at two light intensities, they exhibited decreased total polyunsaturated fatty acids with increased light intensity [31]. Algae lipid contents and growth rates are affected by light intensity, light source, and illumination schedule as discussed in Chapter 3.

Many studies have examined the effects of temperature on growth rate in laboratory cultures, but temperature's influence is more complicated in outdoor cultures due to seasonal and diurnal effects. In tropical areas, a diurnal cycle may show a temperature difference of 20 °C [14]. Increased temperatures cause increased metabolism, so reduced

night temperatures can decrease loss of biomass from respiration. In cold seasons, however, low temperatures can go beyond limiting culture growth and cause culture crashes. A further element to be considered in open outdoor ponds is the expected rainfall. This is important because dilution from heavy rainfall may cause a culture to crash.

Artificial illumination can be provided internally or externally to the reactor, and the illumination scheme can be chosen to simulate diurnal patterns or for continual illumination. Along with increasing bioproductivity due to decreased dark reaction time, internally lit bioreactors can be heat-sterilized to reduce contamination by other organisms [21]. Optical fibres have been proposed for internal illumination. Optical fibres have produced markedly increased yields and hydrogen production from cultures of the bacterium *Rhodopseudomonas palustris* WP3-5; these increases were attributed to provision of additional irradiation area and a more uniform light distribution [32].

In addition, artificially lit PBRs can be designed to take advantage of the maximal absorption wavelengths for the chlorophyll in the algae being grown. This should provide increased photosynthetic efficiency, since only some wavelengths of sunlight are needed for algal growth. As mentioned previously, photosynthetically active radiation extends from 350 to 720 nm [33]. The maximum photosynthetic efficiency has been estimated at 12% assuming that half of solar energy is not absorbed because of wavelength spread and that a fourth is lost through reflection and transmission from the cells [2].

Another advantage of artificial illumination is the possibility of using flashing light. Due to its intermittent nature, flashing light may not heat the reactor as much as continuous light. *Haematococcus pluvialis* cultures internally illuminated by flashing light are more efficient than both externally illuminated flashing light cultures and cultures illuminated continuously to the same average irradiance [34].

2.2.3. Large-Scale Algae Growth and Products

Algae production already occurs on a large-scale. The total world-wide production of algae is estimated at 10,000 tons dry weight (dw) per year [35]. Most of this production occurs in China, with Japan, USA, Taiwan, Australia, and India being other major producers [35]. Humans began using algae for protein; then, the 1970s energy crisis stimulated research on algae for fuel. Early algae research focused on understanding photosynthesis, was performed on very small scales, and mainly used fast growing freshwater algae like *Chlorella* and *Scenedesmus* [36].

Goldman [36] reviewed algae mass culturing from the first pilot plants in 1951 with an average culture yield of 2 g m^{-2} d^{-1} up through 1978, when average yields from 15-25 g m^{-2} d^{-1} were common. During this time period, peak culture yields increased from 11 g m^{-2} d^{-1} to 35 g m^{-2} d^{-1} [36]. This shows the ability to increase yields as the technology develops. However, worldwide research on outdoor mass cultivation indicates that, with present technology and algal strains, annual productivities beyond 100 tons of biomass per hectare are not possible in large-scale cultures [4].

The largest horizontal tubular PBR facility ever constructed was abandoned after failing to reach productivity expectations [22]. This facility, built by Photobioreactors Ltd in Cartagena, Spain, had several kilometre long tube runs, and its productivity was limited by O_2 accumulation [22]. This reactor type may not be scalable to large-scale production.

One of the largest concerns in large-scale production is harvesting. Algae are aquatic plants, so they must be collected from the water in which they are grown using membranes, flocculation, magnetic nanoparticles, and/or centrifugation. This can be very energy intensive because it may involve concentrating the biomass from concentrations below 1 g L^{-1} up to 250 g L^{-1} [37]. Some cells like those of *Haematococcus* become large and heavy as they produce carotenoids or cysts that settle out with rates >1 cm min^{-1} or faster once they coalesce into larger flocks [37]. Flocculation may also be induced by

altering the culture pH by adding sodium hydroxide. This can significantly reduce harvesting costs.

2.2.3.1. Algae Products

Some of the great advantages of using algae as a feedstock are the flexibility of cells and the great variety of species available. Species range from single-celled to giant kelp over 60 m long. Algae exist in freshwater and saltwater; they can also coexist within other organisms as lichen or inside coral reefs. When algae are cultured, changing the environmental conditions can change the cellular composition. For example, when *Nannochloropsis* sp was grown under low light conditions, its cellular light utilization efficiency increased 3.7 times as it increased the number of its photosynthetic units [38]. In addition, algae have quick cultivation cycles. As such, it has been estimated that cells can be harvested 4 to 6 times annually in tropical climates [39]. Although algae can produce many useful products, many species are toxic to humans and other animals. As such, production of unwanted side products must be considered in large-scale cultures.

Several algae are currently grown successfully to produce high-value products. A few of these possible high-value products are industrial food and cosmetic colourings, such as β-carotene (a precursor to vitamin A) and astaxanthin (an antioxidant). Many high-value products are important nutraceuticals for human health, including ω-3 polyunsaturated fatty acids and co-enzyme Q_{10} (an antioxidant). Some ω-3 fatty acids (also termed essential fatty acids) are EPA and docosahexaenoic acid (DHA); these are being studied for nutritional and therapeutic uses. Some of the factors that influence EPA production may also influence total lipid production within algal cells. These factors include culture age, carbon source if grown heterotrophically, nitrogen source, C/N and C/P ratios [16].

Large-scale β-carotene production uses *Dunaliella salina* grown in raceway ponds, where *Dunaliella*'s toleration of high salt concentrations reduces contamination. As they

lack cell walls, it is easier to extract materials from *Dunaliella* cells. Another pigment, astaxanthin, is a carotenoid that provides colour to salmon, shrimp and lobsters. Astaxanthin can be produced from *Haematococcus pluvialis*. Astaxanthin is potentially important for the cosmetics and food industries. Currently, however, synthetic astaxanthin is generally used because of its low cost compared to *H. pluvialis* production, which has high processing costs due to a thick cell wall [37]. Research is underway to improve astaxanthin production efficiency. Flashing lights have been shown to increase the astaxanthin yield from *H. pluvialis* [34]. However, natural *H. pluvialis* will not become economically feasible unless public demand or regulations for use of natural astaxanthin come into place similar to those for β-carotene production [37]. Astaxanthin has also shown possible advantages in disease prevention.

The nutraceuticals market also includes *Crypthecodinium cohnii* grown commercially for DHA. EPA production has been attempted using *Phaeodactylum tricornutum*. Commercial production was unsuccessful in horizontal tubular PBRs but it may be possible using another reactor type [22]. Some macroalgae are being studied for possible anti-HIV, antiobesity, and antidiabetic effects [39]. In addition, various algal compounds are being studied for their potential anti-tumour or cardioprotective activities. For example, Mera Pharmaceuticals are working to develop new pharmaceuticals from the University of Hawaii's cyanobacteria collection, which has already produced >100 bioactive molecules [37].

Algae are also grown for food production. Over 100 algae species are used for foods from wakame to nori [40]. More recently, *Spirulina* have been sold as a nutritional supplement due to its unusually high protein content (up to 70%), ease of digestion, lack of toxins, and pigments [36], [41]. Microalgae are also grown commonly as feed for aquaculture operations. This includes feed for molluscs, shrimp, and fish. Aquaculture

involves growing *Tetraselmis*, *Nannochloropsis*, *Isochrysis*, and *Nitzschia* at costs around \$70 L^{-1} [42]. Farmed salmon, for example, obtain their ω-3 fatty acids from microalgae or prey fish that have eaten microalgae.

Other uses of algae include production of carrageenan, alginic acid and agar, which are then used in industries ranging from paper to adhesives to pharmaceuticals [39]. Algae are also grown to produce phycoerythrin, which is a fluorescent label, and for heavy isotope labelled metabolites [42]. Fossilized diatoms are used as diatomaceous earth inside filters, reflective paint, and polishing agents [40]. Also, macroalgae can bioaccumulate heavy metals. As shown above, algae have tremendous potential for a wide variety of products.

More recently, algae have been studied for biofuel production. Algal biodiesel is discussed in Section 2.3. However, algae can also provide feedstock for several other kinds of energy production. Algae can have carbohydrate levels up to 64% dw [43]. In combination with low lignin levels, this makes many algae species preferable to other lignocellulosic plants for bioethanol production. As many algae are supported by buoyancy in water, they do not require the same structural strength as land plants. Algal ethanol can be produced using fermentation. One study showed a 38% by weight ethanol productivity from microalgae [44]. In addition, biogases can be produced using anaerobic digestion of an algal slurry or gasification of dried biomass produced after extraction of high-value products. Moreover, some cyanobacteria can produce hydrogen.

2.2.3.2. Wastewater Treatment and Algae Growth

One of the best ways to make large-scale algae cultivation cost effective is to combine it with wastewater treatment, which provides fertilizer for the algae while providing an important service. Algae growth for wastewater treatment has been widely successful, especially in areas with high sunlight and available land. Microalgae have been widely researched for removing nitrogen and phosphorous from wastewater. *Chlorella*,

Botryococcus, and *Scenedesmus* are just a few of the many microalgae genera that have been grown on wastewater [45]. Removal of nutrients and/or pollutants from wastewater is termed phycoremediation.

Wastewater from homes and industrial facilities generally contains high levels of organic material and nutrients. However, it may also contain pathogenic microorganisms and toxins. As long as toxin concentrations are not too high, microalgae can remediate them while releasing O_2 that will promote aerobic degradation by bacteria within the culture [45]. With the high level of nutrients and continually varying water composition, heterotrophic algae may be preferable for wastewater treatment systems. Wastewater temperature affects reactions within it with high temperatures increasing fungi and undesirable species [45]. Because the flow of wastewater into the system is continuous, biomass harvesting must also be continuous. This need for continuous operation means that the resulting algae cultures will generally be more dilute than batch systems, and the cultures may be susceptible to contamination and population crashes due to the need to operate for extended periods. Population crashes can occur if predatory zooplankton or protozoa enter the system because they can deplete the system of algae within days.

Due to the large volumes requiring remediation, PBRs are not ideal [45]. The largest outdoor mass culture system in the US is a 1,000,000 L raceway pond built by Oswald in the early 1960s; it treats domestic wastewater while producing a high-protein algal-bacterial product mixture [36]. In Israel, algae wastewater treatment has been performed in systems from 120-1,000 m^2, and growth rates >35 g m^{-2} d^{-1} were achieved for freshwater green algae [36]. However, algae growth for wastewater treatment has a lot of room for scaling up. Large-scale algal wastewater treatment systems, often termed high rate algal ponds, tend to be shallow (0.3–0.6 m), continuously mixed, and operated at hydraulic retention times in the range of 4–10 days [45]. Along with raceway ponds,

cascading systems may be used for algal wastewater treatment. Land requirements may be reduced by starving the algae of nitrogen to increase nutrient removal rates [45].

High rate algal ponds effectively remove nutrients and bacteria but produce effluent rich in small, low-density microalgae. Wastewater treatment research using *Scenedesmus* growth under nutrient and light supplementation produced a dilute culture for shellfish food [36]. Similarly, microalgae can be used for phycoremediation with resulting biomass used for sustainable biofuels. Wastewater from pig farms has been treated cost-effectively with productivities up to 50 t ha^{-1} per year [45]. This biomass could be used for bioenergy production. This is supported by laboratory studies of algae grown on wastewater, which have shown up to 30% dw lipids and up to 505 mg L^{-1} of biomass [45]. Also, wastewater treatment facilities have relaxed economic constraints compared to facilities focused on fuel production, so they can be used as near-term microalgae biofuel production systems even without maximized productivities [17].

2.3. Biodiesel from Algal Oils

Algae oils can be used to produce biodiesel via transesterification. First, however, the oils must be extracted from the cells. Algae biodiesel meets the required biodiesel standards, but no company has yet launched full commercialization of algal biodiesel.

One of the most promising areas for algae biodiesel is production of aviation fuels. Worldwide, the airline industry consumes over 5 million barrels of oil per day [46]. More environmentally sustainable aviation fuel may be possible by partially substituting algal biodiesel into jet fuel blends in place of diesel or kerosene. Algal aviation fuels have been estimated by Boeing to reduce greenhouse gas emissions by 60 to 80% [46].

2.3.1. Understanding Algae Oil Types and Nomenclature

Algae cells contain several types of lipids, and research on algae lipids and biodiesel production tends to concentrate on different types. Some researchers cite total lipid

contents, some measure fatty acids, and others measure only neutral lipids because these contain the acylglycerols. As such, it is useful to clarify the lipid types.

Lipids are classified as either neutral lipids, which are mainly used for energy storage, or polar lipids, which are found in cell membranes. There are many kinds of neutral lipids. The acylglycerols are useful in transesterification for biodiesel production; these include mono-, di-, and triacylglycerols. Other neutral lipids types are hydrocarbons, sterols, ketones, and free fatty acids [47]. Free fatty acids are the building blocks of many other lipids, such that 3 fatty acids bonded to a glycerol backbone form a triacylglycerol. Fatty acids are also used to build polar lipids, which include phospholipids and glycolipids.

Lipids are composed mainly of either chains or rings of carbon atoms held together by single or double bonds. As such, lipids are described by their number of carbon atoms and their number of double bonds. Saturated lipids have no double bonds between carbon atoms. Unsaturated lipids are described by the number of carbons:the number of double bonds, such that C18:1 refers to an 18 carbon chain with one double bond to form a molecule more commonly called oleic acid. This nomenclature is sometimes modified to read C18:1 ω9, which indicates that the double bond begins on the 9^{th} carbon atom from the methyl end of the molecule. When simply referring to molecule length, the form C_{17} may be used, which indicates a 17 carbon chain.

2.3.2. Algal Oil Extraction and Transesterification

Harvesting the algal cells from their growth media is 20-30% of the total production costs for algal biofuels [40]. After harvesting, algae cells are de-watered, and their lipids are extracted and purified prior to undergoing the chemical reactions needed to form biodiesel. Liquid solvent extraction has been used to recover between 4.8 and 96.1% oils from 9 microalgae species [48]. This is far greater recovery than the 10.7 to 25.3% oil obtained from 2 species using mechanical extraction methods like wet milling and

sonication [48]. Oil can be extracted using a variety of solvents, such as hexane, methanol, and supercritical CO_2. Supercritical CO_2 has been used to recover 2.1-77.9% oil from 4 microalgae species [48]. Due to costs, hexane is the most commonly used solvent, but it is an environmental and health hazard. As a result, several alternatives are being studied. One alternative is "in situ transesterification," which forgoes the extraction step.

Biodiesel is commonly prepared via transesterification of fat or oil with an alcohol. Water inhibits transesterification, so materials must be dried prior to reaction to substantially reduce solvent requirements [49]. The requirement to dry materials adds complexity and greatly increases the energy requirements of transesterification, so extraction methods for wet materials are being studied. Algae, which may contain up to 90% water, can be liquefied under moderately high temperature and pressure conditions to release large amounts of oils, even larger amounts than those released by supercritical CO_2 extraction. However, the higher liquefaction temperatures can cleave long chain fatty acids [50].

An alternative wet oil extraction method uses enzymes, such as cellulases, xylanases, and proteases, to decompose cell walls and release the oils. Enzymes can produce oil yields comparable to solvent extraction on a wide range of plant materials [51]. Also, this method operates at lower temperatures than liquefaction and, since it does not use organic solvents, has fewer safety risks and produces hull and meal by-products of superior value for use in animal food. Additional new methods being tested for oil extraction involve use of pulsed electric fields, microwaves, ultrasonic energy, and beads. Although promising in lab tests, these and enzymatic extraction have undergone little testing at larger scales [48].

Once the oil is obtained and dried, it is ready for transesterification. The transesterification reaction may be catalysed by acids, bases, or enzymes, and the process requires an excess of alcohol to drive the reaction equilibrium towards the formation of

biodiesel. The cheapest and thus most commonly used alcohol for transesterification is methanol. The desired methyl esters (aka biodiesel) are formed along with glycerin, as a coproduct, and various impurities that result either from the reversibility of the transesterification reaction or from the presence of contaminants, such as sterols, alcohols, and high-molecular weight hydrocarbons, in the reactant oil [52]. After transesterification, refining is necessary to produce biodiesel that conforms to purity regulations. Refining can be done by washing with distilled water, washing with acid, or solvent extraction; however, each of these methods has associated problems including loss of product due to emulsification [53] and copious wastewater production [52]. A study by Haas and Scott [49] estimated that 14% of the maximum attainable biodiesel yield had been lost during biodiesel washing. These problems can be circumvented by using hollow fibre membranes to extract high quality biodiesel [53]. Membranes take advantage of the miscibility differences between reactant oils and ester products to achieve efficient product separation as the methyl esters pass through a membrane with a pore size too small for oil globules to transverse [52]. This method also allows unreacted materials to be recirculated to increase reaction efficiency.

2.3.3. Meeting Biodiesel Standards

Algae biodiesel must comply with existing standards, such as Europe's Standard EN 14214 and EN 14213 to be compatible with current engines. These standards include limits on the extent of the oil's total unsaturation, its iodine content, and the amount of fatty acid methyl esters with four or more double bonds [3]. To meet standards, oils for biodiesel must contain <12% linolenic acid (C18:3) and <1% polyunsaturated fatty acids with 4 double bonds [54]. Oils from *Nannochloropsis* sp and *Scenedesmus obliquus* meet these standards [54].

The fatty acids used for biodiesel production are typically chains of carbon atoms ranging from eleven to twenty carbons long [55]. Algae oil composition can differ greatly by species, and some species produce high volumes of suitable oils. Han et al [56] analysed the hydrocarbon compositions of two green algae, *Spirogyra* and *Chlorella*, and two blue-green algae, *Nostoc* and *Anacystis*, and they found each species to have a range of hydrocarbons from C_{15} to C_{20}, with C_{17} being the predominant hydrocarbon. Also, Aresta et al [50] found that *Chaetomorpha linum* had a range of saturated and unsaturated fatty acids from C_{14} to C_{24}, with saturated C_{16} being predominant.

However, not all algae are suitable sources for biodiesel production because of the types of oil they produce. Many microalgal oils contain high levels of unsaturated fatty acids [54]. Biodiesel with a high degree of unsaturated fatty acids can react with lubricating oils in engines and form sludge that increases engine wear [57]. Also, fatty acids with four or more double bonds are susceptible to oxidation during storage [3]. However, polyunsaturated oils can be partially hydrogenated through well-known industrial practices. Moreover, the method of oil extraction can have an effect on oil saturation. When comparing thermal liquefaction and supercritical CO_2 extraction, Aresta et al [50] found that the yield of polyunsaturated fatty acids, specifically long chain fatty acids with 2 to 5 double bonds, is higher from supercritical CO_2 extraction than from thermal liquefaction, and they postulated that it was due to high temperature cleaving of long chain fatty acids during thermal liquefaction.

Gouveia and Oliveira [54] examined the lipid compositions from six algae species and found that *Scenedesmus obliquus* had the most adequate fatty acid profile for biodiesel production. However, algae oils may also be used in combination or supplemented by vegetable oils. If used in a mixture, *Nannochloropsis* sp, *Neochloris oleoabundans*, and *Dunaliella tertiolecta* would be suitable for biodiesel production [54]. All four of these

species had iodine values well below the standard, which is advantageous because soy and sunflower oils, which are also used for biodiesel, have iodine values higher than the standard [54].

Several studies have compared biodiesel produced from algae to both conventional diesel fuel and biodiesel standards and found that it compared favourably. Biodiesel prepared from the microalgae *Chlorella protothecoides* was 60.8% oleic acid methyl ester, with other major components being octadecadienoic acid methyl ester and octadecanoic acid methyl ester [58]. Algae biodiesel from heterotrophically grown *Chlorella protothecoides* [59] and mixotrophically grown *Chlorella vulgaris* [60] have both been found comparable to traditional diesel.

The necessity to meet biodiesel standards requires that algae maintain a predictable lipid composition, and the species or mixture of species grown must remain stable throughout annual production. This indicates that PBRs may be preferable for algal biodiesel production because of their improved culture stability. In addition, algae biodiesel must have a comparable density, heating value, and viscosity to traditional diesel.

2.3.4. Economic and Environmental Considerations of Algae Biodiesel

For large-scale algae biodiesel production to become a reality, the relatively high cost of algae production must be reduced to the relatively low cost required for fuel production. Algal biomass production costs have been estimated at \$0.60-\$7 per kilogram; meanwhile, algal biodiesel costs may exceed \$6 L^{-1} [41]. Other projections place biodiesel costs at two times higher than petroleum diesel costs, even using aggressive assumptions about biological productivity [17]. This projection was made with open ponds, and reactor type will greatly affect the economic analysis. When considering continuous cultivation of diatoms for aquaculture, smaller and less productive airlift reactors were more economic than larger PBRs because of reduced labour, minimal start-up/shutdown time loss, and

reduced maintenance and equipment costs [61]. Even allowing for the optimization required, algae's high biomass and lipid productivity make them a strong candidate as a feedstock of commercially viable biodiesel [62].

Algae growth rates and lipid productivities will greatly affect cost estimates. Previous algae oil projections of 80–90 t ha^{-1} per year are unrealistic [4]. As a result, many earlier cost estimates are unreliable. Of course, genetic engineering may significantly increase productivities. Using current algae strains, attainable growth productivities are only a quarter of previous optimistic predictions. Growth of *Nannochloropsis* in flat-panel PBRs predicts annual oil productions of 20 t ha^{-1} over a 10 month period using a two stage production [4]. In tropical areas, oil predictions rose to 30 t ha^{-1} per year due to the increased average radiation of 20 MJ m^{-2} d^{-1} [4].

Costs may be at least partially offset by gasifying the biomass after the oil is extracted to power algae production or harvesting. Alternatively, the biomass remaining after oil extraction could be used as a bioethanol feedstock. Microalgae cell debris from oil extraction using supercritical CO_2 produced 60% more bioethanol than dried whole algal cells [44]. The researchers concluded that oil extraction had released carbohydrates within the algal cell walls and thus made the fermentation more efficient [44]. This beneficial effect indicates that algae biodiesel feasibility may be greatly enhanced when paired with production of other biofuels.

Several algae biofuel start-ups have begun recently. Twelve of these companies are based in coastal US states, one is in New Zealand, and one is in Israel [19]. Algae biofuel companies are working mainly the following genera: *Botryococcus*, *Chlamydomonas*, *Chlorella*, *Dunaliella*, and *Neochloris* [42]. Several of these start-ups have partnered with educational institutes or petrochemical companies. Since 2008, microalgal fuel demonstration projects have begun in the US, South Africa, the Netherlands, Portugal, and

Australia [41]. Many of these projects have not reported which species will be grown, but they include proprietary marine organisms, *Chlorella vulgaris*, and *Isochrysis galbana* [41]. In addition, more than 100 microalgae companies exist around the world [63]. The majority of these are in the US and China. However, several are present in Germany, Japan, India, and Israel.

Along with algae lipid production rates and conversion efficiencies, algae biodiesel profitability will be affected by market forces, which can be assisted by government programmes and financial incentives. For example, in 2008, the UK launched a £26m project to develop algae biofuels with hopes of algae-based biofuels replacing more than 70 billion L y^{-1} of fossil fuels in road transport and aviation by 2030 [64]. In the US, updated Renewable Fuel Standards mandate the production of 36 billion gallons of biofuels by 2022 [65]. A recent global multistakeholder report cites biofuel projections that advanced biofuels, including biodiesel from biomass, will be commercially available by 2025 [66]. Prior to this, commercial-scale biomass to biodiesel demonstrations are predicted by 2015, and advanced biofuels may account for as much as 18% of biofuel production by 2035 [66]. However, even if commercially available by 2025, algae biodiesel is unlikely to be cost competitive with conventional fuels until later.

One obvious case for algae biodiesel is the reduction in CO_2 emissions. If the UK's goal of 70 billion L y^{-1} biodiesel is achieved, it would lead to an annual CO_2 savings of more than 160m tonnes globally [64]. Algae biodiesel can be used as a pure fuel or as a blend with petroleum diesel. In addition to reduced CO_2, biodiesel and biodiesel blends have significantly lower carbon monoxide, particulate matter, hydrocarbon, and toxin emissions than petroleum diesel [1], [17]. If microalgal oil targets of 40 t ha^{-1} per year are reached, biodiesel from microalgae in raceway ponds could have an 80% lower global warming potential than fossil based diesel [67]. Due to the increased power consumption

from mixing, microalgal biodiesel from tubular airlift PBRs is estimated to have higher global warming potential than fossil-derived diesel [67]. These reactors ranged from 5-10 cm diameter, which is smaller than the 19 cm diameter more typical of airlift PBRs. Much of the electricity consumption in the tubular PBRs was used to overcome frictional losses, so larger diameter airlift PBRs may have a lower global warming potential. Along with potential CO_2 emissions, a major environmental consideration is water usage.

When comparing water consumption, algal biodiesel produced in tubular PBRs used significantly less water than open ponds [68]. This occurred because the majority of water usage was required to overcome surface evaporation, which greatly outweighed water used to produce the glass used in PBRs [68]. Along with increased evaporation rates, open pond performance fails to reach laboratory scale results much less theoretical maxima [69]. In addition to reduced water requirements, PBRs may allow use of genetically modified organisms or production of pure cultures. LCA of raceway microalgae cultivation can produce environmentally sustainable biodiesel feedstock, although the cultivation method will significantly impact the feedstock's environmental performance [67]. One concern with LCAs is failure to consider geographic effects on algae growth, even after considering assumptions of nearness to markets and material availability [70]. The geographic location of the facility is an important consideration in choosing the reactor type. When considering growth in an area with sufficient rainfall to overcome evaporation rates, the estimated water usage for open ponds was nearly that of closed ponds [68]. Considering open pond algae growth in US deserts, which would have high irradiation, dry air, and low land costs, estimated water usage was 10 times greater for open ponds than for tubular reactors [68].

In addition, because each species has its own growth rate and lipid content, the species chosen will affect the water usage. Yang et al [71] calculated biodiesel water footprints

from 11 microalgae species and found that *Chlorella vulgaris*, *Chaetoceros gracilis*, *Cyclotella cryptic*, and *Nannochloropsis* sp required significantly less water than other species for biodiesel production. With lower lipid contents, *Dunaliella primolecta* and *Phaeodactylum tricornutum*, and with lower growth rates, *Botryococcus braunii*, were calculated to require the most water per biodiesel output [71].

All calculations assumed freshwater used. Average water usage estimates for PBRs and open ponds were 44 and 216 L water per L of biodiesel respectively [68]. Harto's [68] highest water consumption estimates, for open ponds in the US desert, were 656 L water per L of biodiesel. These values are on the low end of estimates by Yang et al [71], which once converted assuming 0.864 kg L^{-1} algal biodiesel density, ranged from 511-3,159 L water per L of biodiesel. In either case, water consumption could be reduced drastically by water recycling, using seawater, or using wastewater. In *Chlorella vulgaris* biodiesel production, using seawater or wastewater for culturing would decrease freshwater usage by 90%; even just recycling harvest water could reduce water usage by 84% [71].

Microalgae cultivation requires far less water than traditional oilseed crops [17], [68], [71], which leads to lower water requirements for algal biodiesel. The ASP assessed land, water and CO_2 requirements and determined that algal biodiesel could supply substantially more biodiesel than existing oilseed crops [17]. More recently, calculations of water consumption for soybean biodiesel were up to 5 times greater than estimates for algae in PBRs [68]. Estimates for corn bioethanol water consumption vary greatly by irrigation practices within the growth area. In the US, estimates by state ranged from 5-2,138 L water per L of corn bioethanol [72]. In many US states, corn ethanol production requires far more water than algae biodiesel, which also has a much higher energy density.

Algae growth also requires nutrients, especially nitrogen and phosphorous. Yang et al [71] calculated that 0.33 kg nitrogen and 0.71 kg phosphorous are needed per kg algal

biodiesel if production uses freshwater without recycling. Recycling harvest water could reduce nutrient consumption by 55%, and using wastewater could nearly eliminate the need for nutrients [71]. Considering microalgae production, the ASP determined that resource limitations were not an argument against the technology [17]. As a result, the major concerns for large-scale production are economic and not environmental.

2.4. Altering Algal Oil Abundance and Types

A wide variety of algae are present in nature. Estimates vary widely, but a conservative estimate is 72,500 algae species with maybe 44,000 species named [73]. Relatively few strains have been examined for lipid contents. The majority of these were examined as part of the US DOE's ASP, which isolated over 3,000 algae species and screened many of them for lipid contents and growth [17]. However, no species recommendations were given, and the programme was discontinued in 1996 [17].

Both the total oil content and composition of lipids present differ widely among various algal species. Several species contain between 20-50% oil, and up to 80% oil by dry weight is possible in some species [3]. Even so, Rodolfi et al [4] calculated that, even under optimal conditions, maximum oil yield in large-scale outdoor cultivation will not exceed 40 t ha^{-1} using current algal strains and technologies. There are many ways to alter microalgal lipid contents. The effects of environmental factors, such as light intensity, culture volume, and gas composition, are discussed in detail in Chapter 3. The effects of nutrient limitation, cell size, and presence of flagella are covered in Chapter 4. Several other methods for altering lipid contents are discussed in the rest of this chapter.

2.4.1. Why Algae Store Lipids

Algae store lipids for a variety of reasons. The lipids act as energy reserves and are important parts of the cellular membranes. Lipid reserves provide energy when solar irradiance changes and prevents photosynthesis. For most species, irradiance changes occur on a time period of hours or days. However, some algae can exist in extreme

environments, where they have adopted a rest phase to allow them to survive extreme conditions, such as prolonged snow exposure.

Algae can alter their cell membrane lipid composition to maintain the fluidity of their membranes under varying environmental conditions like temperature changes. These lipid changes can include increased production of polar lipids, alteration of the lipid head group, decreased fatty acid chain length to decrease the melting point, and increased proportion of *cis*- to *trans*- fatty acids [74]. The most common change however, especially in cyanobacteria, is fatty acid desaturation.

Some species store triacylglycerols when light intensity is high but conditions are adverse to cell growth; these lipids provide energy reserves to maintain the cell and rebuild it once environmental conditions improve [75]. In addition, an overall high lipid content has been cited as an adaptation strategy to cold environments [74]. Some species, like *Klebsormidium*, produce bodies abundant with starch and lipid granules upon exposure to dehydration stress, and these bodies are able to withstand prolonged dry periods before restarting the population upon the return of environmentally favourable conditions [74].

Other species, such as *Botryococcus braunii*, exist in a colony held together by an extracellular oil matrix exuded by the cells. *B. braunii* strains contain up to 63% dw lipids, with most of this material located inside occluded globules within the colony matrix [76]. Although well known for its high oil content, *B. braunii* is less studied for biodiesel production due to its relatively slow growth rate; it doubles in 48-72 hours depending upon the suitability of growth conditions. In addition, its oils cannot be transesterified to make biodiesel because they are triterpenes rather than triacylglycerols; hence they lack a free O_2 atom, which is essential in transesterification. Instead, oils from *Botryococcus* need to be hydrocracked to produce gasoline and diesel.

2.4.2. Growth Stage Effects

Microalgal lipids tend to be composed of mainly unsaturated fatty acids with a significant percentage of palmitic acid (C16:0) [54]. However, green algae produce different types and amounts of oils during different stages of growth. In one investigation, the green algae *Chlorella vulgaris* and *Scenedesmus obliquus* contained mainly polar and polyunsaturated C_{16} and C_{18} chain fatty acids during early growth, but, during the stationary growth phase, the main lipids changed to neutral and saturated C_{16} and C_{18} chain fatty acids [77]. Similar trends have been observed in strains of the diatom *Cylindrotheca*. Polyunsaturated fatty acids decreased during later growth stages; meanwhile, saturated fatty acids and total lipids increased during later growth stages [78]. This trend was the same for four *Cylindrotheca* strains, although the strains showed some variability in which growth phase had peak concentrations [78]. It is important to note that these green algae and diatom experiments were batch cultures, so nitrogen concentrations decreased steadily throughout and may have affected the lipid composition. However, nitrogen levels remained above 4 μmol L^{-1} throughout growth in the green algae experiment [77]. Overall, the total lipid content increased from 24.4% dw to 64.5% dw in *Chlorella vulgaris* and from 25.7% dw to 47.1% dw in *Scenedesmus obliquus* [77]. Under the same conditions, blue-green algae, *Anacystis nidulans* and *Microcystis aeruginosa*, showed no obvious change in lipid content or composition throughout their growth cycles [77].

2.4.3. Heterotrophic versus Autotrophic Growth

Many algal species can be either autotrophic or heterotrophic, and the growth method affects the cell composition. Autotrophic algae require some essential elements, along with carbon dioxide and water. The essential elements required vary by algal species but always include nitrogen, iron, and phosphorus and may also include silicon. Various formulas exist for estimating an alga's minimal nutritional requirements based upon its cellular composition. These can be useful in determining the media composition for the

culture, but it is equally important to assess the forms in which the nutrients are supplied. For example, nitrogen can be supplied through nitrate (NO_3^-), urea ($(NH_2)_2CO$), or ammonia (NH_3), but the forms are not be equally bioavailable. Also, depending upon the enzymes present in the cells, it may be possible to use cheaper, cruder forms of nutrients, such as distiller's solubles, yeast extract, and meal from vegetable oil production. As the algae grow, they remove nutrients from and deposit metabolic waste products into the media, so continuous production systems require continuous addition of fresh media along with media removal.

Heterotrophic algae can grow on organic carbon sources, so their growth has the advantage of not requiring a light source for the reactor. This means they can be grown in fermenters, which have large-scale availability, relatively low operating costs, and an extensive knowledge base. Moreover, heterotrophic algal cultures can be a thousand times denser than photoautotrophic cultures [79]. Cell densities between 20 and 100 g L^{-1} have been found in heterotrophic cultures [20]. These benefits result in heterotrophic growth generally being more economic than phototrophic growth unless a high-value product is produced [6].

In addition to increased cell densities, some studies have shown increased lipid production within cells grown heterotrophically. Xu et al [58] grew *Chlorella protothecoides* heterotrophically and found that it produced about four times the lipid content that it did under autotrophic conditions. Its lipid content when grown autotrophically was 14.6%, but it produced lipid contents of 54.7% when grown on glucose solution and 55.2% when grown on hydrolysed corn powder [58]. Other studies have shown changes in fatty acid composition and a decreased polyunsaturated fatty acid content when algae were grown heterotrophically [79].

It is well known that algae generally change chemical composition under heterotrophic conditions [11], [20], [58]. However, not all of the chemical composition changes deal with lipid accumulation. For example, Xu et al [58] found that heterotrophic growth caused *C. protothecoides* to lose its chlorophyll. Furthermore, heterotrophic conditions are not suitable for all species of algae, including *Chaetoceros*, *Skeletonema*, and *Thalassiosira* [11]. Another drawback to heterotrophic growth is that it requires an organic carbon source that would have to be grown as a crop plant, unless a suitable source could be found from the waste products of another industry.

An intermediate method of cultivation is under mixotrophic conditions, where photosynthetic growth is supplemented with an organic carbon source. Lebeau and Robert [11] cited a number of studies of algae under mixotrophic growth conditions, and each study reported 8 or 9 fold higher biomass productivities than under photoautotrophic conditions. Growth of *Chlorella vulgaris* under mixotrophic conditions was almost 4 times higher than control conditions with slightly higher lipid content [60].

2.4.4. Nitrogen and Phosphorous Limitation

The synthesis of lipids in algal cells is similar to that occurring in higher plants, but there are some differences, which allow lipid production to continue and even increase under stress conditions in some algal species. For example, when diatoms bloom in sea ice, increased lipid production is often observed. Along with increased lipid production, physiological changes have been observed, such as the formation of conspicuous oil droplets, along with changes in abundance of various lipid classes; these changes have been attributed to mineral nutrient limitation as the algal population bloomed [80].

These changes in nutrient limitation affect starch and lipid concentrations. The green alga *Pseudochlorococcum* sp uses starch for energy storage under nitrogen replete conditions, but it converts its starch to neutral lipids under periods of extended nitrogen

depletion [81]. This increased neutral lipid production under nitrogen limitation is enhanced by high light conditions [81]. Nitrogen limitation also affects lipid composition of other species. Lipids stored by *Nannochloropsis* sp under nitrogen limitation were mainly triacylglycerols [82]. *Tetraselmis suecica* showed increased C14:0, C16:0, C16:1, and C18:1 fatty acids after 5 days of nitrogen limitation leading to 50% dw fatty acids [4]. With increases in neutral lipids and triacylglycerols, nitrogen limitation may be useful for biodiesel production.

Phosphorous limitation has also been studied but not as much as nitrogen limitation. *Nannochloropsis* sp fatty acid contents increased from 13.2% to 50.1% under phosphorous limitation with lipid composition changing from mainly polar lipids and sterols to triacylgylcerides [4]. The increased lipid content from phosphorous limitation was balanced by decreased biomass productivity to result in no additional lipid productivity [4]. Combinations of nitrogen and phosphorous limitation produced results similar to nitrogen limited cultures [4]. Effects of nutrient limitation on microalgae lipid contents are discussed in greater detail in Chapter 4.

2.4.5. Genetic Engineering as a Way to Increase Algae Lipid Production

Considering the large variety and global distribution of algae species, it is likely that many species exist that would be useful for biofuel production. Even so, genetic engineering has been suggested to increase algae oil contents, to overcome photosaturation, and to reduce photoinhibition.

Early genetic engineering efforts targeted Acetyl CoA Carboxylase (ACCase), which is a major enzyme used to synthesize lipids in plants. As such, increasing its production may increase the amount of lipids produced. The US DOE's ASP was the first to isolate and clone ACCase from a diatom [17]. Later, the diatoms *Cyclotella cryptica* and *Navicula saprophila* were transformed using plasmid vectors in an attempt to induce additional

copies of the ACCase gene [83]. This area has been aided tremendously by advances that allow new organisms to be sequenced more quickly and more cheaply.

The most widely studied algae for genetic engineering is *Chlamydomonas reinhardtii* [42], [84]. This work has elucidated many of *C. reinhardtii*'s metabolic pathways that expand the possibilities of genetic engineering. *C. reinhardtii* and *Volvox carteri* are some of the few algae that have demonstrated long-term, stable expression of transgenic proteins [42]. In addition, *C. reinhardtii* has been engineered to reduce its sensitivity to light such that it can be grown under higher light intensities with less photooxidative damage [42].

For biodiesel production, it may be useful to transform an obligate phototroph, like *Phaeodactylum tricornutum*, into a heterotroph [6], [42]. This has also been accomplished with two other algae species [42]. A wide variety of other modifications have been considered too. Some modifications would centre on oil type, such as engineering fatty acid chains towards production of a preferred chain length or increasing neutral lipid production during exponential growth. Other modifications would target oil recovery, such as making cells secrete oils that would normally be stored internally. Yet another target is nutrient use, such as enabling use of atmospheric nitrogen rather than nitrates or increasing efficiency of phosphorous use. As production of high-value products could aid biofuel economic feasibility in the short-term, this is another possible goal of genetic modification. Algae have already been engineered to produce recombinant proteins and peptides. A wide variety of genes have been spliced into algae to produce vaccines, pharmaceuticals, monoclonal antibodies, and other therapeutic proteins [84].

Clearly, genetically modified algae have the potential to be extremely beneficial to biodiesel production. However, using genetically modified algae would require overcoming major regulatory and public appearance hurdles. In addition, the algae would

need to be engineered to prevent replication in the wild, and closed PBRs would likely be required.

2.5. Summary and Thesis Objectives

Algae production has great potential for a wide range of industries from bioenergy to aquaculture to nutraceuticals. This chapter provides a synopsis of algae culturing requirements and an overview of algae biodiesel production. In current commercial production, algae are most commonly cultivated in open ponds. However, there are a wide variety of closed photobioreactor systems, and each system has specific advantages and disadvantages. Large-scale algae cultivation is currently used to produce biomass for aquaculture or as a source of pigments and nutraceuticals. Nonetheless, there is a lot of potential for biodiesel production, and this may be beneficially combined with wastewater treatment.

For biodiesel production, algae will need to have reliably high oil productivities. However, there is still a great deal to be understood about the ways that culturing conditions affect algae growth rates and lipid production. This research targeted that area.

This thesis was the first of its kind within the University of Oxford, so Objectives 1 and 2 were a larger part of this thesis than would have been likely in a department with a long history in algae culturing. In addition, Objective 5 had complications that extended the timeline, so Objectives 3 and 4 took on much larger roles than originally anticipated. As such, this resulting thesis has the following specific objectives:

1. Develop an extensive database of algae research

   This database contains algae growth, lipid content, and lipid productivity information and corresponding environmental parameters from a large number of publications.

2. Identify key trends in algae research

   By combining information from a large number of studies, the most commonly used

and range of environmental conditions used are identified. Several trends in algae growth rates and lipid contents were observed, and areas for future research have been noted.

3. Quantify key parameters in algae growth and lipid production using modelling

Algae studies involve manipulation of a large number of environmental parameters. Several models were developed using linear multiple regression analysis; these models quantify which parameters most impact algae growth and lipid production.

4. Develop genus specific models

Models were made for *Chlorella*, *Isochrysis*, *Nannochloropsis*, *Phaeodactylum*, and *Tetraselmis* genera. These models make it possible to compare the reliability of general algae models with genus specific ones. Comparisons between genera are also possible.

5. Devise and build a 230 L photobioreactor

The majority of algae studies are performed on <10 L cultures. To consider scale-up issues, a 230 L photobioreactor (PBR) was devised, built, and characterized. Several <1 L bottle experiments were performed to develop experimental procedures. *Tetraselmis impellucida* was used in growth experiments, which were run in parallel with Objectives 1 through 4.

6. Test a *Tetraselmis* SGR model using growth experiments

Each of the multiple regression models produced was assessed using several statistical validation checks. In addition, a three-month *Tetraselmis* growth experiment was performed as a real-world test of one *Tetraselmis* SGR model. Methods to improve the PBR for future experiments were noted.

Chapter 3. Algae Trends Visual Overview of Effects from Experimentally Controlled Variables

Microalgae are important sources of materials for biodiesel, nutraceuticals, pigments, and aquaculture production. This chapter aims to provide a better understanding of the effects of culturing parameters on microalgae growth rates and lipid contents. By combining data from 116 publications on 132 microalgae species, this chapter displays several ways that microalgae growth rates and lipid contents are affected by a wide variety of environmental parameters. These parameters include light intensity, light source, illumination schedule, gas flow rate, CO_2 concentration, culture volume, temperature and salinity. These factors have been studied previously, but the resulting data are difficult to use because they are reported individually, use a variety of units, and contain different combinations of environmental parameters. In this chapter, the data were graphed to show trends in specific growth rates (SGRs) and maximum lipid contents (MLCs) under a variety of environmental conditions. This chapter begins with a discussion of the importance of understanding how environmental variables affect algae production and a comparison with previous reviews. Section 3.2 details how the data were collected and converted into consistent units, the limitations of comparing the studies, and the need for standardising data reporting to increase the usability of data from future studies. Section 3.3 discusses effects of light intensity on algae growth and lipids, while Section 3.4 discusses temperature effects. Culture volume effects are discussed in Section 3.5, and the effects of gas flow rate and carbon dioxide supplementation are discussed in Section 3.6. Next, algae growth in various reactor types is revealed in Section 3.7, and Section 3.8 covers other environmental factors to consider.

3.1. Impacts of Environmental Variables on Algae Production

Algae growth and cell composition depend upon a long list of environmental factors that can be controlled. Unfortunately, algae culturing involves such a diversity of

variables that it can be difficult to determine which variables within a study are having the most impact on growth rate and lipid content. Over the last 100 years, a tremendous store of microalgae knowledge has been generated on these variables, but these data are reported in a wide variety of formats that make it difficult to compare studies. By collecting these data and converting them into a consistent set of units, overall trends emerge that were unobservable within individual studies.

This chapter combines the data from a large number of studies to look for trends among species and to identify data gaps. Previous reviews have focussed on verbal descriptions that list collated published data in text or in tables. While providing a lot of information, these reviews can be difficult to distil into trends. Also, most reviews focus on lipid contents and growth rates without relating environmental information. This chapter takes a different approach and concentrates on visual displays to identify the optimal environmental parameters for algae growth and lipid production. Relatively few graphing review studies exist, and this review is much more comprehensive than previous studies. It contains data on 132 species from 116 publications, whereas other large collation studies contain 55 species from 74 publications [85] or do not list the number of species/publications included [5].

This search for overall trends is different from previous studies that concentrate on microalgae culturing factors in pairs, such as light intensity and temperature [28], [86], [87]; salinity and temperature [87], [88], [89]; or light intensity and CO_2 supplementation [90]. Other studies have examined the combined effects of nutrient limitation and light intensity [4], nutrient limitation and temperature [91], and phototrophic/mixotrophic growth with and without CO_2 supplementation [92].

This chapter concentrates on several key environmental parameters manipulated during algae growth. These parameters are light intensity, light source, illumination schedule,

temperature, culture volume, gas flow rate, and CO_2 concentration. This chapter should help focus future research to increase algae lipid and biomass productivities, and it will help new algae researchers gain a quick understanding of the complexities of algae growth. The aim of this chapter is to display a large volume of algae growth and lipid content data as clearly and succinctly as possible. Instead of concentrating on species specific data, this chapter looks at microalgae responses to different growth conditions. Meanwhile, Chapter 4 examines species specific characteristics important in choosing an alga species for large-scale growth; these include cell size, presence of flagella, and lipid contents.

3.2. Database Preparation Methods

An extensive literature review of microalgae growth and lipid content research was performed, and the data were used to populate a database containing information from 131 publications. All available environmental parameter data were used, and this included lighting variables (light source, intensity and schedule), gas variables (flow rate, CO_2 concentration), culture size, culture medium, pH, media type, use of nutrient limitation, and temperature. Additionally, the database contains reported results, such as SGRs, biomass productivities, lipid productivities, and lipid contents. Information was gathered from tables, from data within the text and, when necessary, read off graphs as accurately as possible. This resulted in the data from 116 publications reported in the figures within this chapter. All publications used to generate each figure are cited under that figure. Where possible, algae species names were updated using the most recent strain numbers in databases and publications [85], [93], [94].

To prepare the database, data were entered into an Excel workbook with one row for each experimental setup and with columns containing the data source, each experimental variable, and the results. In this way, data could be sorted and grouped while maintaining links to each data point's source. When no datum was available (i.e. when a study did not

state the illumination schedule used), the corresponding cell was left blank. Additional columns were added to convert data into a consistent set of units. These conversions are discussed in Section 3.2.2. The MLC stated for each setup indicates the MLC obtained using that particular experimental setup rather than a species maximum. For each graph, the dataset was filtered to graph only those results for which all relevant variable data were known. As a result, the number of species represented in each graph is different; this number is included in the title of each graph.

3.2.1. Limitations of Comparing Studies

It is difficult to compare studies on enhancing microalgae growth rates and lipid contents for four main reasons. The first major difficulty is the wide variety of ways in which similar data are presented. For example, algae growth may be reported as SGR, maximum and/or average biomass concentration, cell count, biomass productivity, doubling time, cell weight and volume, or generation time. Each of these ways of measuring growth provides slightly different information, and this makes it difficult to compare data across studies. Additionally, many studies report either areal or volumetric data for biomass or lipid productivity without providing the specific data on reactor measurements, particularly reactor depth, necessary to convert between the two data types.

Secondly, many parameters are reported in a variety of data formats. Table 2 shows a summary; these data formats require conversion to a consistent set of units before the data can be compared. Many of the conversions are easily performed. However, some are given in “per cell” units that are impossible to convert unless corresponding weight and volume information is given for the cells, and this is rarely done. In addition, conversions between volumetric and areal formats require information on the culture vessel size and geometry. Another under reported parameter is the time period of growth before harvesting, which is necessary to convert between growth rates and productivities.

Table 2. Variety of data formats found during the review of published literature

Illumination Units	Biomass Concentration	Lipid Yield	Lipid Productivity	Gas Flow Rate	Salinity
µEinsteins m^{-2} s^{-1} µmol photons m^{-2} s^{-1} µmol PAR photons m^{-2} s^{-1} µmol m^{-2} s^{-1} µmol quanta m^{-2} s^{-1} W m^{-2} mW cm^{-2} lux foot candles metre-candles photons s^{-1} MJ m^{-2} d^{-1} kJ m^{-3} kWhr d^{-1} outdoors	**g L^{-1}** mg mL^{-1} mg AFDW L^{-1} cells $µL^{-1}$ % increase **Biomass Productivity** Volumetric- **g L^{-1} d^{-1}** mg L^{-1} hr^{-1} g L^{-1} $week^{-1}$ kg m^{-3} d^{-1} L hr^{-1} * Areal- g m^{-2} d^{-1}	**g L^{-1}** µg mL^{-1} ng $cell^{-1}$ pg $cell^{-1}$ m^3 ha^{-1}	Volumetric- **mg L^{-1} d^{-1}** g L^{-1} d^{-1} µg L^{-1} hr^{-1} mg L^{-1} $week^{-1}$ pg $cell^{-1}$ Areal- g m^{-2} d^{-1} kg ha^{-1} d^{-1}	vvm or **L L^{-1} min^{-1}** L min^{-1} L min^{-1} $flask^{-1}$	**ppt** ‰ no units µS cm^{-1} mS cm^{-1} g L^{-1} mol L^{-1} psu

*Effluent value used in turbidostat cultures
This table shows the wide variety of data formats commonly used in publications. Recommended units for reporting are shown in bold.

A third problem is that many studies fail to report information on the light source, light intensity, and/or illumination schedule used in phototropic algae growth, even though these variables are a major factor in growth rates and productivities as shown in this chapter. A large proportion of studies did not report the culture volume or illuminated surface area used. Other studies reported bubbling the cultures but failed to provide flow rate information, and others reported using marine species without providing the media salinity. Some studies reported average data, and some reported maximum data.

A fourth obstacle involves data citation chains, where data are cited in a review that is then cited as the data source rather than returning to the original data source. This causes a piece of data, such as the lipid content for a species, to be cited repeatedly as coming from different authors. On the surface, it appears to be several individual results in agreement, which may overinflate the results of one study such that a widely agreed upon value is not as widely supported as it first appears. An associated and serious problem is that this

re-citing loses the details from the original study, so it is difficult to tell what conditions produced that lipid content level. Additionally, the long chain of citations makes it difficult and time-consuming for future researchers to trace their way back to the original source when searching for more details about the experiments used to produce those data.

The microalgae data reported here were produced in many laboratories, which means that SGR and lipid content determination procedures and equipment varied. Also, the cultures used a variety of media, temperatures, culture volumes, irradiances and other parameters. These differences cause variability in the dataset. The figures show individual experimental results rather than a mere species average value, so they provide a more accurate understanding of the dataset.

3.2.2. Converting Units

Before the studies can be consolidated to look for trends, it is necessary to convert the units from the wide variety of formats shown in Table 2 to a consistent format. Several of these conversions were straightforward. In some cases, the lack of details within the publications made it necessary to make assumptions before data could be converted to a consistent set of units. The assumptions made, when necessary, are that lipid content values given as % were assumed to be % dw even if it was not explicitly stated. When the culture volume was not stated but the container volume was, it was assumed to be 60% full if an Erlenmeyer flask and 80% full for other vessels. In two instances, the resultant value from a unit conversion was far outside the range of the other literature data for that species, and such data were excluded from future analyses.

One of the most difficult factors in comparing algae studies is that each study uses a different light source and light intensity. Converting light intensities is complicated because a wide variety of light sensors are used to measure light intensity, which results in the different formats shown in Table 2. Some of these formats are not directly comparable

because some are based on physical parameters, such as Watts m^{-2} or $\mu E\ m^{-2}\ s^{-1}$, while others are based on subjective parameters, such as lux and foot-candles. Light contains energy, so it can be measured in the physical units of energy or quantum units, whose interconversion is dependent on wavelength. However, many light measurement devices commonly available to researchers are based on subjective measurements like the brightness seen by the human eye, which is characterized as luminosity. When based on brightness seen by the human eye, measurements can be misleading in culturing algae, which may grow well in light wavelengths not seen by the human eye. Converting between physical and subjective units leads to approximations because they are based on the relative visibility of different wavelengths to the human eye. The complexity of the light data is shown in Figure 4, which was developed from summarized information in the CSIRO database [95].

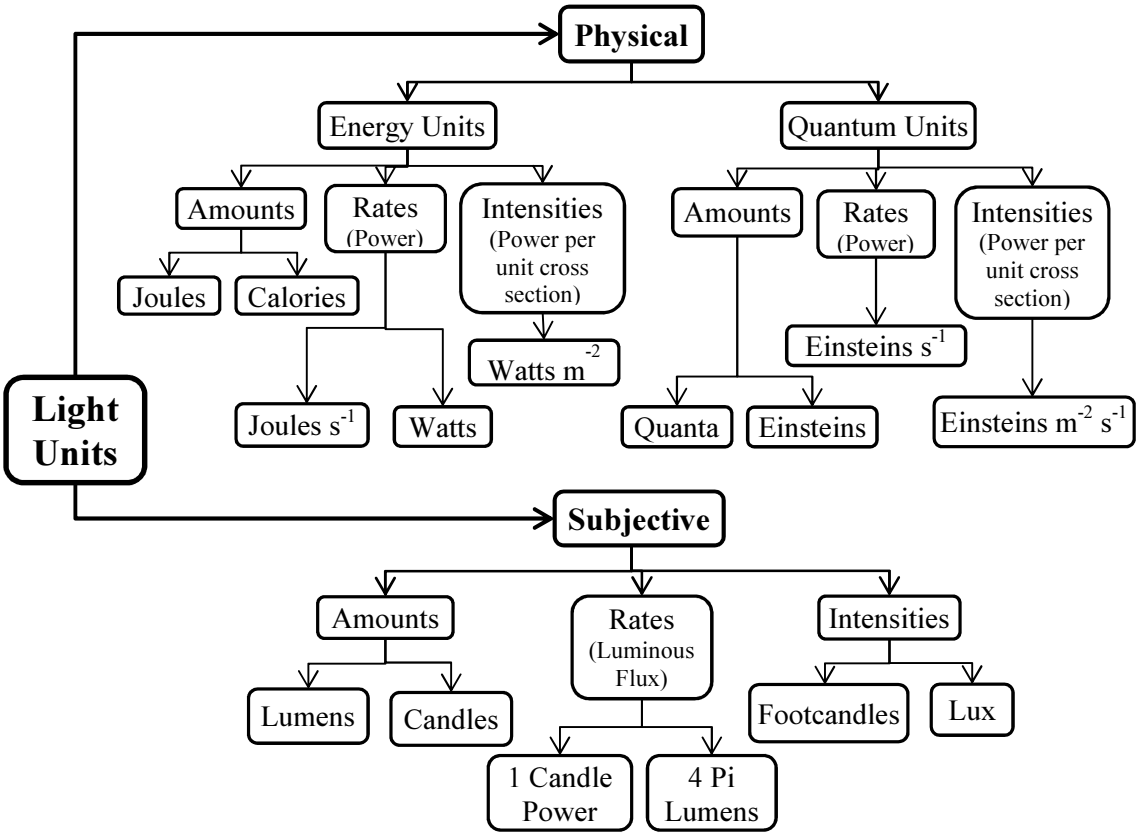

Figure 4. Relationships between physical and subjective light units

Light intensities and growth rates were converted to a single set of units to enable comparisons. Conversions were performed using the parameters in Table 3. Occasionally, insufficient data were available to perform the conversion, such as a lack of reactor depth data needed to convert from areal productivity. Such data were not included in analyses.

Table 3. Conversion parameters used to consolidate light and growth rate data

Variable Type	Light Intensity
Target Units:	$\frac{\mu E}{m^2\ s}$
Equations Used:	1 E = $6x10^{23}$ quanta = 1 mol light 1 E s^{-1} = 1 watt = 1 Joule s^{-1} 1µE m^{-2} s^{-1} = $6x10^{17}$ quanta m^{-2} s^{-1} 1 footcandle = 10.8 lux 1 µmol photons m^{-2} s^{-1} ≈ (constant) × (lux value measured) constant: 0.0135 for fluorescent lamps 0.0165 for incandescent bulbs 0.0135 for unknown light sources 1 metre-candle = 1 lux 1 µmol quanta = 1 µmol photons 1 W m^{-2} = E m^{-2} s^{-1}
Abbreviations: E = einsteins m = meters s = seconds W = watts	

Variable Type	Specific Growth Rate (µ or K')
Target Units:	day^{-1}
Equations Used:	$\mu = \frac{\ln\left(\frac{N_2}{N_1}\right)}{(t_2 - t_1)}$ $\mu X = Q_V = \frac{Q_A \times D}{1000}$ $\mu = \frac{Q_A \times D}{1000X}$ $\mu = \ln 2 \times \frac{Divisions}{Day}$ $\mu = \ln 2 \times \frac{1}{Generation\ time}$ Generation time = Doubling time
Abbreviations: D = container depth N_1 = inoculation concentration N_2 = final concentration Q_A = areal biomass productivity Q_V = volumetric biomass productivity t = time X = biomass concentration	

3.2.3. Standardizing Units and Information Reported

This dataset contains a wide variety of reporting formats as shown in Table 2. Furthermore, some data needed to convert between formats are consistently under-

reported, such as reactor depth, reactor dimensions, and growth period. This lack of standardization in reporting data needs to be addressed because it limits the usability of algae growth and lipid production data.

Standardising units would be beneficial to the algae culturing community by making cross comparisons of algae studies easier. The need for complete reporting of culture conditions has been noted previously [85], but this chapter goes further by identifying several variables that ought be reported to increase data usability. Future research should definitely include culture volume, reactor depth, gas flow rate and illumination schedule, which are commonly under-reported. A recommended set of data for reporting is provided in Table 4 along with recommended units for each variable.

Table 4. Data parameters that should be included in algae articles to facilitate inter-comparison

Study Setup Parameters	**Study Output Parameters**
Species	Average Lipid Content (% dw)
Water Type	Maximum Lipid Content (% dw)
Average pH	Average Biomass Productivity (g L^{-1} d^{-1})
Average Temperature	Maximum Biomass Productivity (g L^{-1} d^{-1})
Reactor Type	Average Lipid Productivity (mg L^{-1} d^{-1})
Reactor Working Volume (as L culture)	Maximum Lipid Productivity (mg L^{-1} d^{-1})
Reactor Depth (m)	Cell Size (µm long x µm wide)
Reactor Ground Area (m^2)	Cell Grouping (singular, clumped, chain)
Reactor Surface Area (m^2)	
Light Source	
Light Intensity (µE m^{-2} s^{-1})	
Illuminated Surface Area (m^2)	
Salinity (ppt)	
If Nutrient Limitation was Used	
If Heterotrophic or Autotrophic Growth	
Gas Type Supplied (% CO_2 if used)	
Gas Volume Used (L L^{-1} min^{-1})	

3.3. Light Intensity Effects on Algae Growth and Lipid Contents

Adequate light supply is a fundamental requirement of any autotrophic algal photobioreactor (PBR). As such, the light intensity supplied is of great importance, and it has been studied extensively. The light source used is somewhat less studied, but it can

also impact algal growth. Algal PBR research has largely been based on solar illuminated reactors because of the cheapness of the energy. In addition, several artificial light sources have been tested, and each source has a unique wavelength spectrum. Tungsten-halogen lamps, for example, provide little light in the blue region of the wavelength spectrum [33].

Light energy is absorbed by chlorophyll and accessory pigments within the algae's chloroplasts. All algae contain chlorophyll a, which has maximal absorption around 430 nm and 660 nm [7]. Most algal species also contain one or more other chlorophylls, chlorophyll b, c_1, c_2, and d, and each of these has a specific maximal absorption wavelength. Accessory pigments extend the range of wavelengths considered to be photosynthetically active radiance to 350 to 720 nm [33]. This indicates that different light sources may affect algae growth. To examine this possibility, algae SGRs obtained under different light intensities were graphed for several light sources.

Figure 5 covers a wide range of light intensities from 11-4,000 $\mu E\ m^{-2}\ s^{-1}$. It is important to note that light intensities given in literature are difficult to interpret because of the different procedures for determining light intensity. Many studies report a light intensity measured near a culture. Others attempt to account for the surface area that is illuminated, and some report the light intensity within the culture. These methods may provide very different measurements for some reactor types, especially tubes and flasks with curved surfaces. As such, these methods likely cause some variability in the dataset.

The highest SGRs are for cultures grown with fluorescent tubes and metal halide lamps. Except for sunlight, all light sources produced SGRs greater than 1 d^{-1}. Figure 5 shows solar cultures tend to have much higher light intensities than other light sources. Most of the high light intensities are for sunlight and light emitting diode (LED) cultures.

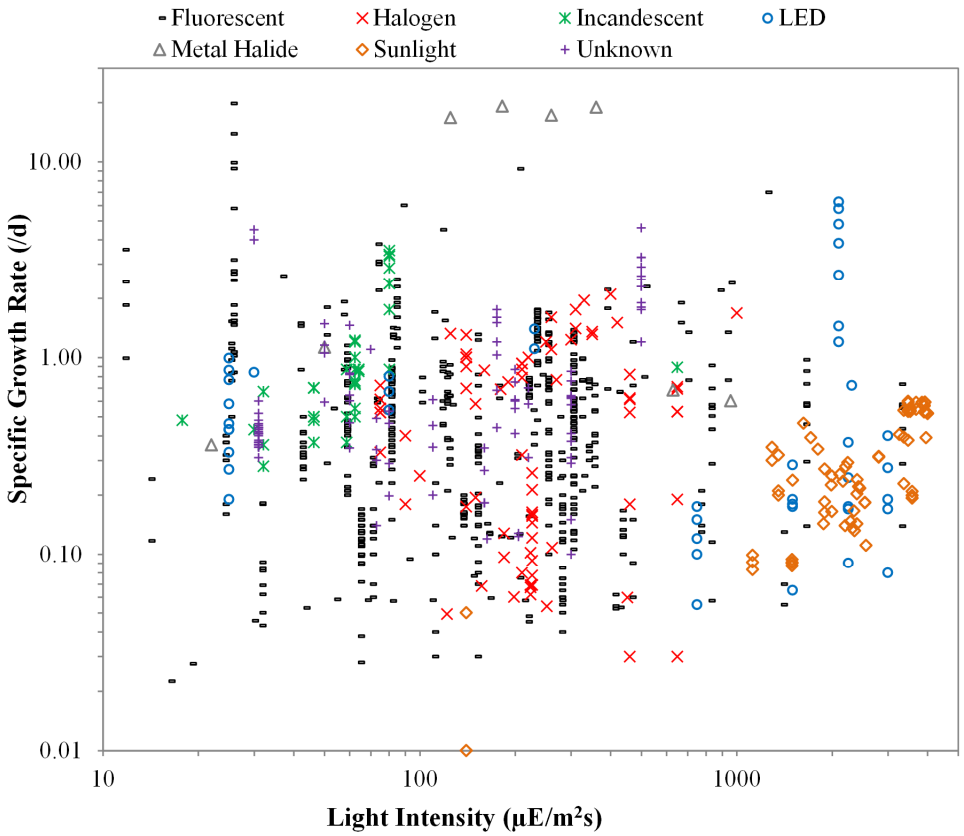

Figure 5. Specific growth rates of 92 algae species by light intensity and light source
This graph includes data from the following research papers: [14], [23], [27], [38], [61], [87], [88], [89], [91], [96], [97], [98], [99], [100], [101], [102], [103], [104], [105], [106], [107], [108], [109], [110], [111], [112], [113], [114], [115], [116], [117], [118], [119], [120], [121], [122], [123], [124], [125], [126], [127], [128], [129], [130], [131], [132], [133], [134], [135], [136], [137], [138], [139], [140], [141], [142], [143], [144], [145], [146], [147], [148], [149], [150], [151], [152], [153], [154], [155], [156], [157], [158], [159], [160], [161], [162], [163], [164]

LEDs are a promising light source because they are small and can be rapidly switched on and off. In addition, LEDs have long life expectancies and are very energy efficient, so they produce relatively little waste heat compared to other light sources [96]. Red LEDs with spectral emissions peaking at 680 nm have been used to grow *Chlorella sorokiniana* and *Chlorella vulgaris* [96], [165]. Blue light wavelengths from 400 to 500 nm produced increases in growth rate and extracellular polysaccharide production in *Porphyridium purpureum* cultures [166]. When growing *Chlorella vulgaris*, red-blue LED combinations were twice as productive as fluorescent lamps [46].

At comparable high light intensities, LEDs produced similar or higher SGRs than sunlight. However, this is more likely due to culture size rather than light intensity

because the LED cultures were 52 mL to 1.7 L, while all but two sunlit cultures were 16-12,000 L. Large culture volumes have several possible effects, including reduced light penetration, presence of dead zones, increased contamination risk, and effects from dilute cultures. Culture volume effects are discussed further in Section 3.5. In addition, the higher light intensities could be causing photoinhibition.

In Figure 5, the lower light intensities, from 25-360 μE m^{-2} s^{-1}, have the highest SGRs, but these cultures are 40 mL (metal halide) and 800 mL (fluorescent). SGRs >1 d^{-1} were achieved at light intensities from 11.6-2,100 μE m^{-2} s^{-1} with most of these data points occurring between 25-650 μE m^{-2} s^{-1}. This result matches previous research showing that *Nannochloropsis* sp cultures grown at irradiances <30 and >650 μE m^{-2} s^{-1} deteriorated rapidly [38]. Seven liter *Nannochloropsis* sp cultures grew at 0.43 d^{-1} under 30 μE m^{-2} s^{-1} but reached 0.89 d^{-1} under 650 μE m^{-2} s^{-1} irradiance [38]. Similarly, *Pseudochlorococcum* sp cultures showed slight photoinhibition at 600 μE m^{-2} s^{-1} and significant inhibition causing decreased cell density at 800 μE m^{-2} s^{-1} [81]. In general, algae SGRs increase with increasing irradiance up to a maximum with further increases causing photoinhibition [81], [167]. Figure 5 shows lower SGRs at high light intensities. Several of these light intensities are above 2,000 μE m^{-2} s^{-1}, which exceeds saturation irradiance [167].

The variability shown in Figure 5 could be due to many factors, including temperature and media used, the inoculation culture's growth phase, and type of measurement equipment used. In addition, Figure 5 includes data from a wide variety of culture volumes. In one study, *Chlorella pyrenoidosa* linear growth rates increased with increased light intensity within a single PBR size, but the correlation was absent when several PBR sizes were compared [168]. The time period considered for SGR calculation will also significantly affect the resulting SGR and may even lead to negative SGRs. Moreover, some algae can acclimate to the light intensity in which they are grown by changing their

number of photosynthetic units and concentration of intracellular pigments. Algae can be very flexible to their environmental conditions. *Nannochloropsis* sp cultures begin to acclimate to a light intensity after twelve hours and reach a steady-state after ninety hours [38]. This can affect the SGR achieved at a particular light intensity. Low light acclimated *Nannochloropsis* sp cells show 4.25 times more chlorophyll a than high light acclimated cultures [38].

Figure 5 makes it clear that most algae growth studies are performed using fluorescent lights. Several reasons for the popularity of fluorescent lights are high energy efficiency, cheapness and availability. Also, fluorescent lamps distribute light nearly uniformly along their length, which increases the potential illumination area. *Isochrysis galbana* grown under fluorescent lamps at light intensities up to 250 W m^{-2} showed increasing growth rates as light intensity increased up to 80 W m^{-2} (369 μE m^{-2}) [97]. Similar experiments on *Tetraselmis* sp showed increased growth up to light saturation at 100 W m^{-2} (461 μE m^{-2}) [97]. The same effect has been seen with *Nannochloropsis* sp grown in outdoor flat panel reactors, where an increase in irradiance from 115 to 230 mmol photons m^{-2} s^{-1} resulted in increased biomass productivity from 0.97 to 1.45 g L^{-1} d^{-1} [4]. The fluorescent cultures in Figure 5 have volumes ranging from 34 mL to 200 L with many unknown culture volumes. At low and medium light intensities, fluorescent tubes produced high SGRs, but, at higher light intensities, fluorescent tubes produced lower SGRs than other light sources. Due to the advantages discussed above, fluorescent tubes are commonly used, but they are not feasible for large-scale culturing because of their energy requirements. Parabolic light collection devices and fiber optics have also been tested; however, the improved energy efficiency of these configurations has generally been offset by their increased cost and difficulty of use [6].

In addition, light intensity may affect whether the cells float or sink. *Porphyridium*

cruentum cells grown in low light intensities settle faster than those grown in high intensities [169]. This occurs because *P. cruentum* cells grown under high light intensities characteristically have a greater volume of vacuoles and a larger proportion of sheath, which may reduce their density [169]. This has important implications for large-scale culture of species that produce large vacuoles or sheaths. Gelatinous sheaths are common in unicellular and filamentous cyanobacteria [170].

Light intensity is the most commonly studied light characteristic. However, illumination period may be as important. In solar illuminated reactors, algae grow in the daylight due to photosynthesis and shrink at night due to respiration. Many studies use continual illumination in an effort to reduce respiration losses of biomass. However, continuous illumination may not be feasible for long-term cultures because most cultures require light/dark periods to maintain correct physiology [6]. Other studies have aimed to mimic natural daylight rhythms using 12/12 or 14/9 hour illumination schedules.

Figure 6 shows a vast array of illumination schedule and light intensity combinations that have been tested. The majority of artificially illuminated algal studies are performed with either continuous or 12 hour illumination. Continuous illumination has been used for a range of light intensities from 16-3,300 $\mu E\ m^{-2}\ s^{-1}$. Figure 6 also shows that many studies do not cite the illumination period; these cases are shown under the category "unknown." This makes it hard to judge the actual irradiance received by the algae. Most of the highest light intensity unknown data points are from sunlit cultures. These studies experience a range of light intensities daily, so no single irradiance level is available. In addition, sunlight studies are exposed to fluctuating light from season, reactor orientation, and geographic location. Outdoor cultures may also be affected by weather or presence of environmental particulates. A review of 27 years of algae mass culturing showed summer yields reaching 30 $g\ m^{-2}\ d^{-1}$ but winter yields significantly lower with peaks around 3.5 g

m^{-2} d^{-1} [36]. Also, since outdoor cultures undergo different growth rates at different times of the year, they will experience different amounts of light limitation due to cell shading throughout the year. As a result, outdoor ponds may need to be operated at different depths and cell densities depending upon the season [14]. These considerations are especially important for industrial scale production of high-value products, where the algae composition must be consistent.

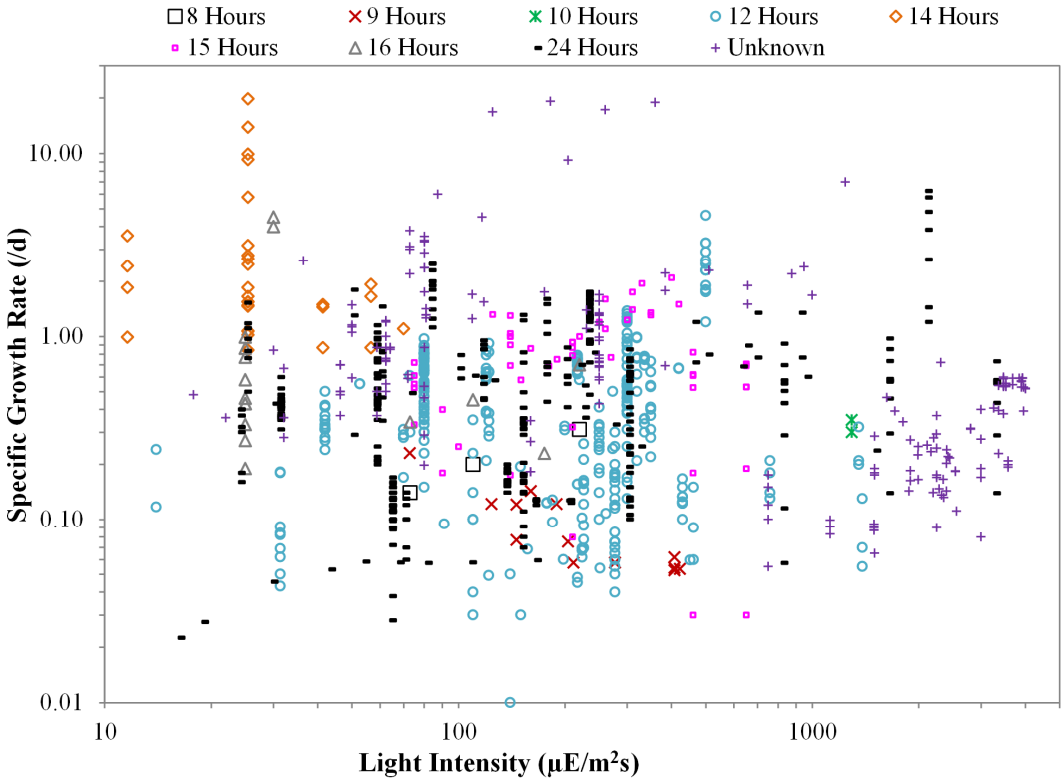

Figure 6. Specific growth rates of 92 algae species as a function of light intensity and illumination schedule
This graph is composed of data from the following sources: [14], [23], [27], [38], [61], [87], [88], [89], [91], [96], [97], [98], [99], [100], [101], [102], [103], [104], [105], [106], [107], [108], [109], [110], [111], [112], [113], [114], [115], [116], [117], [118], [119], [120], [121], [122], [123], [124], [125], [126], [127], [128], [129], [130], [131], [132], [133], [134], [135], [136], [137], [138], [139], [140], [141], [142], [143], [144], [145], [146], [147], [148], [149], [150], [151], [152], [153], [154], [155], [156], [157], [158], [159], [160], [161], [162], [163], [164]

Light intensity can have significant effects on algae composition. Using fluorescent lamps, a 4 times increase in light intensity increased *Chlorella vulgaris* lipid production significantly [46]. *Nannochloropsis* sp shows increased lipid contents when light intensity is increased from 30 to 290 µmol m^{-2} s^{-1} [28]. In another study, increasing light intensity

from 115 to 230 mmol photons m^{-2} s^{-1} caused *Nannochloropsis* sp to increase its fatty acid content from 24.3% to 32.5% [4]. *Isochrysis galbana* has also shown increased lipid contents with increased light intensity up to 30% dw [97]. After similar observations, increased light intensity was tested as a method of increasing lipid content. However, the effect is species dependent. *Tetraselmis* sp showed slightly decreased lipids at low intensities but constant 10% dw lipids up through saturation light intensities [97]. Higher light intensities do not appear to increase lipid contents in marine diatoms either. Marine diatoms *Chaetoceros neogracilis*, *Phaeodactylum tricornutum* B114, and *Cylindrotheca fusiformis* showed decreased total lipids at ≈67.5 μE m^{-2} s^{-1} compared to ≈20.3 μE m^{-2} s^{-1} [31]. No lipid changes were observed in *Nitzschia closterium* or in *Phaeodactylum tricornutum* B118 or B221 between the same two light intensities [31].

Furthermore, very high light intensities appear to reduce lipid contents. Figure 7 shows that most of the >50% dw MLC values are for light intensities below 300 μE m^{-2} s^{-1}. The optimal light intensities appear to be 25-277 μE m^{-2} s^{-1}. Many light sources are not reported in lipid content studies. However, of those reported, fluorescent tubes and sunlight are the most common light sources. Most of the sunlit cultures have a MLC between 30-40% dw. The relative precision of the data may be because only a handful of species are included in the sunlit culture data because of the need for species that can outcompete other species in outdoor conditions. Also, sunlit cultures generally have the highest light intensities. The highest MLCs were achieved using fluorescent lamps and LEDs. In a comparison of microalgae grown under the same conditions, red-blue LEDs were found to produce higher oil contents than red LEDs and much higher than fluorescent lamps [46].

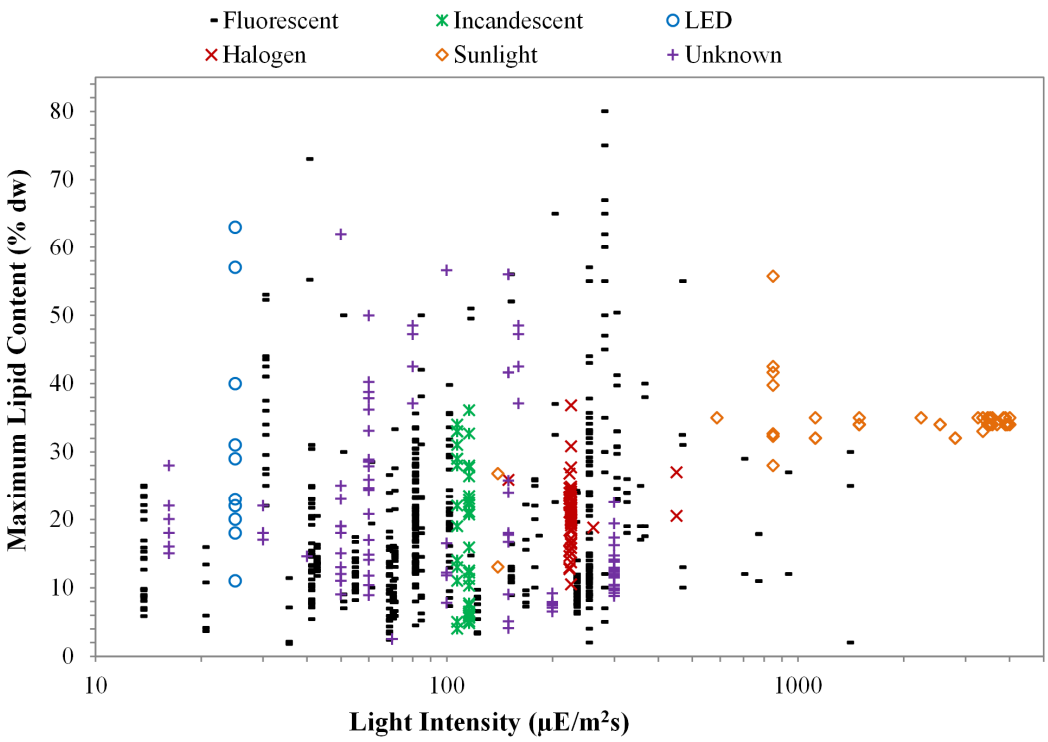

Figure 7. Maximum lipid contents of 96 algae species by light intensity and light source
This graph was produced with data from: [4], [14], [31], [54], [58], [59], [78], [82], [91], [92], [97], [101], [104], [105], [106], [108], [112], [115], [118], [119], [120], [124], [125], [126], [128], [129], [133], [134], [137], [138], [139], [143], [144], [147], [155], [162], [163], [164], [171], [172], [173], [174], [175], [176], [177], [178], [179], [180], [181], [182], [183], [184], [185], [186], [187], [188], [189], [190], [191]

Light intensity can also affect lipid composition. High light intensities have been shown to increase triacylglycerol levels in a few species [75]. *Nannochloropsis salina* showed increased saturated and monounsaturated fatty acids at increased light intensities [4]. Slight photosynthetic inhibition by high light intensities may be necessary for maximum neutral lipid accumulation; as such, 600 µE m^{-2} s^{-1} produced maximum neutral concentrations in *Pseudochlorococcum* sp cultures grown from 20-600 µE m^{-2} s^{-1} [81]. Low light intensities have been shown to increase polyunsaturated fatty acids and decrease saturated ones [192].

The combination of high light intensity and nitrogen limitation may increase lipid contents more than nitrogen limitation alone. Combinations of higher light intensities and nitrogen starvation produced increased lipid storage in *Nannochloropsis salina* cultures in a 20 L alveolar panel under artificial illumination [4]. Similarly, at 600 µE m^{-2} s^{-1},

nitrogen limitation increased the neutral lipid content from 38.3% to 52.1% in *Pseudochlorococcum* sp; meanwhile, 20 µE m^{-2} s^{-1} nitrogen limited cultures had 24.6% neutral lipids [81].

It does not appear that illumination period has a significant effect on MLC as seen in Figure 8. However, this assessment is hindered by the lack of MLC data for cultures grown under less than 12 hours of illumination. It should be noted that all of the values for unknown illumination schedule and >500 µE m^{-2} s^{-1} light intensity are for sunlit cultures. Figure 8 shows that the majority MLCs are for continuous illumination cultures, although several cultures have unknown illumination periods.

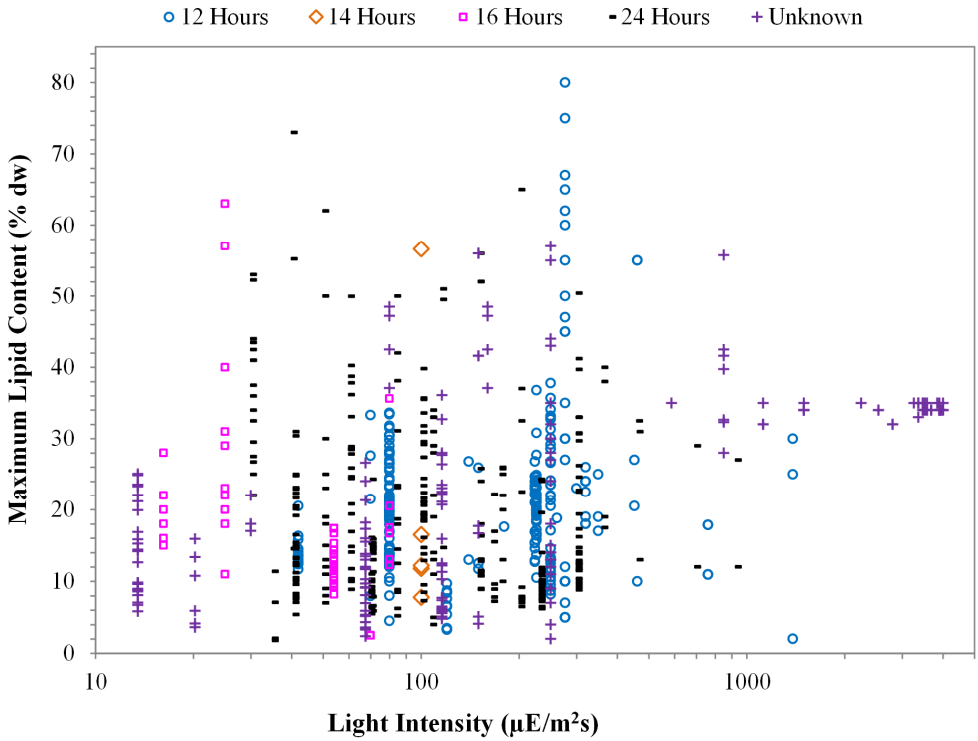

Figure 8. Maximum lipid contents of 96 algae species by light intensity and illumination schedule This graph includes data from the following sources: [4], [14], [31], [54], [58], [59], [78], [82], [91], [92], [97], [101], [104], [105], [106], [108], [112], [115], [118], [119], [120], [124], [125], [126], [128], [129], [133], [134], [137], [138], [139], [143], [144], [147], [155], [162], [163], [164], [171], [172], [173], [174], [175], [176], [177], [178], [179], [180], [181], [182], [183], [184], [185], [186], [187], [188], [189], [190], [191]

A vast array of illumination schedule/light intensity combinations have been used. Considering this, it is difficult to assess the actual irradiance on the cultures in the many publications that fail to report illumination schedules used. This chapter shows that light

intensities <500 μE m^{-2} s^{-1} produced the majority of the high SGRs and MLCs.

In addition to light intensity and illumination schedule, great increases in algal growth efficiency may be possible by using flashing light. Under flashing light conditions, *Haematococcus pluvialis* showed 400% increased astaxanthin production compared to continuous light; this was achieved with an average flashing light intensity of 16.4 μE m^{-2} s^{-1}, although the instantaneous maximum light intensity was >1,700 μE m^{-2} s^{-1} [34].

Light path is another light variable that affects SGRs and lipid contents. Chlorophyll quickly absorbs all light in a dense culture, so short light-path lengths are recommended. Reducing the light path from 30 to 15 mm resulted in a 2.5 times higher biomass productivity in *Chlorella vulgaris* cultures grown in an airlift reactor [23]. Similarly, increased culture productivities and lipid contents were observed when a flat panel PBR was irradiated from two sides compared to when irradiated with equal intensity from only one side [4]. In large diameter reactors, mixing is used to circulate cells so they experience a shorter light-path length.

3.4. Temperature Effects on Algae Growth and Lipid Contents

Algae grow in a wide range of temperatures around the world, but each species has its own optimum range. If the culture temperature gets too high, the lipids within the cells' thylakoid membranes separate, and the chloroplasts will become less efficient and cause photosynthesis to be reversibly reduced [9]. Generally, freshwater algae can handle greater temperature fluctuations than marine algae [6].

Temperature also affects other algal cell processes, such as flagellar regeneration. Several species move using flagella. Some flagellates drop and regenerate flagella as a normal part of their cell cycle [193]. Also, a cell's flagella may be damaged by pH changes or mechanical stress [194]. As such, the flagella must be regenerated. In *Tetraselmis striata*, low temperatures (10 and 15 °C) reduced flagella regeneration rates,

while high temperatures (30 °C) prevented flagella regeneration [195]. Flagellar regeneration was fastest at 20 and 25 °C [195]. For maximal biomass productivity, reactor temperature should be maintained within the optimum range for the species being grown.

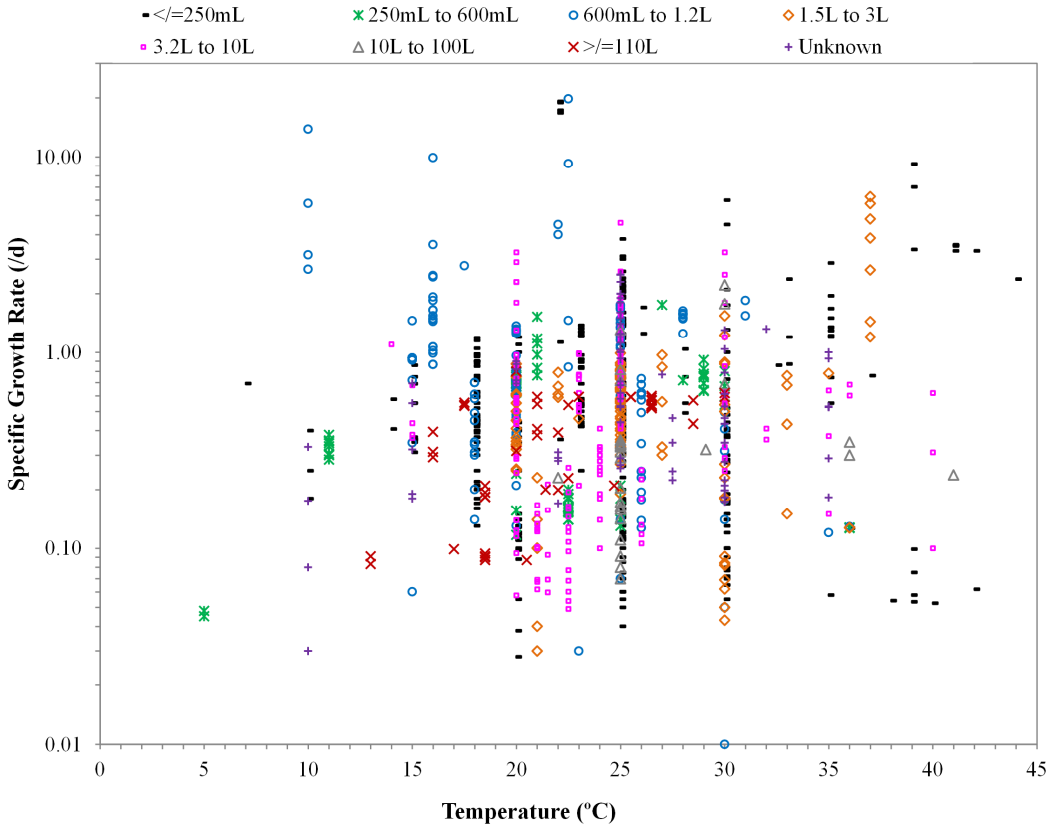

Figure 9. Specific growth rates of 100 algae species as affected by temperature and culture volume This graph was prepared using data from the following sources: [14], [23], [27], [38], [61], [87], [88], [89], [91], [96], [97], [98], [99], [100], [101], [102], [103], [104], [105], [106], [107], [108], [109], [110], [111], [112], [113], [114], [115], [116], [117], [118], [119], [120], [121], [122], [123], [124], [125], [126], [127], [128], [129], [130], [131], [132], [133], [134], [135], [136], [137], [138], [139], [140], [141], [142], [143], [144], [145], [146], [147], [148], [149], [150], [151], [152], [153], [158], [159], [160], [161], [162], [163], [164], [196], [197], [198], [199], [200], [201]

Figure 9 represents the effects of temperature on microalgae SGRs in several culture volumes. Some of the publications in the dataset listed temperature ranges rather than a controlled temperature. When this occurred and an optimal temperature was listed, the optimal temperature was used. When no optimal was provided, the average temperature was used because insufficient data were provided to calculate medians. The highest SGRs were obtained from 22-22.5 °C in cultures <1 L. This matches previous studies of temperature effects on microalgae. *Nannochloropsis* sp grown under 20 or 200 µmol m^{-2}

s^{-1} light intensity at a range of temperatures showed optimal growth rates at 25 °C [28].

In this dataset, algae cultures grew well (2.38-6.24 d^{-1}) at all temperatures from 10-44 °C, but >80% of the SGRs were less than 1 d^{-1}. In Figure 9, cultures ≥10 L show SGRs ranging from 0.07-2.22 d^{-1} over temperatures from 13-41 °C. As temperatures increase, however, increased light intensities are required and evaporation rates increase within the culture [6]. High light intensities are common, as shown in Figure 5, but increased evaporation requires cultures to be grown in saltwater or paired with wastewater treatment.

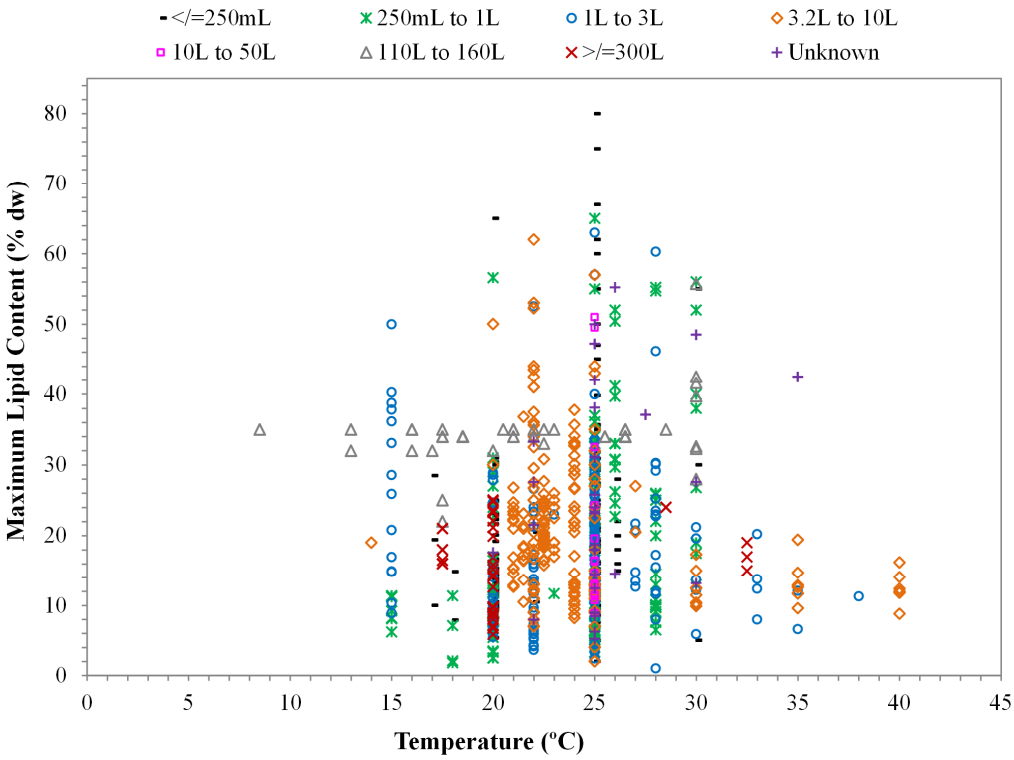

Figure 10. Maximum lipid contents of 99 algae species as affected by temperature and culture volume
The following data sources were used to make this graph: [4], [14], [31], [58], [59], [78], [82], [91], [92], [97], [101], [103], [104], [105], [106], [108], [112], [115], [118], [119], [120], [124], [125], [126], [128], [129], [133], [134], [137], [138], [139], [143], [144], [147], [162], [163], [164], [171], [172], [173], [174], [175], [176], [177], [178], [179], [180], [181], [182], [183], [184], [185], [186], [187], [191], [199], [202], [203]

Figure 10 shows the MLCs of 99 microalgae species grown at a variety of temperatures ranging from 8.5-40 °C. The most common temperature is 25 °C. The largest cultures (≥300 L) have lipid contents between 5.9-25% dw MLC at a range of temperatures from 17.5-32.5 °C. The smallest cultures (≤250 mL) have the highest lipid contents;

furthermore, seven of the top 10 MLCs were from cultures <1 L. The efficiency of small cultures could be a result of improved mass transfer of nutrients or light intensity within the small-scale cultures as compared to larger cultures. The highest MLCs generally occurred from 20-30 °C, with the highest MLCs for several species occurring at 25 °C. Within the dataset, only *Chlorella* cultures were grown above 35 °C, and MLCs were reduced to ≤16.2% dw compared to 63% dw reached at 25 °C. Most of the MLCs >50% dw were obtained using fluorescent lamps.

Temperature control is of additional importance in outdoor cultures. Outdoor ponds in the desert have ample sunlight but regularly reach such low nightly temperatures that consistently high algae productivities are not possible without additional temperature controls [17]. Temperature also affects lipid composition of many algae species. Low temperature growth increases fatty acid unsaturation in *Dunaliella salina* [10] and EPA content in *Skeletonema costatum* [11].

3.5. Culture Volume Effects on Algae Growth and Lipid Contents

Laboratory scale microalgae experiments are commonly performed to assess effects of environmental factors on growth rates and lipid contents. Figure 11 shows SGRs obtained at different culture volumes from 10 mL to 12,000 L. It clearly shows that most experiments are performed on cultures of less than 1 L volume, and there is comparatively little data about cultures over 10 L. Small-scale experiments are often used to predict scaled-up results on large-scale for life cycle analyses or production predictions [70]. However, Figure 11 indicates that small-scale results may not translate well when scaled up for pilot or industrial scale growth. This observation points to concerns about the usefulness of models developed on scales below 10 L being used to predict algae growth in large-scale reactors. Similar concerns have been noted in previous reviews [36]. These considerations indicate that there is a great potential for future research in developing

models from larger volume cultures. Chapters 5 and 6 include models developed using a range of culture volumes spanning most of the range shown in Figure 11.

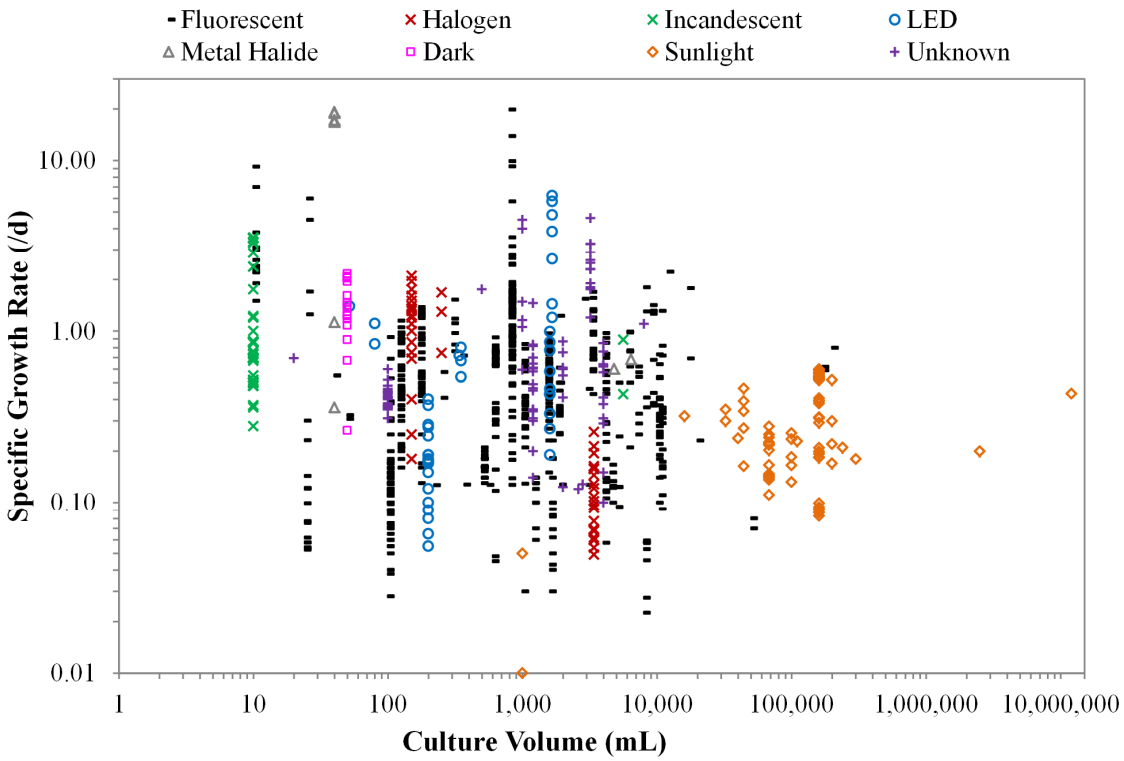

Figure 11. Specific growth rates of 91 algae species by culture volume and light source
This graph includes data from the following sources: [14], [23], [27], [38], [61], [87], [88], [89], [91], [96], [97], [98], [99], [100], [101], [102], [103], [104], [105], [106], [107], [108], [109], [111], [112], [113], [114], [115], [116], [117], [118], [119], [120], [121], [122], [123], [124], [125], [126], [127], [128], [129], [130], [131], [132], [133], [134], [135], [136], [137], [138], [139], [140], [141], [142], [143], [144], [145], [146], [147], [148], [149], [150], [151], [152], [153], [154], [155], [156], [157], [158], [159], [160], [196], [197], [199], [200], [201], [204]

Goldman [36] summarized the beginnings of algal mass culture research from 1951 to 1977 and found that 4-200,000 m^2 cultures yielded an average of 2-27 g m^{-2} d^{-1} algae. Nearly all of these cultures were *Chlorella*, *Scenedesmus*, or unnamed diatoms. Of the 33 mass cultures Goldman [36] studied, only 9 were >100 L and only 5 were >10,000 L. This review covers different, more recent studies on a wider range of algae species, but the data in Figure 11 also show the limited availability of large-scale data. Only 59 of the 1,001 cultures in this dataset are ≥100 L and only 2 are ≥10,000 L. Very little data are available at scales between 300 L and industrial scale levels. Goldman [36] also noted that all but two of the cultures in his review were from relatively small outdoor research facilities.

Microalgae SGRs are largely affected by the culture volume used. Figure 11 shows that the ≤1 L culture volumes tend to have the highest SGRs. This may be due to reduced mass transfer concerns on such small-scales. Also, small-scale cultures tend to lack dark zones, so they have better light passage through the system than large-scale cultures. When growing *Chaetoceros calcitrans* in 2.8 L and 170 L airlift PBRs, similar light intensities produced lower growth rates in the larger PBR [61]. In addition, small-scale cultures are likely to have been grown under extremely well controlled conditions of sterility and temperature.

To determine whether outdoor and laboratory cultures showed significant differences, the two culture types were compared. Outdoor cultures encompass those listed as outdoors, in raceway reactors, in open ponds, or using sunlight as a light source. The median SGR for these 81 cultures was 0.26 d^{-1} in culture volumes ranging from 1-12,000 L. The median SGR from the 920 remaining cultures (termed laboratory cultures) was 0.48 d^{-1} in culture volumes from 10 mL to 200 L. The outdoor culture SGR data encompassed 10 species, while the laboratory culture data contained 90 species (including 9 of the outdoor culture species). Meanwhile, the median of the 76 MLCs for the outdoor cultures was 34% dw with a range from 5.7-55.7% dw in cultures from 1-12,000 L. The 720 laboratory cultures had a median MLC of 16.3% dw with a range from 1-80% dw for cultures from 30 mL to 350 L. The median indoor culture SGR was higher than the median outdoor culture SGR, but the median outdoor MLC was higher than the median indoor MLC. A higher average MLC in outdoor cultures has also been found previously [85]. It is likely that the difference in lipid content is species specific because the outdoor cultures contained data on only 8 species, which were also included in the 97 species in the laboratory cultures group.

Fluorescent tubes are by far the most commonly tested light source in Figure 11;

however, many papers do not cite the light source used. The cultures grown in sunlight tended to have lower SGRs than those grown with fluorescent tubes. Sunlight was the main light source for the large-scale experiments. Even with lower SGRs, large-scale algae cultures can be used for wastewater treatment while providing a side revenue stream or producing biofuel to offset wastewater treatment plant needs. The larger volume, sunlit cultures' SGRs were likely affected by diurnal light fluctuations that resulted in periods of photoinhibition due to extremely high light levels and photolimitation due to periods of low light levels near dawn and dusk. Along with diurnal fluctuations, seasonal fluctuations may be significant. Outdoor cultures grown from October to November in Nanjing, China showed significant decreases in biomass productivity as temperature and light levels decreased in November [192]. Other outdoor culture light fluctuations were discussed in Section 3.3.

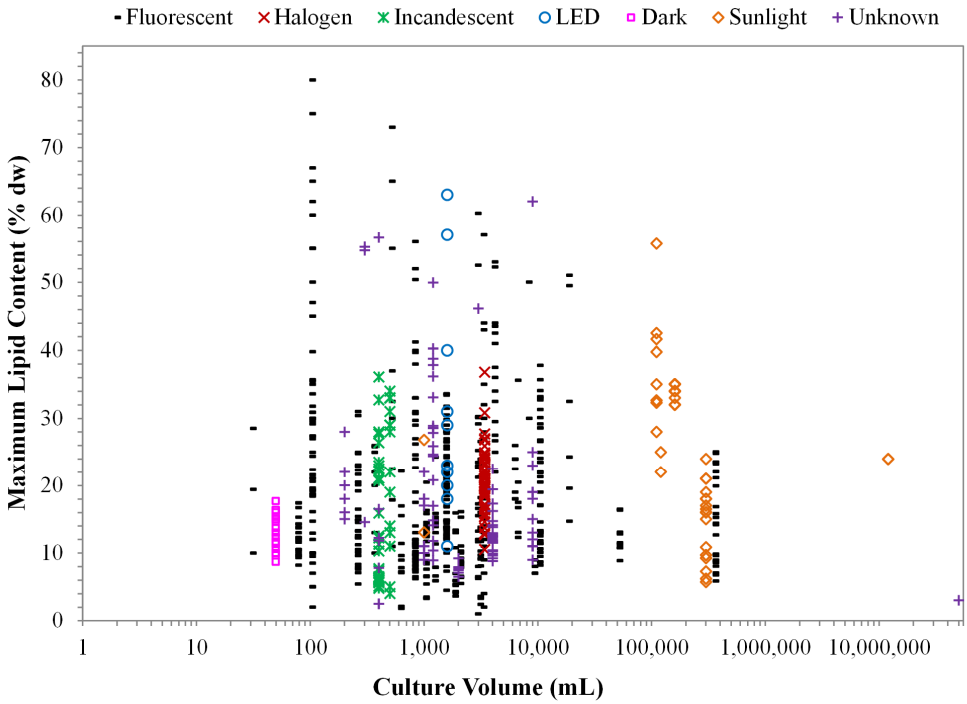

Figure 12. Maximum lipid contents of 97 algae species by culture volume and light source
This graph includes data from the following sources: [4], [14], [31], [58], [78], [82], [91], [92], [97], [101], [103], [104], [105], [106], [108], [112], [115], [118], [119], [120], [124], [125], [126], [128], [129], [133], [134], [137], [138], [139], [143], [144], [147], [155], [171], [172], [173], [175], [176], [177], [178], [179], [180], [181], [182], [183], [184], [185], [186], [187], [188], [189], [190], [191], [199], [203], [205]

Figure 12 shows MLCs of 97 algae species grown at different culture volumes. Most data were available for cultures between 1-3 L. The highest MLC values were from 100 mL and 500 mL cultures. The majority of the MLCs were between 5-40% dw from 30 mL to 350 L. Dark cultures had lower MLCs than any light source type.

Several sunlit cultures >110 L had 30-40% dw MLCs. In Figure 12, higher MLCs were produced in small volume, fluorescent tube cultures than in larger sunlit cultures. Similarly, the marine microalga *Pavlova viridis* produced lower total lipid contents in 60 L outdoor tubular PBRs than in 3 L indoor tubular PBRs [192]. Also, outdoor November cultures had significantly reduced lipids compared to outdoor October cultures, which had higher temperature and light levels [192]. Very few industrial scale data were available.

One major trend identified in this review is that culture volume has a major impact on SGR for a wide variety of algae species. Smaller cultures were consistently found to produce higher SGRs. This result is likely due to increased mass transfer within a small liquid volume. This effect may be due in part to the simple internal construction of small containers like test tubes, flasks and bottles compared to more complicated algae growth containers needed for large-scale cultures. These construction differences mean small-scale containers are likely to have different mixing methods than large-scale cultures. Many small-scale cultures are mixed with hand swirling or bubbling, while large-scale cultures are more likely to be paddlewheel mixed. Additionally, small containers are likely to have less area for cell shading, although this effect will depend upon the cell density within the container. Furthermore, small containers are easier to keep sterile and allow improved temperature control. These variables complicate scale-up and reduce the reliability of large-scale production estimates based on small-scale experiments.

This finding is significant because it implies that algae growth models developed from small-scale experiments, especially those <1 L volume, may not be reliable predictors for

algae growth on a large-scale, even if the same species, temperature, and light intensity are used. Additional factors inherent in large-scale production, such as salinity changes from evaporation, wash out from flooding, lack of control over sterility, temperature and light, will further increase the unreliability of models developed from lab scale experiments. This finding also implies that overcoming mass transfer limitations within large-scale cultures will significantly increase their algae production potential.

3.6. Algae Growth and Lipid Contents as Affected by Gas Flow Rate and Carbon Dioxide

Algae cultures are often sparged to mix cells, provide CO_2 and remove O_2. Thorough mixing is essential to evenly distribute nutrients, heat, gas, and light throughout the reactor chamber and to prevent dead zones from forming within the reactor. This is especially important in dense cultures, where the media flow environment is more constrained. As gas is added to the reactor, the gas pressure creates turbulence to reduce biomass settling and to aid mass transfer within the reactor. The amount of energy needed for mixing depends in part upon the density difference between the algal cells being suspended and the reactor media used. Sparging is commonly used, but many studies fail to provide information on gas flow rates.

Figure 13 shows the SGRs of algae grown with different gas flow rates. Most of the experiments were performed with a gas flow rate of 0.6-1.4 L L^{-1} min^{-1}. Generally, the highest SGR at each gas flow rate increased as gas flow rate increased up to 1.6 L L^{-1} min^{-1} and then decreased. This trend was also noted by Sanchez Miron et al [22], who explained it as increased agitation improving light-dark cycling within light limited cultures. The decreased SGRs at higher gas flow rates may be due to increased shear stress. Barbosa et al [206] examined shear stress effects and found increased cell death above 30 m s^{-1} for *Dunaliella salina* and above 50 m s^{-1} for *Dunaliella tertiolecta*. They determined that bubble formation at the sparger caused significantly more cell death than bubble rising or

bursting and recommended using larger nozzles [206].

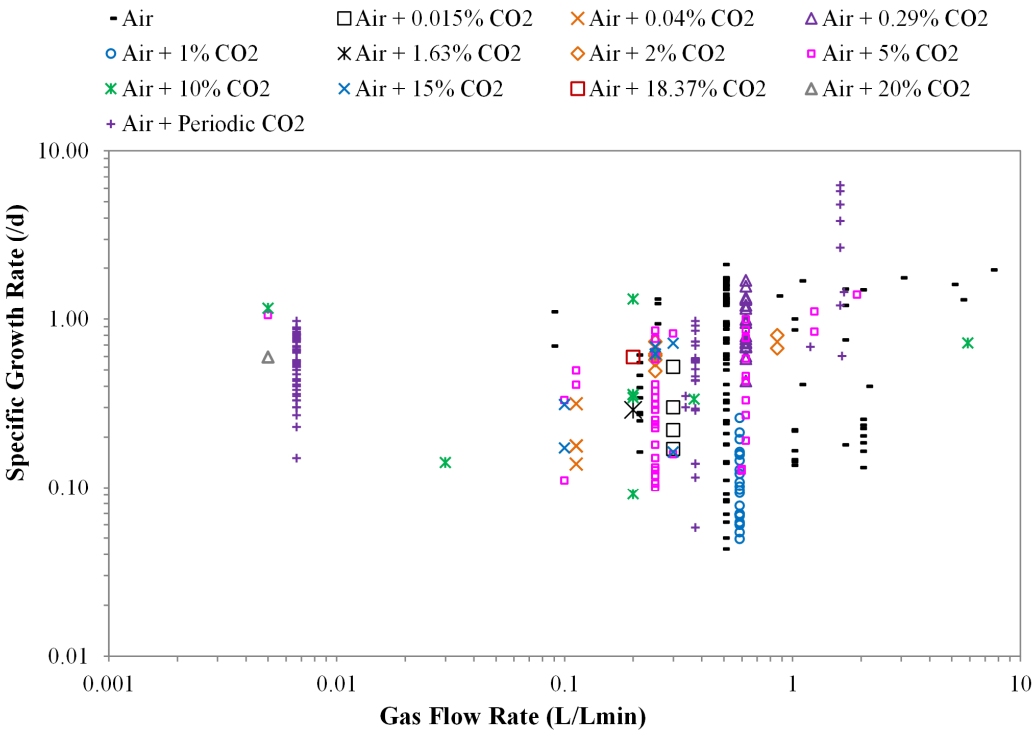

Figure 13. Specific growth rates for 50 algae species by gas flow rate and gas composition
This graph was produced using data from these studies: [27], [61], [91], [96], [98], [102], [105], [106], [107], [109], [110], [117], [118], [120], [123], [129], [130], [131], [132], [133], [134], [137], [138], [139], [141], [143], [144], [145], [146], [147], [148], [153], [156], [157], [204]. When necessary, the gas flow rates were converted by dividing the gas flow rate in L min^{-1} by the culture volume in L.

Attempts to increase algal productivity have included CO_2 supplementation, which has the added benefits of CO_2 sequestration and pH control. In the US desert, several 1,000 m^2 open ponds demonstrated that injected CO_2 could be used with >90% efficiency so long as the physical setup and pH were carefully controlled [17]. In this setup, single day algae productivities up to 50 g m^{-2} d^{-1} were achieved [17].

All algae species have an optimum pH range for growth. As algae grow, they consume CO_2, which increases the culture pH. Once pH levels rise above 9.5, growth is inhibited in most green, red, and brown algae [207]. A few algae are able to grow at pH levels above 9.5, such as *Spirulina* [20] and *Corallina* [207]. Around the pH of seawater, 7.2-8.2, CO_2 is predominately in the form of bicarbonate (HCO_3^-) ions [208]. At pH levels > 9, the predominant CO_2 form switches to carbonate (CO_3^{2-}) ions [208]. This reduced growth

may be due to reduced bioavailability of CO_3^{2-} ions. Figure 13 shows that CO_2 additions have covered a large range from 0-20%.

CO_2 is necessary for photosynthesis, so it may be predicted that higher CO_2 concentrations would increase SGRs until pH is reduced substantially. In Figure 13, the cultures with the highest CO_2 addition levels, those ≥15% CO_2, failed to achieve SGRs over 1 d^{-1}. At 20% CO_2 supplementation, *Thalassiosira weissflogii* growth rate was greatly decreased compared to growth under 0-10% CO_2 supplementation [98]. It is possible that the high CO_2 additions reduced the culture pH below optimal levels. In a study on *Nannochloropsis oculata*, as CO_2 levels increased from 2-15%, pH levels decreased from 7.8 to 7.0 [106]. A similar trend was found using *Chlorella* sp cultures, where CO_2 levels increasing from 2-15% produced corresponding pH decreases from 7.6 to 6.8 [105]. Along with affecting growth rates, pH changes affect how cells behave within a reactor. *Pleurochrysis carterae* and *Emiliania huxleyi* were grown in saltwater at several pH levels but, when pH was reduced to 7.4 for *Pleurochrysis carterae* and 7.2 for *Emiliania huxleyi*, the cells started to clump and stick to the PBR walls such that semicontinuous culture could not be maintained [14].

Algae growth is also considered as a CO_2 sequestration method. Cultures with 5% and 10% CO_2 additions reached SGRs of 1.39 d^{-1} and 1.31 d^{-1} respectively. Additional CO_2 may be sequestered by altering the culture procedures. When high density *Chlorella* sp cultures were pre-adapted to 2% CO_2 and then grown at 10% and 15% CO_2 concentrations, the cultures grew quickly [105].

Figure 13 also shows data from several experiments that added CO_2 periodically to maintain culture pH levels. Air with periodic CO_2 additions provided the highest SGRs; of these, 1.63 L L^{-1} min^{-1} aerated cultures had the highest SGRs. Generally, this dataset does not show CO_2 addition greatly increasing SGRs over air alone. Even so, it should be noted

that most studies showing CO_2 addition for pH maintenance do not report the amount of CO_2 added. Also, the results of CO_2 addition may be species specific. *Thalassiosira weissflogii* grown under CO_2 supplementation from 0-10% showed no significant change in growth rate [98]. Furthermore, it is possible that the cultures for which there are gas flow rate and CO_2 addition data were limited by other factors, such as provision of nutrients, temperature, or light intensity. It is also important to note that evaporation is a major consideration when growing algae cultures, especially bubbled cultures. Increased gas flow rates tend to increase media lost due to evaporation. Evaporation effects and how they were overcome were generally not reported, so these data may be biased by unreported salinity changes within the marine cultures in the dataset.

Figure 14 examines whether gas flow rate has a noticeable effect on cells of different sizes. The cells were grouped by size class with 0.2-2 μm as picoplankton, 2-20 μm as nanoplankton, 20-200 μm as microplankton, and 200 μm-2 mm as mesoplankton. The highest picoplankton SGRs were obtained at a gas flow rate of 1.67 L L^{-1} min^{-1}. Nanoplankton was the most common size class in the dataset, and SGRs >1 d^{-1} were achieved at gas flow rates from 0.005-5.1 L L^{-1} min^{-1}. These observations follow the expected results that the smallest cell size groups can be well mixed at low gas flow rates. This dataset contains only one mesoplankton value and comparatively few microplankton values, so it is unclear if these species require higher gas flow rates. The optimal gas flow rate range is 0.5-3 L L^{-1} min^{-1}, but this range may differ depending upon bubble size, reactor layout and sparger hole spacing.

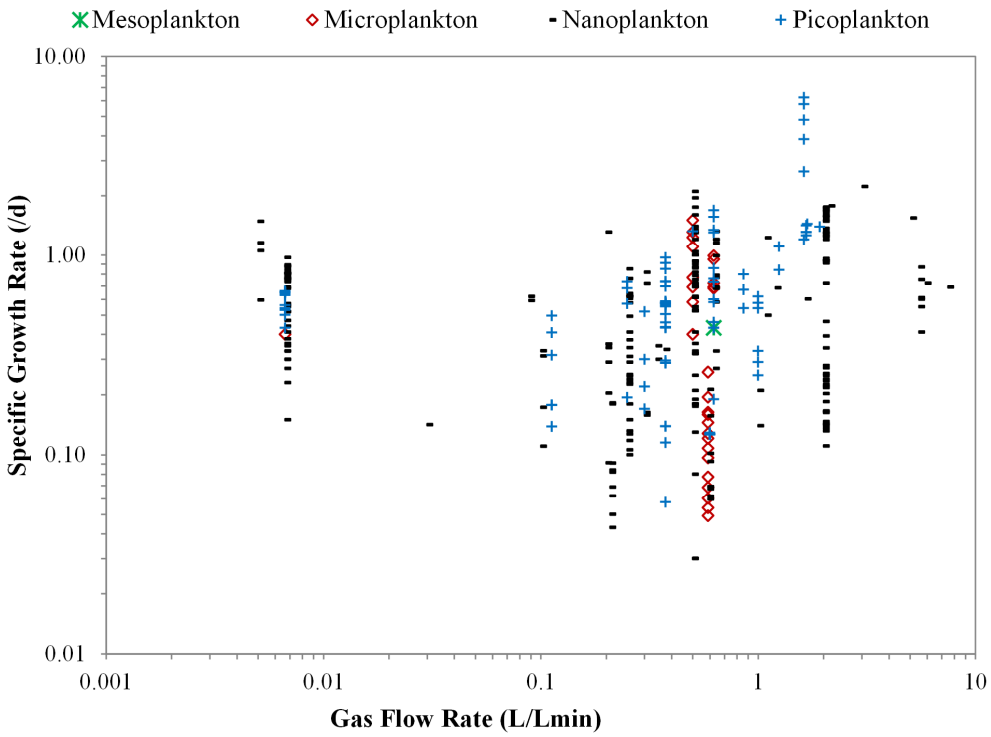

Figure 14. Specific growth rates of 50 algae species by gas flow rate and cell size
This graph includes data from the following publications: [27], [61], [91], [96], [98], [102], [105], [106], [107], [109], [110], [117], [118], [120], [123], [129], [130], [131], [132], [133], [134], [137], [138], [139], [141], [143], [144], [145], [146], [147], [148], [153], [156], [157], [204]

The highest MLCs in Figure 15 were >60% dw, and they were obtained with air + 5% CO_2, air, and air + periodic CO_2 addition; these lipid contents were produced using gas flow rates from 0.02-0.6 L L^{-1} min^{-1}. All MLCs >50% dw were produced using 0.02-1.5 L L^{-1} min^{-1} flow rates. This indicates that lower gas flow rates are sufficient, which should reduce power consumption of large-scale cultures. The highest CO_2 additions of 10% and 15% produced MLCs from 9-33% dw. The highest gas flow rate, 5.5 L L^{-1} min^{-1}, produced low lipid contents from 6.5-9.2% dw. When the data were grouped by size class and examined, it was clear that the >35% dw MLCs occurred in picoplankton and nanoplankton. The mesoplankton produced the lowest MLCs as a group; these MLCs ranged from 4-9.6% dw.

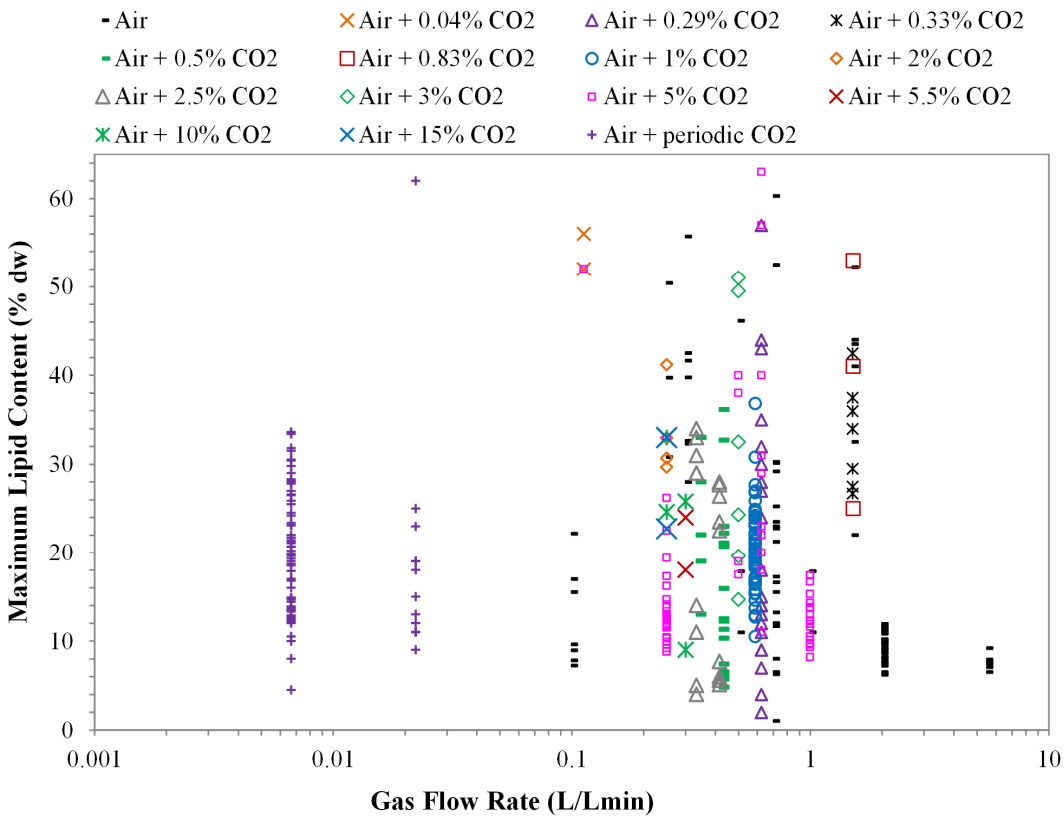

Figure 15. Maximum lipid contents of 67 algae species by gas flow rate and type
This was produced using data from: [4], [58], [91], [105], [106], [118], [120], [129], [133], [134], [137], [138], [139], [143], [144], [147], [172], [173], [174], [176], [177], [178], [179], [181], [182], [203]

Relatively few gas flow rate data were available in the 116 publications included in this chapter. Low gas flow rates were sufficient to high SGRs and high lipid contents. Supplementing sparger gas with CO_2 did not significantly increase the SGRs.

3.7. Algae Growth in Various Reactor Types

Algae are grown in a wide variety of containers covering a range of volumes from test tubes to raceway ponds. These open reactors and PBRs are summarized in Figure 16. The highest SGRs occurred in flat plate and turbidostat reactors at volumes ≤800 mL. Specifically, the highest SGRs occurred around 22 °C in *Chlorella vulgaris* and *Nitzschia closterium* cultures. All of the SGRs ≥2.3 d^{-1} occurred in turbidostats, flat plate PBRs, test tubes, flasks, and bottles. Each of these cultures were grown at volumes ≤3.2 L; the only exceptions were 6 SGRs from 2.3-4.5 d^{-1} grown in undisclosed containers of either 1 L or unreported volumes.

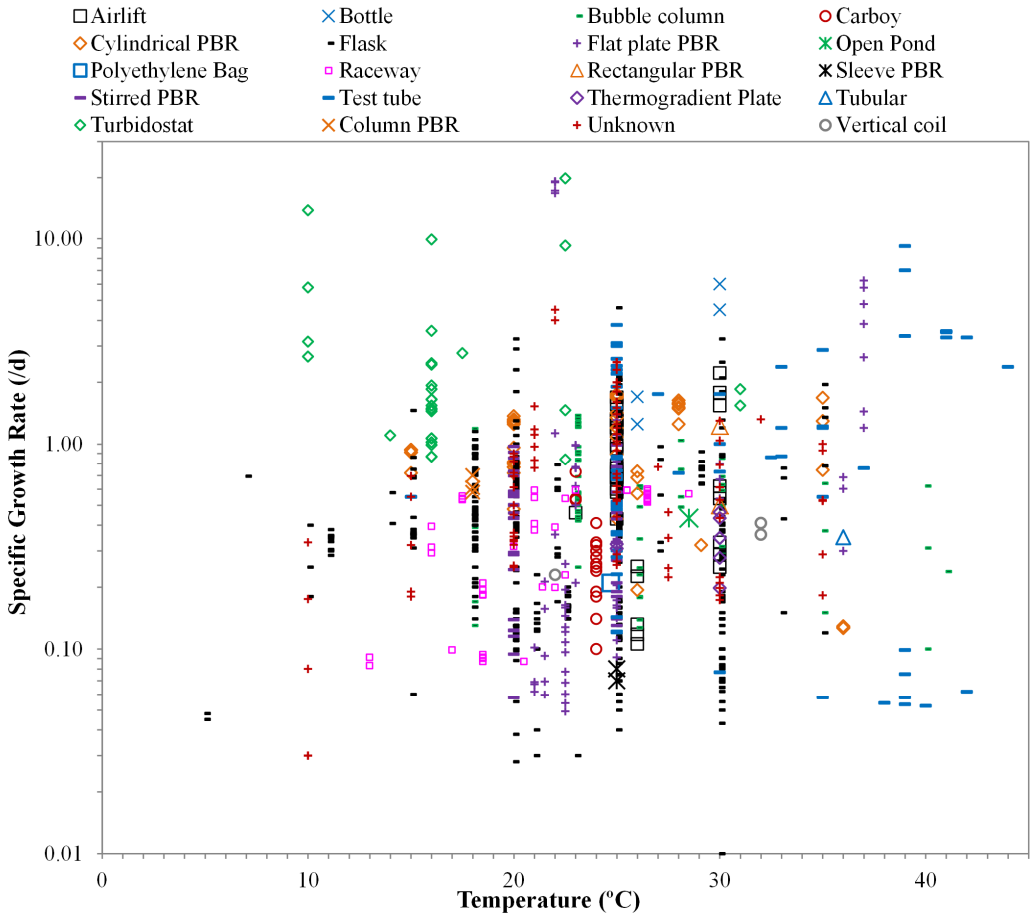

Figure 16. Specific growth rates of 100 algae species by temperature and reactor type
This figure was produced using data from the following sources: [14], [23], [27], [38], [61], [87], [88], [89], [91], [96], [97], [98], [99], [100], [101], [102], [103], [104], [105], [106], [107], [108], [109], [110], [111], [112], [113], [114], [115], [116], [117], [118], [119], [120], [121], [122], [123], [124], [125], [126], [127], [128], [129], [130], [131], [132], [133], [134], [135], [136], [137], [138], [139], [140], [141], [142], [143], [144], [145], [146], [147], [148], [149], [150], [151], [152], [153], [158], [159], [160], [161], [162], [163], [164], [196], [197], [198], [199], [200], [201]

SGRs >2.3 d^{-1} were obtained over a wide range of temperatures from 10-44 °C in 10 mL to 3.2 L cultures. At high temperatures (≥38 °C), test tube cultures produced SGRs up to 9.2 d^{-1}. Meanwhile, at low temperatures, turbidostat cultures of *Tetraselmis* sp achieved SGRs of 13.9 d^{-1} (10 °C) and 9.9 d^{-1} at (16 °C).

Raceway and open ponds were the only reactors to reach culture volumes >240 L. The cultures grown in these pond types were all between 0.08-0.6 d^{-1}, although the temperature ranged from 13-28.5 °C. These relatively low SGRs in raceway ponds match calculations like those by Chisti [3] who calculated volumetric biomass productivities of a closed tubular PBR and a racetrack facility and found that the closed PBR was 13 times more

productive. There are several possible reasons for the reduced productivity in large volume ponds. These include light and mass transfer limitations, and large volume ponds have increased salinity due to evaporation over a large surface area. The raceway and open ponds in this dataset contained from 110-12,000 L, but the highest SGRs were obtained at 160 L.

Bubble columns with culture volumes ranging from 170 mL to 170 L produced SGRs from 0.1-1.38 d^{-1}. Column PBRs from 220 mL to 200 L produced slightly higher SGRs ranging from 0.13-1.75 d^{-1}. Airlift columns were larger and showed increased SGRs of 0.11-2.22 d^{-1} in cultures from 2.8-170 L.

Each reactor type has advantages and disadvantages. Bubble columns, airlift reactors, and flat plate reactors have better O_2 removal efficiencies than tubular reactors. The short light path that occurs in a flat-plate PBR gives it a uniform light distribution. Bubble-column and airlift reactors are easier to scale-up than other bioreactor types, in part because they have been used for many years in industries such as beer manufacturing. However, these reactors are less efficiently externally illuminated compared to flat-plate, horizontal, and inclined tubular PBRs [21]. This reduced illumination is caused by a combination of the larger reactor diameter needed for efficient gas transfer in a large culture volume and by the large angle relative to incoming solar radiation, which causes a significant fraction of incident solar energy to be reflected off the reactor [8]. Due to this reflection, the reactor surface should be considered. Light reflection and refraction occurs when the light enters the culture medium at a non-normal angle. This means that flat plate and rectangular PBRs experience less reflection and refraction than reactors with tightly curved surfaces, such as tubular PBRs, flasks and test tubes.

Reactor choice may also affect the algae species used. Some species stick in tubular or Biocoil reactors [20], [21]. Also, oleaginous species are likely to have low specific

gravities, so they may be unsuitable for airlift and bubble column reactors due to floating [6]. Species with high specific gravities may be difficult to keep suspended, especially in reactors with dead zones. Also, open reactors are limited to the relatively few algae that require conditions specialized enough to preclude significant growth by competing and predatory species. Such algae include *Dunaliella salina*, which grows well in extremely saline conditions, and *Spirulina*, which grows best with high pH and bicarbonate concentrations [20].

3.8. Other Factors

Along with the variables discussed above, other environmental factors may have significant effects on SGR and MLC. Several of these factors, such as culture age and use of heterotrophic growth, were discussed in Chapter 2. As a culture's density changes, so does its light requirements. This is important to note because algae cultures can be limited by too much or too little light. As a result, some researchers have tested modifying light intensity as a culture develops in a reactor. Sequentially increasing light supply as culture density increases produces increased growth rates compared to cultures grown under constant light [149], [209]. This practice is also likely to increase culturing energy efficiency [149].

Energy efficiency is also strongly affected by the hydrodynamics in the reactor. Bubble size and gas holdup affect light penetration, gas-liquid mass transfer, mixing and shear stress [22]. However, no data were available on gas bubble size distributions, and few gas holdup data were available in this dataset. As such, it was not possible to estimate the efficiency with which the supplied CO_2 was transferred to the culture media.

The growth system operation method is another potentially important parameter to consider. This review includes batch, continuous and semi-continuous operation modes. A previous review of 30 years of algae mass culturing found semi-continuous operation to

be prevalent with only a couple of fully continuous experiments noted [36]. The relative lack of data on continuous systems may be of concern if algae growth is combined with domestic wastewater treatment, which would require continuous operation.

3.9. Conclusions

This chapter shows the effects of several variables including: gas supply, volume, and temperature on algae growth rates and lipid contents. Effects may vary by algae species, but, by combining data from 116 publications, several general trends have been identified.

Light intensity and schedule: SGRs >1 d^{-1} have been achieved at light intensities from 11.6-2,100 μE m^{-2} s^{-1} using all light sources except sunlight. Sunlit cultures tend to experience much higher light intensities than other light sources, and most sunlit cultures have a MLC between 30-40% dw. Optimal light intensities for lipid content production were found to be 25-277 μE m^{-2} s^{-1}. A culture's illumination schedule is also important, although it is often unreported. The majority of artificially illuminated algal studies are performed with either continuous or 12 hour illumination.

Temperature: Algae cultures grew well at all temperatures from 10-44 °C, but the highest SGRs occurred in small cultures around 22 °C. The highest MLCs generally occurred from 20-30 °C, with the highest MLCs for several species occurring at 25 °C.

Culture volume and reactor type: Culture volume has a major impact on SGR for a wide variety of algae species. Smaller cultures consistently produced higher SGRs. Most experiments are performed on cultures of less than 1 L volume, and there are comparatively little data on cultures over 10 L. This dataset indicates that small-scale results do not translate well when scaled up for pilot or industrial scale growth. All of the SGRs ≥2.3 d^{-1} occurred in PBRs and lab experiments. Raceway and open ponds were the only reactors to reach culture volumes >240 L, and these reactors had SGRs ≤0.6 d^{-1}.

Gas flow and CO_2: Sparging is commonly used to mix cultures and supply CO_2, but relatively little gas flow rate data are reported. Overall, lower gas flow rates were sufficient for high SGRs and MLCs, which should reduce power consumption in large-scale cultures. Also, this dataset does not show CO_2 addition greatly increasing SGRs over air alone. However, air with periodic CO_2 additions for pH control provided the highest SGRs. Another major consideration in bubbled cultures is evaporation.

Data reporting: There is a substantial algae growth and lipid content dataset available in published literature. However, comparing studies is difficult because a wide variety of data formats are commonly used, and many experimental setup parameters are under-reported. The usability of data from future studies can be improved by agreeing upon widely accepted standards for data reporting. To this end, a recommended set of culturing parameters and formats has been provided in Table 4.

Chapter 4. Microalgae Species Choice Considerations for Large-scale Growth: Cell Size, Grouping, Flagellates, Lipid Contents, and Productivity Trade-offs

Algae culturing depends on many factors. Effects of several culturing parameters were discussed in Chapter 3 with an emphasis on overall trends among microalgae. However, several species specific considerations also affect algae culturing. These include factors that may affect hydrodynamics, such as cell size and presence of flagella, and the potential to increase lipids under nutrient limitation. These topics are discussed within this chapter.

Additional details on the usefulness and uniqueness of the review in this chapter are provided in Section 4.1. Section 4.2 outlines the building of the database used for this review. Several important characteristics to consider when choosing a species for large-scale production are detailed in Section 4.3. Cell sizes and effects are specified in Section 4.4, which also provides cell lengths for 146 microalgae species. Then, Section 4.5 discusses the effects of nutrients on lipid contents in 75 marine and 31 freshwater species. Section 4.6 looks at lipids by algae Class, and Section 4.7 examines algae lipid productivity as affected by light intensity and culture volume. In Section 4.8, trade-offs are studied between lipid productivities, MLCs, biomass productivities, and SGRs. Next, Section 4.9 covers flagellate algae because they can actively move within a reactor. Finally, several trends particularly worth highlighting are summarised in Section 4.10.

4.1. Usefulness of this Chapter

Microalgae SGRs and MLCs can be enhanced by controlling a variety of culturing parameters as discussed in Chapter 3. However, successful large-scale microalgae growth requires careful species choice considering a variety of characteristics like those detailed in Table 5. This chapter graphically combines data from 131 publications on 128 microalgae species to provide a broader understanding of many algae characteristics. These include cell size, grouping, and presence of flagella, which may all affect movement of cells within a reactor. In addition, cell size information is provided for 146 species. Lipid contents are

provided for 31 freshwater and 75 marine species with nutrient limitation effects included for most species. Potential effects of culture volumes and light intensities are shown on lipid productivities. In addition, possible trade-offs between lipid productivity, biomass productivity, MLC, and SGR are discussed.

Microalgae research has progressed significantly since the first algal mass culture studies were performed in the 1950s. Microalgae are now cultured to produce many high value products including EPA, DHA, astaxanthin, and β-carotene. Many reviews discuss these and other high value products along with general algae mass culturing [11], [20], [210], [211]. Algae biodiesel is also commonly studied with a particular focus on identifying optimal algal species for production [118], [212]. Although these reviews contain information from many sources, the information is often convoluted. They tend to be verbal summaries with occasional tables of previous research. This chapter takes an alternative, visual approach. It coves many topics, and it will be particularly helpful for researchers new to the field who want to gain a quick understanding of many aspects of microalgae useful in culturing. Reviews presenting data graphically are rare, but a few exist that display species averaged data [5], [85]. Along with species averaged data, this chapter presents several parameters as individual experimental results, which gives a more accurate assessment of the data spread.

4.2. Methods

The database discussed in Section 3.2 was expanded to include additional characterizing data for each species. The additional data include Class, water type (freshwater or saltwater), cell grouping, cell morphology, and cell dimensions. Much of the information was available within the publications themselves, but when absent the missing data were obtained from major online algae databases, algae identification textbooks, and published works on algae physiology. The online databases used were the

Provasoli-Guillard National Center for Marine Algae and Microbiota (NCMA Provasoli-Guillard), University of Texas at Austin Culture Collection (UTEX), Culture Collection of Algae and Protozoa (CCAP), Australian National Algae Culture Collection of the Commonwealth Scientific and Industrial Research Organization (CSIRO), Protist Information Server, and the European Diatom Database. Each figure is captioned with references to the data sources used to generate it.

Conversions and assumptions were discussed in Section 3.2, along with limitations within the dataset. Some figures required the use of averaging or max/min functions to consolidate the data as a species average, maximum or minimum; such data treatments are noted in the respective figures and text. Also, algal taxonomy has changed a lot over the time period included in this dataset. Species names were updated using the most recent strain numbers in databases and publications [85], [93], [94]. Some example name changes are *Ettlia oleoabundans* instead of *Neochloris oleoabundans* and *Skeletonema costatum* instead of *Skeletonema marinoi*. Also, a few species live in saline or hypersaline environments, and these species were grouped with marine species within this chapter.

4.3. Choosing Algae Species

Algae are mass cultured for a variety of purposes. When considering industrial scale growth, algae species choice is one of the most important decisions to be made, and it requires consideration of a large number of parameters. These parameters cover both overall strain behaviours and physical properties of the cells. To illustrate, desirable properties when choosing an algal species for biodiesel production are shown in Table 5. Many of these same considerations apply to algae mass culturing for any purpose.

Table 5. Desirable properties in choosing algae species for biodiesel production

Desired Properties	**Reasons Desirable**
Overall Strain Properties	
Robust and flexible strain	Able to survive environmental fluctuations, especially if culture is grown outdoors
High productivity	To reduce footprint of the algae growth plant
Reasonably high natural oil content	Higher lipid contents increase biomass processing efficiency
Quick growth rate	Doubling 1-3 times/day increases productivity
Accumulates lipids under nutrient deficiency	Can then use nutrient starvation near harvest time to increase the % lipids
Temperature optimum near that available at proposed culture facility	Will reduce costs of cooling/heating the culture
Able to grow well at a range of temperatures and salinities	This will reduce the impacts from fluctuations that occur within the facility
Able to resist shear stress from mixing	To reduce cell breakage during culture mixing
Little sticking or clumping	To reduce cleaning costs and reduce possibility of undesirable cell settling
Grows in seawater or recycled fresh water	To reduce possible water shortages and environmental impacts
Able to dominate outdoor cultures over extended periods	To handle interspecies contamination likely to occur within an outdoor culture
Responds reliably to flocculation attempts	To reduce harvesting costs
Relatively easy to grow	To reduce operational problems and costs
Physical Properties of the Cell	
Appropriate lipid composition	May need lipids from a mixture of species to get proper composition for biodiesel production
Stable lipid composition	A lipid composition that does not fluctuate wildly by the cell's life cycle stage will increase predictability of facility output
Low ratio of polyunsaturated fatty acids	A high polyunsaturated fatty acid concentration may necessitate a hydrogenation step in the biodiesel production process
Produce a high-value product in addition to oils	Having a small volume, high cost side product will improve the economic feasibility of the facility
Cell size	Small cells increase harvesting costs
No hard cell wall	Presence of a hard wall is likely to increase processing complexity and costs
No toxin production	To reduce disposal costs and environmental concerns

Some factors should be considered in combination. For example, a combination of high biomass areal productivity and lipid content will result in a high lipid yield per area, which will greatly influence production costs. Meanwhile, high lipid content alone will improve biomass processing efficiency [4]. Another consideration is strain source. The optimal species depends upon the industrial facility's geographic location. Due to the difficulties of maintaining a laboratory selected monoculture for weeks outdoors, the optimum species is likely to be different at each culture facility, and a dominant native species is likely to be the best [17]. The local species can be screened with respect to the characteristics mentioned in Table 5. An algal strain isolated locally may increase culture stability, but it also needs to be able to dominate the culture year-round [4]. Alternatively, a facility may switch between strains to maximize productivity throughout the year [17].

Co-products may increase a facility's economic feasibility. In the short-term, high-value products may provide an important product stream for commercial production of algal biodiesel. Once algal biodiesel production reaches volumes to replace a few percent of total diesel requirements, prices for current high-value products would drop due to their increased availability [41]. However, considering the wide variety of uses for algae discussed in Section 2.2.3.1, it is likely that co-products would remain an important revenue stream for algal biodiesel production. In this case, the algae would potentially produce at least three products: (i) oil, (ii) a high-value product, and (iii) a high-protein cell carbohydrate that can be processed into animal food, gasified for energy production, or fermented for ethanol production. High-value products include nutraceuticals, pigments, and potential medicines as discussed in Section 2.2.3.1. Alternatively, algal biodiesel production could be coupled with wastewater treatment.

4.4. Cell Sizes and Possible Effects

Microalgae have a variety of cell sizes. Cell size data were obtained for 146 algae species. These cells range in size from 1-375 μm, but the median cell length is 9.9 μm.

The small size of many non-motile species enhances their entrainability within turbulent eddies, which may aid the cells in increasing the portion of their life cycles spent within the light section of the water column [213], [214]. Unless motile, larger cells may be more likely to settle within the reactor or to require increased energy for suspension. Motility and cell protrusions are discussed further in Section 4.9. Cell surface area per unit volume varies with cell size, but this ratio can be enhanced by shape deformations from spherical. These deformations can include elongation in one or two planes to form needle or plate shapes, surface convolution, or addition of cellular protrusions like horns or spines. These deformations can improve the cell's likelihood of eddy entrainment, and the increased surface area per volume ratio improves gas and nutrient exchange across the cell surface.

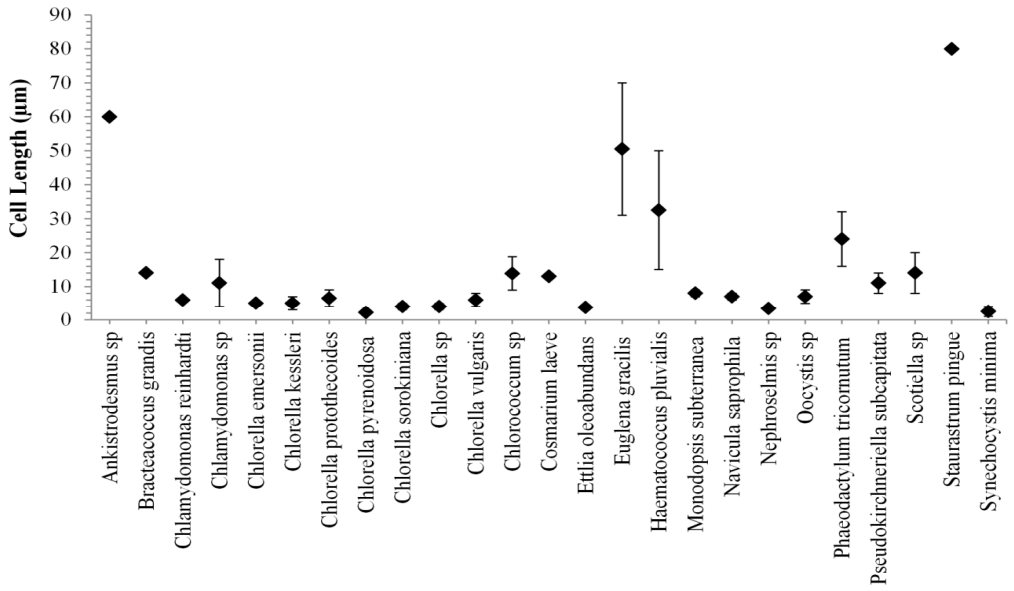

Figure 17. Average and range of cell lengths of 25 freshwater unicellular species
This chart was prepared using data from the following sources: [93], [94], [108], [118], [138], [163], [215], [216], [217], [218], [219], [220], [221], [222], [223]

The majority of algae species in this dataset are unicellular. Figure 17 and Figure 18 show the average and range of cell lengths for 111 unicellular freshwater and marine microalgae species. The length measurements were taken as the longest dimension of each cell. The median freshwater cell length is 7 µm, and the median marine cell length is 9 µm. Open ocean salinity is generally 35 ppt, but seawater salinity can range from trace

near melting glaciers or estuaries to 40 ppt in the Red Sea [213].

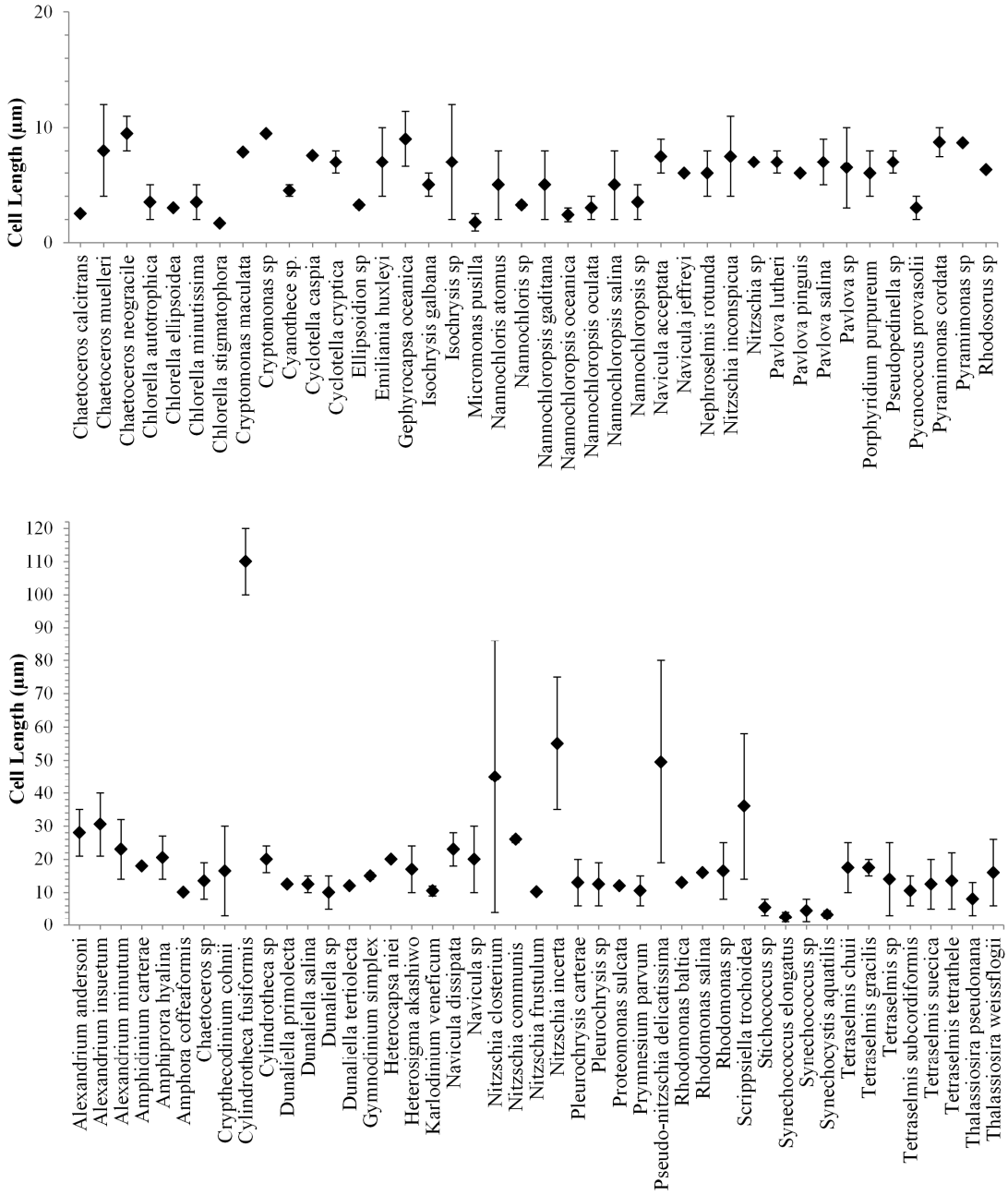

Figure 18. Average and range of cell lengths of 86 marine unicellular species
This graph was prepared using data from the following sources: [4], [61], [82], [88], [93], [94], [103], [108], [112], [118], [125], [128], [138], [142], [147], [157], [163], [164], [216], [218], [224], [225], [226], [227], [228], [229], [230], [231], [232], [233], [234], [235], [236], [237], [238], [239], [240]

Some microalgae exist in a variety of groupings. Many of these groupings are highly structured into certain shapes and specific numbers of cells. A few species tend to group into highly structured short chains of 2, 4, or 8 cells; *Scenedesmus acutus* and *Scenedesmus ecornis* are examples. Other species, such as *Skeletonema costatum*,

regularly form longer chains around 16 cells long. Filamentous algae exist in much longer chains of cells, and these include *Spirulina* sp, *Ulothrix zonata*, and *Oscillatoria* sp. Another common algae grouping is formation of organized colonies. The colony forming species, *Pediastrum*, has individual cells in plate-like structures, while *Volvox* cells form a sphere-like structure. The structured arrangement of these short chains, filaments, and colonies makes it possible for some species groupings to reach volumes of 10^3-10^5 μm^3 while maintaining surface:volume ratios > 1 [213]. As such, the structured groupings of cell chains and filaments help provide their composite cells with advantages of increased size, such as reduced predation, while only slightly increasing settling rates compared to a spherical grouping of the same cell volume. Similarly, the unique arrangements of specific numbers of cells from colonial species can reduce their settling rates below that expected by their volume. For example, *Asterionella* colonies group into 8 cells forming a rimless spoked wheel or into spiral staircases formed by layers of 8 cells [213].

Alternatively, some species' cells aggregate into unstructured clumps. One example is *Botryococcus braunii*, which exudes oils that aid in cell clumping. Other species exude extracellular polysaccharides. Clearly, a species' typical grouping pattern will affect the hydrodynamics of the cells within a reactor and may restrict the growth of some species to certain reactor types. Figure 19 shows the average cell lengths for 35 species of grouped cells. For grouped cells, the length refers to the length of a single cell within the group. The median grouped cell length is 13.8 μm, but the cell lengths range from 2-280 μm. Since they exist in assemblies, grouped cells have a larger apparent surface area than provided by the dimensions of each individual cell.

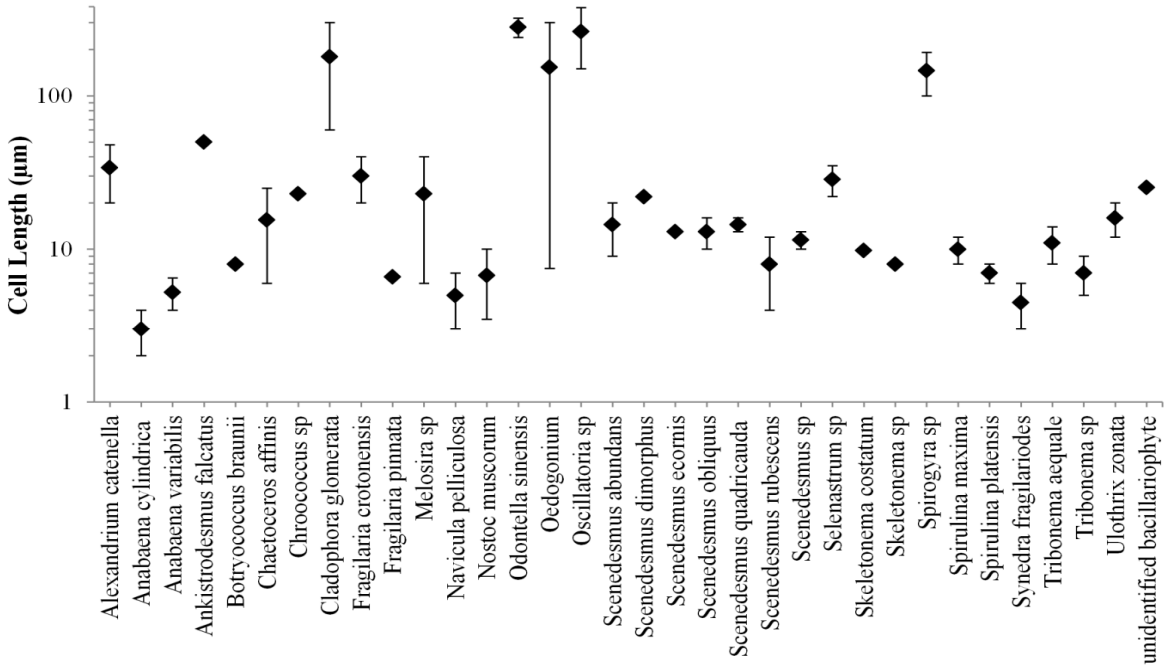

Figure 19. Average and range of cell lengths for the 35 grouped species studied
This chart contains microalgae that exist in clumps, filaments, short chains or colonies of cells. The length measurements are for an individual cell within the grouping. This chart was made with the following data sources: [17], [93], [94], [118], [128], [138], [217], [218], [241], [242], [243], [244], [245], [246], [247], [248]

Within a species, cells can vary in size due to age or environmental conditions. This is indicated by the ranges in Figure 17 to Figure 19. In some cases, only one length measurement was available for a species, so no range was possible. Even so, these figures provide a starting point for cell sizes for a wide range of microalgae species.

SGRs and MLCs in cells of different sizes are examined in Figure 20 and Figure 21 with the dataset grouped by size class. The cultures in this dataset were illuminated with several illumination schedules ranging from 8 to 24 hours. The most common illumination schedules were 24 hours and 12 hours respectively. Furthermore, the cultures were irradiated with light intensities ranging from 11.6-3,270 µE m^{-2} s^{-1}. Both illumination schedule and light intensity may affect SGRs and MLCs. In an attempt to clarify the input from the various light intensity/illumination schedule combinations, a new variable was calculated. It is called the illumination flux, and it includes the light intensity per hour multiplied by the hours/day the culture was illuminated. Figure 20 shows that all size

classes have similar SGRs across a wide range of illumination fluxes. Meanwhile, Figure 21 shows that the smallest algae classes, picoplankton and nanoplankton, have the highest MLCs. However, this dataset contains only a few mesoplankton data.

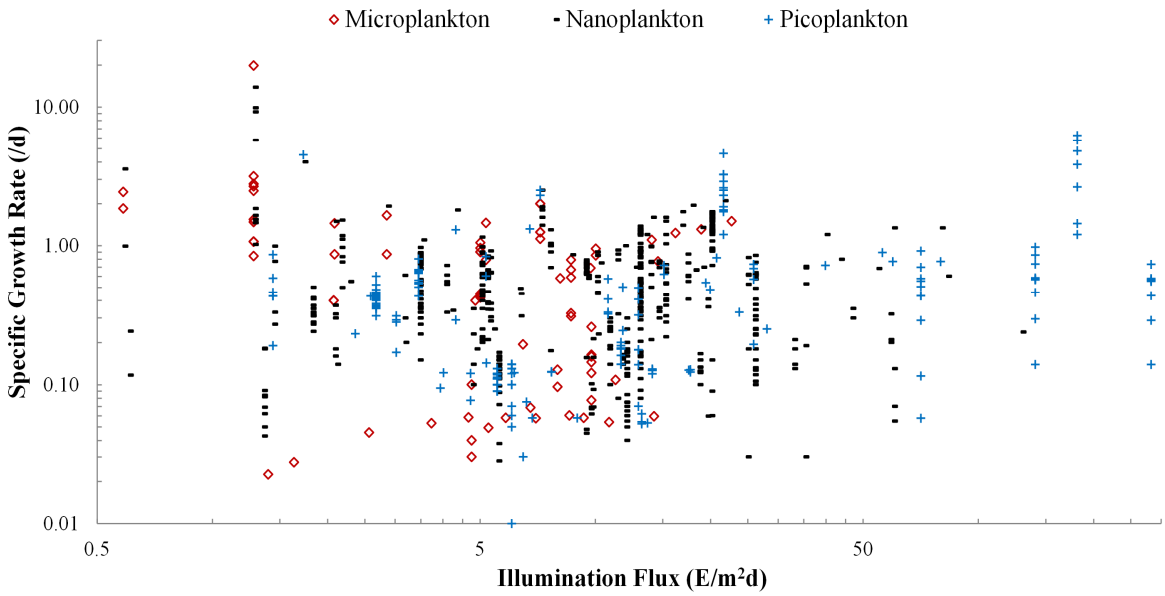

Figure 20. Specific growth rates of 79 species by illumination flux and cell size
This figure was produced using data from the following publications: [14], [27], [38], [87], [88], [89], [91], [97], [99], [100], [101], [102], [104], [105], [106], [107], [108], [109], [110], [111], [112], [113], [114], [115], [116], [117], [119], [120], [122], [124], [125], [126], [127], [128], [129], [130], [131], [132], [133], [134], [135], [137], [138], [139], [140], [141], [143], [144], [145], [146], [147], [148], [149], [151], [152], [153], [154], [155], [158], [159], [161], [162], [164], [199]

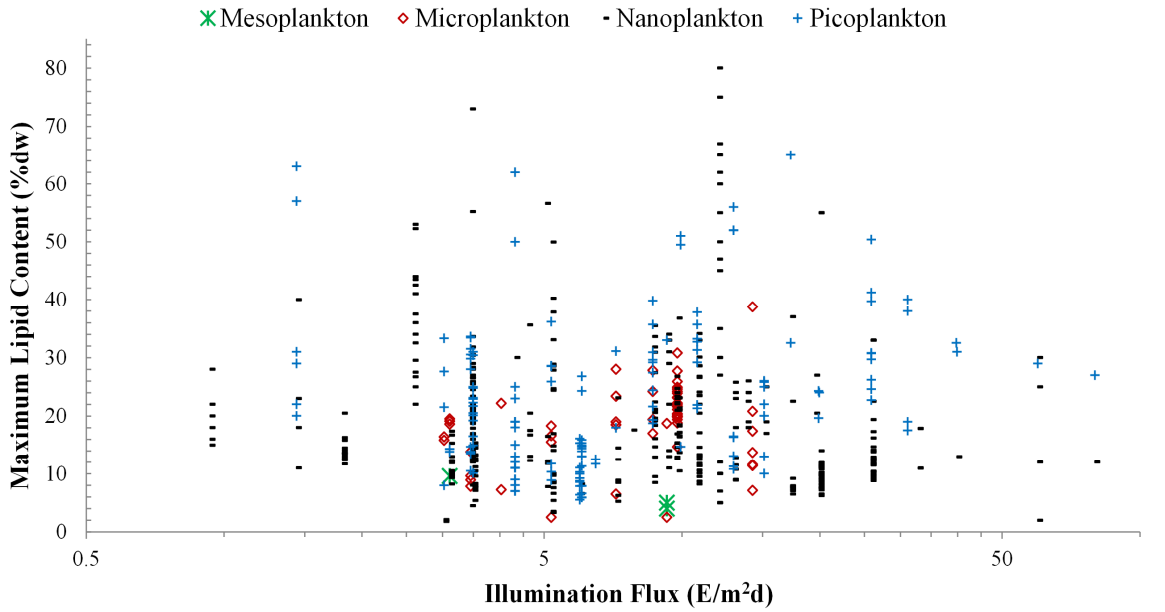

Figure 21. Maximum lipid contents of 85 species by illumination flux and cell size
This graph includes data from the following sources: [4], [14], [58], [59], [91], [92], [97], [101], [104], [105], [106], [108], [112], [115], [119], [120], [124], [125], [126], [128], [129], [133], [134], [137], [138], [139], [143], [144], [147], [155], [162], [164], [171], [172], [173], [174], [175], [176], [178], [179], [180], [181], [182], [184], [185], [186], [187], [188], [190], [199]

Cell size, presence of protrusions like spines, and groupings are all species specific cell properties that can affect cell settling rates. In addition, algal cells appear to have some direct control over their settling rates. Living cells have shown 2-4 times slower settling rates than killed cells of the same species [213]. How cells alter their settling rates is not well understood, but it likely assists cells in settling faster when exposed to negative conditions, such as excessive illumination or nutrient limitation [213]. In addition to settling rates, cell size and groupings may affect the appropriateness of an alga species for large-scale growth in a certain reactor type.

4.5. Nutrient Effects on Lipid Content

Water source is a major concern in large-scale algae culturing. Marine algae may be advantageous for industrial production because of the relative ease of procuring large volumes of saltwater for facilities located near the coast. Also, LCA indicates saltwater species have better energy and greenhouse gas performance than freshwater species in both open ponds and closed PBRs [15]. Even so, use of natural seawater for culturing has a few disadvantages, such as possible pollution in the intake water and the fact that seawater composition varies. On the other hand, freshwater species are preferred for algae production linked with wastewater treatment. This is the case even though LCA shows freshwater systems have lower biomass yields and thus higher land requirements than marine systems [15]. Figure 22 shows that this dataset is biased towards marine species with 75 marine species and only 31 freshwater species. The most common nutrient replete lipid content range is 10-20% dw for both algae types. This is slightly lower than previously found nutrient replete lipid content averages of 22% dw for freshwater and 24% dw for marine species [85].

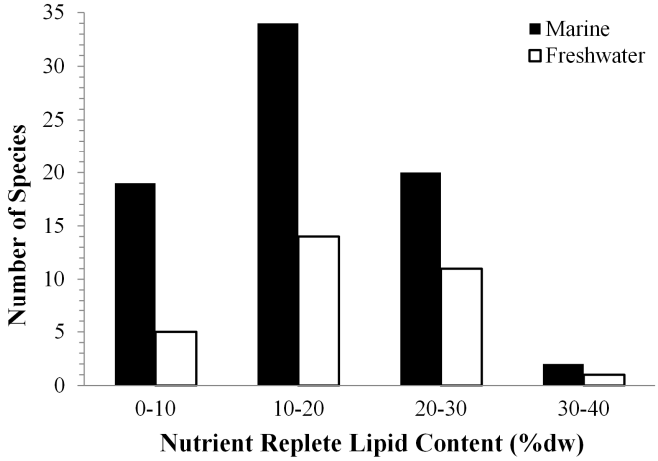

Figure 22. Average nutrient replete lipid contents for marine and freshwater microalgae
This chart enumerates species with average nutrient replete lipid contents falling within the indicated ranges for marine and freshwater species. Data for each species are averaged from these sources: [4], [14], [31], [54], [58], [59], [78], [82], [91], [92], [97], [101], [103], [104], [105], [106], [108], [112], [115], [118], [119], [120], [124], [125], [126], [128], [129], [133], [134], [137], [138], [139], [143], [144], [147], [155], [162], [163], [164], [171], [172], [173], [174], [175], [176], [177], [178], [179], [180], [181], [182], [183], [184], [185], [186], [187], [188], [190], [191], [199], [203], [249], [250], [251]

Both total oil content and lipid composition differ widely among algal species. Figure 23 shows the average nutrient replete lipid contents for 31 freshwater species. Where available, nitrogen limited and silicon limited data are included.

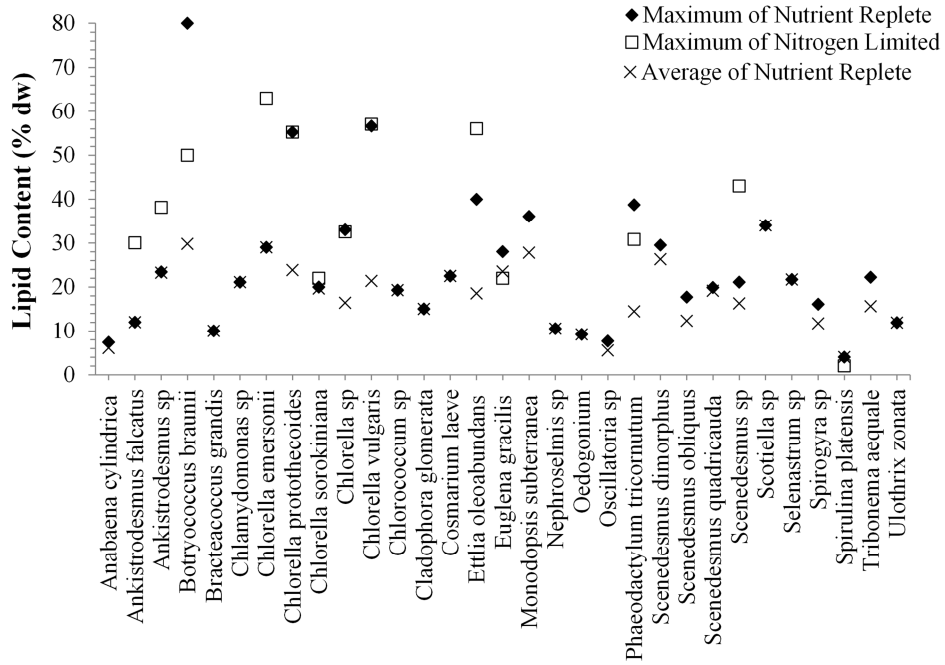

Figure 23. Lipid contents of 31 freshwater species
This chart shows microalgae grown under nutrient replete and limited conditions. Each data point is the species maximum value for that condition. Average nutrient replete lipid contents are also shown for each species. Data were obtained from the following sources: [4], [54], [58], [59], [91], [108], [118], [120], [124], [126], [134], [138], [162], [172], [174], [176], [177], [179], [180], [182], [185], [187], [189], [190], [203], [249], [250]

Figure 24 shows the same lipid content data for 75 marine species. It should be noted that a few species were grown heterotrophically as well as autotrophically. Heterotrophic growth is a very small proportion of the dataset, but it does account for the MLC in *Chlorella protothecoides*. Similar MLCs in *Chlorella vulgaris* were obtained under autotrophic growth.

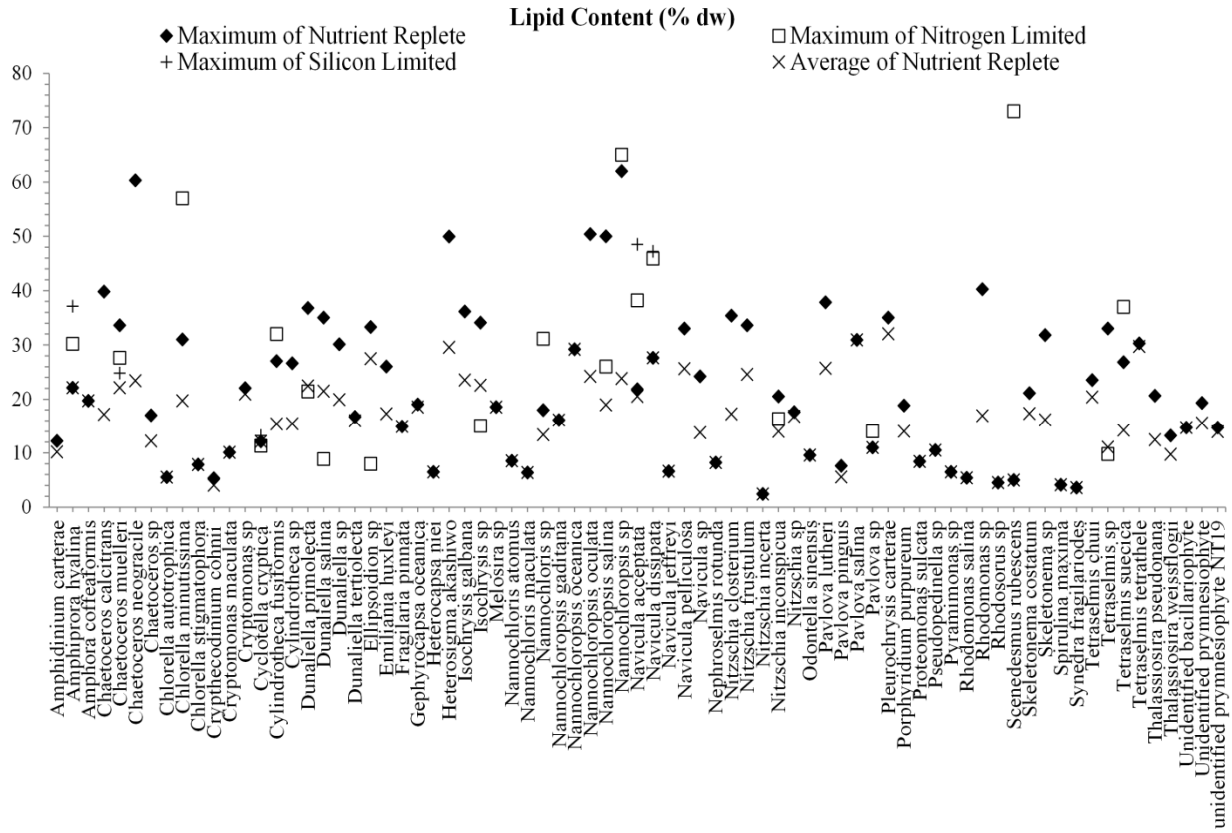

Figure 24. Lipid contents of 75 marine species
This figure shows species grown under nutrient replete [filled diamonds], nitrogen limitation [empty squares], and silica limitation [plus signs] conditions. Each data point is the maximum value for that condition for each species within the dataset. The average nutrient replete lipid contents [x values] are also shown for each species. This graph was prepared using data from the following publications: [4], [14], [31], [54], [78], [82], [92], [97], [101], [103], [104], [105], [106], [108], [112], [115], [118], [119], [120], [125], [128], [129], [133], [137], [138], [139], [143], [144], [147], [155], [162], [163], [164], [171], [173], [175], [176], [178], [179], [181], [183], [184], [186], [188], [191], [199], [203], [205], [251]

Many algae studies state that algae store lipids under environmental stressors, such as nutrient limitation and light and temperature changes. Stored algal lipids act as energy reserves and are important components of cellular membranes. Lipid reserves provide energy when solar irradiance decreases such that photosynthesis is not possible. Culturing

microalgae under nutrient deficiencies, such as nitrogen or silica starvation, has been shown to increase their lipid contents [11], [17], [81], [163], [252]. Similar results are displayed in Figure 23 and Figure 24; nitrogen limitation showed increased lipid contents in many species. Silica limitation has been less studied, but it also appears to increase lipid contents in some cases. Using a much smaller dataset with some overlapping sources, Griffiths and Harrison [85] found that average lipid contents increased to 138% and 168% of nutrient replete conditions under nitrogen limitation and silicon limitation respectively. Among the 55 species in their study, the average nitrogen limited lipid content of 27% dw was close to the nutrient replete lipid content of 23% dw [85]. They found a greater increase in lipid content under silicon deprivation with an increase from 24% to 41% dw [85]. As silica is a major component of diatom cell walls, silica limitation tends to induce lipid accumulation in diatoms; meanwhile, nitrogen limitation tends to induce lipid accumulation in green algae [17].

With sufficient light availability, nitrogen deprived cultures continue photosynthesis but fixed carbon is diverted to lipid or carbohydrate synthesis [4], [82]. The green alga *Pseudochlorococcum* sp switches from carbohydrate to neutral lipid production when grown under extended high light, nutrient limited conditions [81]. *Nannochloropsis* sp lipid contents may increase to 55% dw under nitrogen limitation [82]. Nitrogen depleted cultures of *Ettlia oleoabundans* showed increased lipid contents from 20% to 56% dw [91]. In another study, *Ettlia oleoabundans* grown under nitrogen starvation showed a 50% increase in fatty acid content with no significant change in fatty acid profile [54].

Lipid contents within the species in Figure 23 and Figure 24 vary over a large range from 2-80% dw. Only 11 species (10.4% of the species in the dataset) had MLCs ≥50% dw. However, 42 species reached >30% dw lipids. If they also have high biomass productivities, these species could be advantageous for industrial lipid production.

Figure 24 also shows that some species do not accumulate lipids under nitrogen limitation. Particularly, *Dunaliella salina* and *Isochrysis* sp, show decreased lipid contents under nitrogen limitation, and *Tetraselmis* sp shows similar lipid contents. This result agrees with previous research showing that some species, such as *Dunaliella* and *Tetraselmis*, show decreased lipid production under stress conditions and increased carbohydrate production instead [74]. Another study found that *Chlorella* sp and *Scenedesmus* sp grown in media until all nitrogen had been removed showed no change in lipid content, reduced productivity, and growth cessation within a week [4].

It has been postulated that algae produce lipids under conditions of mineral nutrient limitation as a sink for the electron carriers that would have been used to produce new cells had sufficient nutrients been available [253]. Johansen et al [163] found that silicon starvation increased cellular lipids in several species including *Navicula acceptata*, *Chaetoceros muelleri*, *Amphiprora hyalina*, and *Navicula dissipata*. *Navicula pelliculosa* also show increased lipid contents after 50 hours of silicon starvation [252]. Along with the lipid content changes discussed here, cellular lipid composition changes under nutrient deficiency.

4.6. Algae Class Lipids

Algae have a complex taxonomical structure, but they are primarily grouped into Phyla by colour and then into Classes according to structures visible under microscopic examination. Online algae databases were used to determine the Class for each species. In some cases, the databases disagreed about which Class should harbour a species. Disagreements were found in whether some species should be classed as Trebouxiophyceae or Chlorophyceae, Prymnesiophyceae or Pavlovophyceae, and Porphyridiophyceae or Rhodophyceae. When this occurred, the Class used was that given in the NCMA Provasoli-Guillard or, if unavailable, the UTEX database. Figure 25 shows

the medians and ranges of nutrient replete lipid contents for the algae in this chapter. This dataset is compared to the ranges provided in a commonly cited table by Borowitzka [254]. Figure 25 indicates that the Bacillariophyceae, Chlorophyceae, Chrysophyceae, and Eustigmatophyceae Classes have promise for oil production. This matches previous observations that many algae within the Chlorophyceae, Bacillariophyceae, Chrysophyceae, and Xanthophyceae Classes accumulate large amounts of oils [255]. Also, the US DOE ASP collected >3,000 algae strains with in-depth studies on growth and lipid production of 51 strains, and they found that the best candidates for algae lipid production were in the Chlorophyceae and the Bacillariophyceae classes [17].

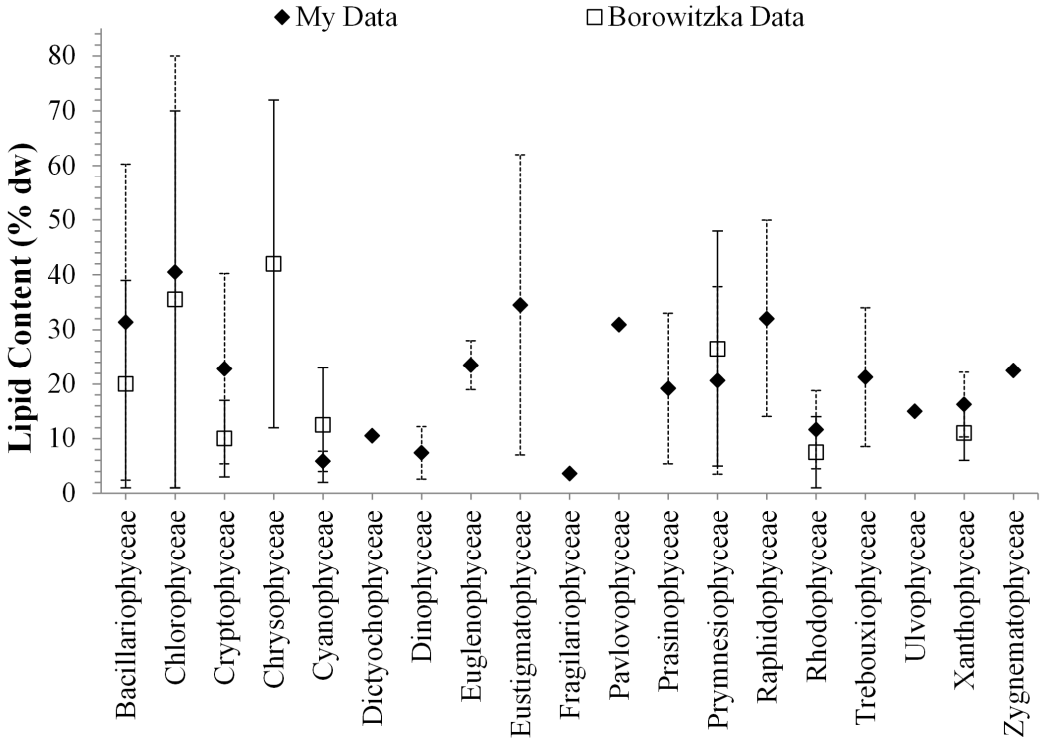

Figure 25. Average and range of nutrient replete lipid contents by algae class
This chart shows the average values and ranges of the nutrient replete lipid contents of the species in the database grouped by algae Class. This chart was prepared using these data sources: [4], [14], [31], [54], [58], [59], [78], [82], [91], [92], [97], [101], [103], [104], [105], [106], [108], [112], [115], [118], [119], [120], [124], [125], [126], [128], [129], [133], [134], [137], [138], [139], [143], [144], [147], [155], [162], [163], [164], [171], [172], [173], [174], [175], [176], [177], [178], [179], [180], [181], [182], [183], [184], [185], [186], [187], [188], [190], [191], [199], [203], [249], [250], [251]. The data are graphed alongside Class lipid content averages and ranges prepared by Borowitzka [254].

The average Chlorophyceae nutrient replete lipid content in this dataset was 40.5% dw, which is higher than found in previous reviews of 23% dw [85] and 35.5% dw [254]. An example is *Ettlia oleoabundans*, which is a freshwater Chlorophyte commonly studied for biodiesel production. When growing Chlorophytes, Griffiths and Harrison [85] found that nitrogen deprivation increased the average lipid content from 23% dw to 41% dw. They also found that most Chlorophytes had 20-30% dw lipid contents when nutrient replete with a far wider range of 18-64% dw under nitrogen deprivation [85]; however, this trend did not occur in the other classes. When comparing representatives from several algal classes, Collyer and Fogg [179] found that, unlike other classes, algae in Rhodophyceae and Myxophyceae (now termed Cyanophyceae) did not accumulate lipids under low nitrogen concentrations, even though the species could produce reasonable fat contents. In addition, Cyanobacteria have a markedly lower fat content from 5-13% dw without accumulating lipids under nitrogen limitation [85].

4.7. Algae Lipid Productivity

Algae lipid productivity depends upon both growth rate and lipid content. Algae SGRs and MLCs may be indirectly related. As a result, lipid productivity may be a more important selection parameter than either lipid content or growth rate when choosing a species for large-scale lipid production [85].

Whereas other studies have concentrated on optimal species, this chapter considers more general effects of light intensity, light source, illumination schedule, and culture volume on lipid productivity. Figure 26 shows lipid productivities for 61 microalgae species at a range of light intensities. The most common light sources in this dataset are fluorescent tubes, although many light sources are unknown. Using fluorescent tubes, high lipid productivities were found under light intensities from 115-460 $\mu E\ m^{-2}\ s^{-1}$. Sunlit cultures also produced reasonably high lipid productivities around 850 $\mu E\ m^{-2}\ s^{-1}$ light

intensity. By combining increased sunlight and severe nitrogen limitation, Rodolfi et al [4] found increased lipid productivity in outdoor *Nannochloropsis* sp cultures. In this dataset, LED, halogen, and incandescent bulbs produced significantly lower lipid productivities. The highest lipid producing species were *Nannochloropsis* sp, *Chlorella* sp, and *Phaeodactylum tricornutum*. When considering temperature effects, the highest lipid productivities for 66 microalgae species occurred at several temperatures from 20-28 °C (figure not shown).

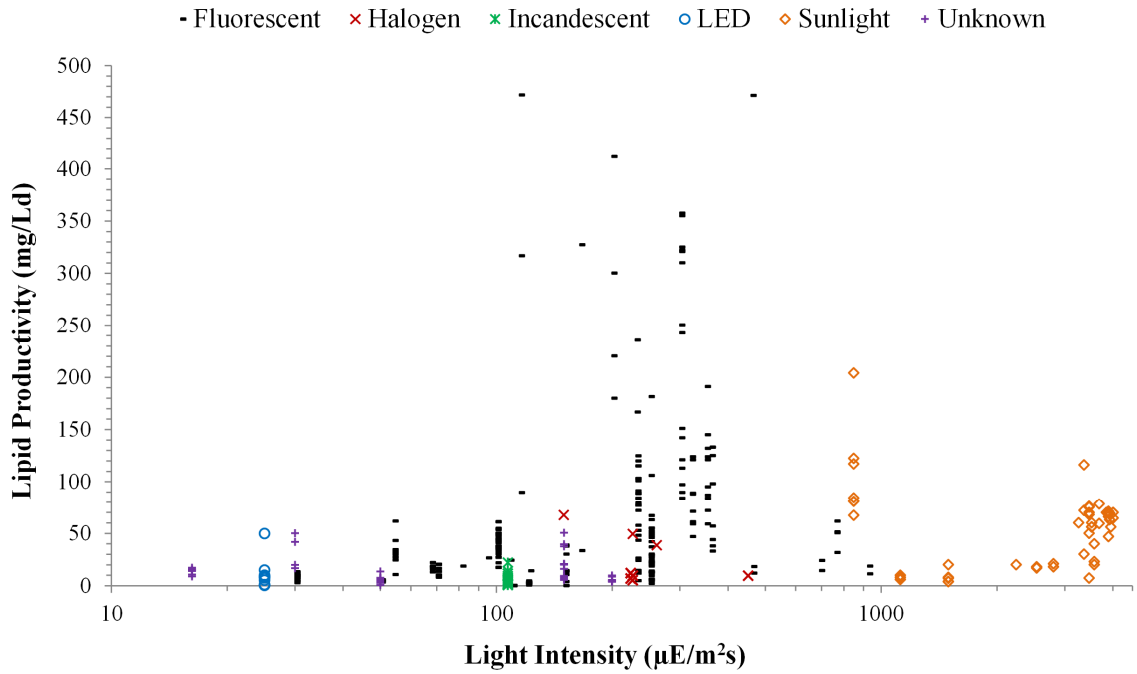

Figure 26. Lipid productivities 61 algal species at various light intensities and light sources
This includes data from the following publications: [4], [14], [54], [82], [91], [92], [97], [105], [106], [108], [116], [118], [119], [120], [126], [128], [129], [134], [143], [144], [147], [172], [173], [174], [178], [179], [181], [182], [187], [189], [199], [256]

Figure 27 shows lipid productivities produced at a range of culture volumes. In this dataset, only one study indicated lipid productivities over 1000 mg L^{-1} d^{-1} [203]. These extremely high lipid productivities occurred in 3 L flask cultures of *Chlorella vulgaris*, *Chaetoceros neogracile*, and *Tetraselmis tetrathele*. These values are significantly higher than other *Chlorella vulgaris* studies in this dataset, which had lipid productivities from 6.2-70 mg L^{-1} d^{-1} at similar volumes [4], [108], [118], [120], [172], [179]. Similarly, other

Chaetoceros studies showed <25 mg L^{-1} d^{-1} lipids in 100 mL cultures [4], and other *Tetraselmis* studies ranged from 0.2-300 mg L^{-1} d^{-1} lipids in 100 mL-10 L cultures [4], [97], [116], [118], [119], [129], [144], [147]. Lipid productivities >500 mg L^{-1} d^{-1} were also found in 3 L flasks of *Nannochloropsis oculata* and *Chaetoceros muelleri* [203] and in 5 L heterotrophic *Chlorella protothecoides* cultures [58]. Lipid productivities >350 mg L^{-1} d^{-1} were obtained in 300 mL to 18 L cultures of *Nannochloropsis* sp, *Chlorella* sp, *Tetraselmis chuii*, and *Dunaliella* sp. The largest cultures (>300 L) produced an average lipid productivity of 24.8 mg L^{-1} d^{-1} with values ranging from 0.19-54.2 mg L^{-1} d^{-1}. The average lipid productivity for cultures >2,000 µE m^{-2} s^{-1} is 53.8 mg L^{-1} d^{-1}. Figure 27 also includes some heterotrophic dark cultures with lipid productivities ranging from 58.5-222 mg L^{-1} d^{-1}.

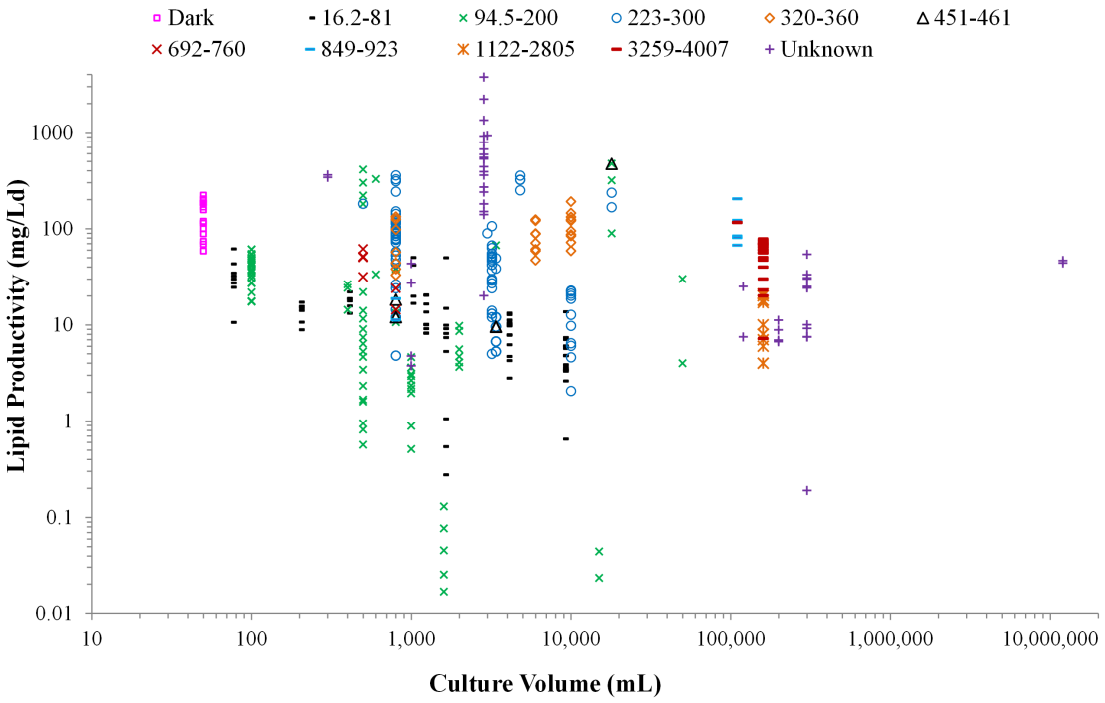

Figure 27. Lipid productivities of 66 species by culture volume and light intensity
The data are grouped by light intensity ranges with units of µE m^{-2} s^{-1}. This chart contains data from the following sources: [4], [14], [58], [82], [91], [92], [97], [103], [104], [105], [106], [108], [116], [118], [119], [120], [126], [128], [129], [134], [143], [144], [147], [172], [173], [178], [179], [181], [182], [187], [189], [199], [203], [204], [256]

Understanding the effects of environmental parameters is essential because large-scale algae production is not limited by fundamental engineering issues but by the need for more

fundamental research aimed towards developing high productivity algal strains [17]. Figure 26 and Figure 27 show that the highest lipid productivities were produced in small culture volumes grown under fluorescent lamps. Lipid productivities >100 mg L^{-1} d^{-1} were possible in small, dark heterotrophic cultures. Large-scale sunlit cultures produced lower lipid productivities, but the largest cultures (12,000 L) achieved 44 mg L^{-1} d^{-1} lipids.

4.8. Productivity and Lipid Content Trade-offs

Energy taken into algal cells is incorporated into new biomass, used for maintenance or converted into storage components, such as lipids or carbohydrates. As a result, there are trade-offs between growth rates, lipid contents, and productivities. These parameters were examined to identify trends. A high MLC is desirable to improve oil extraction efficiency. However, Figure 28 shows that MLC is not a reliable indicator of lipid productivity. This was also observed in a previous, smaller study [85]. This may be especially true when using nutrient limitation to increase MLC. Algal oil accumulation through nitrogen-deficiency does not tend to increase oil productivity because the higher oil content tends to be more than offset by the lower biomass productivities attained under nutrient shortage [4], [17]. Rodolfi et al [4] reasoned these effects to be due to the high metabolic cost for lipid biosynthesis. It is possible that this limitation may be minimized by using a two stage setup of optimized algal growth followed by nutrient limitation to increase cell oil contents. To reduce costs, an open pond-PBR combination could be used. Rodolfi et al [4] recommended growing *Nannochloropsis* sp under nutrient sufficient conditions in a PBR followed by a very short oil accumulation phase in an open pond under nitrogen starvation. For some species, an alternate method of overcoming the trade-off between growth and MLC may be mixotrophic growth. *Chlorella vulgaris* grown under nutrient limitation showed lipid increases from 9.2 to 55.3% dw but growth diminished from 1.05 to 0.31 g L^{-1}; however, mixotrophic growth combined with nutrient limitation increased

lipids to 48.5% dw at 4.07 g L^{-1} [60].

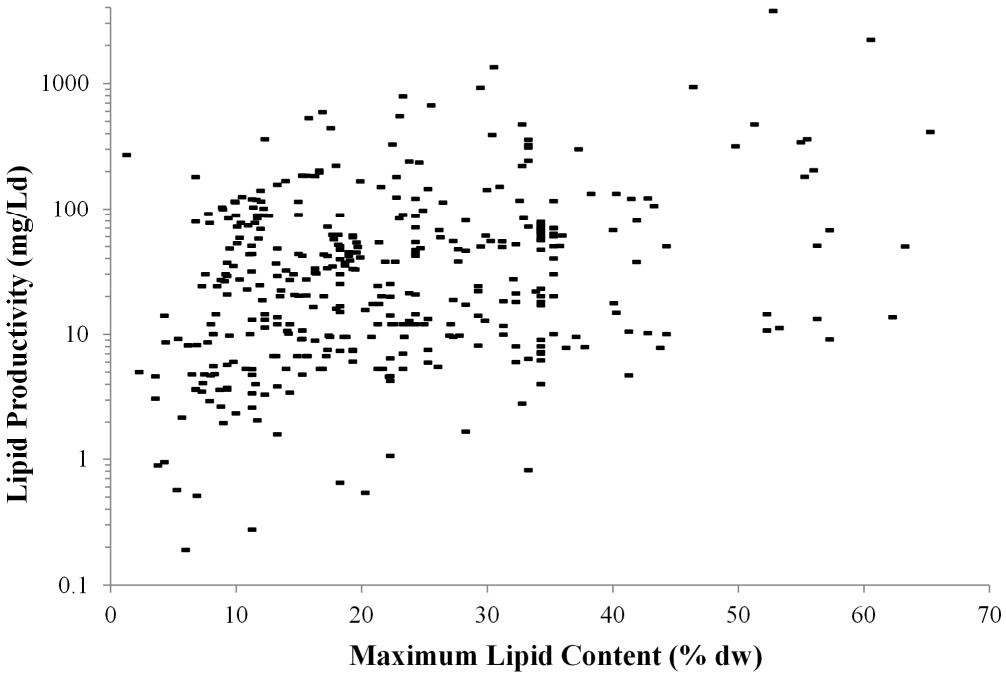

Figure 28. Lipid productivity versus maximum lipid content for 62 microalgal species
This chart was prepared using data from the following publications: [4], [14], [54], [58], [82], [91], [92], [97], [103], [104], [105], [106], [108], [118], [119], [120], [126], [128], [129], [134], [143], [144], [147], [172], [173], [174], [178], [179], [181], [182], [187], [189], [199], [203]

Biomass productivity is an important parameter for large-scale algae production. However, there is even less correlation between biomass productivity and MLC, as shown in Figure 29. Biomass productivities <1 g L^{-1} were observed in algae with MLCs ranging from 1-65% dw. This wide lipid content range shows that the dataset is composed of a mixture of species accumulating lipids and species accumulating carbohydrates; in addition, the algae are grown under a variety of temperatures, light intensities, and salinities that may be affecting lipid production. The highest biomass productivity in this dataset is 7.1 g L^{-1} d^{-1}, which was obtained for *Chlorella vulgaris* at 35 g L^{-1} salinity. *Tetraselmis tetrathele*, *Chaetoceros neogracile*, *Nannochloropsis oculata*, and *Tetraselmis* sp also had high biomass productivities. Most of the cultures with high lipid contents, such as *Nannochloropsis* sp and *Chlorella emersonii*, had low biomass productivities. Rodolfi et al [4] reported a similar observation when they examined 30 microalgae species and found that strains with higher lipid contents tended to show lower biomass

productivities. Of the 56 species in Figure 29, cultures with MLCs >35% dw had biomass productivities <0.93 g L^{-1} d^{-1}. A few cultures defied this trend; these were *Chlorella vulgaris*, *Chaetoceros neogracile*, and *Chlorella protothecoides*. As such, these species may be good places to look for high lipid content fast growers. It is also possible that they achieved this result due to favourable culture conditions.

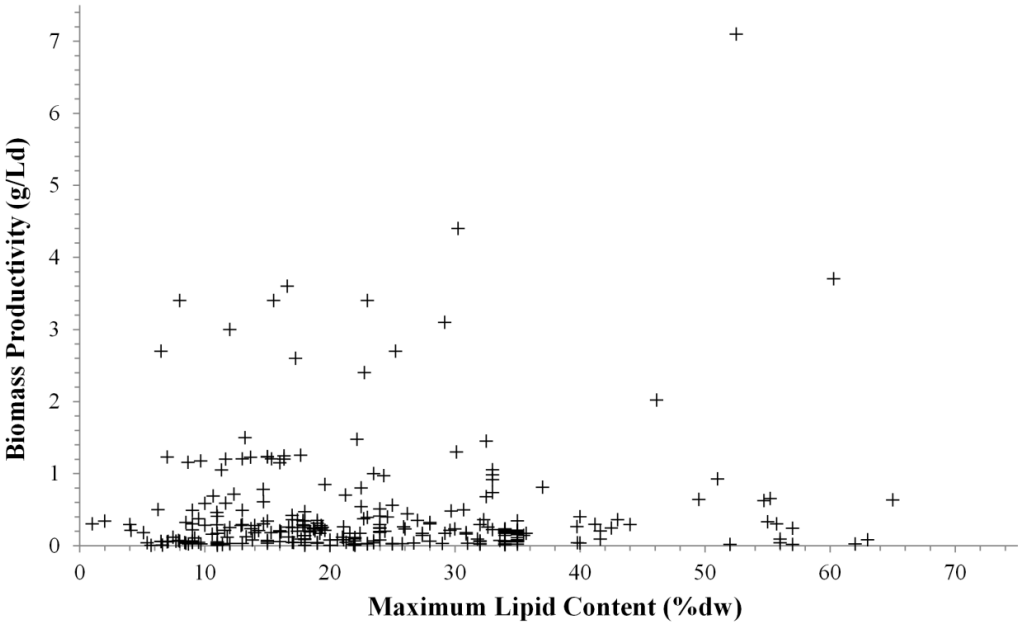

Figure 29. Biomass productivities versus maximum lipid contents for 56 algae species
This chart was prepared using data from the following sources: [4], [14], [54], [58], [82], [91], [92], [103], [104], [105], [106], [118], [119], [120], [126], [128], [134], [143], [147], [172], [173], [174], [178], [181], [182], [187], [189], [199], [203]

Although the relationships between lipid content and either biomass or lipid productivity are not clear, there is a much closer relationship between lipid productivity and biomass productivity as shown in Figure 30. This occurs partially because lipid productivity is a combination of lipid content and biomass productivity. However, the top biomass producers are not necessarily the top lipid producers. This dataset shows a linear trend between lipid and biomass productivities with an R^2 of 0.74. Since only one study produced lipid productivities over 1000 mg L^{-1} d^{-1}, Figure 30 is limited to lipid productivities <1000 mg L^{-1} d^{-1} and shows a trendline R^2 of 0.72. Lipid productivities ≥100 mg L^{-1} d^{-1} occurred for algae with biomass productivities from 0.24-3.6 g L^{-1} d^{-1}.

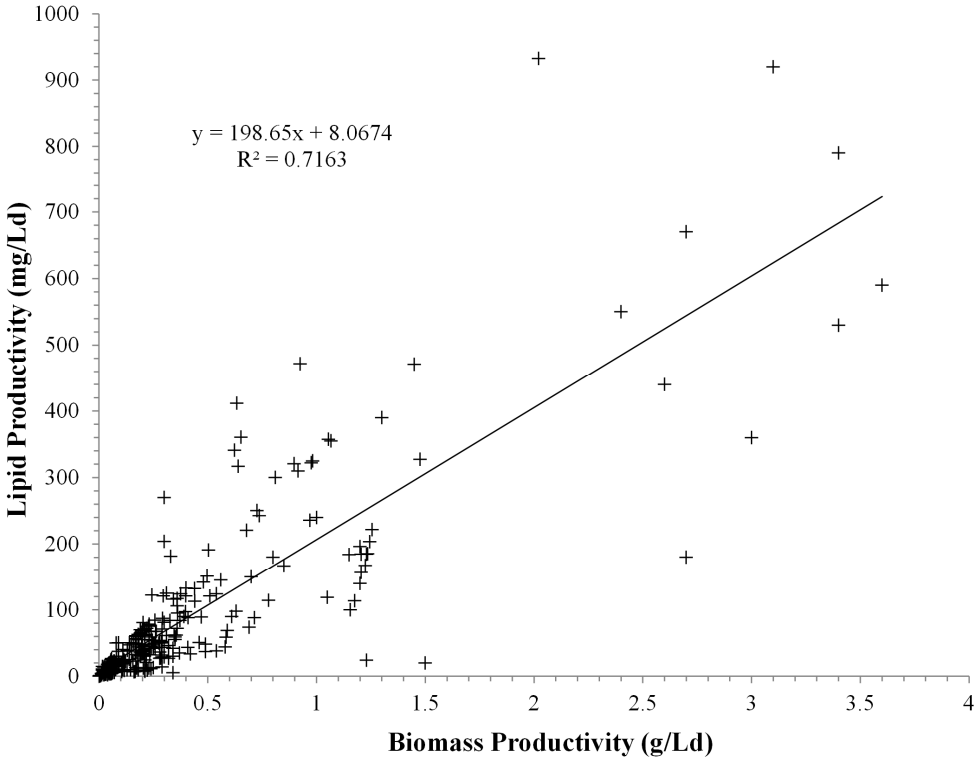

Figure 30. Lipid productivity versus biomass productivity for 54 algae species
This chart includes data from the following sources: [4], [14], [54], [58], [82], [91], [92], [103], [104], [105], [106], [118], [119], [120], [126], [128], [134], [143], [144], [147], [172], [173], [174], [178], [181], [182], [187], [189], [199], [203], [204], [256]

Some of the variability in these trade-off considerations may result from the inclusion of nutrient limited cultures within the dataset. For example, some cultures grown under continually low nitrogen levels show a general trend of decreased media nitrogen levels decreasing the biomass productivity while increasing the lipid content, which leaves lipid productivity unchanged [4]. This result has been seen in a number of species under either nitrogen or silica deprivation, and the overall lipid productivity is often reduced during nutrient deficiency [17]. However, not all species show this trend. *Nannochloropsis* sp grown in nitrogen exhausted media showed a short period of greatly increased lipid content (to 60% dw) with limited loss of biomass productivity; this resulted in an average lipid productivity of 204 mg L^{-1} d^{-1} for a few days [4]. Similar results were achieved with *Pseudochlorococcum* sp neutral lipid productivities reaching 350 mg L^{-1} d^{-1} upon harvesting after 6 days of nitrogen limitation [81].

The environmental conditions used during an experiment may produce a range of SGRs and MLCs for each species. In an attempt to clarify relationships between SGRs and MLCs, the experimental information was condensed to obtain an average SGR and an average MLC for each species. Figure 31 shows no significant correlation between lipid content and SGR for the algae in this dataset. The top eleven averaged MLCs occurred in species with an average SGR <0.7 d^{-1}. On the other hand, the two fastest growing species, *Nannochloris* sp and *Nitzschia closterium*, have 19 and 17% dw MLCs respectively.

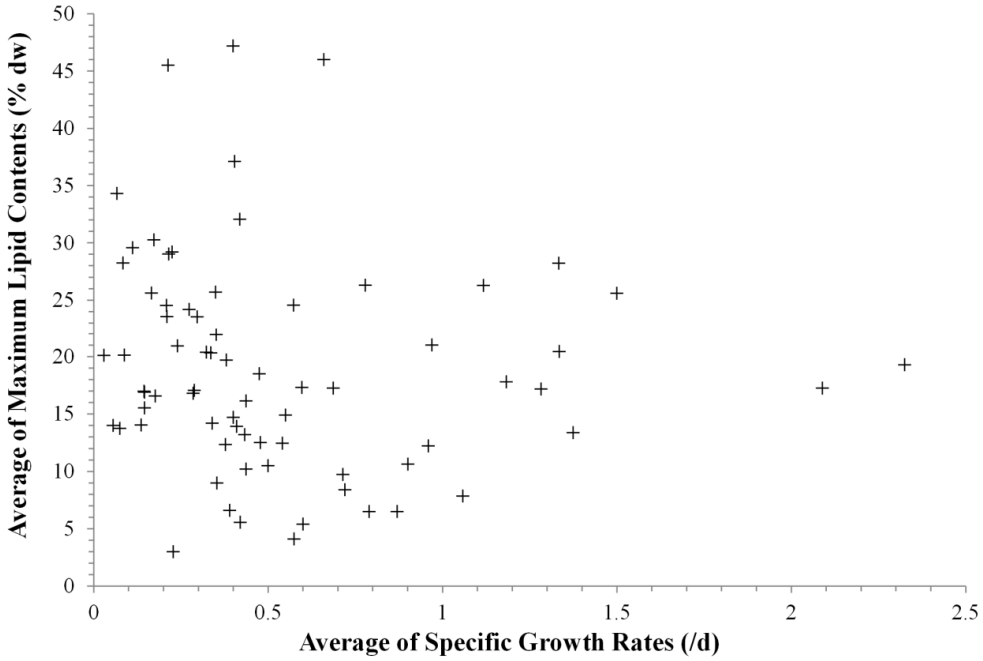

Figure 31. Relationship between average specific growth rates and average of maximum lipid contents for 72 algae species
This graph contains averages of the SGRs and MLCs for 72 species from the following publications: [4], [14], [23], [27], [31], [38], [54], [58], [59], [61], [78], [82], [87], [88], [89], [91], [92], [96], [97], [98], [99], [100], [101], [102], [103], [104], [105], [106], [107], [108], [109], [110], [111], [112], [113], [114], [115], [116], [117], [118], [119], [120], [121], [122], [123], [124], [125], [126], [127], [128], [129], [130], [131], [132], [133], [134], [135], [136], [137], [138], [139], [140], [141], [142], [143], [144], [145], [146], [147], [148], [149], [150], [151], [152], [153], [154], [155], [156], [157], [158], [159], [160], [161], [162], [163], [164], [171], [172], [173], [174], [175], [176], [177], [178], [179], [180], [181], [182], [183], [184], [185], [186], [187], [188], [189], [190], [191], [196], [197], [198], [199], [200], [201], [203], [204], [205], [249], [250], [251], [257]

In one study using saturating light intensities, *Isochrysis galbana* had a lower growth rate than *Tetraselmis* sp, but its higher lipid content gave productivities double those reached by *Tetraselmis* sp [97]. In Figure 31, *Chlorella vulgaris*, *Navicula pelliculosa*, and *Ankistrodesmus* sp have average SGRs >1 d^{-1} and MLCs above 25% dw, so they may

be able to produce large lipid productivities.

4.9. Flagellate Microalgae

Most algae cells are denser than their culture media. Freshwater density is approximately 1.0 g cm^{-3}, and seawater densities range from 1.021-1.028 g cm^{-3}. The density of algal cells, meanwhile, can range from 1.03-1.10 g cm^{-3} for cells without cell walls to 2.6-2.7 g cm^{-3} for cells covered with scales or coccoliths [170]. In their natural environment, algae either swim actively or use buoyancy to enhance their time within the light portion of the water column.

Cells are more buoyant when they have increased surface area per volume. Some species have spines that may be minor, such as small protrusions, or long and needle-like. These spines increase the cell surface area, which affects their hydrodynamic properties and helps them become entrained within water eddies. These eddies may push the cells up into the water column, such that, along with reduced sinking rates, the cells remain longer within the illuminated section of the water column. These structures may also help decrease predation. With many potential functions, it is unsurprising that a large proportion of the species within this chapter, 41.7%, had long cellular extensions (flagella or spines) and that 2.9% had minor extensions. Buoyancy can also be actively controlled in several ways. Many species use gas vacuoles, and some can accumulate mucilage. In addition, some marine organisms use ionic regulation to alter density.

Many motile algae swim using flagella, such as *Tetraselmis chuii*, *Isochrysis* sp, and *Pleurochrysis carterae*. Swimming algae may move in short quick bursts using a wide variety of swimming patterns including corkscrew, wobbling, helical, and breaststroke motions. The flagella length and number determine the type of swimming stroke used by motile algae. For instance, flagellates can swim by corkscrewing with one flagella or by using a breaststroke motion if the cell has pairs of flagella. Algae have been measured

swimming at rates between 50-500 μm s^{-1} [170], [214]. Other sources list 3-30 μm s^{-1} for nanoplankton, 200-500 μm s^{-1} for larger microalgae, and nearly 1 mm s^{-1} for some large colonies [213].

Flagella may be present singularly or in 1 or more pairs. Flagella can range in length from approximately half their cell length to more than twice their cell length. A cell's radius is often 15-40 times the radius of its flagellum [170]. In larger cells, the flagellum frequently has hairs to increase its effective radius [170]. Several algae species have flagella for most or all of their life cycles, while other species only have flagella for a portion of their life cycles, such as during sexual reproduction.

Actively swimming algae may react differently than passive cells within a PBR. For example, *Tetraselmis cordiformis* cells have been seen swimming to a suitable position from a light source before attaching to the substrate with two flagella on each side of the cell [258]. Also, turbulence modeling indicates that motile cells may have a significant advantage in waters with patchy turbulence because motile cells pushed out of their preferred environment by turbulence can move back towards it [214]. Figure 32 considers flagellate algae, which are likely to be swimming actively within their culture containers. SGRs >1 d^{-1} were reached for light intensities from 11.6-923 μE m^{-2} s^{-1}. The flagellate data are more even across a range of light intensities than the data for all species. In addition to the data displayed, the dataset contained three higher SGRs for 800 mL *Tetraselmis* sp cultures under 14 hour illumination at 25 μE m^{-2} s^{-1}; these cultures reached 13.9 d^{-1} at 10 °C, 9.9 d^{-1} at 16 °C, and 9.24 d^{-1} at 22.5 °C. Also, the log x-axis in Figure 32 does not allow inclusion of the 17, 50 mL dark cultures of *Crypthecodinium cohnii*, which had SGRs from 0.26-2.16 d^{-1} and MLCs from 8.7-17.7% dw. In Figure 32, several illumination schedules were used ranging from 8 to 24 hours illumination. Illumination schedules were unknown for several cultures, especially high light intensity cultures

illuminated by sunlight. The highest SGRs in the dataset occurred for low light intensities using a 14 hour illumination schedule. Illumination schedule may affect flagellates more than other algae.

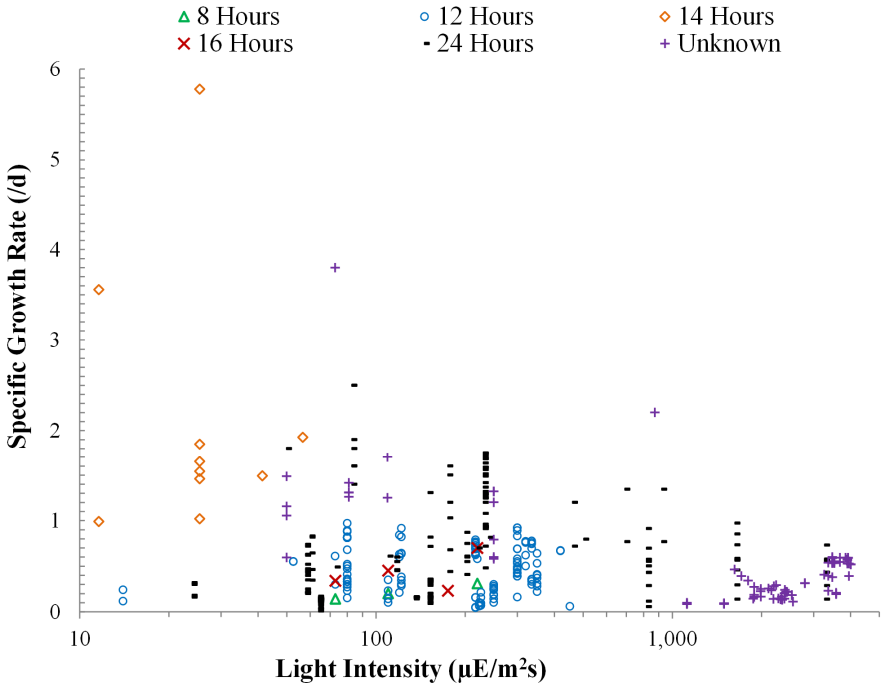

Figure 32. Specific growth rates of 28 flagellates by light intensity and illumination schedule This graph includes data from the following sources: [14], [87], [97], [98], [99], [112], [114], [115], [116], [118], [119], [122], [127], [128], [129], [130], [137], [138], [139], [142], [144], [147], [151], [152], [153], [156], [157], [159], [160], [161], [162], [199]

When measuring composition of flagellated and non-flagellated *Tetraselmis striata* cells within a synchronized culture over a 14:10 hour light:dark cycle, Reize and Melkonian [195] found that over 80% of cells had flagella during the first 6 hours of light but only 10% were flagellates at 10.5 hours. After 14 hours, the dark period began, and the percent flagellated increased from 14.5 hours until the dark regime ended with ≈80% of cells flagellated. Cell division began in earnest after 10.5 hours, jumped up over 50% around 14.5 hours then decreased rapidly until the dark regime ended [195]. Division in the dark stage is common to most algal flagellates; *Scherffelia dubia* has been shown to divide in the light stage but under conditions unlike its natural environment [259].

Figure 33 shows that many flagellate lipid contents are 30-40% dw at light intensities from 40.5-4,000 µE m^{-2} s^{-1}. The most common illumination schedule used was 12 hours.

Eight species reached MLCs >35% dw, including *Dunaliella primolecta*, *Heterosigma akashiwo*, and *Tetraselmis suecica*.

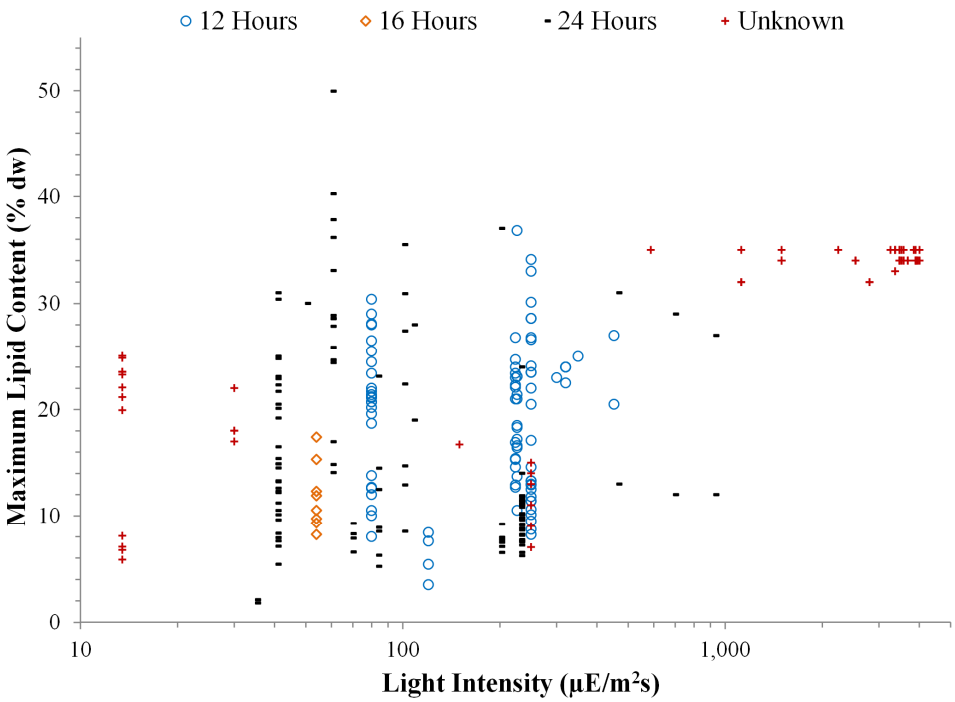

Figure 33. Maximum lipid contents of 25 flagellates by light intensity and illumination
This chart includes data from the following sources: [4], [14], [54], [97], [112], [115], [118], [119], [128], [129], [137], [138], [139], [144], [147], [162], [171], [173], [175], [176], [179], [184], [189], [191], [199]

4.10. Conclusions

This chapter provides a visual overview of several important parameters in algae culturing. Unlike Chapter 3, which concentrated on variables controlled during culturing, this chapter concentrates on characteristics inherent in a species. Data from 131 publications on 128 microalgae species were combined to identify general trends.

Cell size and grouping: Cell lengths were provided for 146 species. Most of the species in this dataset are unicellular with median cell lengths of 7 µm for freshwater and 9 µm for marine species. When grouped into size classes, each size class produced similar SGRs across a wide range of illumination fluxes. The smallest algae classes, picoplankton and nanoplankton, produced the highest MLCs.

Class Lipids and Nutrient Effects: Several algae classes show promise for oil production, including Bacillariophyceae, Chlorophyceae, Chrysophyceae, and Eustigmatophyceae.

The most common nutrient replete lipid content range is 10-20% dw among the 75 marine and 31 freshwater species. In many species, nitrogen limitation showed increased lipid contents. Fewer data were available for silica limitation, but this may also increase lipid contents. A few species were identified that do not follow this trend.

Lipid Productivity: Several lipid productivities over 150 mg L^{-1} d^{-1} were produced in small-scale cultures grown under fluorescent lamps from 115-460 μE m^{-2} s^{-1}. Reasonably high lipid productivities were found in sunlit cultures around 850 μE m^{-2} s^{-1} light intensity, but light intensities >2,000 μE m^{-2} s^{-1} reduced lipids to an average of 53.8 mg L^{-1} d^{-1}. The largest cultures (>300 L) produced an average of 24.8 mg L^{-1} d^{-1} lipids but with a wide dispersion.

Trade-offs: Cells put energy into growth, storage often as lipids, or maintenance. As such, trade-offs occur between productivities, MLCs, and SGRs. Most of the cultures with MLCs >35% dw had biomass productivities <0.93 g L^{-1} d^{-1}, although a few cultures defied this trend. MLC was not a reliable indicator of SGR, lipid productivity, or biomass productivity. A much closer relationship occurred between lipid productivity and biomass productivity, but the top biomass producers were not necessarily the top lipid producers.

Flagellates: The presence of flagella affects how a cell moves within a reactor. Over 44% of the species within this chapter had flagella, spines or other extensions. Flagellate algae reached SGRs >1 d^{-1} for light intensities from 11.6-923 μE m^{-2} s^{-1}. The highest SGRs occurred for low light intensities with 14 hour illumination. Many flagellate lipid contents are 30-40% dw at light intensities from 40.5-4,000 μE m^{-2} s^{-1}.

Chapter 5. Multiple Regression Models to Assess Algae Growth and Lipid Production

To enhance algae feasibility for large-scale culturing, it is desirable to have high VLPs, which result from a combination of SGRs and MLCs. Algae growth and composition depend upon a wide variety of environmental factors, such as light intensity, temperature, and salinity. These and other factors have been widely studied, but, as discussed in Chapter 3, their interactions are complex. This complexity makes it difficult to quantify the degree to which each culture variable affects algae growth rates and lipid production.

A set of general and simple predictive models was prepared to assess SGRs, MLCs, and VLPs under a variety of environmental conditions. The use of the term model in this thesis refers to statistical models rather than fundamental theoretical models based on kinetics, stoichiometry, or mass balance. The multiple regression models developed here are a complementary method of extracting useful information from a large dataset with many variables and potentially interacting factors. As statistical models capable of considering a large number of variables, these models have promise in explaining complex systems like algae growth. Several multivariate analyses were performed to generate these models, which can determine which culture parameters were significant predictors of growth rates and lipid production. Also, the variability in growth and lipid production contributed by each environmental parameter can be quantified.

This chapter begins with a discussion in Section 5.1 of non-species specific models and why they are important. Then, Section 5.2 details the necessary pre-screening data considerations, and Section 5.3 follows with the theory behind multiple regression and model validity checks. Next, several SGR, MLC, and VLP models are described in Sections 5.4, 5.5, and 5.6 respectively. Finally, the major findings from each model are discussed in Section 5.7 along with notes on how to improve future models.

5.1. Importance of Non-species Specific Models

A large number of algae growth models have been produced. Many of these have been based on experiments for a single species grown under a small number of conditions [260], [261], [262], [263]. However, scaling-up results from small-scale and/or short-term experiments may not provide reliable estimates of large-scale production. Quinn et al [70] collated algae oil productivity estimates from 10 studies from 2007-2010 and found estimates ranging from 12-184 m^3 ha^{-1} per year. In addition, many published models were developed for a specific reactor type, including air lift [261], plate [70], and raceway reactors [264]. However, the models presented here provide a more general estimate that is independent of reactor type.

Many models are based on theoretical calculations and assume an average light intensity within the PBR [70], [265], [266]. However, average light intensity depends upon illumination schedule as well as light intensity. Moreover, determining the average light intensity requires quantifying the light distribution within the PBR. Some models account for light distribution [168], light distribution and temperature [260], [267], or light distribution with nutrient depletion [268]. Other models look at the effects of mixing on light/dark cycles within the reactor [261], [269]. Most of the theoretical algae growth models calculate light attenuation using Lambert-Beer's law or a variation of it [70], [266], [268], [269], [270]. Lambert-Beer's law is a simple equation, but it is only applicable when scattering effects can be neglected. This indicates that models using the Lambert-Beer law are highly dependent upon the species' cell size and other properties, and that these models may be less accurate for dense cultures or cultures with long light paths. Light distribution also depends upon the light source's properties and position. For example, several models have been developed specifically for internally illuminated reactors and may assume one or more multiple internal radiators [271] or the use of fibre optics [272]. Light distribution is also affected by the physical outlay of the reactor, the

algae culture's optical properties, and the cells' physiologies. One culture trait that may be required is the scattering properties of the cells [273]. Unfortunately, such properties are not readily measured using the available equipment in many labs, so they must often be assumed.

The assumptions made in theoretical models can greatly affect the predictions generated. In addition, theoretical models tend to involve complex calculations. Unlike theoretical models, multiple linear regression attempts to assess relationships between a large number of variables to predict processes. Multiple regression models have been used extensively to predict chlorophyll-a, and therefore algae growth, from physical and biological water quality parameters in reservoirs [274], [275]. They have also been used to look at phytoplankton and zooplankton communities, grazing interactions, and herbicide exposures within lakes and streams [276], [277], [278], [279], [280]. Algae multiple regression models have been sporadically made for determining growth rates of rotifers when fed algae [281], maximizing CO_2 fixation [282], and looking at nutrient supplies to biomass ratios [283]. Multiple regression has rarely been used to predict algae growth, and that was done looking at environmental factors affecting a single species [86], [284], [285]. However, multiple regression has not been used to assess general algae growth or lipid contents under controlled conditions, which is the goal of this study.

The models described here are particularly useful when predictions need to be made without specialized laboratory equipment. This occurs because these models use variables that are either set by the experimenter or are relatively easy to measure. Also, these models should provide accurate initial estimates because they are based on experimental results generated on many algae species by a variety of researchers.

Furthermore, this work will be useful in predicting growth of a species under specific conditions given a handful of easily obtainable variables. Unlike species specific growth

prediction models, these models can be used to obtain results for a generic algae species under a given set of study conditions. These non-species specific results may be particularly applicable for use in life cycle analyses or carbon capture calculations performed before a specific species has been chosen. In addition, this work will be useful anticipating the results of different growth regimes on a species.

5.2. Data Pre-screening

The database described in Chapters 3 and 4 was used to prepare several models to predict algae SGRs, MLCs and VLPs. These models were prepared using standard multiple linear regression. Before modelling, the data were screened for compliance with model assumptions. Data pre-screening consists of three major tasks. Section 5.2.1 details checking if the dataset is normally distributed and performing transformations to normalize the dataset. Another issue is how to handle missing data as discussed in Section 5.2.2.

5.2.1. Checking for Normal Distribution and Transforming Data

Multiple regression assumes that the dataset is normally distributed, which means it is not skewed and has low kurtosis. Skewness is a measure of how symmetric a data distribution is, and it is given by Equation 7 for calculating skewness from z-scores [286].

(7) $$Skewness = \frac{n}{(n-1)(n-2)} \sum_{i=1}^{n} {z_i}^3$$

Negative skewness indicates that most data is below the dataset's mean, and positive skewness indicates most data is above the mean. The z^3 value indicates that data points far from the mean, i.e. those with large standard deviations and large z-scores, affect the total more than those closer. In positively and negatively skewed datasets, the median is probably a better representation than mean for the dataset [286]. The assumption of normality is the basis of multiple regression, and statistical inferences from non-normal datasets may rapidly become less robust as the dataset departs from normality [287]. However, most real-world datasets are not normally distributed [287]. Unless there is a

reason not to, Tabachnick and Fidell [287] recommend using transformations to increase normality of datasets prior to multiple regression.

Histograms were prepared for each predictor and outcome variable using IBM SPSS FREQUENCIES version 21. A case is a set of predictor and outcome variable data relating to a single experiment. The database was split into three files, where each file contained only cases with SGR or MLC or VLP data. The histograms showed that many variables were skewed and had some kurtosis.

Several transformations were tested to determine which was best in reducing the number of outliers, in improving normality, linearity and homoscedasticity of residuals, and in reducing skewness. Each variable was tested as is and as transformed using Log, Inverse, and Square Root transformations. When necessary, a constant was added to allow calculation of a transformation. P-P plots assess each variable's expected versus observed probabilities, so SPSS P-P plots were produced to assess which transformation, if any, improved the dataset's normality. Normal distributions show P-P plots along the diagonal and detrended P-P plots having approximately equal data above and below zero. The optimal P-P plots for each variable are shown in Sections 5.4, 5.5, and 5.6. In each case, the transformation producing the most normal distribution was used in further analyses.

5.2.2. Missing Data

The database was populated using data reported in published works, so it contained several missing variables. When no datum was available (i.e. when a study did not state the light illumination used), the cell was labelled missing. The dataset was analysed using SPSS EXPLORE, and the missing data did not have a particular pattern. However, Little's Missing Completely at Random test indicates that the data may not be missing completely at random. SPSS REGRESSION uses listwise deletion to remove cases with a missing value prior to performing regression analyses. If the data is not missing completely at

random, listwise deletion of cases with missing variables may improperly skew results [287]. Furthermore, listwise deletion can greatly decrease the number of cases, N, and thereby remove a great deal of data. Due to the wide range of studies and large number of sources used to produce the database, some variables contain a large amount missing data. As shown in Table 6, some culture parameters are commonly reported by researchers; these include volume, temperature, and light intensity. However, gas flow rate, pH, and salinity were commonly unreported. When a publication provided the SGR and MLC, the VLP was calculated if it had not already been provided.

Table 6. Missing data within the SGR, MLC and VLP datasets

Dataset[1]	**Vol**	**Temp**	**pH_{Avg}**	**GFR**	**$\%CO_2$**	**LI**
SGR	7.5	6.8	37.8	39.7	36.1	6.2
MLC	6.2	6.3	39.1	36.0	31.3	6.7
VLP	2.8	8.6	36.6	32.4	27.0	8.6
Dataset[1]	**IS**	**Salinity**	**CW_{Min}**[2]	**SGR**	**MLC**	**VLP**
SGR	18.4	38.5	0.5	--	40.5	44.7
MLC	21.9	39.9	0.6	37.3	--	34.9
VLP	22.0	43.5	0.0	34.6	9.9	--

[1] The missing data for each parameter are expressed as % of the total dataset for that value.
[2] Several of the missing minimum cell width data points were completed using species values from other sources as detailed in Chapter 4.

Missing data can be completed using several methods, including inserting mean values, expectation-maximization or regression. It has been noted that multiple imputation is the most recommended method to complete missing data because it does not assume data are randomly missing and retains the sampling variability [287], [288]. However, in SPSS, multiple imputation is not recommended for datasets with lots of missing values. Methods of data completion are not designed to compensate for such high missing percentages, so it was not possible to test the result differences between regression runs on complete and incomplete datasets. Tabachnick and Fidell [287] note that deciding how to handle missing data is an important decision, even though it is a choice among several bad alternatives.

This study used listwise deletion, which greatly decreased the N values. Even with this

caveat, these models are first steps towards reliable algae growth, lipid content, and lipid productivity models that use easily obtainable experimental data and easily obtainable experimental results to predict effects. Future work may increase the robustness of these models by increasing the database size to reduce the variables percentage missing.

5.3. Multiple Regression and Model Validity

The theory behind multiple regression analyses is discussed in Section 5.3.1. Models developed by multiple regression must be rigorously tested for validity. These validity checks are detailed in Section 5.3.2. The abbreviations and units for each variable are summarized in Section 5.3.3.

5.3.1. Multiple Regression Theory

Multiple regression uses several independent or "predictor" variables to predict one dependent or "outcome" variable. The analysis evaluates whether the given predictor variables are sufficient to predict the outcome and identifies which predictor variable most strongly predicts the outcome [289]. In linear multiple regression, the method of least squares is used to produce regression coefficients that have been computed to minimize the sum of squared deviations between predicted and actual Y values. Multiple regression equations for two predictor variables, x_1 and x_2, are shown below as given in a standard textbook [290].

$$\begin{aligned} \sum y &= nb_0 + b_1 \sum x_1 + b_2 \sum x_2 \\ \sum x_1 y &= b_0 \sum x_1 + b_1 \sum {x_1}^2 + b_2 \sum x_1 x_2 \\ \sum x_2 y &= b_0 \sum x_2 + b_1 \sum x_1 x_2 + b_2 \sum {x_2}^2 \end{aligned}$$

The regression coefficient, b, shows the predicted change in the outcome variable, y, for a one-unit increase in the predictor variable controlling for all other predictor variables in the analysis [289]. Standard multiple regression treats all variables equally by controlling for all other predictor variables. Furthermore, standard multiple regression assigns each predictor variable only the area of its unique contribution to the results;

overlapping areas are not assigned to any predictor variable [287]. As such, standard multiple regression assesses the relationship between variables; however, it does not imply causality [287]. This occurs because one cannot exclude the possibility that the cause is an unidentified variable.

Models produced here were generated using IBM SPSS Statistics version 21. First, SPSS FREQUENCIES and P-P Plots were used to analyse datasets for compliance with model assumptions as discussed in Section 5.2. Then, SPSS REGRESSION was used to produce models. Numerous standard multivariate regression analyses were performed to determine the relationships of several predictor variables (i.e. light intensity, cell size, culture volume) on an outcome variable (either SGR, MLC or VLP). Several combinations of predictor variables were run for each of the three outcome variables tested. Generally, when more predictor variables were included in the analysis, a higher R^2 value was achieved. However, adding variables was stopped before the point at which including more predictor variables substantially decreased the number of data points in the analysis. Some possible predictor variables, such as areal biomass productivity, lipid yield, and areal lipid productivity, had insufficient data that limited the size of the dataset; these variables were not modelled.

5.3.2. Model Validity Checks

The models were tested in several ways to ensure their validity. These validity checks are as follows: multicollinearity, ratio of N to the number of predictor variables, univariate outliers, regression coefficient t-tests, semipartial correlation, F test, and bivariate scatterplots of the residuals. The purpose of each validity check is detailed below. For each model, the validity check results are summarized alongside the models in Sections 5.4, 5.5, and 5.6.

The models were checked for multicollinearity with predictor variables removed when

multicollinearity was indicated by a collinearity VIF statistic >10.0. Multicollinearity occurs when two predictor variables are too highly correlated, which causes the R^2 value of the model to be greatly inflated [287]. Each analysis aimed to include predictor variables that are strongly correlated with the outcome variable but not with each other. The goal was to identify the smallest group of predictor variables necessary to predict the outcome variable [287].

For each model, the ratio of N to predictor variables was calculated to ensure that the dataset was large enough to produce a meaningful solution from linear regression. For most models, the following rules of thumb were used as recommended by Tabachnick and Fidell [287]:

To test multiple correlation: $N \geq 50 + 8m$

To test individual predictors: $N \geq 104 + m$

In these equations, m = number of predictor variables, and the largest N value among the two equations is used for comparison. In some models, the expected squared partial correlations were large enough to indicate a larger effect size. In these cases, the dataset was confirmed as sufficiently large by using this correlation, denoted as pr^2, for the independent variable with the smallest effect. Equation 8 shows Green's rule of thumb [291].

(8) $$N \geq \frac{8}{f^2} + (m - 1) \qquad \text{where } f^2 = \frac{pr^2}{1 - pr^2}$$

For several variables, transformations were used to improve normality and reduce univariate outliers. Multivariate outliers can also occur, where a combination of variables makes the data point an outlier and may affect the precision of regression weight estimates [287]. Multivariate outliers, as identified using Mahalanobis distance, must be removed iteratively because some outliers mask others [287]. In some situations, removing cases based on Mahalanobis distance would result in a large reduction in N, which could limit

the models' applicability. For consistency, the models produced here do not consider Mahalanobis distance, but some notations were included to indicate results from datasets reduced by comparing Mahalanobis distance to Chi-square, χ^2, with a criterion of p=0.001. Each of these models may be used to manipulate the outcome variable, so each model includes some predictor variables that can be manipulated [287]. Each regression coefficient was analysed by the t-test to determine its significance. The t-test significance level used was $p \leq 0.05$. For each model, the significant regression coefficients were identified as a way to help identify which variables have the most impact on predicting the outcome variable. However, the multiple regression solution is very sensitive to the combination of variables used to produce the model [287]. As such, a predictor variable's noted significance depends upon the other predictor variables included in the analysis. If multiple predictor variables assess the same facet of an outcome variable, each predictor variable will appear less important than if the others were not included in the analysis.

Assuming that the predictor variables are uncorrelated with each other, those with higher standardized absolute value coefficients or with larger correlations are more important to the solution than those coefficients with lower standardized absolute values [287]. Unstandardized coefficients are harder to interpret, and it is more difficult to assess the importance of predictor variables. The squared semipartial correlation, sr_i^2, shows the predictor variable's unique contribution to R^2. For standard multiple regression, this means the amount that R^2 is reduced without that predictor variable.

Each model was assessed by the F test, which tests the null hypothesis that all correlations between the outcome variable, the predictor variables, and all regression coefficients are zero. In each model developed, the F test was passed, which indicates that the relationships are not a result of chance. Adjusted R^2 values were also calculated to account for any inflation in the sample R from chance fluctuations that may have occurred

due to number of predictor variables or to the sample size used [287]. Residuals are the differences between obtained and predicted outcome variable scores. Bivariate scatterplots of the residuals for each pair of variables were prepared and examined to check that they were roughly oval-shaped, which is the expected distribution for linear variables.

Artificial neural networks may produce alternate models, which in some cases have shown higher R^2 values. However, multiple regression is good at showing capabilities of specific values. Some studies combined multiple regression with artificial neural networks [292], [293], [294] and found that artificial neural network models tend to show higher R^2 values. However, neural network models do not provide information on relationships between the outcome variable and predictor variables, and they are specific to the experimental setups for which they were prepared [293], [295]. In future, the database used in this study could be used to produce artificial neural networks.

5.3.3. Model Abbreviations and Units

Each model is summarized in tables within Sections 5.4, 5.5, and 5.6. To allow this, several abbreviations were necessary as shown in Table 7. The units for each variable modelled are also listed.

Table 7. Abbreviations and units for each variable modelled

Abbreviation	Variable	Unit
$\%CO_2$	% CO_2 added to gas supply by volume	%
$C_{L/W}$	ratio of average cell length/average cell width	--
CW_{Min}	minimum cell width	µm
dw	dry weight	--
GFR	gas flow rate	$L\ L^{-1}\ min^{-1}$
LI	light intensity	$\mu E\ m^{-2}\ s^{-1}$
IS	illumination schedule	hr
MLC	maximum lipid content	% dw
pH_{Avg}	average pH	--
SGR	specific growth rate	d^{-1}
Temp	temperature	°C
VLP	volumetric lipid productivity	$mg\ L^{-1}\ d^{-1}$
Vol	culture volume	mL
Salinity	salinity	ppt

5.4. Specific Growth Rate Models

Several SGR models were developed using the database subset of cases with SGRs. First, each modelling variable was analysed to determine whether it fit the normal distribution, and several transformations were evaluated. P-P plots were produced to determine the optimal transformation for each variable. Optimal P-P plots of all variables are shown in Figure 34. Next, several models were produced.

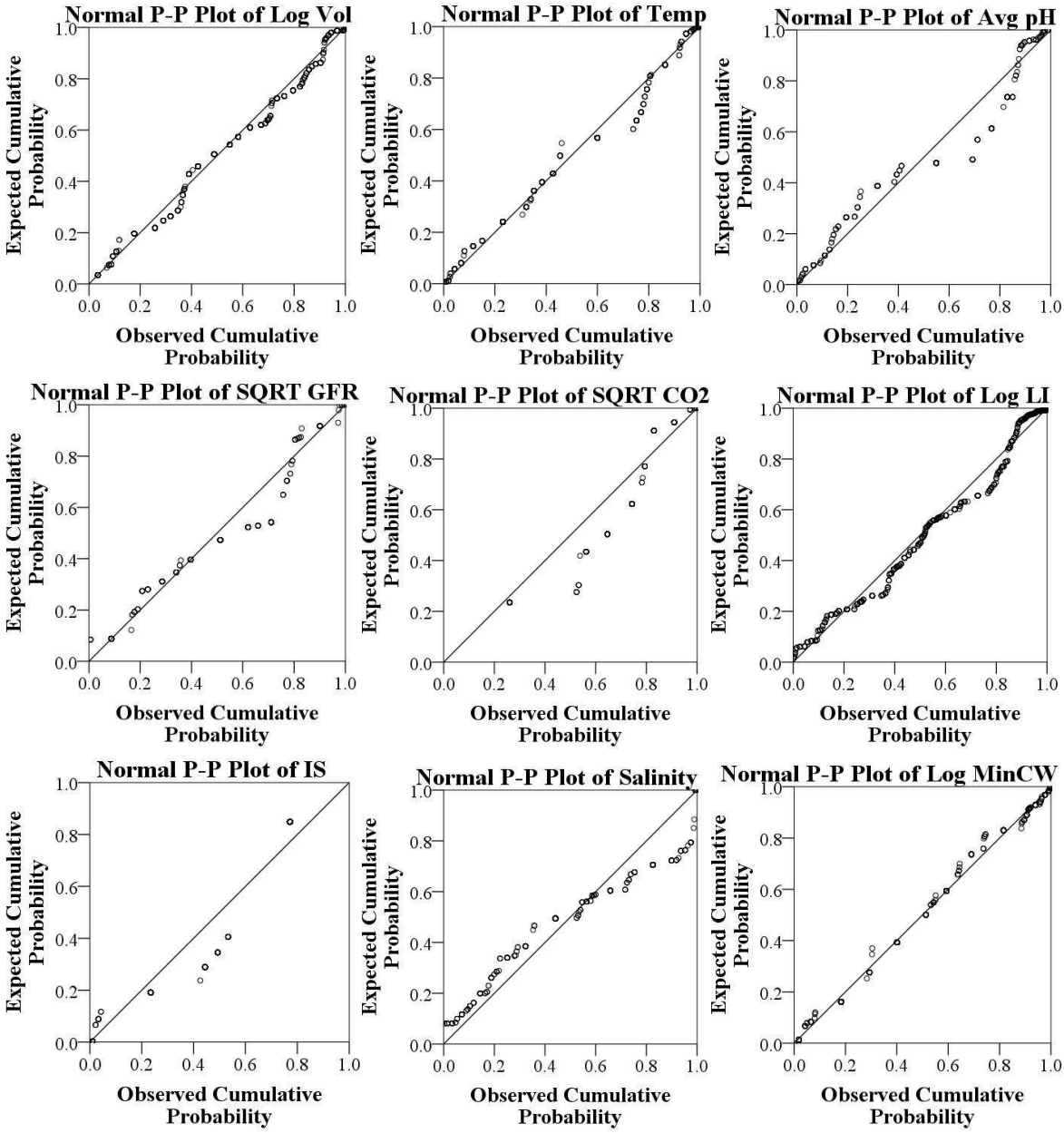

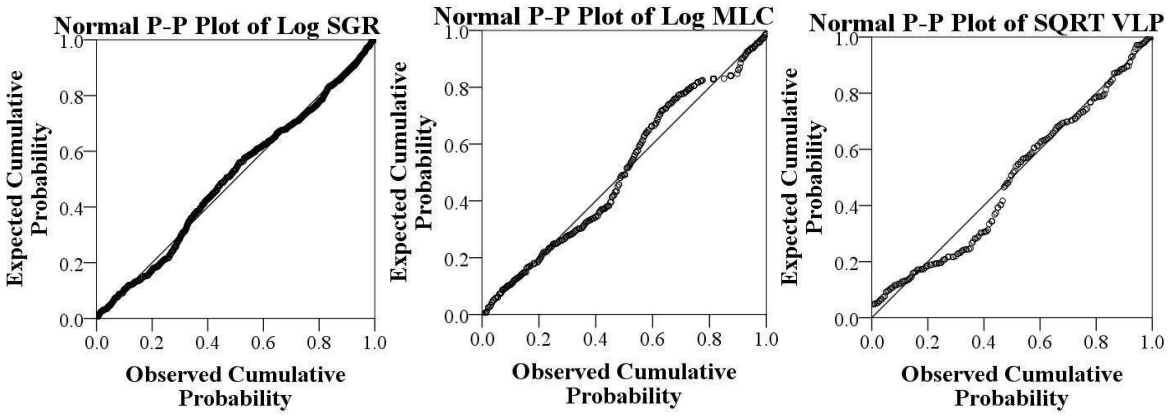

Figure 34. P-P plots of variables used to develop specific growth rate models
This figure shows the expected versus the actual probabilities of the residuals for each variable. Each variable is shown using the transformation used to develop the SGR models.

Five models were developed to quantify the effects of several predictor variables on SGRs. Model SGR_A was produced using only four experimental variables, and it is shown in Table 8. Model SGR_A has an R^2 of 0.275 for 295 cases covering 48 algae species as reported in 31 publications. However, by removing outliers identified using Mahalanobis distance, the R^2 can be increased to 0.415 for 273 cases. The dataset used to produce Model SGR_A used culture volumes from 24 mL to 240 L and temperatures from 10-42 °C. The cultures were grown under a range of light intensities from 25-3270 $\mu E\ m^{-2}\ s^{-1}$ for 9-24 hours per day. The gas flow rates used ranged from 0.007-5.5 $L\ L^{-1}\ min^{-1}$ with 0-18.37% CO_2 added. Of the parameters in this model, nearly all of the variation in SGRs was accounted for by the $\%CO_2$ added to the culture and the illumination schedule.

Cell dimensions were incorporated into Model SGR_B, which has an R^2 of 0.231 for 331 cases covering 46 algae species as reported in 34 publications. By removing outliers identified using Mahalanobis distance, the R^2 can be increased to 0.475 for 285 cases. Model SGR_B was produced using culture volumes from 52 mL to 240 L and temperatures from 10-41 °C. The cultures were grown under a range of light intensities from 25-3270 $\mu E\ m^{-2}\ s^{-1}$ for 10-24 hours per day. The gas flow rates used ranged from 0.005-7.5 $L\ L^{-1}\ min^{-1}$ with 0-20% CO_2 added. The cells used in this study had average dimensions ranging from 1.6-280 µm long by 1.6-13 µm wide. Of the parameters in this model, 15% of the

variation in SGRs was accounted for by volume.

Table 8. General specific growth rate models

Model Name	Dependent Variable	Regression Equation[1]							
SGR_A	Log SGR	y = -0.099(**Log Vol**) – 0.169(**SQRT %CO_2**) – 0.111(**Log LI**) + 0.034(**IS**) – 0.299							
		N	pr^2	R	R^2	R_{Adj}	SE	F	$F_{Critical}$
		295	0.024	0.525	0.275	0.265	0.36	27.521	2.40
SGR_B	Log SGR	y = -0.238(**Log Vol**) + 0.123(**SQRT GFR**) – 0.092(**SQRT %CO_2**) + 0.346(**Inv $C_{L/W}$**) + 0.180							
		N	pr^2	R	R^2	R_{Adj}	SE	F	$F_{Critical}$
		331	0.009	0.481	0.231	0.22	0.36	24.544	2.40
SGR_C	Log SGR	y = 1.154(**pH_{Avg}**) – 0.223(Log MLC) + 0.055(**SQRT GFR**) + 0.429(SQRT %CO_2) – 9.708							
		N	pr^2	R	R^2	R_{Adj}	SE	F	$F_{Critical}$
		91	0.022	0.787	0.619	0.601	0.16	34.932	2.48
SGR_D	Log SGR	y = 0.572(**Log Vol**) + 0.009(Temp) + 0.211(**pH_{Avg}**) – 0.198(**Log LI**) + 0.059(**IS**) + 0.001(Log MLC) – 4.423							
		N	pr^2	R	R^2	R_{Adj}	SE	F	$F_{Critical}$
		107	0.107	0.723	0.523	0.495	0.21	18.301	2.19
SGR_E	Log SGR	y = 2.396(**Log Vol**) – 0.146(**pH_{Avg}**) + 0.614(**Log MLC**) + 0.85(**SQRT GFR**) – 7.485							
		N	pr^2	R	R^2	R_{Adj}	SE	F	$F_{Critical}$
		91	.073	0.838	0.702	0.688	0.14	50.543	2.48

[1] Significant variables are shown in bold. The t-test significance level used was $p \leq 0.05$.

Model SGR_C has an R^2 of 0.619 for 91 cases covering 18 algae species as reported in 7 publications. Model SGR_C was produced covering culture volumes from 500-1500 mL and temperatures from 15-35 °C. The cultures were grown under a range of light intensities from 80-760 μE m^{-2} s^{-1} for 12 or 24 hours per day. The gas flow rates ranged from 0.007-2 L L^{-1} min^{-1} with 0-15% CO_2 added. Of the parameters in Model SGR_C, 54% of the variation in SGRs was accounted for by gas flow rate, 26% by pH, and 18% by %CO_2 added.

Model SGR_D, as shown in Table 8, was produced to predict SGRs when cultures are not aerated. Using these units gave a model that predicts 52% of the variability in 23 algae

species as reported in 11 publications. Removing 3 outliers based on Mahalanobis distance would increase the R^2 to 0.684. The dataset includes cultures grown from 500 mL-6 L with MLCs ranging from 6.2-33.6% dw. The temperatures used ranged from 15-35 °C, and the average culture pH values ranged from 6.8-9.0. Also, the dataset included algae grown under 80-923.3 μE m^{-2} s^{-1} light intensity for 12 or 24 hours per day. In this dataset, illumination schedule accounted for 44% of the variability in SGRs.

As shown in Table 8, Model SGR_E predicts 70% of the variability in SGRs from 18 algal species from 7 publications. The algae dataset contains cultures from 500-1500 mL grown from 15-35 °C with average pH values from 6.8-8.6. The cultures were aerated from 0.007-2 L L^{-1} min^{-1} and 0-15% CO_2 added. Gas flow rate accounted for 61% and volume accounted for 27% of the variability in SGRs in this dataset.

These models help illuminate the contributions of several variables to predicting SGRs of algae grown under a wide variety of conditions. Salinity was also studied, but it did not produce a significant regression coefficient within the SGR cases included in these models. These models indicate that gas flow rate, illumination schedule, volume, average pH, and CO_2 % added account for the most variability within the cases included in this study.

5.5. Maximum Lipid Content Models

Several MLC models were developed using the database subset of cases with MLCs. tested. First, each variable to be modelled was analysed to determine whether it fit the normal distribution, and several transformations were analysed by producing P-P plots. The optimal P-P plots are shown in Figure 35.

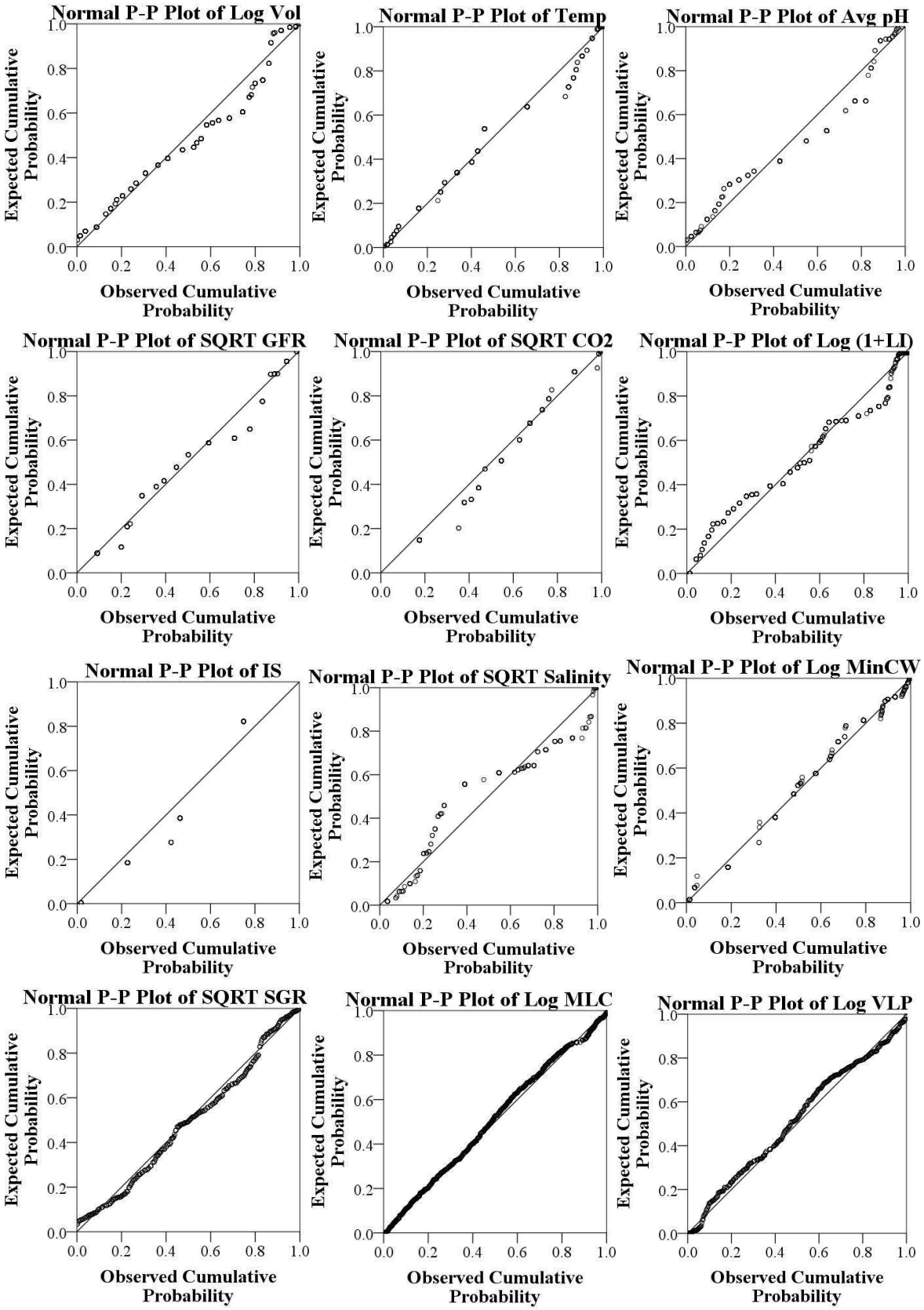

Figure 35. P-P plots of variables used to make maximum lipid content models
This figure shows the expected versus the actual probabilities of the residuals for each variable. Each variable is shown using the transformation used to develop the MLC models.

Five models were developed to assess the contributions of several variables towards algae MLCs. Model MLC_A is a non-species specific model to predict MLCs using only experimentally controlled variables. This model, shown in Table 9, uses 31 species from 12 published sources. The dataset includes cultures grown from 14-35 °C at volumes from 500 mL-110 L. The average pH values ranged from 6.59-8.6, the gas flow rates used were 0.007- 2 L L^{-1} min^{-1}, and the light intensities ran from 30-850 μE m^{-2} s^{-1}. Additional predictor variables tested were CO_2 % within the gas supplied and illumination schedule used, but these variables did not improve the model's R^2 value. Model MLC_A has an R^2 of 0.351. Using this database, a model containing only a handful of environmental parameters predicted 35% of the variation in MLCs for 31 algae species in 159 trials. Volume and average pH respectively accounted for 10.1% and 9.3% of variation in MLCs.

Table 9. General maximum lipid content models

Model Name	Dependent Variable	Regression Equation[1]							
MLC_A	Log MLC	y = 0.153(**Log Vol**) – 0.205(**pH_{Avg}**) – 0.16(**SQRT GFR**) – 0.092(**Log (1 + LI)**) + 2.684							
		N	pr^2	R	R^2	R_{Adj}	SE	F	$F_{Critical}$
		159	0.01	0.593	0.351	0.334	0.19	20.831	2.43
MLC_B	Log MLC	y = 0.304(**SQRT SGR**) – 0.412(**SQRT GFR**) – 0.014(**Temp**) – 0.178(**pH_{Avg}**) + 2.962							
		N	pr^2	R	R^2	R_{Adj}	SE	F	$F_{Critical}$
		91	0.131	0.742	0.550	0.530	0.14	26.329	2.48
MLC_C	Log MLC	y = -0.372(**SQRT SGR**) – 0.226(**SQRT GFR**) – 0.449(**Log (1 + LI)**) + 0.276(**Log VLP**) + 2.367							
		N	pr^2	R	R^2	R_{Adj}	SE	F	$F_{Critical}$
		82	0.12	0.779	0.607	0.587	0.19	29.694	2.49
MLC_D	Log MLC	y = -0.387(**SQRT SGR**) – 0.219(**SQRT GFR**) – 0.423(**Log (1+LI)**) + 0.261(**Log VLP**) – 0.135(Log CW_{Min}) + 2.413							
		N	pr^2	R	R^2	R_{Adj}	SE	F	$F_{Critical}$
		82	0.12	0.782	0.612	0.587	0.19	23.968	2.33
MLC_E	Log MLC	y = 0.173(**SQRT SGR**) + 0.283(**pH_{Avg}**) – 0.022(**SQRT Salinity**) – 1.145							
		N	pr^2	R	R^2	R_{Adj}	SE	F	$F_{Critical}$
		81	0.149	0.739	0.546	0.528	0.14	30.855	2.72

[1] Significant variables are shown in bold. The t-test significance level used was $p \leq 0.05$.

Models MLC_B, MLC_C, and MLC_D incorporate gas flow rate and SGR along with a variety of other variables. Model MLC_B, which is displayed in Table 9, uses 18 species from 7 sources. Model MLC_B's dataset includes 500-1.5 L cultures grown from 15-35 °C using average pH values from 6.8-8.6. The cultures were aerated from 0.007-2 L L^{-1} min^{-1} using air supplemented from 0-15% CO_2, and light intensities ranging from 80-760 μE m^{-2} s^{-1}. In Model MLC_B, 37% of the MLC variability was accounted for by the gas flow rate used. All of the model's predictor variables are significant, and all but 2.6% of the R^2 is attributable to unique sources.

Model MLC_C is a similar model using light intensity and VLP data rather than temperature and average pH data. Model MLC_C uses 20 species from 9 sources. Model MLC_C used a dataset of 500 mL-3.4 L cultures aerated from 0.11-5.5 L L^{-1} min^{-1} with 0-15% CO_2 added to the gas supply. The cultures used light intensities from 25-760 μE m^{-2} s^{-1} and obtained SGRs from 0.11-1.75 d^{-1} and VLPs from 0.28-357.5 mg L^{-1} d^{-1}. Cell dimensions were also added to see their effects on the model's ability to predict variation in MLC values. Within the dataset, average cell lengths ranged from 2.5-280 μm, and average cell widths ranged from 2.5-11.5 μm. As Model MLC_D shows in Table 9, adding minimum cell width as a variable caused a slight increase in R^2, but it was not a significant variable. It is important to note, however, that the regression coefficient significance tests are only sensitive to the unique variance that an independent variable adds to the R^2 [287]. Light intensity and VLP accounted for 31% and 25% of the variability MLC in Model MLC_C and Model MLC_D respectively.

Model MLC_E considers salinity effects on algae. These data are only for algae species that can be grown under saline conditions ranging from 3.8 ppt to 211.8 ppt. Overall, this dataset includes 23 species from 7 published studies. The dataset contains algae grown from 1-160 L at temperatures from 13-35 °C. The average pH values ranged from 8-9.7,

and the SGRs achieved were 0.03-2.5 d^{-1}. Salinity is a significant regression coefficient in this model using a t-test at $p \leq 0.05$. Although this model was produced using only 81 cases, it satisfies the N to predictor variables ratio because of the high correlations between the variables, as indicated by the smallest pr^2 being 0.149. In Model MLC_E, nearly 30% of the variability in MLCs was accounted for by average pH.

To summarize, Model MLC_A indicated volume and average pH accounting for the most variation in R^2. Model MLC_B did not include volume but showed gas flow rate accounting for the most R^2 variation. Model MLC_E also leaves out volume, and the most variation in R^2 was due to average pH. When light intensity and VLP were included, as in Model MLC_C and MLC_D, light intensity accounted for the most variation in R^2 followed by VLP. These models point to the predictor variables most likely to account for variation within MLCs for a wide variety of species grown under many conditions.

5.6. Lipid Productivity Models

Two VLP models were developed using the database subset of cases containing volumetric lipid productivities. First, each modelling variable was analysed to determine whether it fit the normal distribution, and several transformations were tested. P-P plots were produced to determine the optimal transformations, as shown in Figure 36.

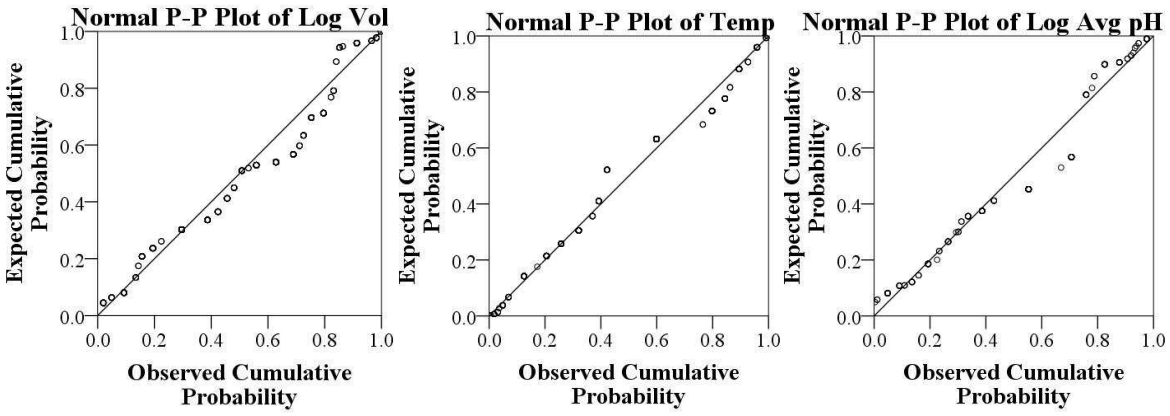

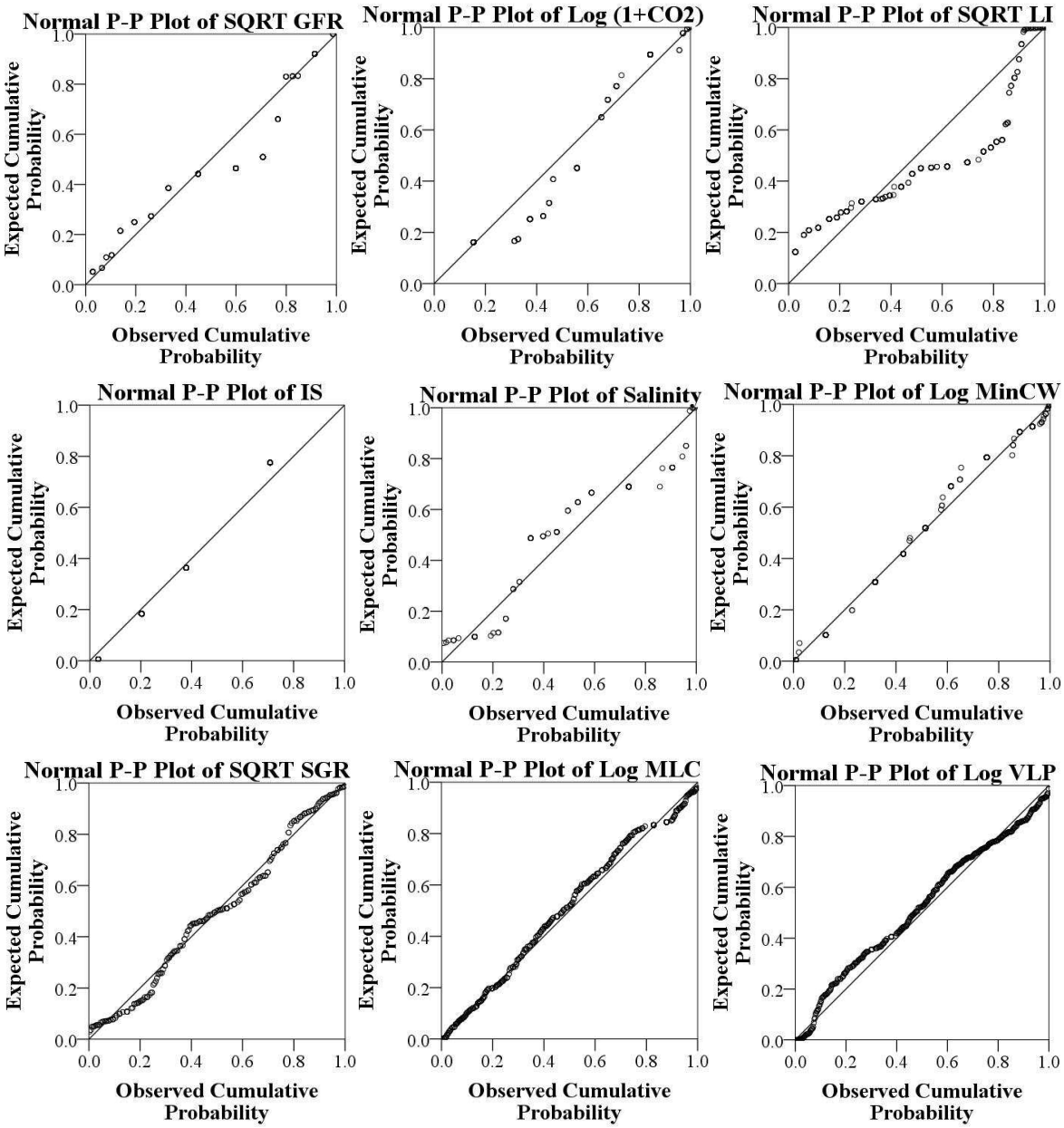

Figure 36. P-P plots of variables used to make lipid productivity models
This figure shows the expected versus the actual probabilities of the residuals for each variable. Each variable is shown using the transformation used to develop the VLP models.

Two models were produced to assess effects of several predictor variables on lipid productivity. Model VLP_A uses only experimental variables to estimate algae lipid productivity. This model uses data from 18 published studies, and includes 44 algae species. The dataset contains 75 mL-18 L cultures from 14-30 °C. The cultures were supplemented with 0-28% CO_2. The cultures were grown under 25-760 μE m^{-2} s^{-1} light intensities for 12, 16, or 24 hours per day. Removing multivariate outliers from Model

VLP_A's dataset based on a Mahalanobis distance greater than 20.515 (χ^2, 0.001) increases the R^2 to 0.658. Table 10 shows the statistics for Model VLP_A. Light intensity accounts for nearly 28%, and illumination schedule accounts for 16% of the variation in lipid productivities within the dataset.

Table 10. General volumetric lipid productivity models

Model Name	Dependent Variable	Regression Equation[1]							
VLP_A	Log VLP	y = -0.066(Log Vol) – 0.007(Temp) + 0.549(**Log (1+%CO_2)**) + 0.082(**SQRT LI**) + 0.056(**IS**) – 0.758							
		N	pr^2	R	R^2	R_{Adj}	SE	F	$F_{Critical}$
		221	0.033	0.697	0.486	0.474	0.48	40.723	2.26
VLP_B	Log VLP	y = -0.083(Log Vol) – 0.008(Temp) + 0.526(**Log (1+%CO_2)**) + 0.085(**SQRT LI**) + 0.045(**IS**) – 0.485(**Log CW_{Min}**) – 0.178							
		N	pr^2	R	R^2	R_{Adj}	SE	F	$F_{Critical}$
		221	0.033	0.710	0.504	0.490	0.47	36.211	2.14

[1] Significant variables are shown in bold. The t-test significance level used was $p \leq 0.05$.

Model VLP_B was produced to estimate VLPs with cell size included as an additional predictor variable. This model contains data from 44 species in 18 publications, as described for Model VLP_A. The dataset contained cells of average cell length from 2.4-262.5 µm and average cell width from 2.3-27.5 µm. Cell size is a significant variable in Model VLP_B, but the majority of the VLP variability, 29%, is predicted by light intensity.

Salinity may also be a significant predictor of VLP; however, insufficient data were available to prepare models with salinity as a predictor. These VLP models show that lipid productivity can be accurately estimated for algae. Model VLP_A includes only variables set by the experimenter, so it may be useful in designing facilities to produce lipids.

5.7. Model Discussion

The most significant variables affecting microalgae SGR, MLC and VLP were identified using datasets containing data from several species. These models have other potential uses too. They could be used to predict SGRs, MLCs, and VLPs under specified environmental conditions. They could also be used to predict what conditions will cause

maximum or minimum SGRs, VLPs, or MLCs.

These models are based on 81 species from 53 published studies. An additional 78 publications were included in the database used to generate these models, but the models were generated from cases without missing values. The cultures in the study were grown on scales from 24 mL-240 L, so they may give more accurate predictions than models produced from lab scale experiments alone. Furthermore, the significant variables were identified using a wide variety of experimental and species specific variables. The species within these datasets have average cell lengths ranging from 1.6-280 μm. Cells with longer cell lengths may have greater surface areas and are generally more likely to settle within the reactor and to require increased energy to remain mixed. Cell sizes were included in each model type to look for possible effects on SGR, MLC, and VLP. Along with containing a wide variety of environmental conditions and species, the data used to prepare these models were generated by many researchers in many labs, so they should represent an accurate representation of algae data.

Three models were developed to estimate SGRs using a handful of easily obtainable variables, and they indicated that volume, illumination schedule, and CO_2 % added account for the most variability within the cases included in this study. Light intensity was also a significant variable. These results are useful because they indicate the importance of more than light intensity, which is commonly found significant. For example, a photosynthetic yield model based on *Monodus subterraneus* grown in 450 mL bubble columns found productivity was directly correlated with light intensity; this model gave an R^2 of 0.92 but showed high error bars [296]. Also, a stepwise multiple regression study ($R^2 = 0.845$) on *Gracilaria tenuistipitata* found that light intensity and salinity were significant predictors of growth [284]. Sediment was also modelled but was not significant [284]. Since more culturing parameters were considered in the models

developed here, this work will be useful in anticipating the results of many different growth regimes on a species.

The models discussed here had R^2 values ranging from 0.351-0.782. This compares favourably to other multiple regression models containing multiple algae species. Models considering blooms of *Microcystis* in a mixed population produced R^2 values ranging from 0.11-0.73 [277]. Meanwhile models considering macroinvertebrate species abundance within a population under several environmental conditions reported R^2 values from 0.07-0.39 [276]. These models were reported as highly predictive. It is true that a model with a low R^2 value can provide valuable information on statistically significant predictors, but it does not have the ability to predict accurately.

In this study, the MLC models showed temperature and light intensity to be significant predictors of MLC. These results have also been found in other studies, whose data is not included in this database. Multiple regression of *Nannochloropsis oculata* growth in outdoor vertical flat-plate PBRs indicated that up to half of the variation in total lipids could be accounted for by temperature and total global radiation [12]. Temperature alone explained 38% of the variation [12]. This *N. oculata* model did not consider gas flow rate effects on lipid content; however, in Model MLC_B, the gas flow rate used was found to predict even more variation than temperature. In fact, nearly 49% of the variability in MLCs was accounted for by the gas flow rate used. Model MLC_B was produced using 15 algae species grown under a variety of conditions. Model MLC_B indicates that temperature is a significant predictor of variability but is inversely related to MLC. This result is supported by small-scale studies on *Dunaliella salina* showed increased lipids at 12 °C compared to 30 °C [10]. Also, Renaud et al [139] grew tropical algae and *Isochrysis* sp at temperatures from 25-35 °C, and they found that most of their species, *Rhodomonas* sp, *Cryptomonas* sp, prymnesiophyte NT19, and *Isochrysis* sp, achieved highest lipid contents

over temperatures from 27-30 °C. Meanwhile, *Chaetoceros* sp produced the most lipids at 25 °C [139]. These result show an overall inverse relationship between temperature and MLC, which is in agreement with the relationship predicted in Model MLC_B.

Model MLC_A predicted >35% of variability in MLCs obtained for 31 species grown in fresh and saltwater on scales from 500 mL to 110 L with average pH values from 6.59-8.6. Of the parameters in this model, volume and average pH respectively accounted for 10.1% and 9.2% of variation in MLCs. This model helps enumerate the importance of the environmental variables in growing algae, and it shows that trends are possible to determine even when considering a large number of potential predictor variables. Two VLP models were prepared, and illumination schedule was found to be significant in accounting for VLP variability within the dataset. Light intensity was also found to be significant in accounting for variability in VLPs within the dataset.

5.8. Methods of Improving Future Models

This work is an attempt to make better use of published data as collated for thesis objective 2. Due to the large dataset used to produce the models, the results have lower correlation coefficients than they would if they were generated by comparing only like with like datasets, such as using data from experiments with the same species, nutrient concentrations, and lighting regimes. Also, these models do not account for variability from experimental errors owing to the wide range of experiments, growth and lipid content testing procedures, and experimental apparatus used to generate the datasets.

A variety of statistics were prepared to validate each model as recommended by Wang and Jain [297]. In summary, all of the models detailed here have F values much greater than their F critical values; this indicates that all of the models are likely to have statistically significant predictive capability. These models provide good estimates; however, they can still be enhanced by considering additional factors. Accounting for

lipid contents under nitrogen or other nutrient limitation could enhance the predictive capabilities of the MLC models. Another potential source of residual variability in these models is the fact that the initial growth phase of the culture is often not accounted for in published studies. Cultures inoculated in growth phases other than exponential are likely to experience lag phases that can significantly affect the SGR over a set period. Other variables not modelled here that may affect SGR, MLC and VLP are culture density, photon utilization efficiency, photoinhibition, and non-linear responses to environmental conditions [12]. These models may be further refined by adding categorical information, such as culture media, heterotrophic or autotrophic growth, and nitrogen source.

In future, these models could also be examined for the presence of suppressor variables. If present, a suppressor variable weakens or changes the relationship between two variables such that, if the suppressor variable is controlled for statistically, the true relationship between the two variables is stronger or occurs in the opposite direction than seen when the suppressor variable is included.

In addition, some variables could be grouped and modelled to increase the predictive capability of these models. For example, the data could be grouped by growth phase at time of lipid measurement. This could be important because some algae produce different types of oils during different phases of growth, as discussed in Section 2.4.2. Along with growth phase, fatty acid composition could be grouped to account for its changes under various environmental conditions. Season is another possible grouping that could enhance the models. Olofsson et al [12] found that *Nannochloropsis oculata* grown for two years in outdoor PBRs contained 20-30% dw lipids from summer to autumn but only 11-22% dw lipids from winter to spring. Clearly, understanding the season's effects on lipid content within algae grown in outdoor PBRs is necessary for industrial scale algae growth. It is also possible that species specific properties account for some of the remaining

variability in SGR, MLC, and VLP. This hypothesis is examined in Chapter 6.

Other models predict biomass yield [261], volumetric biomass productivity [273], [296] or areal biomass productivity [298]. These models show excellent predictive capabilities, but they are not applicable to other algae species, reactor types, or less controlled environmental conditions. Meanwhile, the models developed here were generated from a much more varied and comprehensive dataset.

5.9. Conclusions

Microalgae have great promise as sources of biodiesel, nutraceuticals, pigments, and food for aquaculture. However, high SGRs, MLCs, and VLPs are essential to make industrial scale microalgae production feasible for a wider range of products. A wide variety of environmental parameters affect the growth rates of various algae, including light intensity, light source, illumination schedule, gas flow rate, CO_2 concentration, culture volume, temperature and salinity. The models discussed here assess the significance of predictor variables on SGRs, MLCs, and VLPs.

A range of models was developed depending on the data available. Using only four environmental parameters, over 40% of the variation in SGRs was predicted for 48 algae species, and 35% of variability in MLCs was predicted from 31 species. Nearly 49% of variation in VLPs for 44 species was accounted for by five environmental parameters. Together, these models help identify variables that should be concentrated on during algae production facility design, biomass life cycle analyses, and carbon capture estimations. These models are especially useful because they are composed of variables that are relatively easy to obtain with limited specialized equipment.

Chapter 6. Genus Specific Models

Microalgae species choice has major impacts on the possible productivity for biodiesel production, but relatively few species have been studied. This number is increasing rapidly as more screening studies are done on recent isolates from wild populations of algae. Several general models were discussed in Chapter 5, but one question raised was the possibility of genus specific models enhancing predictive capabilities.

Of all of the species in the database mentioned in Chapters 3-5, the genera with the most data were selected to produce genera specific models using multiple regression analysis. Section 6.2 describes each of these genera, which are *Chlorella*, *Isochrysis*, *Nannochloropsis*, *Phaeodactylum*, and *Tetraselmis*. SGR models are shown in Section 6.3, and MLC models are given in Section 6.4. Several VLP models are described in Section 6.5. Where possible, each of these models was compared to previously produced models for those genera in Section 6.6. Finally, Section 6.7 discusses the genus specific models in relation to the general models produced in Chapter 5.

6.1. Model Development Methods

Using the database detailed in Chapters 3 and 4, several genus specific models were produced. The modeling procedures are the same as those detailed in Chapter 5. The units and abbreviations for each variable used in the models are the same as shown in Table 7.

These models were prepared using SPSS v21. First, data for each genus were assessed for normality and tested with log, inverse, and square root transformations. Then, the models were produced using SPSS v21 and tested for validity. P-P plots were used to determine if transformations were necessary and, if so, which were most appropriate for each variable. When more than one transformation P-P plot was near normal, univariate regression equations were formed to identify the transformation (if any) with the highest R^2 value for use in multiple regression models. These univariate regressions were also used to identify independent variables with $R^2 > 0.1$ for inclusion in draft multiple

regression models; this method has been used in similar multiple regression studies [299].

6.2. Description of Each Genus

Multiple regression models were produced for several microalgae genera. These include *Chlorella*, *Isochrysis*, *Nannochloropsis*, *Phaeodactylum*, and *Tetraselmis*. Each of these genera is described briefly below.

Chlorella: *Chlorella* are single celled, round algae without flagella, and they range in diameter from 1.6-12 µm. They may be classed as Chlorophyceae or Trebouxiphyceae. *Chlorella* may be grown in marine and freshwater and are commonly cultured in a wide variety of media. *Chlorella* were one of the first genera to be grown on a large-scale and have been grown commercially since the 1960s [36]. Large-scale *Chlorella* production occurs around the world, especially in Taiwan, Germany, and Japan [41]. *Chlorella* are often used for human nutrition, cosmetics production, and aquaculture feed [36], [41], [42]. Successful industrial-scale growth is accomplished using a high inoculant level and harvesting the culture quickly before the reactor has time to become contaminated. Also, *Chlorella* can be grown phototrophically, mixotrophically, and heterotrophically.

Isochrysis: *Isochrysis* are unicellular marine organisms in the Class Prymnesiophyceae. The cells are oval shaped with two equal flagella. Their cell widths range from 2-7 µm and lengths from 2-12 µm. *Isochrysis* are commonly used as feed for bivalve larvae [300].

Nannochloropsis: *Nannochloropsis* are marine organisms in the Eustigmatophyceae Class. The cells can be round or oval-shaped, and they range from 1-8 µm long and from 1-4 µm wide. *Nannochloropsis* can produce EPA for nutritional supplements, and they are grown as food sources for aquaculture operations. They are also a promising oil source due to their growth rates and ability to accumulate lipids under nitrogen depletion [4].

Phaeodactylum: *Phaeodactylum* are unicellular marine organisms in the Bacillariophyceae Class. They can grow in brackish water, and some species can also

grow in freshwater. The cells can be rod-shaped with short extensions at both ends similar to a boat shape; they can also be crooked or joined into a T shape. *Phaeodactylum* cells range from 2-6 µm wide and 11.5-32 µm long.

Tetraselmis: Tetraselmis is a genus of unicellular green algae with flagella, and it includes many marine and a few freshwater species. *Tetraselmis* species are in the Prasinophyceae Class, and they are found in temperate areas around the world. Motile *Tetraselmis* cells have four equal length flagella (2 pairs) attached at the bottom of an apical depression. The flagella are approximately half as long as the cell's length. Cells may be oval-shaped or round, and they are generally 3-25 µm long by 3-20 µm wide. *Tetraselmis* cells use their flagella to swim with a breaststroke motion and have been noted to swim in long straight lines with abrupt direction changes [193]. *Tetraselmis suecica* swims at an average rate of 180 µm s^{-1} [170]. *Tetraselmis* may be grown in a wide variety of media, including Conway, Erdschreiber, E/4, F, F2, K, L1, Miquels modified, and Z8 media. *Tetraselmis* are commercially produced as food for aquaculture operations [42], [205].

6.3. SGR Models

6.3.1. *Isochrysis* Models

Several SGR models were developed using the database subset of *Isochrysis* cases with specific growth rates. This dataset includes the 2 *Isochrysis* species shown in Table 11.

Table 11. *Isochrysis* species and sources used to develop models

Species	**Source**
Isochrysis galbana	[97], [103], [115], [130], [197]
Isochrysis sp	[99], [118], [119], [137], [138], [139], [162]

First, each variable to be modelled was analysed to determine whether it fits the normal distribution, and several transformations were tested. P-P plots were produced to determine the optimal transformation for each variable. Figure 37 shows the P-P plots for the variables with the optimal transformation.

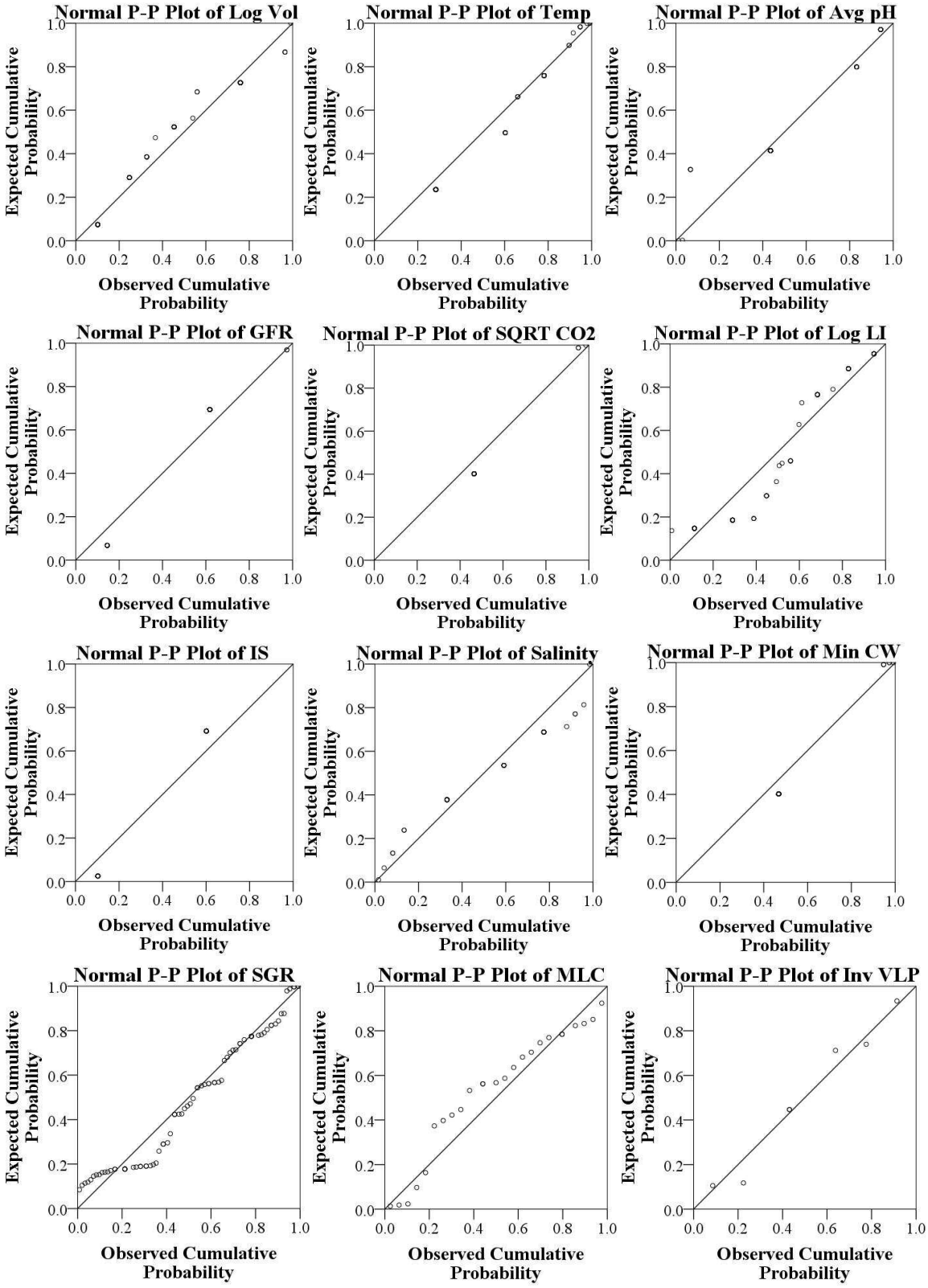

Figure 37. P-P plots of variables used to make *Isochrysis* specific growth rate models
This figure shows the expected versus the actual probabilities of the residuals for each variable. Each variable is shown using the transformation used to develop the models.

Table 12 shows a model that predicts nearly 47% of the variation in SGRs for two *Isochrysis* species in 6 publications. This model includes data from 500 mL-4 L cultures

grown using sparged air with 0-1.5% CO_2 added at a gas flow rate from 0.007-0.63 L per L culture per min. CO_2 alone accounts for 18.3% of the variation in SGRs. Adding temperature to *Isochrysis* SGR_A increases the R^2 to 0.498 with the same N. Using the same dataset, model *Isochrysis* SGR_B predicts over 51% of the variability in SGRs by including temperature and light intensity, even though neither variable is significant. The dataset includes temperatures from 20-35 °C and light intensities from 80-3,270 µE m^{-2} s^{-1}. If minimum cell width is added to *Isochrysis* SGR_B, the R^2 increases slightly to 0.52.

Table 12. *Isochrysis* specific growth rate models

Model Name	Dependent Variable	Regression Equation[1]							
Isochrysis SGR_A	SGR	y = -0.482(Log Vol) + 0.727(**SQRT %CO_2**) + 2.251							
		N	pr^2	R	R^2	R_{Adj}	SE	F	$F_{Critical}$
		43	0.432	0.682	0.465	0.439	0.25	17.048	3.23
Isochrysis SGR_B	SGR	y = -0.594(Log Vol) + 0.749(**SQRT %CO_2**) – 0.036(Temp) – 0.155(Log LI) + 3.871							
		N	pr^2	R	R^2	R_{Adj}	SE	F	$F_{Critical}$
		43	0.187	0.717	0.514	0.463	0.24	10.040	2.62

[1] Significant variables are shown in bold. The t-test significance level used was $p \leq 0.05$.

6.3.2. *Phaeodactylum* Models

Two SGR models were developed using the database subset of *Phaeodactylum tricornutum* cases with specific growth rates as summarized in Table 13.

Table 13. *Phaeodactylum tricornutum* sources used in models

Species	**Source**
Phaeodactylum tricornutum	[115], [118], [143], [152], [154], [197]

First, each modelling variable was analysed to determine whether it fit the normal distribution. Several transformations were also evaluated. P-P plots were produced to determine the optimal transformation for each variable, as shown in Figure 38.

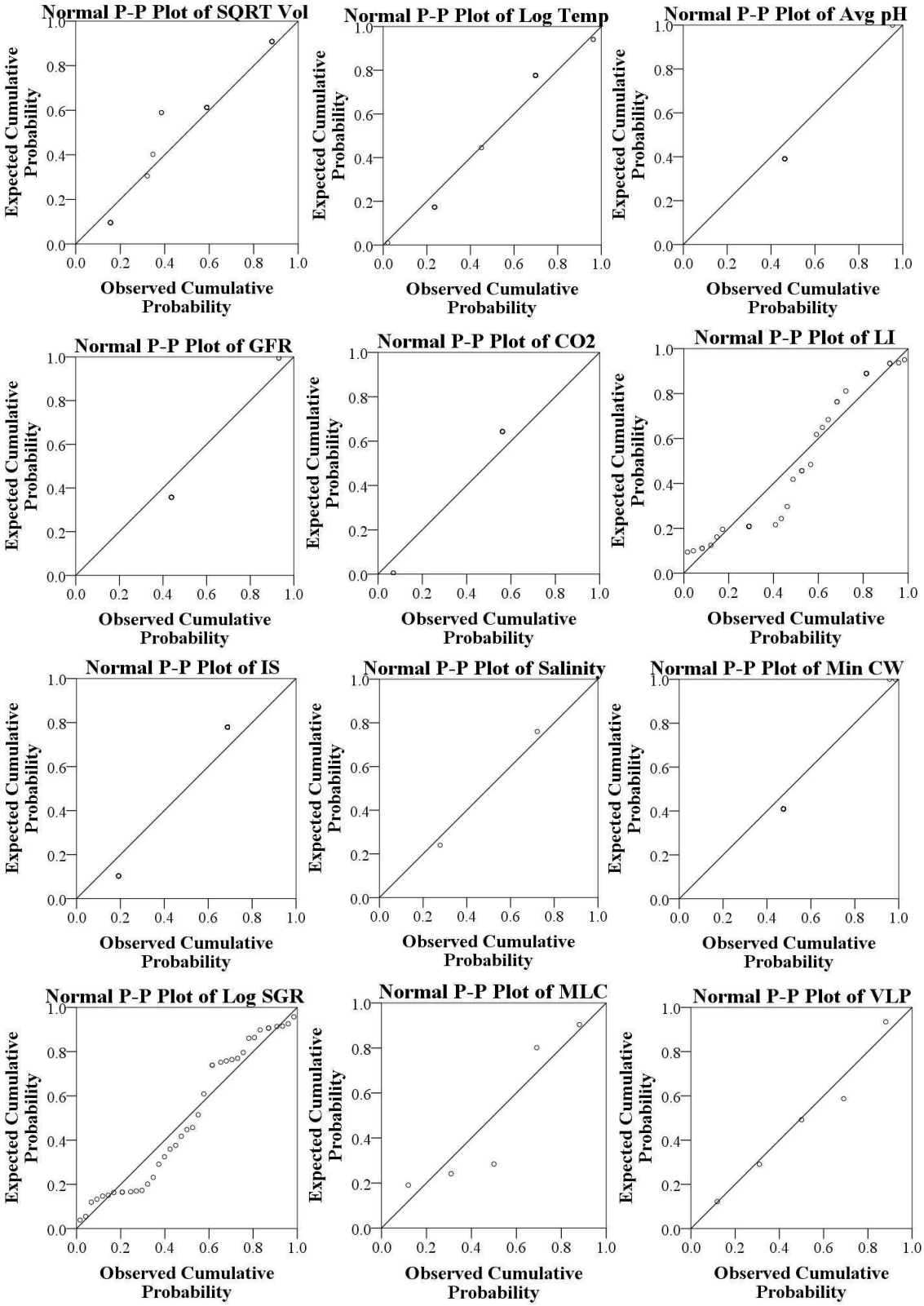

Figure 38. P-P plots of variables used to make *Phaeodactylum* specific growth rate models This figure shows the expected versus the actual probabilities of the residuals for each variable. Each variable is shown using the transformation used to develop the models.

Table 14 shows that over 72% of the variation in *Phaeodactylum tricornutum* SGRs from 6 publications can be predicted using only culture volume. Model *Phaeodactylum*

SGR_A includes data from 120 mL-8 L cultures. Model *Phaeodactylum* SGR_B also includes temperature and has an R^2 of 0.551. Model *Phaeodactylum* SGR_B was produced using data from 5 publications on 120 mL-3.4 L cultures grown at temperatures from 15-25 °C.

Table 14. *Phaeodactylum* specific growth rate models

Model Name	Dependent Variable	Regression Equation[1]							
Phaeodactylum SGR_A	Log SGR	y = -0.015(**SQRT Vol**) + 0.009							
		N	pr^2	R	R^2	R_{Adj}	SE	F	$F_{Critical}$
		39	0.85	0.85	0.723	0.715	0.28	96.404	4.11
Phaeodactylum SGR_B	Log SGR	y = -0.012(**SQRT Vol**) – 1.247(Log Temp) + 1.524							
		N	pr^2	R	R^2	R_{Adj}	SE	F	$F_{Critical}$
		30	0.686	0.742	0.551	0.517	0.31	16.551	3.35

[1] Significant variables are shown in bold. The t-test significance level used was $p \leq 0.05$.

6.3.3. *Tetraselmis* Models

Six SGR models were developed using the database subset of *Tetraselmis* cases with specific growth rate data. This dataset includes 5 species as shown in Table 15.

Table 15. *Tetraselmis* species and sources used in *Tetraselmis* specific growth rate models

Species	**Source**
Tetraselmis chuii	[159]
Tetraselmis gracilis	[100], [158], [257]
Tetraselmis sp	[97], [99], [119], [127], [129], [138], [147], [156]
Tetraselmis subcordiformis	[153]
Tetraselmis suecica	[114], [115], [116], [118], [122], [144], [151], [196], [197], [200]

First, each variable to be modelled was analysed to determine whether it fits the normal distribution, and several transformations were tested. P-P plots were generated to determine the optimal transformation for each variable. These are shown in Figure 39.

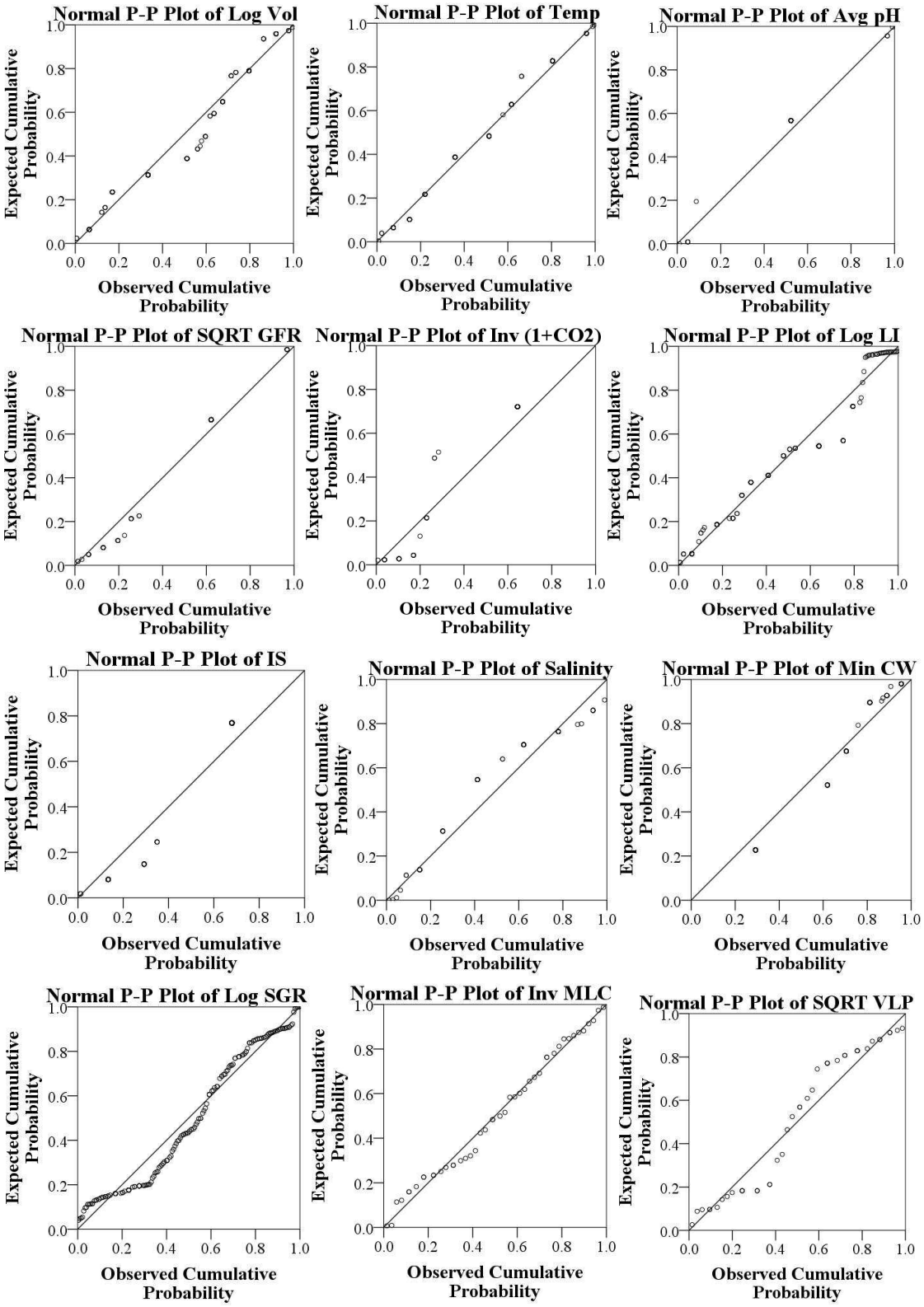

Figure 39. P-P plots of variables used to make *Tetraselmis* specific growth rate models
This figure shows the expected versus the actual probabilities of the residuals for each variable. Each variable is shown using the transformation used to develop the models.

Model *Tetraselmis* SGR_A, as shown in Table 16, predicts over 56% of the variation in SGRs for 3 *Tetraselmis* species in 7 publications using only three variables. This model

includes data from cultures grown over a wide range of volumes from 800 mL-100 L. These cultures were sparged with air containing 0-18.4% CO_2 added at gas flow rates from 0.007-5.5 L L^{-1} min^{-1}. Light intensities ranged from 80-2,558 μE m^{-2} s^{-1}. Light intensity predicts 44% of the variability, and CO_2 % added predicts almost 12% of the variation of SGRs. When considering volume rather than light intensity, as in *Tetraselmis* SGR_B, the model is improved to an R^2 of 0.613 using the same dataset. In *Tetraselmis* SGR_B, 50% of the variability in SGRs is accounted for by culture volume.

Table 16. *Tetraselmis* specific growth rate models

Model Name	Dependent Variable	Regression Equation[1]							
Tetraselmis SGR_A	Log SGR	y = 0.113(SQRT GFR) – 0.669(**Log LI**) + 0.69(**Inv (1 + %CO_2)**) + 0.699							
		N	pr^2	R	R^2	R_{Adj}	SE	F	$F_{Critical}$
		82	0.303	0.75	0.562	0.545	0.29	33.378	2.72
Tetraselmis SGR_B	Log SGR	y = 0.07(SQRT GFR) – 0.381(**Log Vol**) + 0.206(Inv (1 + %CO_2)) + 0.838							
		N	pr^2	R	R^2	R_{Adj}	SE	F	$F_{Critical}$
		82	0.11	0.783	0.613	0.598	0.27	41.166	2.72
Tetraselmis SGR_C	Log SGR	y = -0.334(**SQRT GFR**) + 0.022(**SQRT VLP**) + 2.633(**Inv (1 + %CO_2)**) – 2.202							
		N	pr^2	R	R^2	R_{Adj}	SE	F	$F_{Critical}$
		38	0.193	0.94	0.883	0.872	0.13	85.337	2.88
Tetraselmis SGR_D	Log SGR	y = -0.678(**SQRT GFR**) + 1.257(**Avg pH**) – 10.901							
		N	pr^2	R	R^2	R_{Adj}	SE	F	$F_{Critical}$
		47	0.148	0.861	0.742	0.730	0.20	63.308	3.21
Tetraselmis SGR_E	Log SGR	y = 0.260(**SQRT GFR**) + 0.395(Log LI) + 0.045(**IS**) - 2.446							
		N	pr^2	R	R^2	R_{Adj}	SE	F	$F_{Critical}$
		56	0.322	0.685	0.470	0.439	0.32	15.359	2.78
Tetraselmis SGR_F	Log SGR	y = -0.991(**Log Vol**) + 0.031(**SQRT VLP**) + 2.765							
		N	pr^2	R	R^2	R_{Adj}	SE	F	$F_{Critical}$
		43	0.490	0.781	0.61	0.59	0.23	31.237	3.23

[1] Significant variables are shown in bold. The t-test significance level used was $p \leq 0.05$.

Model *Tetraselmis* SGR_C, as shown in Table 16, predicts over 88% of the variation in SGRs for 2 species in 4 publications using only three variables. This model dataset is

from cultures grown at volumes from 800 mL-3.4 L. These cultures were sparged with 0-1% CO_2 supplemented air at gas flow rates from 0.59-5.5 L L^{-1} min^{-1}; VLPs ranged from 4-125 mg L^{-1} d^{-1}. $\%CO_2$ added predicts 38% of the SGR variation.

Model *Tetraselmis* SGR_D considers average pH for aerated cultures and predicts 74% of the variability in SGRs with nearly all being predicted by gas flow rate. The dataset used to generate this model covers gas flow rates from 0.007-2 L L^{-1} min^{-1}, but it only includes a small average pH range from 8-8.3. Model *Tetraselmis* SGR_E has an R^2 of 0.47 with illumination schedule accounting for 14% of the variability, and gas flow rate accounting for 6.3%. *Tetraselmis* SGR_E includes data from 5 publications on 3 *Tetraselmis* species, and it includes cultures illuminated for 12 or 24 hours at light intensities of 80-230 µE m^{-2} s^{-1}. The cultures were aerated with air containing 0-18.4% CO_2 added at gas flow rates from 0.007-5.5 L L^{-1} min^{-1}.

Model *Tetraselmis* SGR_F was prepared without considering aeration. *Tetraselmis* SGR_F predicts 61% of the variability in SGRs for data from 6 publications on 2 *Tetraselmis* species. The dataset includes cultures from 800 mL-3.4 L with VLPs from 0.017-125 mg L^{-1} d^{-1}. Culture volume accounts for 28% of the variability with VLP accounting for 5.6%. The remaining variability is from non-unique sources.

6.4. MLC Models

6.4.1. *Phaeodactylum* Models

Two MLC models were produced using the database subset of *Phaeodactylum* cases with maximum lipid contents; all were *Phaeodactylum tricornutum* as shown in Table 17.

Table 17. *Phaeodactylum tricornutum* sources used in maximum lipid content models

Species	**Source**
Phaeodactylum tricornutum	[4], [31], [115], [118], [143], [173], [175], [178], [180], [183], [186]

Each modelling variable was analysed to determine if it fit the normal distribution, and several transformations were tested using P-P plots; optimals are shown in Figure 40.

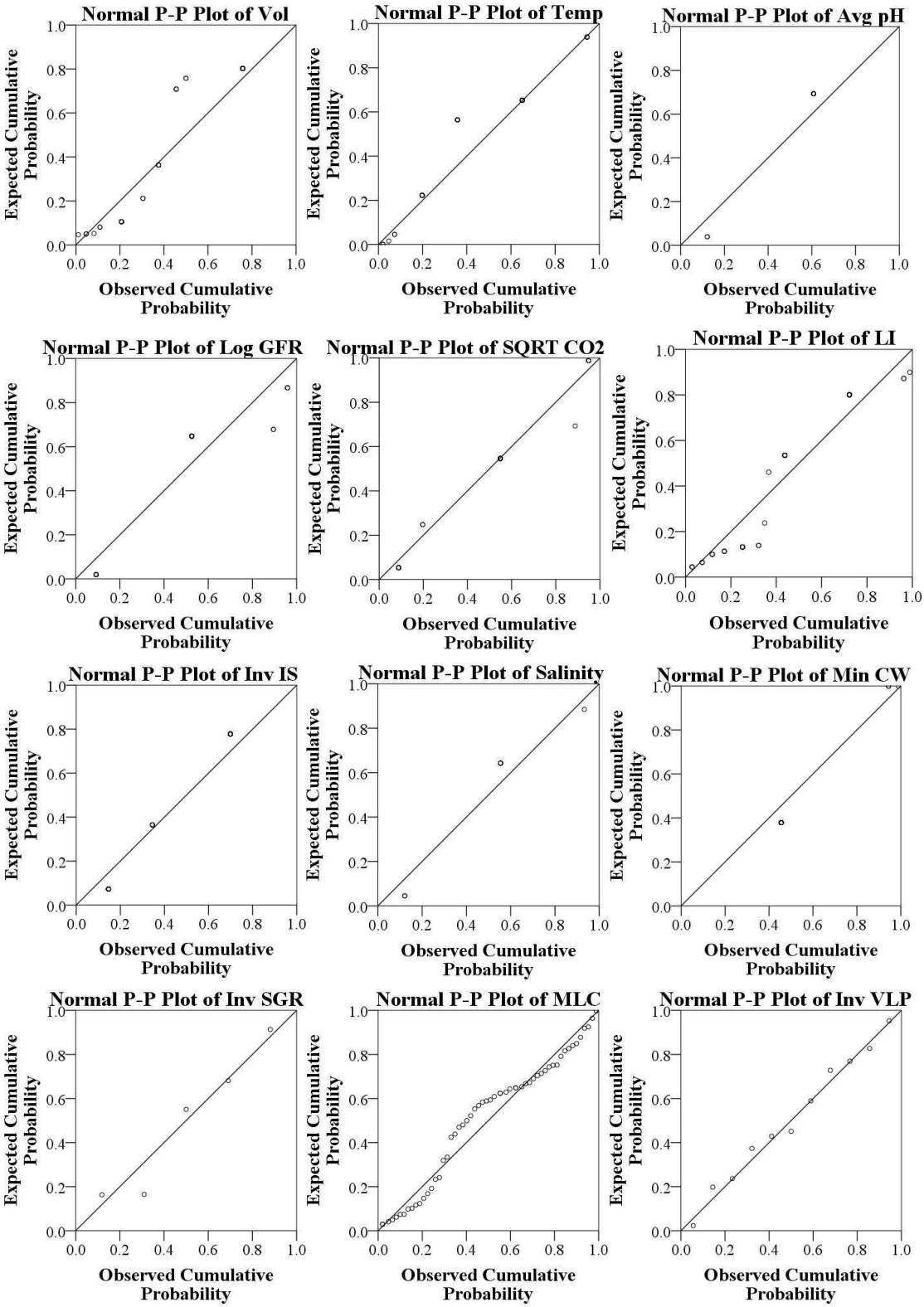

Figure 40. P-P plots of variables used in *Phaeodactylum* maximum lipid content models
This figure shows the expected versus the actual probabilities of the residuals for each variable. Each variable is shown using the transformation used to develop the models.

Table 18 shows Model *Phaeodactylum* MLC_A, which predicts nearly half of the variation in MLCs from 4 publications. This model includes data from 75 mL-3.4 L

cultures that were sparged with air containing 0-5% CO_2 added at gas flow rates from 0.1-1 L L^{-1} min^{-1}. Culture volume alone accounts for 21% of the variation in MLCs.

Table 18. *Phaeodactylum tricornutum* maximum lipid content models

Model Name	Dependent Variable	Regression Equation[1]							
Phaeodactylum MLC_A	MLC	y = 0.002(**Vol**) + 2.949(Log GFR) + 14.151							
		N	pr^2	R	R^2	R_{Adj}	SE	F	$F_{Critical}$
		39	0.507	0.685	0.469	0.439	4.03	15.882	3.26
Phaeodactylum MLC_B	MLC	y = 0.001(Vol) + 0.038(**LI**) + 8.275							
		N	pr^2	R	R^2	R_{Adj}	SE	F	$F_{Critical}$
		56	0.493	0.569	0.323	0.298	6.42	12.659	3.17

[1] Significant variables are shown in bold. The t-test significance level used was $p \leq 0.05$.

If light intensity is considered instead of aeration, as in *Phaeodactylum* MLC_B, 32% of the variation is accounted for in MLCs from 11 publications. This model includes data from 30 mL-3.4 L cultures that were illuminated using 20-261 µE m^{-2} s^{-1} light intensities. In this dataset, light intensity is the largest single predictor accounting for 8% of the variation in MLCs.

6.4.2. *Tetraselmis* Models

Two MLC models were developed using the database subset of *Tetraselmis* cases with maximum lipid contents. This dataset includes the 4 *Tetraselmis* species in Table 19.

Table 19. *Tetraselmis* species and sources used in *Tetraselmis* maximum lipid content models

Species	**Source**
Tetraselmis chuii	[203]
Tetraselmis sp	[4], [97], [119], [129], [138], [147], [203]
Tetraselmis suecica	[4], [115], [118], [144], [171], [184], [191], [205]
Tetraselmis tetrathele	[203]

First, each variable to be modelled was analysed to determine whether it fits the normal distribution, and several transformations were tested. P-P plots were produced to ascertain the optimal transformation for each variable, and optimal P-P plots are in Figure 41.

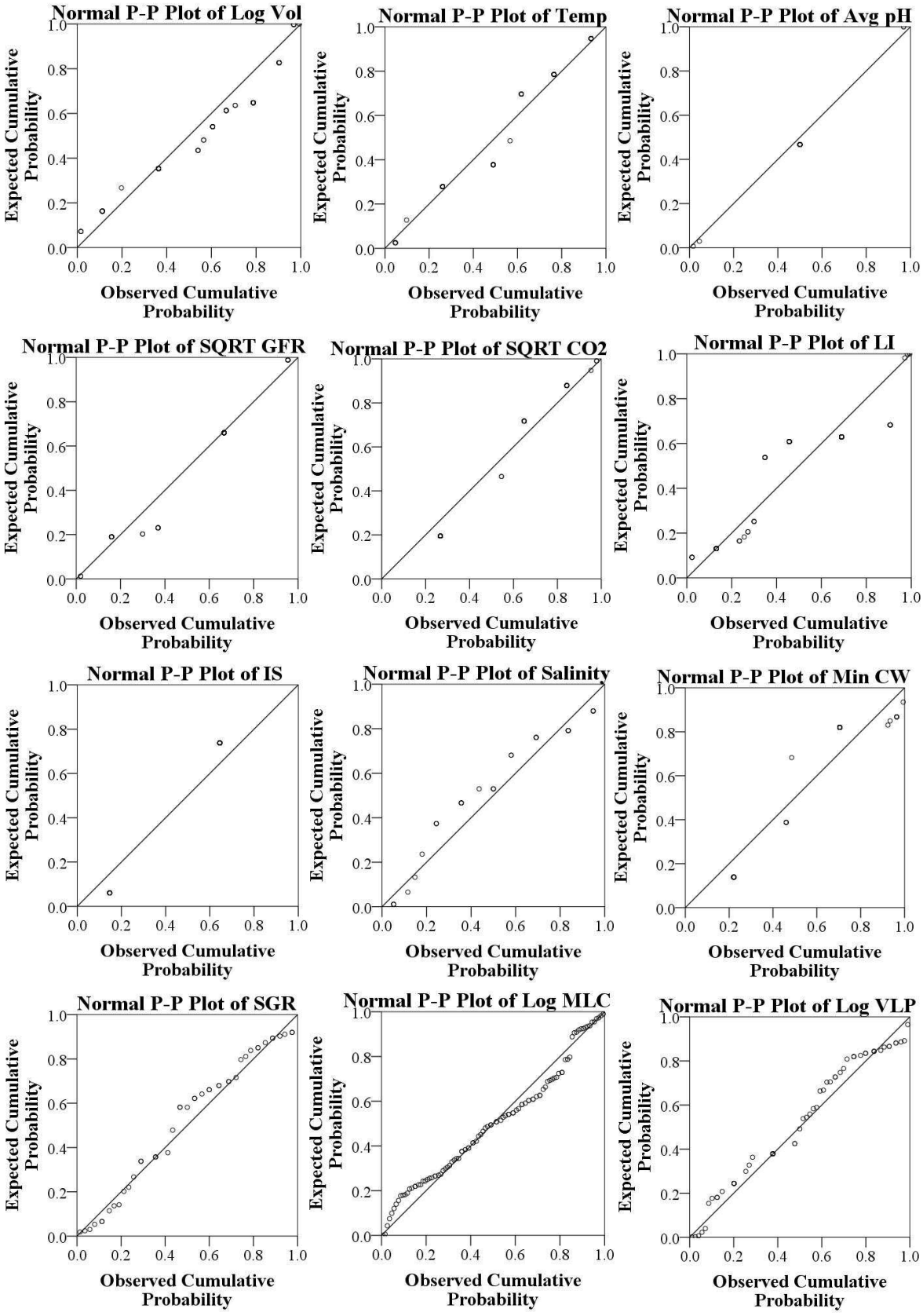

Figure 41. P-P plots of variables used to make *Tetraselmis* maximum lipid content models
This figure shows the expected versus the actual probabilities of the residuals for each variable. Each variable is shown using the transformation used to develop the *Tetraselmis* MLC models.

Table 19 shows Model *Tetraselmis* MLC_A, which predicts 33% of the variation in MLCs from 6 publications covering 4 *Tetraselmis* species. This model includes data from 800 mL-3.4 L cultures that were sparged with air containing 0-1% CO_2 added at gas flow rates from 0.007-5.5 L L^{-1} min^{-1}. CO_2 % added was the largest predictor variable and accounted for 5.9% of the unique variation in MLCs. The remaining variation was accounted for using a combination of predictor variables.

Table 20. *Tetraselmis* maximum lipid content models

Model Name	Dependent Variable	Regression Equation[1]							
Tetraselmis MLC_A	Log MLC	y = 0.039(Log Vol) – 0.102(SQRT GFR) + 0.206(**SQRT CO_2**) + 1.005							
		N	pr^2	R	R^2	R_{Adj}	SE	F	$F_{Critical}$
		57	0.453	0.574	0.33	0.292	0.20	8.692	2.78
Tetraselmis MLC_B	Log MLC	y = -0.023(**IS**) – 0.027(SQRT GFR) + 1.554							
		N	pr^2	R	R^2	R_{Adj}	SE	F	$F_{Critical}$
		49	0.699	0.834	0.696	0.683	0.096	52.692	3.20

[1] Significant variables are shown in bold. The t-test significance level used was $p \leq 0.05$.

Model *Tetraselmis* MLC_B predicts 70% of the variation in MLCs from 4 publications on *Tetraselmis* sp and *Tetraselmis suecica*. This model includes data from small-scale cultures sparged with air containing 0-1% CO_2 added at gas flow rates from 0.007-5.5 L L^{-1} min^{-1}. The cultures were grown at light intensities from 80-231 µE m^{-2} s^{-1} for 12 or 24 hours. Illumination schedule was the largest predictor variable and accounted for 21% of the unique variation in MLCs.

6.5. VLP Models

6.5.1. *Chlorella* Models

Four VLP models were prepared containing only variables controlled during culturing. The models were developed using the database subset of *Chlorella* cases with volumetric lipid productivities. This dataset comprises 6 *Chlorella* species summarized in Table 21.

Table 21. *Chlorella* volumetric lipid productivity model species and data sources

Species	**Source**
Chlorella emersonii	[120]
Chlorella minutissima	[120], [173]
Chlorella protothecoides	[58], [120]
Chlorella sorokiniana	[4], [120]
Chlorella sp	[4], [105], [256]
Chlorella vulgaris	[54], [108], [118], [120], [172], [174], [179], [203]

First, each modelling variable was analysed to determine whether it fit the normal distribution, and several transformations were tested. P-P plots were produced to find the optimal transformation. Each variable's optimal P-P plot is shown in Figure 42.

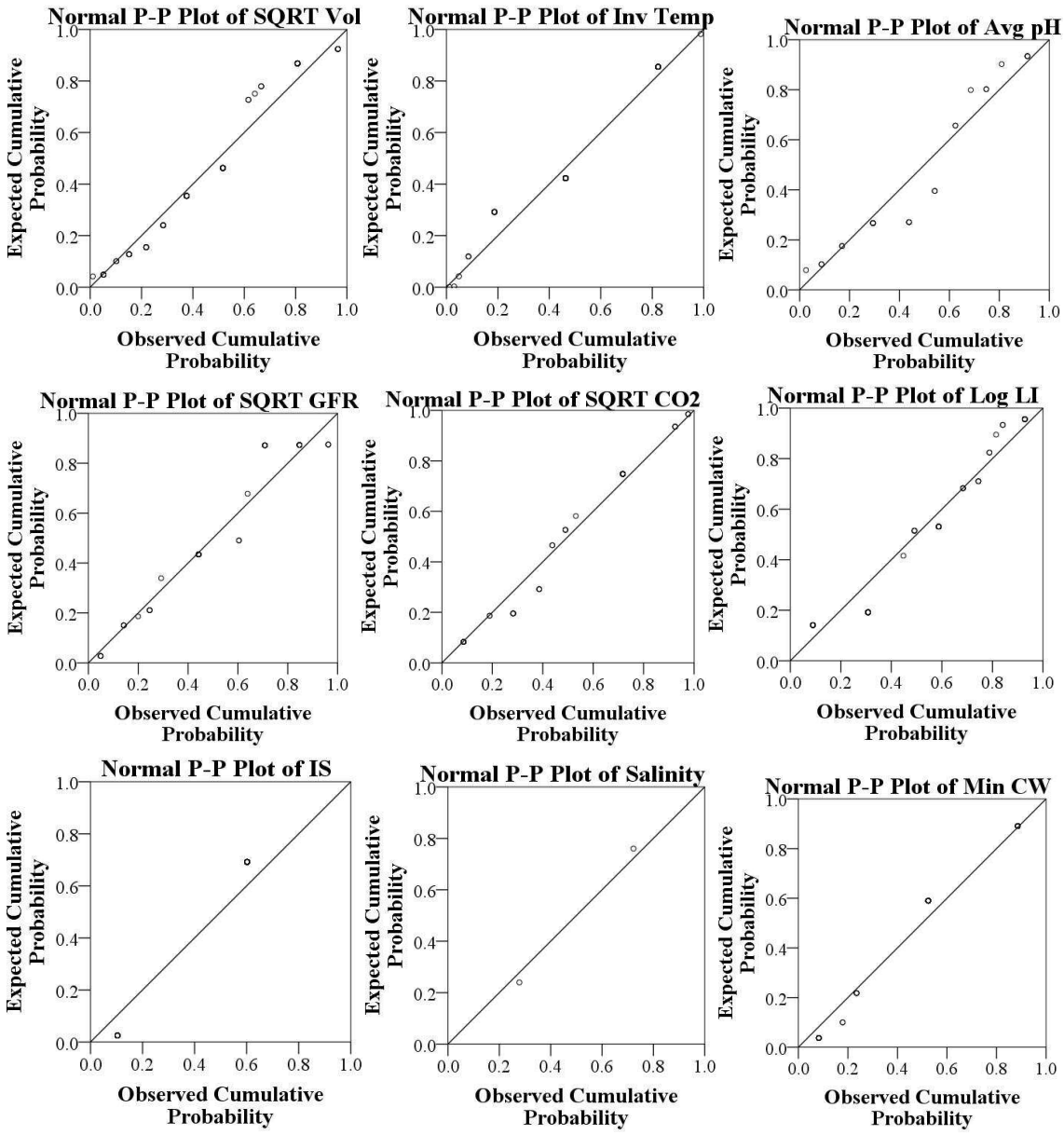

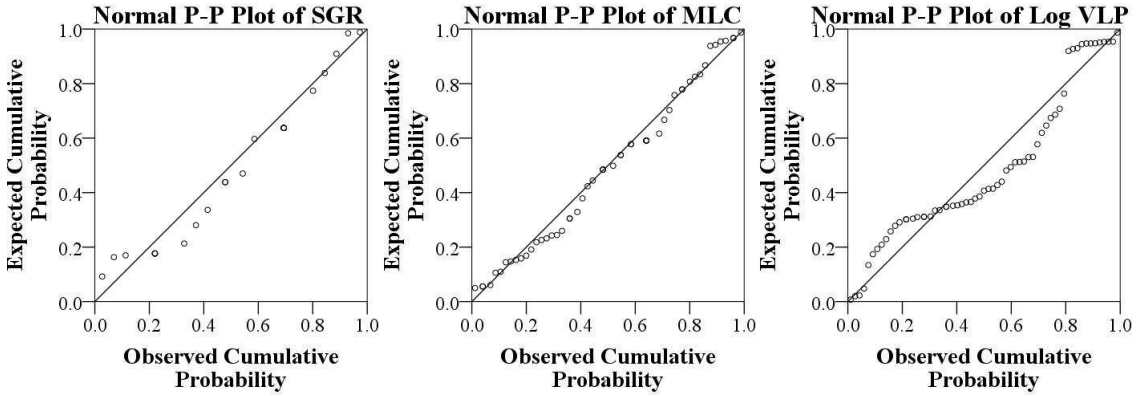

Figure 42. P-P plots of variables used to make *Chlorella* lipid productivity models
This figure shows the expected versus the actual probabilities of the residuals for each variable. Each variable is shown using the transformation used to develop the models.

Model *Chlorella* VLP_A, as shown in Table 22, shows that light intensity alone predicts nearly 65% of the variation in VLPs for 6 *Chlorella* species from 11 publications. This model uses data from 75 mL-4.8 L cultures grown at light intensities of 25-300 μE m^{-2} s^{-1}.

Table 22. *Chlorella* volumetric lipid productivity models

Model Name	Dependent Variable	Regression Equation[1]							
Chlorella VLP_A	Log VLP	y = 1.394(**Log LI**) – 1.281							
		N	pr^2	R	R^2	R_{Adj}	SE	F	$F_{Critical}$
		56	0.803	0.803	0.645	0.639	0.41	98.266	4.2
Chlorella VLP_B	Log VLP	y = 1.447(**Log LI**) + 0.064(SQRT GFR) – 1.398							
		N	pr^2	R	R^2	R_{Adj}	SE	F	$F_{Critical}$
		40	0.62	0.818	0.67	0.652	0.45	37.544	3.25
Chlorella VLP_C	Log VLP	y = 23.274(Inv Temp) + 1.534(**Log LI**) – 2.469							
		N	pr^2	R	R^2	R_{Adj}	SE	F	$F_{Critical}$
		48	0.315	0.828	0.686	0.672	0.42	49.211	3.20
Chlorella VLP_D	Log VLP	y = -0.071(SQRT %CO_2) + 5.617(Inv Temp) + 1.674(**Log LI**) – 0.009(IS) – 1.634							
		N	pr^2	R	R^2	R_{Adj}	SE	F	$F_{Critical}$
		43	0.177	0.844	0.713	0.683	0.43	23.622	2.62

[1] Significant variables are shown in bold. The t-test significance level used was $p \leq 0.05$.

If gas flow rate and light intensity are considered, as in *Chlorella* VLP_B, the model R^2 increases to 0.67. *Chlorella* VLP_B was produced using data for 6 *Chlorella* species from 7 publications. The dataset's light intensities range from 25-300 μE m^{-2} s^{-1}, and the gas flow rates range from 0.042-1.5 L L^{-1} min^{-1} with 0-15% CO_2 added to the airflow. Light

intensity is the most significant predictor variable and accounts for 29% of the variation in VLPs.

When considering temperature rather than gas flow rate, as in *Chlorella* VLP_C, the model is improved to an R^2 of 0.686. Model *Chlorella* VLP_C was produced using data from 9 publications on 6 *Chlorella* species. The dataset includes light intensities ranging from 25-300 μE m^{-2} s^{-1} and temperatures ranging from 20-38 °C. At 59%, light intensity accounts for most of the variability in VLPs.

Model *Chlorella* VLP_C predicts 71% of the variation in VLPs using four predictor variables. Light intensity accounts for 16% of that variability with nearly all of the remaining variability attributable to a combination of variables. Model *Chlorella* VLP_C was produced using data from 7 publications on 6 *Chlorella* species. The dataset covers cultures grown under 25-300 μE m^{-2} s^{-1} light intensities for 16 or 24 hours per day. The culture temperatures ranged from 20-26 °C, and the aeration included 0-15% CO_2 added.

6.5.2. *Nannochloropsis* Models

Five VLP models were developed using the database subset of *Nannochloropsis* cases with volumetric lipid productivities. This dataset includes 5 *Nannochloropsis* species as summarized in Table 23.

Table 23. *Nannochloropsis* species and sources used in volumetric lipid productivity models

Species	**Source**
Nannochloropsis oceanica	[4]
Nannochloropsis oculata	[106], [108], [173], [203]
Nannochloropsis salina	[104]
Nannochloropsis sp	[4], [54], [82], [92], [118], [119], [181], [204]

First, each variable to be modelled was analysed to determine whether it fit the normal distribution, and several transformations were tested. P-P plots were produced to discover the optimal transformation for each variable. Figure 43 shows the optimal P-P plots.

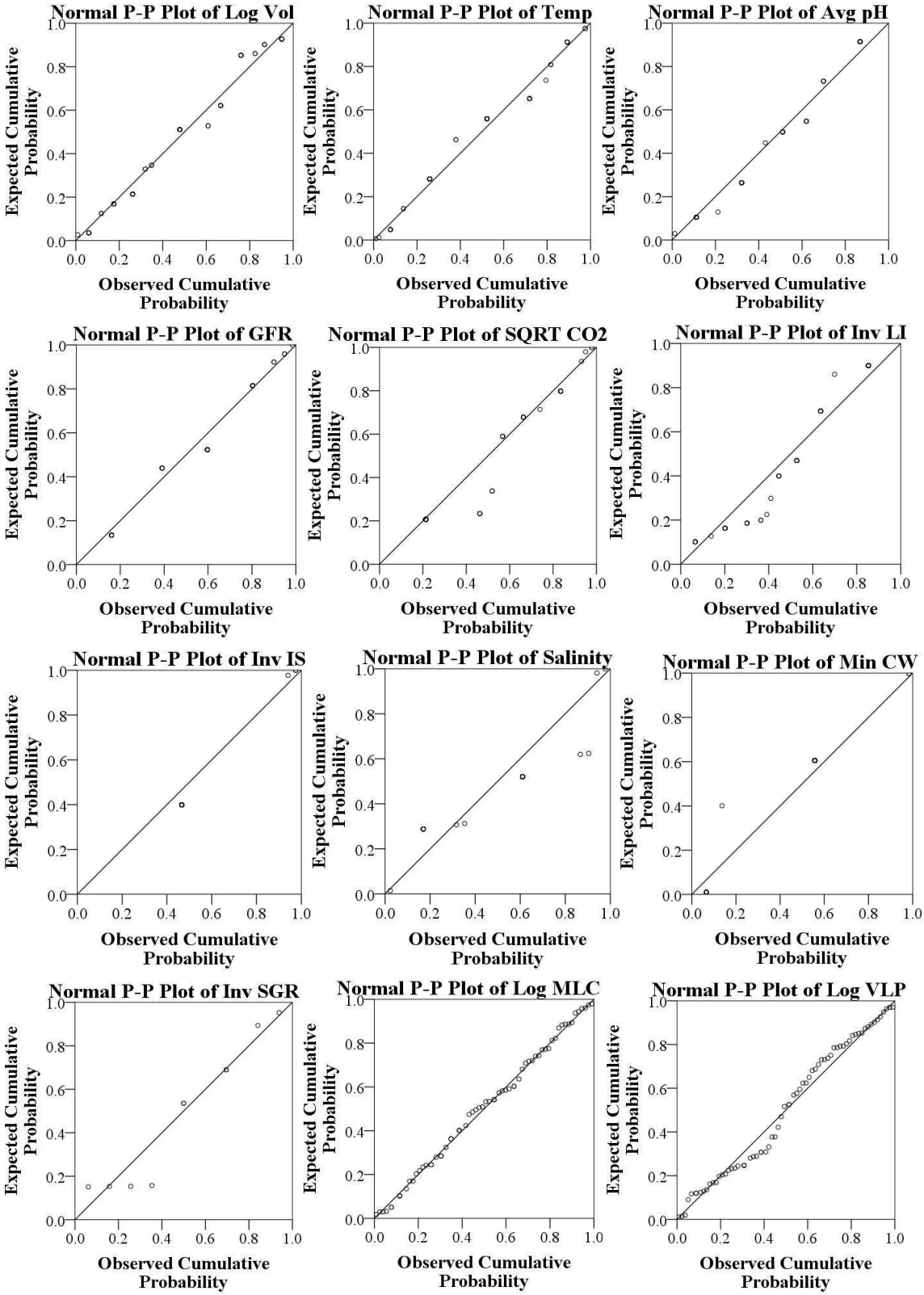

Figure 43. P-P plots of variables used to make *Nannochloropsis* lipid productivity models
This figure shows the expected versus the actual probabilities of the residuals for each variable. Each variable is shown using the transformation used to develop the models.

As shown in Table 24, *Nannochloropsis* VLP_A uses only light intensity to account for 69% of the variability in VLPs from 3 *Nannochloropsis* species for 10 publications. The

cultures include volumes from 75 mL-110 L grown at light intensities from 50-850 μE m^{-2} s^{-1}. With the addition of gas flow rate, *Nannochloropsis* VLP_B predicts 82% of the variability in *Nannochloropsis* sp and *N. oculata* VLPs from 5 publications. These cultures were aerated at 0.022-1 L L^{-1} min^{-1} with 0-15% CO_2 added and illuminated with 50-850 μE m^{-2} s^{-1}. Light intensity accounts for 36% of the variability, and 40% of the R^2 is attributable to non-unique sources. If Log MLC is added to *Nannochloropsis* VLP_B, the R^2 is increased to 0.862 with the same N and all predictor variables are significant.

Table 24. *Nannochloropsis* volumetric lipid productivity models

Model Name	Dependent Variable	Regression Equation[1]							
Nannochloropsis VLP_A	Log VLP	y = -79.557(**Inv LI**) + 2.308							
		N	pr^2	R	R^2	R_{Adj}	SE	F	$F_{Critical}$
		55	0.832	0.832	0.693	0.687	0.39	119.53	4.02
Nannochloropsis VLP_B	Log VLP	y = -65.89(**Inv LI**) + 0.972(**GFR**) + 1.944							
		N	pr^2	R	R^2	R_{Adj}	SE	F	$F_{Critical}$
		35	0.542	0.907	0.823	0.812	0.34	74.405	3.29
Nannochloropsis VLP_C	Log VLP	y = -66.285(**Inv LI**) – 0.622(**pH_{Avg}**) + 7.128							
		N	pr^2	R	R^2	R_{Adj}	SE	F	$F_{Critical}$
		37	0.805	0.912	0.831	0.822	0.35	83.863	3.28
Nannochloropsis VLP_D	Log VLP	y = -51.274(**Inv LI**) + 2.265(**GFR**) – 0.064(pH_{Avg}) – 0.023(Temp) + 2.641							
		N	pr^2	R	R^2	R_{Adj}	SE	F	$F_{Critical}$
		32	0.511	0.952	0.907	0.893	0.27	65.660	2.72
Nannochloropsis VLP_E	Log VLP	y = 2.218(**GFR**) – 0.621(**pH_{Avg}**) + 1.083(**Log MLC**) + 4.45							
		N	pr^2	R	R^2	R_{Adj}	SE	F	$F_{Critical}$
		32	0.479	0.960	0.921	0.913	0.24	108.98	2.95

[1] Significant variables are shown in bold. The t-test significance level used was $p \leq 0.05$.

Considering average pH, Model *Nannochloropsis* VLP_C accounts for 83% of the variability in VLPs from 5 publications on 2 species. The model dataset includes cultures grown under 50-850 μE m^{-2} s^{-1} illumination with average pH values ranging from 7-8.3. In Model *Nannochloropsis* VLP_C, most of the VLP variability is from non-unique sources, 16% is accounted for by light intensity, and 2.5% by average pH. Adding Log MLC to

Nannochloropsis VLP_C increases the R^2 to 0.897 with all variables significant and the same N.

Nannochloropsis VLP_D uses four culturing parameters to predict nearly 91% of the variability in VLPs within *N.* sp and *N. oculata* from 3 publications. The dataset includes cultures aerated with 0-15% CO_2 added at a gas flow rate from 0.02-0.5 L L^{-1} min^{-1}. The cultures were grown at 14-30 °C under light intensities of 50-850 µE m^{-2} s^{-1} and had average pH values from 7-8.3. Gas flow rate accounted for 6.1% of the variability in VLPs, light intensity accounted for 4.2%, and nearly all of the remaining variability was attributed to non-unique sources.

Finally, MLC is considered in *Nannochloropsis* VLP_E, which was produced using 2 *Nannochloropsis* species from 3 publications. The model was produced using data from cultures aerated with 0-15% CO_2 added to air at a gas flow rate of 0.02-0.5 L L^{-1} min^{-1}. The cultures had average pH values from 7-8.3 and 9-62% dw MLCs. *Nannochloropsis* VLP_E has an R^2 of 0.921 with most variability accounted by non-unique sources. If average pH is replaced by light intensity, the R^2 is 0.862 with 35 cases and all predictor variables being significant.

6.5.3. *Tetraselmis* Models

Five VLP models were developed using the database subset of *Tetraselmis* cases with volumetric lipid productivities; this dataset includes the 4 *Tetraselmis* species in Table 25.

Table 25. *Tetraselmis* species and sources used in volumetric lipid productivity models

Species	**Source**
Tetraselmis chuii	[203]
Tetraselmis sp	[4], [97], [119], [129], [147], [203]
Tetraselmis suecica	[4], [116], [118], [144]
Tetraselmis tetrathele	[203]

First, each modelling variable was analysed to determine whether it fit the normal distribution. Several transformations were tested, and P-P plots were created to determine the optimal transformation for each variable. Figure 44 shows the optimal P-P plots.

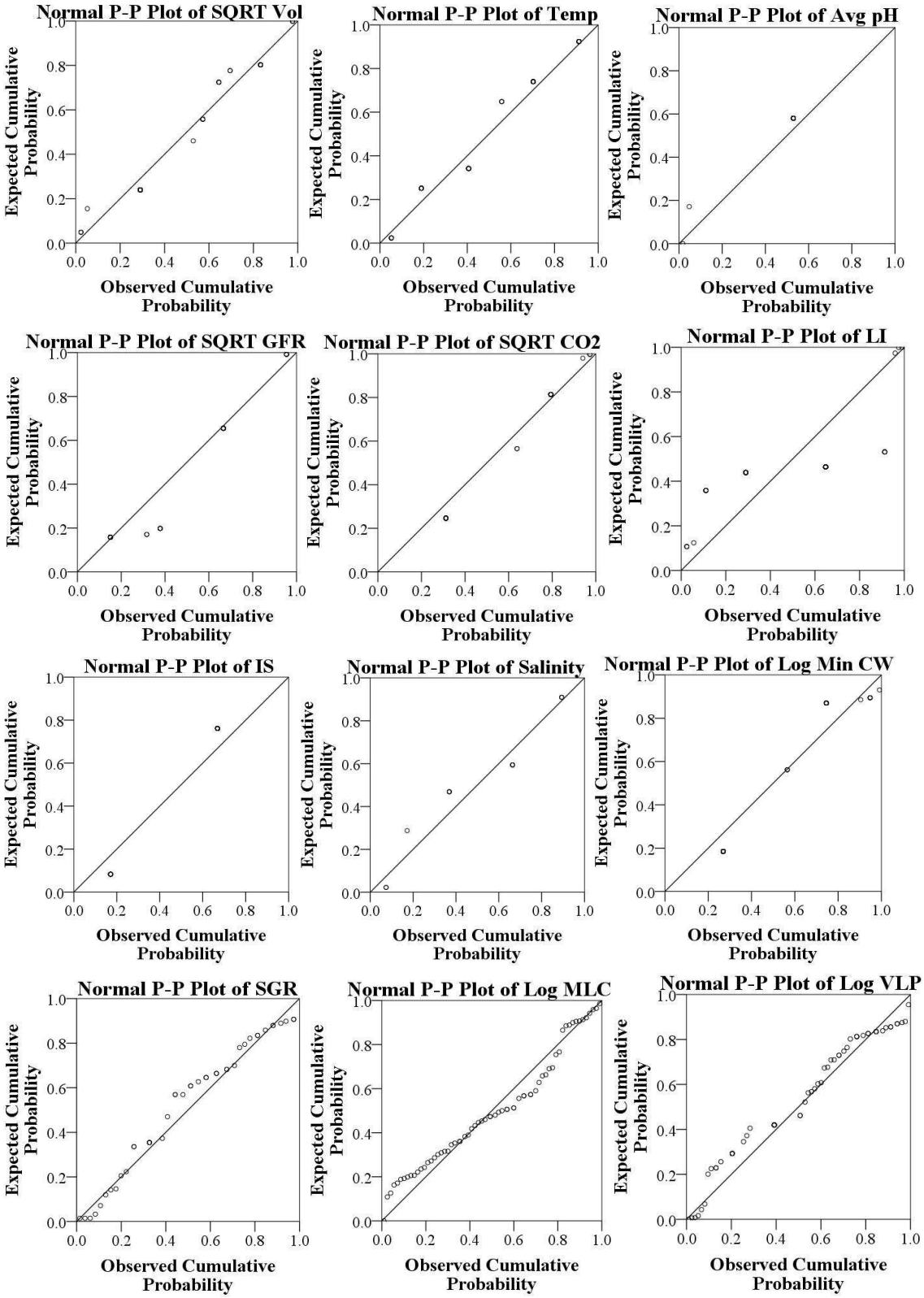

Figure 44. P-P plots of variables used to make *Tetraselmis* lipid productivity models
This figure shows the expected versus the actual probabilities of the residuals for each variable. Each variable is shown using the transformation used to develop the models.

Several *Tetraselmis* VLP models are shown in Table 26. *Tetraselmis* VLP_A shows that 56% of the variability in VLPs from *T. suecica* and *Tetraselmis* sp from 4 publications.

However, the cultures had a small average pH range from 7-8 and were from 500 mL-1.6 L cultures. With the addition of culture volume, Model *Tetraselmis* VLP_B accounts for 68% of the variability in VLPs from the same dataset. Culture volume accounts for 12% of the variability, and 56% of the R^2 is attributable to non-unique sources.

Table 26. *Tetraselmis* volumetric lipid productivity models

Model Name	Dependent Variable	Regression Equation[1]							
Tetraselmis VLP_A	Log VLP	$y = 3.184(\mathbf{pH_{Avg}}) - 23.783$							
		N	pr^2	R	R^2	R_{Adj}	SE	F	$F_{Critical}$
		34	0.75	0.75	0.562	0.548	0.50	41.07	4.15
Tetraselmis VLP_B	Log VLP	$y = 1.295(pH_{Avg}) - 0.183(\mathbf{SQRT\ Vol}) - 3.543$							
		N	pr^2	R	R^2	R_{Adj}	SE	F	$F_{Critical}$
		34	0.75	0.825	0.681	0.661	0.43	33.149	3.30
Tetraselmis VLP_C	Log VLP	$y = -0.037(\mathbf{SQRT\ Vol}) - 0.289(SQRT\ GFR) + 3.160$							
		N	pr^2	R	R^2	R_{Adj}	SE	F	$F_{Critical}$
		57	0.265	0.66	0.436	0.415	0.52	20.847	3.17
Tetraselmis VLP_D	Log VLP	$y = -0.068(\mathbf{SQRT\ Vol}) + 0.185(SQRT\ GFR) + 1.482(\mathbf{SQRT\ CO_2}) + 3.390$							
		N	pr^2	R	R^2	R_{Adj}	SE	F	$F_{Critical}$
		57	0.227	0.834	0.696	0.678	0.39	40.366	2.78
Tetraselmis VLP_E	Log VLP	$y = 0.976(\mathbf{SGR}) + 0.344$							
		N	pr^2	R	R^2	R_{Adj}	SE	F	$F_{Critical}$
		43	0.676	0.676	0.457	0.44	0.52	34.573	4.08

[1] Significant variables are shown in bold. The t-test significance level used was $p \leq 0.05$.

Model *Tetraselmis* VLP_C uses culture volume and gas flow rate to account for 44% of the variability in 4 species' VLPs from 5 publications. Culture volume has a unique contribution of 36.5% to the model R^2. The model's dataset includes cultures with volumes of 800 mL-3.4 L. The cultures were aerated at 0.59-5.5 L L^{-1} min^{-1} with 0-1% CO_2 added. With the addition of $\%CO_2$ added, Model *Tetraselmis* VLP_D has an increased R^2 of 0.696 using the same dataset. Culture volume accounts for 62%, and $\%CO_2$ added accounts for 26% of the variability in VLPs within the dataset. Model *Tetraselmis* VLP_E contains only SGR and accounts for 46% of the variability in *T. suecica* and *Tetraselmis* sp

VLPs from 6 publications. The SGRs in the dataset range from 0.06-1.75 d^{-1}.

6.6. Genus Specific Model Discussion

This chapter details several genera specific models prepared to assess the effects of environmental variables on SGRs, MLCs, and VLPs. Where possible, these models are compared below with published models from species within each genera. Comparisions are also made with published multiple regression models for other species. A 2nd order polynomial model of *Dunaliella tertiolecta* SGRs in an air-lift PBR considers light/dark cycle durations and light fraction as predictor variables; this model had an R^2 of 0.978 [261]. Increased light fraction was significant [261]. In addition, logistic regression analyses of *Spirulina platensis* data considering controlled light, temperature, and nutrients produced models for maximum cell concentration with R^2_{adj} of 0.80-0.82, for total chlorophyll with R^2_{adj} of 0.52-0.72, for cell productivity with R^2_{adj} of 0.81-0.87, and for chlorophyll productivity with R^2_{adj} of 0.60-0.73 [86]. Many of these R^2_{adj} values are similar to those obtained for genus specific models in this chapter. Some of the models developed here have lower R^2 values, but they include data from several species within a genus, and the data were produced under a variety of conditions in multiple labs.

A few of these models have N values as low as 35. However, all pass Green's rule of thumb for cases because the variables have large effect sizes, as calculated in Equation 8. Multiple regression models based on data from a set of experiments within a lab tend to have much smaller N values [86], [285], [301], [302]. These smaller N values are likely reasons for the very high R^2 values obtained. However, they indicate lower statistical reliability and less generalizable conclusions.

***Chlorella* models**

Several *Chlorella* VLP models were produced to determine the effects of several environmental variables. The *Chlorella* VLP models indicate that light intensity is

significant in predicting *Chlorella* lipid productivities. This aligns with a *C. vulgaris* study showing growth proportional to the square root of light intensity [46]. Also, a multiple regression analysis of *C. minutissima* grown in a 1.8 L stirred bioreactor produced a 2nd order polynomial growth model with light intensity, cultivation time, and nitrate concentration as significant variables; the model had an R^2 of 0.921 [302]. These models support the *Chlorella* VLP models developed here, which have an R^2 value of 0.645 with light intensity alone and increasing R^2 values as additional predictor variables are added.

The *Chlorella* VLP models in Table 22 also considered gas flow rate, temperature, $\%CO_2$ added, and illumination schedule. Each of these variables has been considered in previous *Chlorella* models using multiple regression to produce 2nd order polynomial equations. Photoautotrophic *C. vulgaris* CO_2 fixation within a bubble column PBR was modelled with $R^2 = 0.94$ considering aeration and CO_2 concentrations [282]. Stepwise multiple linear regression has also been used to assess the effects of temperature and cell density on *C. vulgaris* SGRs when immobilized within alginate beads. A combination of temperature and initial cell density within a bead accounted for 85.7% of SGR variation, with nearly all (77%) accounted for by temperature alone [280]. When modelling *C. vulgaris* growth among control and toxicity impacted sites, temperature predicts most of the variation ($R^2 = 0.96$) in SGRs but is limited to the range of 8.6-15.1 °C [280]. In another study, temperature was considered along with glucose and nitrate addition for small-scale heterotrophically grown *Chlorella* sp to produce a lipid productivity model with an R^2 of 0.991 [285]. A *C. vulgaris* MLC model was developed using 30 combinations of nutrients and incubation periods in small-scale experiments; the model R^2 was 0.9636 [60]. Nutrient addition was also considered in small-scale *C. protothecoides* experiments used to develop models for biomass production (R^2 of 0.961) and for lipid accumulation (R^2 of 0.984) [303].

***Isochrysis* models**

The two *Isochrysis* models produced here indicated that $\%CO_2$ added accounted for the most variability in SGRs. Culture volume, temperature, and light intensity were added to $\%CO_2$ for Model *Isochrysis* SGR_B, which produced an R^2 of 0.51. This is very close to an *I. galbana* SGR model (R^2=0.53) considering temperature, light intensity, and biomass density [304]. In Model *Isochrysis* SGR_B, temperature, culture volume, and light intensity were not significant variables. The *I. galbana* model also indicated that temperature did not have a significant effect on SGR; however, it found *I. galbana* SGRs to be negatively correlated with biomass density and positively correlated with light intensity [304].

Only two previous *Isochrysis* multiple regression models were found. Along with SGR, *I. galbana* productivity was assessed using stepwise regression (R^2=0.36) and considering temperature, light intensity, and biomass density [304]. Productivity was positively correlated with light intensity and biomass density, and temperature did not have a significant effect [304]. Secondly, models of nitrogen and phosphorous ratios within algae under different nutrient conditions were found [283]. One model indicated 75% of the variability in *I. galbana* SGRs was accounted for by nitrogen:phosphorous supply ratio [283]. A 2nd order quadratic SGR model for *I. galbana* phosphorous requirements had an R^2_{Adj} value of 0.787, and a linear model of nitrogen requirements had an R^2_{Adj} of 0.747 [283]. Effects of supplied nutrients on biomass nitrogen:phosphorous ratio were also modelled (R^2_{Adj} = 0.3) [283].

***Nannochloropsis* models**

Five *Nannochloropsis* VLP models were produced using a variety of environmental variables. Light intensity and gas flow rate were significant predictors of *Nannochloropsis* VLP in every model that incorporated them. Average culture pH was significant in two models, and MLC was also significant. *Nannochloropsis* VLP_D incorporates temperature,

light intensity, pH, and gas flow rate with an R^2 of 0.91. Spolaore [301] used these variables to produce a 2nd order polynomial model for *N. oculata* maximum growth rate with an R^2 of 0.93. Model *Nannochloropsis* VLP_D predicts nearly as much variability as the species-specific *N. oculata* model by Spolaore. However, Model *Nannochloropsis* VLP_D has a wider applicability because it includes data from two species in 800 mL-110 L cultures, while Spolaore's model was based on 2.5 L bubble column experiments.

A literature search revealed few multiple regression models for *Nannochloropsis* species. Instead, bulk biomass growth and lipid accumulation models were found using 16 species-specific parameters, such as light saturation, photon efficiency, and nitrogen uptake; these models were validated using *N. oculata* growth in outdoor PBRs with an average growth over prediction of 3% and 8% standard error in lipids [70]. By comparison, the *Nannochloropsis* VLP models detailed in this chapter are easier to use and have high predictive capabilities.

***Phaeodactylum* models**

Two *Phaeodactylum* SGR models were prepared. Model *Phaeodactylum* SGR_A shows over 72% of the variation in SGRs was predicted by culture volume. Temperature effects were also considered but were not significant. Three publications were found to have modeled *Phaeodactylum* SGRs. A kinetic model was produced for *Phaeodactylum tricornutum* SGRs in batch cultures [263]. When modelling temperature, pH, and light intensity, the temperature was found to be optimum at 20.4 °C and 22.3 °C for aerated and non-aerated cultures respectively [263]. Stepwise multiple regression was used to produce a *P. tricornutum* SGR model considering temperature, turbidity, and total suspended solids as predictor variables; only turbidity was significant with R^2 of 0.945 [279]. Multiple regression was also used to estimate *P. tricornutum* SGRs as affected by nitrogen:phosphorous supply ratio with an R^2 of 0.92 [283]. In addition, 2nd order

quadratic models for *P. tricornutum* SGRs were produced using nitrogen and phosphorous quotas with R^2_{Adj} values of 0.925 and 0.890 respectively [283]. Nutrient supplies' effects on biomass nitrogen:phosphorous ratio were modelled with R^2_{Adj} value of 0.7 [283].

Two *Phaeodactylum* MLC models were prepared using culture volume, light intensity, and gas flow rate. Culture volume and light intensity were both significant variables. No published *Phaeodactylum* MLC models were found for comparison.

***Tetraselmis* models**

Six *Tetraselmis* SGR models were prepared using several combinations of predictor variables. Light intensity, $\%CO_2$ added, gas flow rate, culture volume, average culture pH, illumination schedule, and VLP were all significant predictors of *Tetraselmis* SGRs depending on the variables included in the models. Few *Tetraselmis* multiple regression models have been prepared previously. Of these, no models were found that assessed the effects of culturing variables on *Tetraselmis* SGRs, MLCs, or VLPs. As such, the models developed here could be very useful in future aquaculture and biodiesel manufacturing operations. Since no published models were available for comparison, one *Tetraselmis* SGR model was validated in Chapter 9.

One of the two published *Tetraselmis* multiple regression analyses analysed SGRs of rotifers, which can be used as feed in aquaculture operations. The SGRs of rotifers and ciliates grown on *T. tetrathele* were modelled with R^2 values ranging from 0.08 to 0.65 [281]. In addition, *Tetraselmis* motility has been studied. *T. subcordiformis* movement was examined to determine photosynthetic inhibition under multiple light intensities and types; this was accomplished by iteratively solving an exponential decay function [305].

Two *Tetraselmis* MLC models were prepared considering culture volume, gas flow rate, $\%CO_2$ added, and illumination schedule. $\%CO_2$ added and illumination schedule were both significant variables. In addition, five *Tetraselmis* VLP models were developed

using average pH, culture volume, gas flow rate, %CO_2 added, and SGR. All of these variables, except gas flow rate, were significant in at least one model. Culture volume was a significant predictor of *Tetraselmis* VLPs in every model using it. No published *Tetraselmis* MLC or VLP multiple regression models were found for comparison.

Of the models produced here, illumination schedule was found to be a significant predictor variable within the *Tetraselmis* SGR and MLC models that included it. In both cases, illumination schedule was the largest predictor of unique variability in R^2. This supports the indications in Section 4.9 that illumination schedule may be particularly important for flagellate species.

6.7. Comparing Genus Specific and General Models

As expected, genus specific models commonly produced higher R^2 values than the corresponding general models for SGR, MLC, and VLP in Chapter 5. However, the models here have lower N values and are less generalizable than those in Chapter 5. Also, the Chapter 5 models are useful when a specific species has not been chosen or when the results are meant to give an overview of algae responses in general to predictor variables.

The genera specific models often account for greater variability than the general models, and they should be used if the algae species is known. In addition, some problems require the use of more specialized models. For example, the species specific efficiency to convert CO_2 into lipids is important because it is proportional to the biodiesel cost [62].

The general SGR models found that culture volume, illumination schedule, and CO_2 % added accounted for the most variability within the cases included in this study. Light intensity was also a significant variable. This is mirrored in the genera specific SGR models. *Isochrysis* SGR models indicated that %CO_2 added accounted for the most variability in SGRs. Model *Phaeodactylum* SGR_A shows over 72% of the variation in SGRs was predicted by culture volume. Light intensity, %CO_2 added, gas flow rate,

culture volume, average culture pH, illumination schedule, and VLP were all significant predictors of *Tetraselmis* SGRs depending on the variables included in the models.

The general MLC models showed gas flow rate, temperature and light intensity to be significant predictors of MLC. Culture volume and average pH were also significant but to a lesser extent. Some of these variables were also significant in the genera specific models. *Phaeodactylum* MLC models indicated that culture volume and light intensity were significant variables. *Tetraselmis* MLC models found $\%CO_2$ added and illumination schedule were both significant variables.

The general VLP models indicated that illumination schedule was significant in accounting for VLP variability within the dataset. The genera specific models showed additional variables. Light intensity is significant in predicting *Chlorella* lipid productivities. Light intensity and gas flow rate were both significant predictors of *Nannochloropsis* VLP in every model that incorporated them. Average culture pH and MLC were also significant in *Nannochloropsis* VLP models. *Tetraselmis* VLP models indicated that culture volume, illumination schedule, average pH, $\%CO_2$ added, and SGR were all significant predictors of *Tetraselmis* VLPs.

6.8. Conclusions

Several genera specific models were prepared for SGRs, MLCs, and VLPs in *Chlorella*, *Isochrysis*, *Phaeodactylum*, *Nannochloropsis*, and *Tetraselmis*. These models greatly extend the range of previous species-specific multiple regression models developed in literature. They are useful in identifying the impacts of various culturing parameters on SGRs, MLCs, and VLPs.

Chapter 7. Trial Experiments to prepare for 230 L Photobioreactor Growth

One of the biggest constraints to using algae for biodiesel production is the lack of knowledge to effectively scale up algal cultures from 1 L, where growth is relatively well understood, to commercial scale. Although algae are currently grown at commercial scale, their use is limited to production of low volume, high value products. This production has very different considerations than those needed for the high volume, low value production of algae for biodiesel. The analysis of published data in Chapter 3 demonstrated that most algae experiments are performed on cultures <1 L in volume. A 140 L working volume photobioreactor (PBR) was built to enhance understanding of the scale-up process. Due to the increased time and costs involved in running the 140 L PBR, initial experiments were performed at 200 mL and 500 mL volumes.

Tetraselmis were grown in all experiments because they are marine algae with promising lipid productivities for biodiesel production. In addition, they are flagellates and are large enough to be seen clearly at 400X magnification. A great deal of work has been performed on *Tetraselmis* sp and *T. suecica*. Less is known about *T. impellucida*, so it was chosen for growth. The experiments detailed here were performed alongside the database and modelling work discussed earlier. As such, *Tetraselmis* was not chosen in response to the results found in those chapters.

T. impellucida was grown using culture conditions described in Section 7.1. Initial light source and mixing experiments are detailed in Sections 7.2 and 7.3. Several improvements were made to the bottle experiment setup as discussed in Section 7.4. Next, optical density to biomass conversions are given in Section 7.5. *Tetraselmis* light requirements are covered in Section 7.6, and light source and light intensity 500 mL bottle experiments are detailed in Section 7.7. Finally, sterilization procedures are assessed in Section 7.8.

7.1. *Tetraselmis* Culturing Conditions

Tetraselmis impellucida (PLY 429) was obtained from the Plymouth Culture Collection, UK. The 15 mL initial culture was in ErdSchrieber media. Initial maintenance cultures were in ErdSchrieber media, and their daughter cultures were grown in 50/50 ErdSchrieber/f2 media. This was replaced with f2 media in later maintenance cultures using the f2 recipe from CSIRO [225]. The media was based on artificial saltwater (ASW) made from DI water and Instant Ocean artificial seawater with a specific gravity of 1.022. The *Tetraselmis* stock cultures were maintained in an Innova 4230 refrigerated incubator shaker from New Brunswick Scientific. Maintenance cultures were kept at 15 °C and subcultured regularly in 500 mL Erlenmeyer flasks with 300 mL of media and 30 mL of previous culture. Small cultures were hand swirled regularly to re-suspend algae. Cultures were scaled up to 1 L, 3 L, and 4 L volumes for inoculation into larger experiments. These larger cultures were mixed using continual mixing at 115 rpm on a shaker table within the incubator and supplemented with periodic hand swirling.

7.2. *Tetraselmis* 200 mL Light Source Experiments

Initial growth experiments were performed to compare the effects of fluorescent and halogen lights at different intensities. Cultures were grown in 200 mL tissue culture bottles using the setup shown in Figure 45. The bottles were gently bubbled with air filtered by a 0.3 μm filter. Two light sources were tested: 2 fluorescent tube lights (Phyllips Master; TLD 58 W 840; Recyclable CE; Made in France) or 2 halogen bulb lights (Bell K09 HY; 240 V 60 W; daylight blue bulb). The initial trials were carried out in duplicate with the bottles stacked to provide a range of light intensities. The bottles were sterile and kept in a laminar flow hood after lid removal. The lids were wiped with ethanol, and lids and tubing were ultraviolet (UV) irradiated for an hour prior to use. 190 mL of f2 media were poured into each bottle, and 27 mL of inoculating culture were added to each. Each sample was taken immediately after the culture was well mixed. Samples

were counted using a Sedwick-Rafter haemocytometer and trypan blue dye to measure cell concentration and viability. Light intensities, room temperature, pH, and culture temperature were measured. The bottles experienced significant evaporation, so culture volumes were recorded on Days 0, 3, 8 and 14.

A.  B. 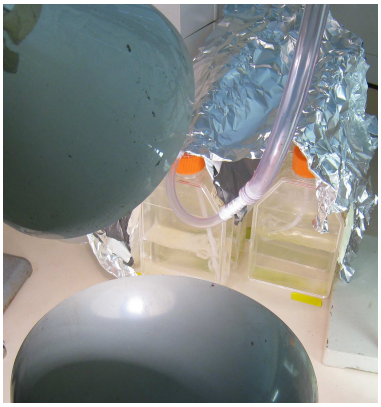

Figure 45. Experimental setup testing fluorescent and halogen lights and light intensities *T. impellucida* growth was assessed using fluorescent (A) and halogen (B) lamps

The halogen bottles experienced light intensities ranging from 70,000 lux for the Halogen High Light bottle to 19,800 lux for the Halogen Low Light bottle. Meanwhile, the fluorescent tube bottles felt light intensities 312,000 lux for the Fluorescent High Light bottle to 21,000 lux for the Fluorescent Low Light bottle. Along with higher light intensities, the bottles nearest the light sources were hotter than the bottles farthest from them. For the tube lights, the differences between the high and low light bottles ranged from 2.4-3.7 °C. For bulb lights, the differences between the high and low light bottles ranged from 5.4-6 °C.

As Figure 46 shows, the bottles with the highest light intensities produced the lowest final cell concentrations. The highest cell concentrations were in bottles farther from the light source, but the deviation between the duplicate trials increases as the days of growth increases. There was less variation in the halogen than in the fluorescent experiments. In addition, noticeable cell size changes were observed at the different light intensities.

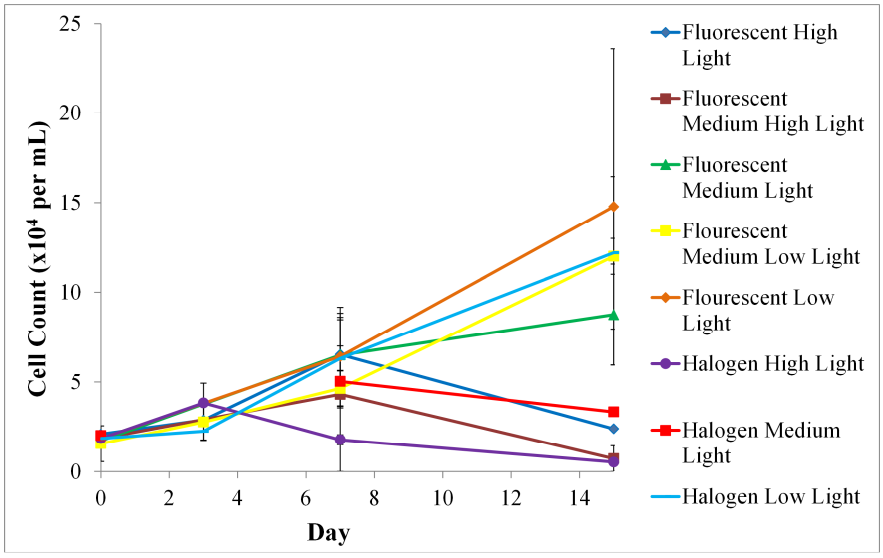

Figure 46. *T. impellucida* growth under fluorescent tubes and halogen lamps
This graph shows average cell count results from duplicate trials. The error bars show the standard error of the mean for each trial.

The fluorescent trials retained cell viabilities >80% for all light intensities except for the highest light intensity bottles. Overall, the halogen trials had lower cell viabilities and lower growth rates than the fluorescent trials. In the halogen high light intensity, cell viability was reduced to 56% and 23.4% in the duplicates under a light intensity of 42,500 lux. For both light sources, the highest light intensity bottle temperatures were around 3.5 °C hotter, which may have caused the decreased growth and viability. The halogen medium and low light intensity bottles had temperatures close to the fluorescent bottles. If light intensity were the predominating factor affecting the growth rate, then the fluorescent medium low and low light intensity trials would be very similar to the high and medium halogen trials. This did not occur, so the differences in growth rate must be at least partially from other effects, such as temperature or wavelength. These trials clearly show reduced growth under high light intensities as seen in Figure 47.

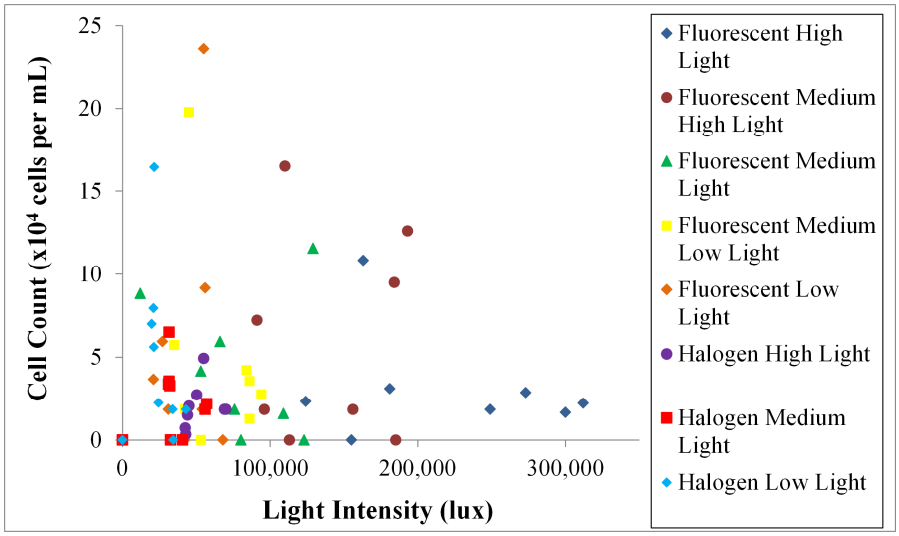

Figure 47. Effects of light intensity on growth under fluorescent and halogen lights

The cultures were bubbled for mixing, but this produced differential evaporation. On Days 3 and 8, media was added to account for evaporation, but this likely caused salinity differences among the cultures. The differences in temperature, light intensity, or salinity may have caused the cells to bleach in the highest light intensity, highest temperature bottles as seen in Figure 48.

A. 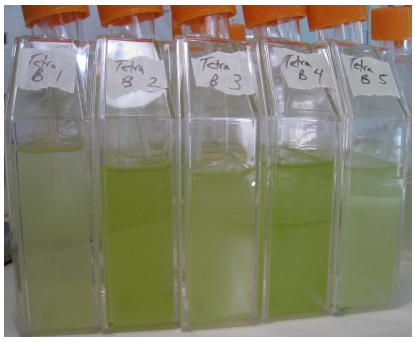 B. 
Figure 48. Bleaching seen in *T. impellucida* cultures grown under several light intensities
T. impellucida cultures grown under fluorescent (A) and halogen (B) lamps. The highest light intensity cultures are on the left with decreasing light intensity to the right.

7.3. Stirring Effects on *Tetraselmis* 200 mL Experiments

Several methods of stirring algae cultures are available, so the effects of mixing were examined in 200 mL glass jars. The following three stirring methods were tested: bubbling, hand swirling, and magnetic stirring. Trials were carried out in duplicate with two levels of stirring for each method. The setup was the same as described in Section 7.2, but each lid contained only one hole for sampling except for the bubbling trials. Each jar

contained 140 mL of f2 media with 18 mL of inoculating culture. The jars were lined single file approximately 2-6 cm in front of two fluorescent tube lights (Phyllips Master; TLD 58 W 840) to give all jars light intensities ranging from 347,000 lux to 210,000 lux. The bubbling jars were gently bubbled with air filtered by a 0.3 µm filter. In the hand swirling trials, the jars were gently swirled until well mixed either daily or every two days.

The jars experienced temperatures ranging from 22.4-24.1 °C, except for the magnetic stirred jars which were 26.1-26.9 °C. As shown in Figure 49, the three lowest final cell concentrations are from the jars that underwent magnetic stirring. Several of the cultures showed reduced cell concentrations after Day 7, which caused some negative SGRs. However, all of the mixing trials retained cell viabilities >70%, except for the magnetically stirred jars and one hand swirling every 2 days. In addition, noticeable cell size changes occurred by mixing speed and type.

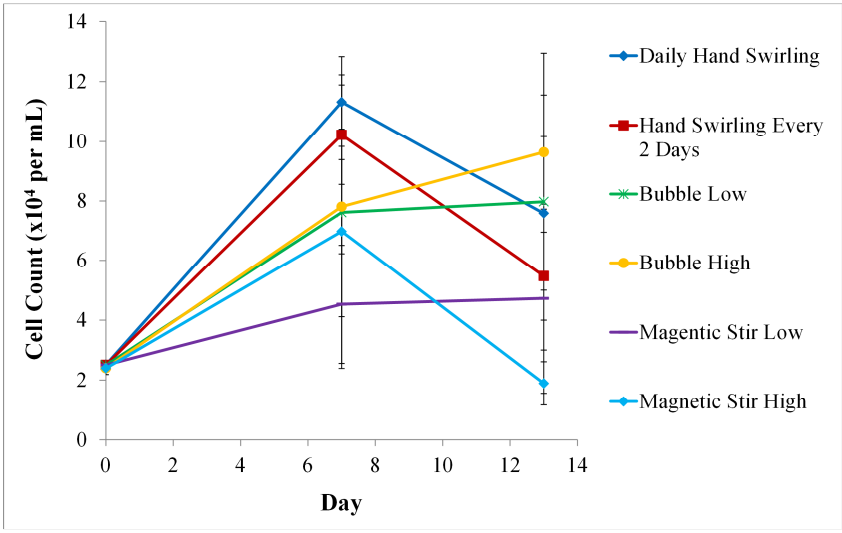

Figure 49. *T. impellucida* growth using several mixing methods
This graph shows average cell count results from duplicate trials. The error bars show the standard error of the mean for each trial.

7.4. Improving Bottle Experiment Setup

The experiments discussed in Section 7.2 and 7.3 experienced significant cell settling and evaporation. The bubbling trials used a tube inserted into the bottle, but the actual bubbling rate received by each culture varied. In some cases, the bubbling was very low or stopped periodically, and in others bubbling was vigorous. Moreover, some of the tubes

curled to release bubbles nearer the culture surface, which reduced mixing. These differences caused some cultures to lose lots of media through evaporation, which likely caused salinity differences. All of these issues increased the variation between replicates.

The bubbling issues were overcome by designing a stainless steel sparger and lid setup that could be sterilized easily and that fit 500 mL Erlenmeyer flasks. The metal sparger retains its shape and has 1 mm holes spaced by 10 mm apart. The holes were drilled on alternating sides of the sparger to reduce settling around it.

These experiments assessed growth using cell counts. Cell counts allow identification of contaminants and dismissal of cell fragments. In addition, dyes like trypan blue can be added to determine cell viability. However, cell counts are tedious and time consuming when many samples need to be counted; this can lead to reduced accuracy. As a result, later experiments used optical density measurements to increase the speed and accuracy of growth rate determination. Optical density measurements do not distinguish between live and dead cells, and they may be less sensitive at higher cell densities. However, regular observations confirmed that dead cells were only a small proportion of the population.

Alternate methods to assess biomass include measurement of chlorophyll a, particulate organic carbon, DNA, and protein. In addition, Nile Red fluorescence can be used to visualize neutral lipids within cells in solution. This allows lipid concentration changes to be tracked but may overestimate the lipid concentration. However, the necessary equipment was unavailable, so these methods must be saved for future experiments.

7.5. Optical Density to Determine Culture Concentrations

Algae culture concentrations have been determined at several wavelengths including 450, 540, 625, 680, and 750 nm [4], [54], [58], [91], [102], [111], [117], [124], [178], [198], [201], [256]. In view of this, measurements were made at a variety of wavelengths as shown in Table 27; media was used as a blank.

Table 27. Absorbances of *T. impellucida* cultures at different wavelengths

Sample	**400 nm**	**450 nm**	**500 nm**	**540 nm**	**550 nm**	**600 nm**	**625 nm**
1	0.114	0.087		0.052			0.048
2	0.172	0.171		0.138			0.066
3	0.140	0.120	0.103		0.090	0.093	
4	0.179	0.165	0.154		0.141	0.138	
Sample	**650 nm**	**680 nm**	**700 nm**	**750 nm**	**800 nm**	**850 nm**	
1		0.027		0.091			
2		0.059		0.089			
3	0.094		0.083	0.079	0.077	0.077	
4	0.137		0.127	0.121	0.120	0.118	

As Table 28 shows, the media contains particles that settle after several seconds, which means that the blank cuvette would need to be refilled with each sample. Instead, deionized (DI) water was used as a blank in future readings. Table 29 shows that 420 nm is the optimal wavelength for analysis of *T. impellucida* cultures, and this wavelength was used to measure optical densities in experiments.

Table 28. Absorbances of media at different wavelengths with DI water as the blank

	400 nm	**420 nm**	**450 nm**	**500 nm**	**540 nm**	**550 nm**	**600 nm**
immediate	0.186	0.185	0.179	0.201	0.210	0.220	0.228
settled	0.175	0.138	0.155	0.191	0.205	0.210	0.224
	625 nm	**650 nm**	**680 nm**	**700 nm**	**750 nm**	**800 nm**	**850 nm**
immediate	0.239	0.229	0.231	0.239	0.246	0.262	0.265
settled	0.231	0.240	0.225	0.233	0.244	0.247	0.259

Table 29. Absorbance of *T. impellucida* culture at different wavelengths with DI water as the blank

400 nm	**420 nm**	**450 nm**	**500 nm**	**540 nm**	**550 nm**	**600 nm**
0.315	0.402	0.295	0.284	0.28	0.279	0.273
625 nm	**650 nm**	**680 nm**	**700 nm**	**750 nm**	**800 nm**	**850 nm**
0.282	0.284	0.285	0.273	0.269	0.283	0.273

Dry weight and optical density measurements were performed to convert the absorbance measurements to cell concentrations. Several sample concentrations were prepared by diluting a *T. impellucida* culture with media; the concentrations prepared were 100%, 50%, 25%, and 0%. Triplicate samples were read optically at 420 nm, and triplicate 20 mL samples were filtered for dry weight measurements using the procedures outlined by Zhu and Lee [251].

In marine algae, many of the salts in the media remain when the sample is filtered for

dry weight determinations; this increases the apparent weight of the algae. Zhu and Lee [251] found that dry weight of un-rinsed marine algae samples was at least 1.2 times higher than rinsed samples. They examined the effects of several rinses and found that ammonium solutions were suitable. Zhu and Lee [251] also found that the ash free dry weights (AFDW) of distilled water rinsed samples of *I. galbana* and *Dunaliella* sp. were significantly lower than ammonium salt rinsed samples. It was postulated that *Isochrysis* and *Dunaliella* cells had no cell walls and so were more susceptible to changes in osmotic pressure, which are likely when marine algae are rinsed with distilled water.

Rinsing is necessary because some sea salts evaporate at 95 °C, the sample drying temperature, and some sea salts evaporate at 540 °C, the temperature at which ashing occurs. Meanwhile, other sea salts do not evaporate; therefore rinsing is necessary to determine accurate dry weights for marine algae samples. The applied vacuum strength can also affect the amount of salts retained on the filter [79], so the 0% concentration contains some salts. Each sample was rinsed with 20 mL of 0.5 M ammonium bicarbonate to remove excess salts, and the samples were dried at 95 °C until the percentage difference between weighings was less than 4%. Figure 50 shows the relationship used to convert absorbance readings into dry weight measurements.

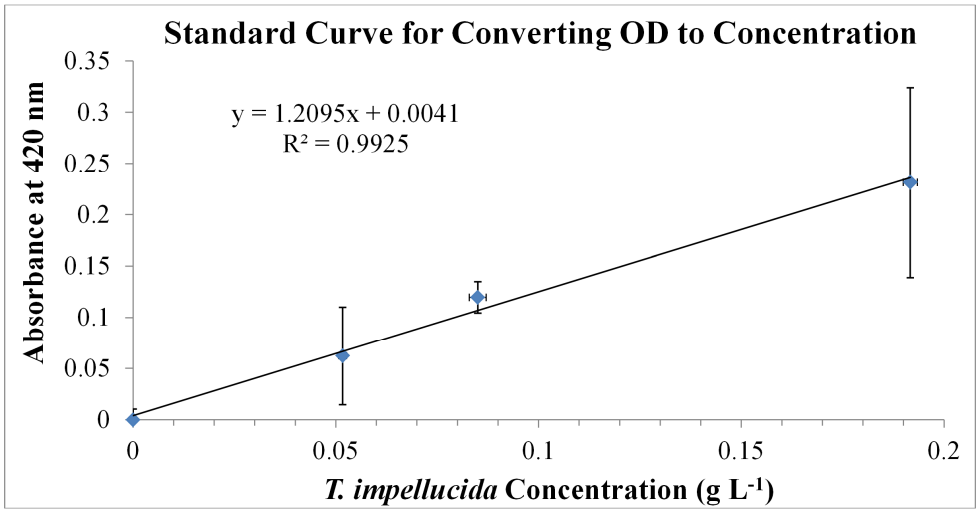

Figure 50. Relationship of *T. impellucida* dry weight and absorbance readings at 420 nm This graph shows average results from triplicate trials, and the error bars indicate standard deviation.

Although the filtered samples were rinsed with 0.5 M ammonium bicarbonate, some salts remained on the 0% concentration filters. This salt weight was subtracted from all concentration levels to account for the presence of salts. Moreover, the 0% samples had a small absorbance from the media, so it was subtracted from all sample absorbance values.

The *T. impellucida* cultures have a dry weight of 0.19 g L^{-1} ± 0.093 and an AFDW of 0.14 g L^{-1} ± 0.067. The *T. impellucida* AFDW was measured using the method of Zhu and Lee [251] with 20 mL culture samples in triplicate. Aliquots were filtered through preweighed, precombusted (450 °C, 2 hr) glass-fiber (Whatman GF/F, 47 mm, 0.7 µm pore) filters. *T. impellucida* has a high percentage of inorganics. This indicates that *T. impellucida* may have a theca (cell wall) and flagella covered in layers of scales, which has been observed in other *Tetraselmis* species [306]. These scales may afford *T. impellucida* greater protection for the stresses induced by mixing during cultivation of dense cultures. However, they could also make *T. impellucida* harder to digest during lipid extraction.

7.6. *Tetraselmis* Light Requirements

As discussed in Chapter 2, algal cells produce the energy for growth via the light driven photosynthesis reaction. This reaction occurs inside the cells' chloroplasts via a two step process involving a "light reaction" and a "dark reaction." The light energy is used to excite photons that are transported through the chloroplasts' photosystems to produce glucose. The total energy used depends upon the light's wavelength.

By comparing the amount of light energy stored in glucose to the amount that was absorbed, the cells' photosynthetic efficiency can be calculated. The efficiency depends on many factors, including dark respiration, fraction of incident radiation useful for photosynthesis, light reflection, and shading from other cells. Considering these factors, a practical photosynthetic efficiency estimate is 8%, which is considered high [307].

Various algae species contain different combinations of chlorophylls and accessory

pigments. These pigments extend the range of wavelengths absorbed for photosynthesis. This is important, especially in the 350-550 nm region; for example, several cultures have shown total pigment absorption at 440 nm to be 2-3 times that of chlorophyll a alone [308]. Zapata, Rodriguez and Garrido [309] used high-performance liquid chromatography to identify the chlorophyll and carotenoid compositions of ten algae species, and they found that *Tetraselmis suecica* had primarily chlorophyll a, followed by chlorophyll b with almost no chlorophyll c. This analysis agrees with earlier work from Whyte [191], who found that *T. suecica* had more than twice as much chlorophyll a as chlorophyll b and no chlorophyll c. Due to these differences in chlorophyll type and amount, it is likely that the absorption spectra of different species will differ, and this has been observed. Absorption spectra are similar but unique to each species [308], [310]. Figure 51(B) shows that the three *Tetraselmis* species tested have very similar absorption spectra with maximal absorbance at 430, 470, 680 and 660 nm.

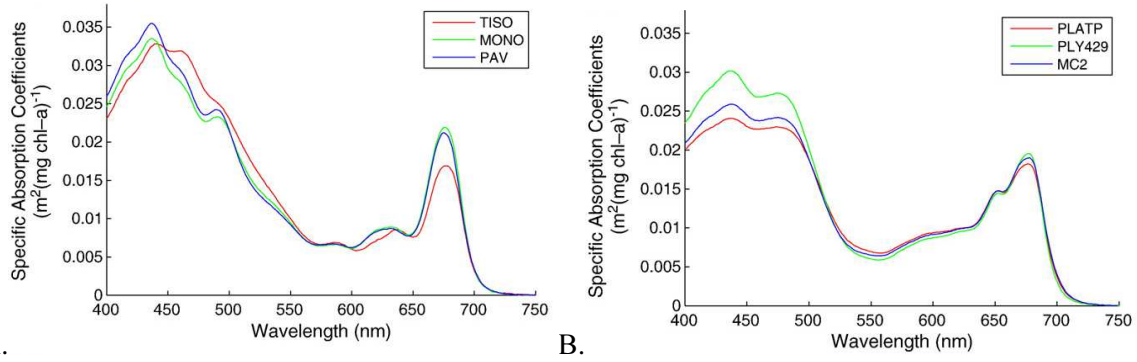

Figure 51. Absorbance spectra for 6 marine algae species within two phyla
These absorbance spectra by algae Class indicate that the Haptophytes, *Isochrysis* sp., *Pavlova lutheri* and *Pavlova* sp, in (A) have different absorption spectra than the Chlorophytes, *Tetraselmis striata*, *Tetraselmis* sp and *Tetraselmis* sp Chui, in (C) [310].

These differences in wavelength absorption ability translate into different growth rates when algae are grown under different light sources. When *T. gracilis* was grown under red, blue-green, and white lights, it grew best under red light [100]. *T. gracilis* harvested red and blue-green light more efficiently than white light [100]. Considering this, the optimal lights for *Tetraselmis* growth experiments were chosen as discussed in Section 7.7.

7.7. *Tetraselmis* 300 mL White and Mixed Light Experiments

A wide variety of artificial light sources are available for algae growth, including incandescent, metal halide, low pressure sodium and LED lamps. However, fluorescent lamps are the best choice because they are less expensive and have a lower heat output than the others except LEDs. Furthermore, fluorescent lamps are available in a variety of wavelength configurations and a variety of lengths and diameters. A combination of fluorescent lamps is necessary to maximise light output at *Tetraselmis*'s maximum absorption wavelengths of 430, 470 and 680 nm. Arcadia Marine Blue Actinic (blue) and Arcadia Original Tropical (white) 25 W lamps were chosen.

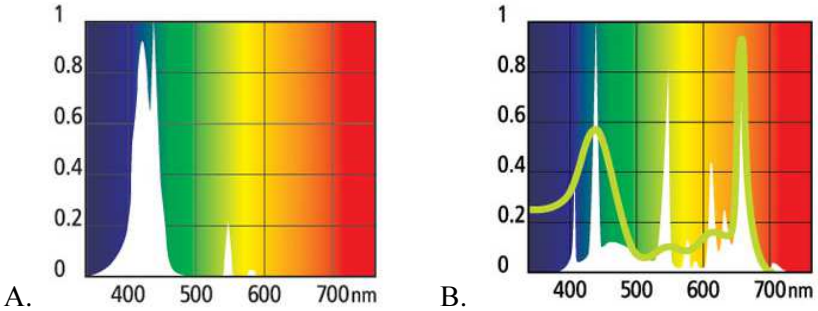

Figure 52. Spectra of lights used in growth experiments
Output Spectra of Arcadia Marine Blue Actinic (A) and Arcadia Original Tropical Fluorescent (B) Lamps [311]

As discussed in Chapter 3, a wide range of light intensities have been tested for algal growth. Less information is available for *Tetraselmis* species, but four *Tetraselmis* species have been grown at a variety of light intensities from 11.61-923.3 μE m^{-2} s^{-1}. The optimal light intensity for *T. impellucida* growth may differ depending on the light source used. To test this hypothesis, 550 mL flask cultures were grown at multiple light intensities; the experiment was performed once with two white lights and once with one white and one blue light. Experiments were performed with 4 replicates of each light source at two light intensities using the setup shown in Figure 53. A wire mesh screen covered was used over half of the lights to produce a range of light intensities. At 25 W, each of the two bulbs would emit 206.8 μE m^{-2} s^{-1} overall with approximately 1/8 of the total going to each flask.

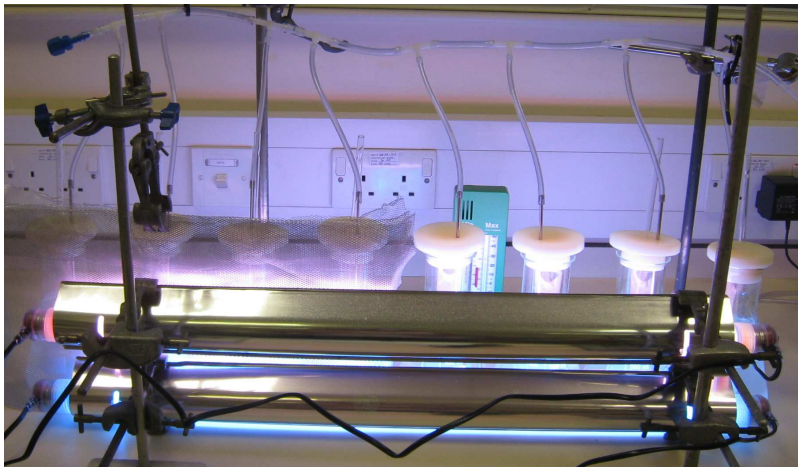

Figure 53. Experimental setup for light intensity and light source experiments

When looking at *T. impellucida* growth under two white lights, the light intensities were 12.3 klux, 153.1 klux (3 flasks), 359.2 klux (3 flasks) and 40.6 klux from left to right of Figure 53. The setup included 550 mL media with 30 mL inoculation per flask; the airflow was 1 bar, 4.3 L min^{-1}. The ASW was sterilized using filtration.

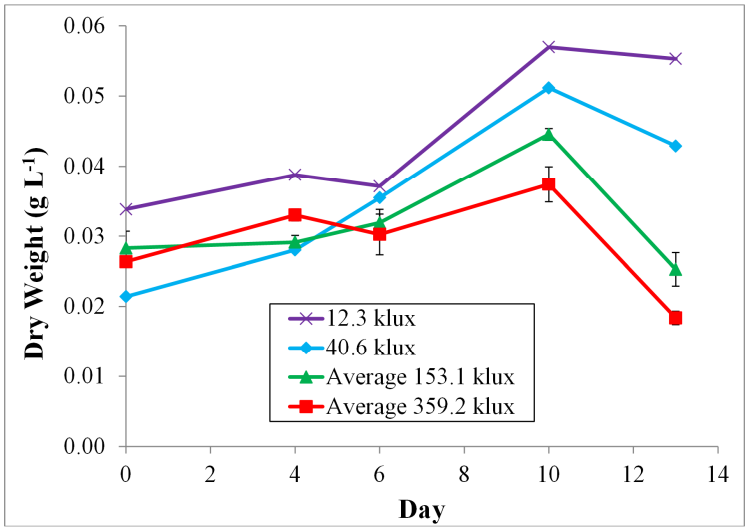

Figure 54. *T. impellucida* growth using white lights and several light intensities
This graph shows average results from triplicate trials at 153 and 359 klux, and the error bars show the standard deviation. The 12 and 40 klux results are from singular runs carried out alongside the triplicate trials.

As shown in Figure 54, all cultures grew until Day 10, when all growth began to decline; this matches observations that the 153.1 klux and 359.2 klux intensity cultures which bleached around Day 10 to become the colours seen in Figure 57 for Day 13. The highest growth was obtained at the lowest light intensity. The 359.2 klux and 153.1 klux cultures grown in triplicate, and the standard deviations were <0.002 g L^{-1} for both sets.

This indicates that, although the 12.3 klux and 40.6 klux cultures were not replicated, the observation that lower light intensities favour growth is accurate.

As in Figure 56, visual observations on Day 13 samples showed that the 12.3 klux and 40.6 klux cultures contained many healthy cells singly and in groupings with the 12.3 klux cells being slightly lighter green. The term "groupings" refers to several cells within one membrane as shown in Figure 55. The cell colour differences seen in Figure 56 result in colour differences in the cultures as shown in Figure 57. In the vegetative state, some *Tetraselmis* species produce cell sheaths, may account for the clear pieces shown in Figure 58. The three 153.1 klux cultures all had fainter green cells as individuals and small groupings, but they also contained some clear cells. The clear cells were intact but either unhealthy or dead. The three 359.2 klux cultures all had very few cells that were mostly clear, and two of them contained small filaments shown in Figure 59.

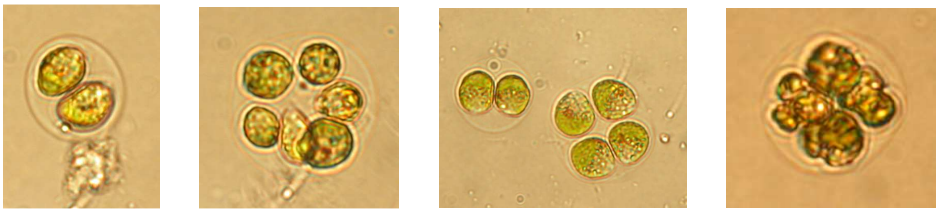

Figure 55. *T. impellucida* cell groupings at 500x magnification

359.2 klux 153.1 klux

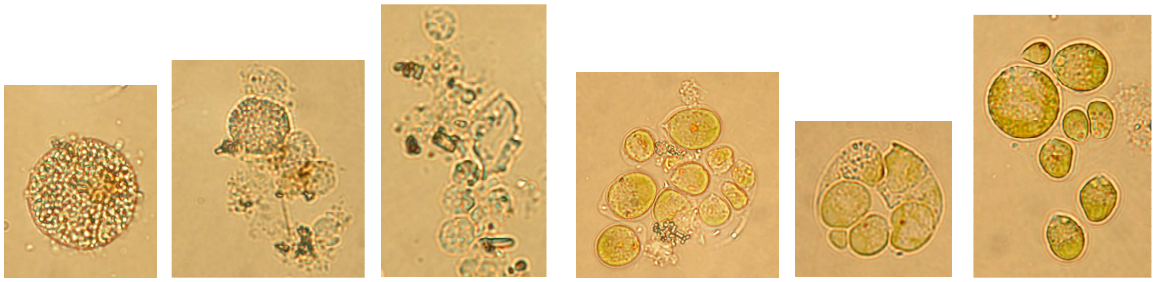

40.6 klux 12.3 klux

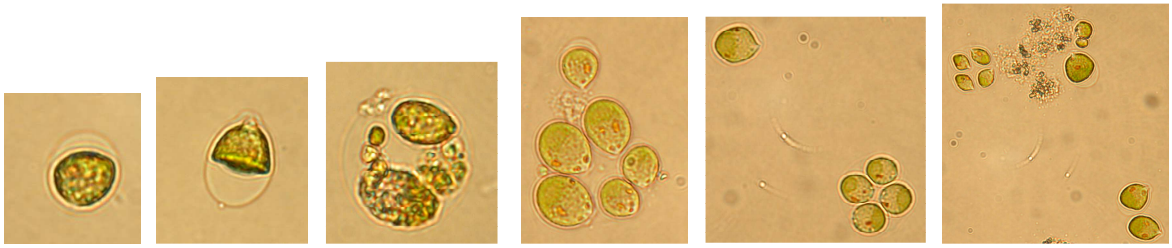

Figure 56. Three images from each light intensity of the white light *T. impellucida* cultures

Figure 57. White light *T. impellucida* cultures on Day 13

Figure 58. Clear pieces found in white light 359.2 klux and 40.6 klux *T. impellucida* cultures at 500x magnification

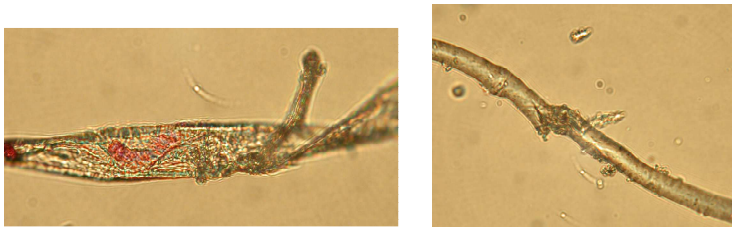

Figure 59. Filaments in 359.2 klux *T. impellucida* cultures at 500X magnification

Figure 60 shows the pH and temperatures within the 12.3 klux and 40.6 klux flasks. Both flasks showed similar pH values that increased slightly throughout the experiment and temperatures of 20.8-22.6 °C. On Day 13, all flasks were measured for pH and temperature, with the four light intensities having pH values of 8.72, 8.74, 8.65 and 8.67 in order of increasing light intensity. All flask temperatures were within 1.1 °C with the highest and lowest temperatures in the 359.2 klux and 12.3 klux and 40.6 klux light intensity flasks respectively. Regular conductivity measurements taken on the 40.6 klux and 12.3 klux cultures showed that the cultures started with the same conductivity of 40.5 mS, and the conductivities increased slightly as the experiment progressed.

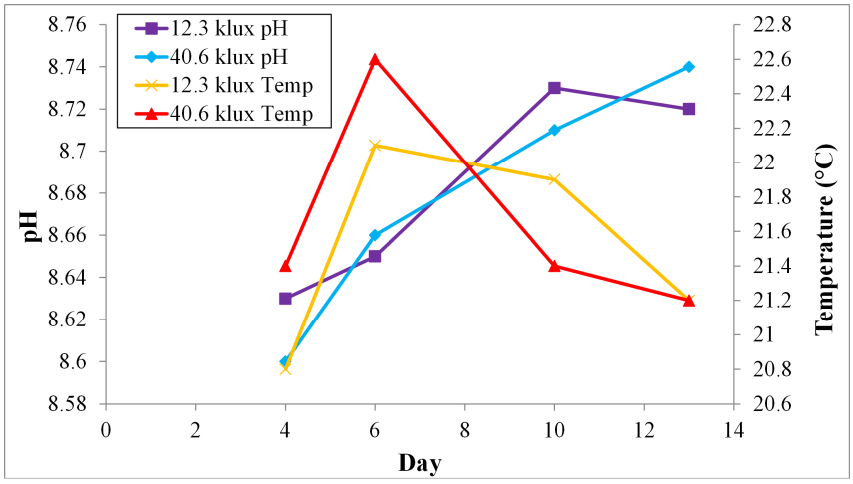

Figure 60. Temperature and pH measurements during white light *T. impellucida* cultures

Conductivity measurements showed the highest values in the 40.6 klux and 359.2 klux cultures with average values of 46.8 mS and 45.7 mS respectively. The 153.1 klux and 12.3 klux cultures had final conductivities of 43.3 mS and 42.4 mS respectively. Nutrient measurements on Day 13 showed that nutrients were not limiting.

In a separate experiment, the effects of mixed lights were assessed using flasks containing 550 mL media with 30 mL inoculation per flask; the airflow was 0.5 bar, 4.7 L min^{-1}. As shown in Figure 53, the flasks on each end of the line (one high and one low light) receive less light than their neighbours. From left to right, the mixed light flasks in Figure 53 receive 13.4 klux, 186.7 klux (3 flasks), 390.5 klux (3 flasks) and 26.4 klux.

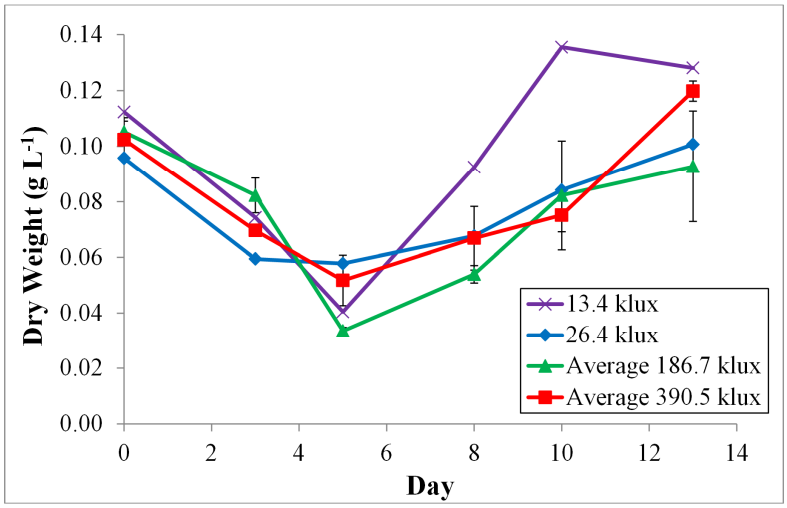

Figure 61. *T. impellucida* growth using mixed lights and several light intensities
This graph shows average results from triplicate trials at 186 and 390 klux, and the error bars show the standard deviation. The 13 and 26 klux results are from singular runs carried out alongside the triplicate trials.

Figure 61 shows biomass produced under mixed lights; these measurements match visual observations of the cultures at Day 13 as shown in Figure 62. The 13.4 klux culture showed the highest final concentration. Visual observations on Day 13 samples showed that the 26.4 klux culture contained many healthy cells that were mainly in groupings. The 13.4 klux culture also contained many healthy cells that were both individual and in small groupings. The three 186.7 klux cultures all had several green cells as individuals and small groupings, but they also contained some clear cells. The clear cells were intact but either unhealthy or dead. The three 390.5 klux cultures all had noticeably fewer cells than the other cultures, and many of their cells were clear. The cells appeared similar to those from Figure 56. Also, the 390.5 klux cultures all contained some clear pieces that may be cell sheaths or pieces of filaments as seen in Figure 58 and Figure 59.

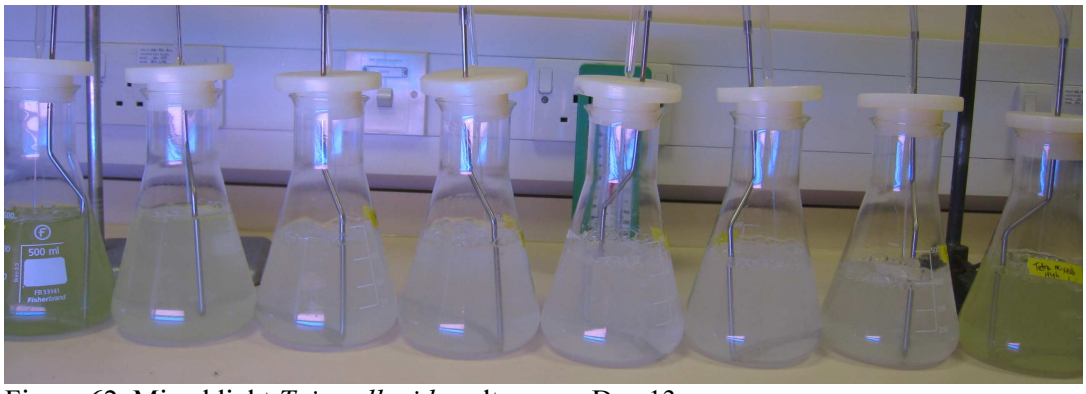

Figure 62. Mixed light *T. impellucida* cultures on Day 13

Figure 63 shows the pH and temperatures within the 13.4 klux and 26.4 klux flasks. Both flasks showed similar pH values and temperatures of 21-25.4 °C. On Day 13, all flasks were measured for pH and temperature, with the four light intensities having pH values of 8.31, 8.2, 8.23 and 8.17 in order of increasing light intensity. All flask temperatures were within 1.5 °C with the highest and lowest temperatures in the 390.5 klux and 13.4 klux light intensity flasks respectively.

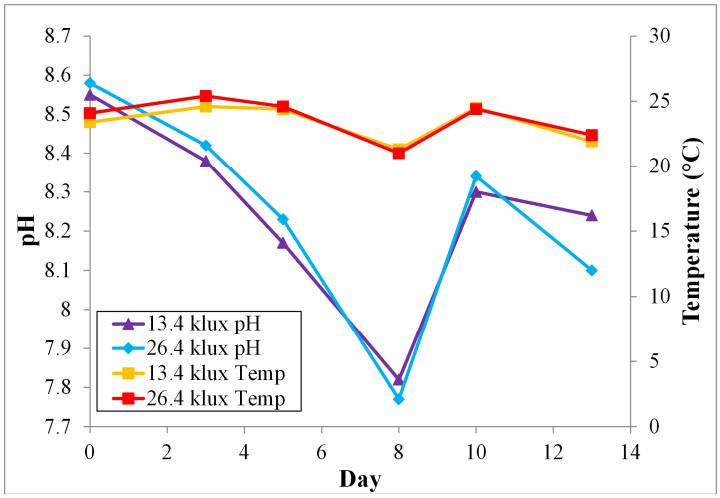

Figure 63. Temperature and pH measurements during mixed light *T. impellucida* cultures

Conductivity measurements showed the highest values in the 390.5 klux and 26.4 klux cultures with average values of 49.6 mS and 49.5 mS respectively. The 186.7 klux and 13.4 klux cultures had final conductivities of 45.4 mS and 45.2 mS respectively. Nutrient measurements on Day 13 indicated that nutrients were not limiting during the experiment.

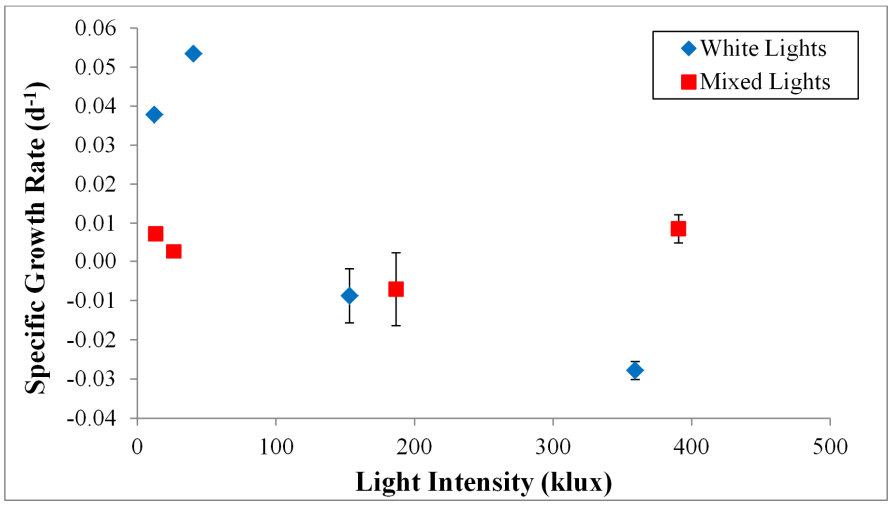

Figure 64. Specific growth rates of *T. impellucida* grown under white and mixed lights
This graph shows average results from triplicate white light trials at 153 and 359 klux and triplicate mixed light trials at 186 and 390 klux. These error bars show the standard deviation. The white light trial 12 and 40 klux and mixed light trial 13 and 26 klux results are from singular runs carried out alongside the triplicate trials.

The SGR calculations showed that growth was greatest for the two low intensity white light cultures at 12.3 klux and 40.6 klux. The mixed light cultures were less dependent upon light intensity but also had a higher standard deviation. It is clear from Figure 64 that algae cultures at 550 mL scale are unlikely to be light limited unless the cultures are dense.

7.8. Sterilization Experiments

The 230 L PBR is too large for conventional sterilization procedures like autoclaving, and steam and UV sterilization are not possible. As a result, it was necessary to test several sterilization procedures before the 230 L PBR could be used for algae growth. When growing algae, sterilization is most important to prevent contamination by other phototrophs; contamination by fungi and bacteria is less likely because of the lack of organic carbon in the media [6]. Chemical sterilization with bleach is the preferred method for sterilizing large volumes of saltwater.

Chemical sterilization with bleach is the preferred method for sterilizing this volume of saltwater. Three bleach sterilization procedures were identified for culturing large volumes of algae [300], [312]. To determine the optimal procedure for *T. impellucida,* all three procedures were tested in duplicate 500 mL cultures with tap water as a control. They were grown in f2 media with 15 mL inoculation volume. The experiments were 0.25 mL bleach followed by 0.075 mL neutralizer, 0.5 mL bleach/0.125 mL neutralizer, and 2.5 mL bleach/0.625 mL neutralizer. Cultures were prepared and grown using one Arcadia Marine Blue Actinic and one Arcadia Original Tropical 25 W lamp that together produced at an average light intensity of 39.5 klux. Cultures were aerated with humidified, filtered air at a flow rate of 5 L min^{-1}, 1 bar pressure. The experimental setup is shown in Figure 65. Throughout the experiment, air temperature around the flasks ranged from 20-28 °C.

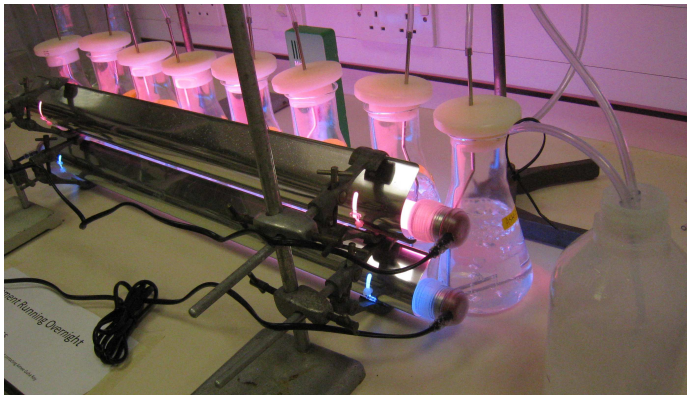

Figure 65. Experimental setup during sterilization experiments

None of the procedures tested in Figure 66 showed high growth. Regular analyses indicated that the cultures all had sufficient nitrate levels and a constant pH throughout the experiment. However, water analyses showed that all flasks contained residual chlorine from 0.8-3 ppm, which is likely to have reduced *Tetraselmis* growth rates. As such, a second sterilization experiment was performed to test the effects of higher neutralizer concentrations. This experiment involved the same flask, light and gas setup used in Figure 65, but the inoculation level was increased to produce duplicate 500 mL cultures with 38 mL inoculants (7.6% rather than 3% inoculants). Also, the gas flow rate was increased to 2 bar and 5 L min^{-1}. The sterilization procedures tested were 2.5 mL of chlorine with either 0.83 mL or 1.25 mL of neutralizer; positive and negative controls consisted of tap water and autoclaved saltwater prepared from DI water. Throughout the experiment, the air temperature around the flasks ranged from 19-25.5 °C.

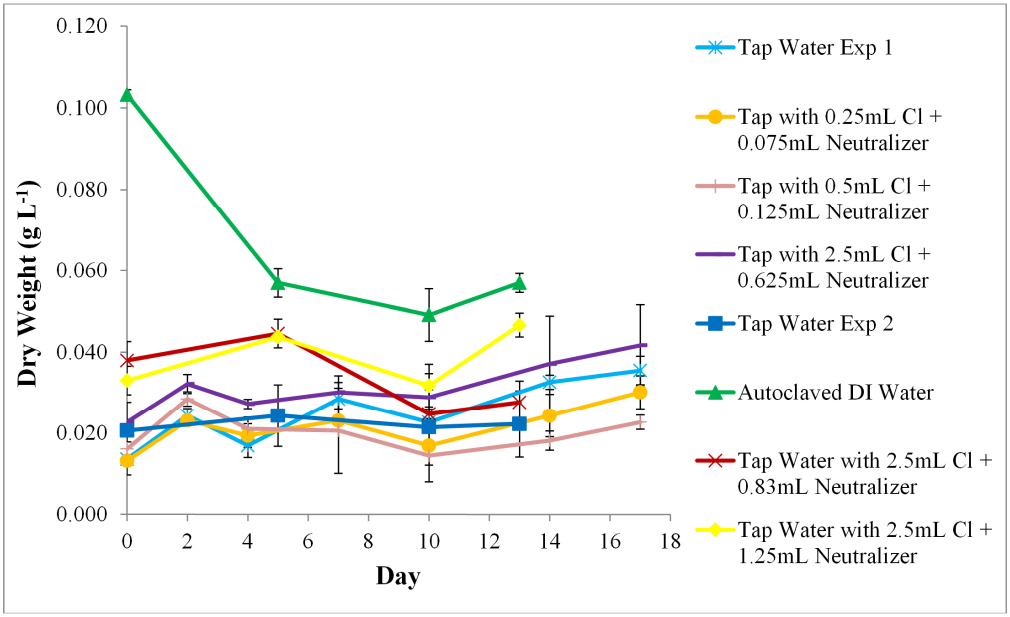

Figure 66. Growth of *T. impellucida* under three sterilization schemes
This graph shows average results from duplicate runs during three sterilization experiments. The error bars indicate standard deviation.

The highest final concentrations were achieved in autoclaved DI water and tap water with 1.25 mL neutralizer. However, the final concentration is dependent on the starting level, so a better growth estimate is to calculate the SGR, which is shown in Figure 67. At

Day 5, the ASW flasks were darker green then the others, while the autoclaved DI water algae were greenish white. All flasks were showing noticeable algae growth except for the tap water with 0.83 mL neutralizer. Furthermore, on Day 5, a proportion of algae had adhered to all flask bottoms, so additional swirling was needed to mix the cultures before sampling. During the experiment, culture tap water with 1.25 mL neutralizer B stopped bubbling; this was corrected and reoccurred three times. However, the sample showed approximately the same growth as its duplicate, which had bubbled continuously. On Day 13, pH readings showed that the autoclaved DI water flasks had an average pH of 8.36 compared to pH levels of 8.64, 8.73, and 8.70 for the tap water, tap water with 1.25 mL neutralizer, and tap water with 2.5 mL neutralizer samples. This is a possible reason that the autoclaved DI samples had a slightly higher final dry weight reading. Note that the standard deviation of the tap water sample may be high because tap water A received only 2.7 mL nutrients, while all other samples received 5 mL nutrients.

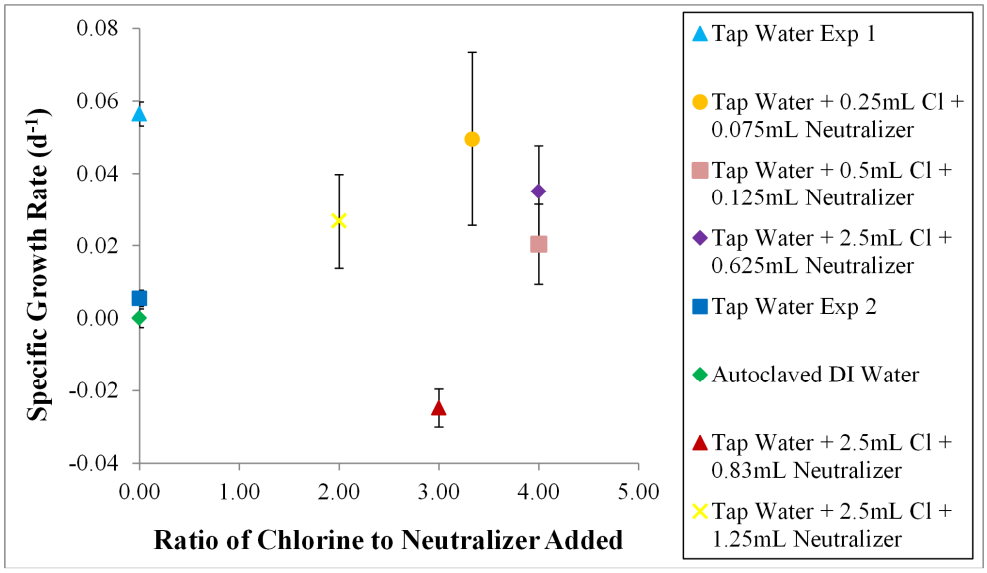

Figure 67. Specific growth rates of *T. impellucida* in various sterilization schemes
This graph shows average results from duplicate runs during three sterilization experiments. The error bars indicate standard deviation.

When saltwater is autoclaved, many of the salts settle out. After autoclaving, the media is stored in a refrigerator until a couple hours before use, when it is removed to warm to room temperature. The autoclaved media was shaken until all salts were

dissolved, but the media was cloudy, which accounts for its higher initial absorbance reading. After a couple days, the media cleared to match other samples. To account for this, μ calculations were performed on with Day 5 as N_1 rather than Day 0 as in other samples. From Figure 67, it is clear that none of the chlorine schemes produced significant growth compared to tap water, and there was a lot of variation between the samples. The autoclaved, media flasks also showed no significant growth, although the same media was used in maintenance cultures. This indicates that the reason for slow growth rates may have been an environmental factor, such as temperature, or another factor common to all flasks, such as the growth phase of the inoculation culture. Later experiments in the PBR, as detailed in Chapter 9, showed a significant lag phase of >17 days, so it is possible that these experiments would have grown more if allowed to run longer. Even so, it is clear that cultures with a higher neutralizer to chlorine ratio grew better than cultures with a lower ratio. This could be due to excess chlorine in the tap water. To overcome this, it was decided that future experiments would be performed with saltwater made from DI water rather than from tap water.

7.9. Conclusions

A wide variety of experiments were performed to prepare for larger-scale experiments in the PBR. These included examinations of light source, light intensity, mixing type, mixing speed for effects on *T. impellucida* growth rates. In addition, several sterilization procedures were tested. Few significant findings were produced from these initial trials, but they were necessary to prepare procedures and settings for PBR experiments. In addition, the standard curve for converting optical density to biomass concentration was used in all *Tetraselmis* growth experiments.

These experiments also made it possible to develop an improved experimental setup for future bottle experiments. Fluorescent high light intensity trials showed cell viabilities

≥70%, where halogen high light trials were reduced to ≤56%. The light intensity experiments indicated that lower light intensities were preferable for *Tetraselmis* growth. During all light intensity and light source experiments, cell size changes and culture bleaching were observed. It would be interesting for these observations to be studied in future experiments. Another interesting observation for future study was noticeable differences in colour of *T. impellucida* cultures grown in f2, ErdSchrieber, and 50/50 f2/ErdSchrieber media.

Chapter 8. Hydrodynamics of a Rectangular Internal Air-lift Photobioreactor for Microalgae Growth

A 230 L internally illuminated PBR was built to grow algae. The reactor was built for easy changing of light sources, light intensities, and optical paths. Before being used to grow algae, it was characterized as described in this chapter. Reactor characterization centred on fluid movement and bubbling. Section 8.1 describes the theory behind bubbling, CO_2 supplementation, and shear stress within an algal PBR. Section 8.2 discusses the planning and construction of the 230 L PBR. Several tubing sizes, hole diameters, and hole spacings were tested in Section 8.3. Next, Section 8.4 details reactor fluid movement and bubbling under several gas flow rates without baffles, with three baffles, with saltwater instead of tap water.

8.1. Theory

Within a bioreactor, mixing is essential to aid distribution of nutrients and CO_2 and to cycle cells between areas of light and dark. Algae require light, CO_2, and nutrients to grow. In addition, the temperature needs to remain stable near the optimal growth temperature and waste products like O_2 need to be removed. Gases are generally transferred into a bioreactor by bubbling.

Bubbling: Energy is added to the reactor to increase mass transfer rates; this occurs as bubbles enter the liquid phase and force the liquid to move. As a bubble moves upward from a sparger hole, the liquid above is pushed aside and below the bubble's wake causes turbulent mixing. Gas holdup is the reactor volume fraction occupied by gas. It determines many important reactor properties, including overall mass transfer rate, circulation rate, and gas residence time [21]. When Sierra et al [29] studied flat-panel PBRs, they found that gas holdup and volumetric mass transfer rates both increased linearly as the air flow rate was increased. However, the maximum air flow rate they tested was 0.32 v v^{-1} min^{-1} (volume of air per volume of culture per minute), which is

equivalent to a superficial gas velocity of 0.0076 m s^{-1} [29]. It is possible that an upper limit to this relationship exists. Ugwu et al [21] found that, as gas flow rate increases, so does bubble diameter, which reduces mass transfer rates. Along with mass transfer, bubble size can affect light penetration, mixing and shear stress [22].

CO_2 Supply and pH Control: Cells need sufficient CO_2 to enhance growth rates. Due to cost considerations, air is often bubbled through PBRs as the CO_2 source. However, CO_2 only composes about 0.038% (v/v) of air, so very dense algal cultures may require CO_2 enriched air to prevent CO_2 limitation. CO_2 is added to the reactor as a gas, so the rate of CO_2 transfer from the air bubble to the reactor media limits the cellular growth rate. CO_2 must diffuse from the pure CO_2 gas phase within the bubble, across the physical interfacial area that occurs at the boundary layer between the gas and liquid, and into the bulk liquid phase. This causes the dissolved CO_2 concentration around the bubble to increase. This aqueous CO_2 disperses into the bulk liquid phase and into contact with the algae cells suspended there. Aqueous CO_2 must then diffuse across the liquid/solid interface of the algae cell walls. This reduces the dissolved CO_2 concentration in the bulk liquid phase and thereby increases the driving force for more CO_2 to dissolve. Once inside the cell, CO_2 is transported from the cell wall to its chloroplasts to undergo photosynthesis.

Mass transfer resistance within a bioreactor is dominated by the resistance between the gas and liquid phases, so CO_2 mass transfer can be approximated by Equation 9 from [8].

(9) $$N_{CO2} = k_L \times a \times (C_{CO2L}{}^{*} - C_{CO2L})$$

where: N_{CO2} is the molar flux of CO_2 at the gas-liquid interface
k_L is the liquid-phase mass transfer coefficient
'a' is the specific area available for mass transfer
$C_{CO2L}{}^{*}$ is the CO_2 concentration in the culture medium adjacent to the bubble and in equilibrium with its actual partial pressure on the gas side
C_{CO2L} = CO_2 concentration in the bulk culture medium

Anything that affects "k_L" or "a" will affect the transfer of CO_2 into the system. "k_L" and "a" may be affected by bubbles, metabolites released by the cells, and other substances

that may modify the medium's surface tension [8]. Also, as the liquid tangential flow rate increases, the liquid boundary layer thins, which generally increases k_La. Overall, the amount of carbon transferred into the system depends upon both gas bubbling rate and partial pressure of CO_2 in the gas [8].

CO_2 dissolves in water, where it exists in equilibrium in a variety of forms including bicarbonate ions, carbonic acid, carbonate ions, and aqueous CO_2. This allows CO_2 in solution to act as a buffer by quickly converting between the forms to maintain equilibrium, and, as a result, changes in pH can be used to determine the CO_2 concentration within the reactor. This fact can be used to ensure that sufficient CO_2 is added to the reactor by injecting CO_2 whenever the reactor medium's pH rises.

It is important to maintain the reactor's pH near the species' optimum to obtain maximal growth. Many species can survive at pH values outside of optimum but doing so requires an expenditure of energy as the cells use active transport mechanisms to generate large pH gradients across their cell walls [13]. As a result of this additional energy expenditure, biomass growth is slowed or halted. Furthermore, the change in pH affects the formation of cellular components. For example, Rowley and Pirt [13] found that *Aspergillus nidulans* undergoes a 20-fold change in melanin formation rate when the solution pH is changed from 7 to 7.9. Also, pH has been shown to affect the production of the fatty acid, EPA, in some algae. EPA production was optimized in *Nitzschia laevis* at pH 7.5 and in *Phaeodactylum tricornutum* at pH 8.5 [11].

Several studies have also been performed on the prospect of using industrial waste gases with high CO_2 concentrations, such as those emitted by cement plants or power stations, to grow algae in PBRs. This approach provides a cheap supply of CO_2 enriched air with the bonus of also supplying nitrogen for the algae. In addition, this type of PBR system can act as a partial pollution control system for the industrial facility using it.

However, most studies have been performed on "artificial industrial emissions" that are generally only CO_2 mixed with air. These studies do not account for the effects of SOx or NOx emissions, high temperatures, or other contaminants likely to occur in these emission releases. In addition, CO_2 inputs from power plants may need to be diluted. When CO_2 concentrations were >2%, much of the influent CO_2 flowed out of the PBR directly [105].

Oxygen Removal: As algae perform photosynthesis, the cells release O_2 as a waste product, which must be removed at such a rate that its concentration is kept below the saturation level. This is necessary because a build-up of O_2 in the reactor will cause the photosynthetic reaction equilibrium to shift towards the reactants, and photosynthesis will be inhibited. This consequence has been shown on a variety of algae, where studies found that oxygen levels high above saturation inhibited photosynthesis [8], [29]. At very high O_2 concentrations, this effect can cause cells to decompose. Moreover, under intense sunlight, high concentrations of dissolved oxygen can damage cells by photooxidation [3].

Some reactor types remove oxygen more efficiently than others. For example, fermenter-type and bubble-column reactors have little difficulty with oxygen removal. Their designs include a head space for the oxygen to escape solution. Tubular PBRs, on the other hand, risk damage to algal cells from oxygen build-up unless supplementary steps are taken during design. This occurs due to the lack of air space within the tubes, which causes dissolved oxygen to become increasingly concentrated along the tube's length. As a result, tubular PBR tubing has a limited continuous run length and must incorporate a gas-exchange unit or degassing zone, where dissolved oxygen can be stripped by bubbled air [3], [8]. Tubular PBRs may also require CO_2 addition at various points along the reactor's length to prevent a pH gradient from forming and to ensure that the entire reactor has sufficient CO_2 to encourage photosynthesis.

Shear stress: In general, increased turbulence within a PBR increases algal growth as cells are more easily mixed with CO_2, nutrients, and light. However, mixing must not be so vigorous as to damage cells by shear stress. Other than sparging, mixing may be accomplished using a mechanical pump or an airlift pump. Mechanical pumps are used because of their ease of design and operation, but they are more damaging to biomass than airlift pumps [3]. Some of the cells may be sheared as they circulate through the pump, especially if the pump is operated at high speeds. Some species are more sensitive to shear stress than others. Diatoms, which contain a rigid siliceous cell wall, are very sensitive to shear stress [11]. In fact, a general rule of thumb for algae sensitivities to shear stress is, in terms of increasing sensitivity to shear: green algae < blue-green algae < diatoms < dinoflagellates [313]. As a green alga, *Tetraselmis* should not be overly sensitive to shear.

Cell stress has been shown to occur when mixing is so vigorous that fluid microeddies are as large as the cells themselves [22], [29]. Several studies have been performed to determine the reasons that sparging can cause cell death but debates continue. Some studies have reported that low intensity sparging could kill cells caught by rising bubbles when the bubbles break at the media surface [8], [11]. A contrasting study reported that cell death was mainly due to bubble formation at the sparger, as opposed to bubbles bursting at the chamber's liquid surface or rising through the chamber [261]. This study was performed on the microalgal strains *Dunaliella tertiolecta* and *D. salina*, and Barbosa et al [261] also concluded that small diameter nozzles were more detrimental than larger ones and that cell damage from sparging was strain dependant. Cell damage may also be reduced by using baffles to provide more efficient mixing at lower overall levels of shear. In addition, supplements that modify interfacial properties can be added to the reactor. One example is carboxymethyl cellulose, which has been shown to protect algal cells against hydrodynamic stress caused by aeration [11].

Since increased turbulence can damage cells, cell damage is less likely in horizontal tubular reactors, where the culture velocity is quite slow. Due to this slower velocity and reduced mixing, flow through a tubular reactor is more like plug flow than through flat-plate, airlift, and bubble-column reactors, which all incorporate greater mixing within the reactor. Unlike tubular PBRs, bubble-column reactors do not generally exhibit plug flow behaviour. Studies on bubble-column reactors containing water showed that they have well-mixed gas and liquid phases as long as the gas flow rate is large relative to the liquid flow rate and the column height and column diameter are of similar magnitude [307].

Cell Motility: Turbulent eddies have lengths on the order of millimetres. The ratio of driving to viscous forces, calculated as the Reynolds number (Re) is used to determine whether ordered or turbulent flow is present. In water, flow moves from laminar to turbulent at a transitional range Re of 500 to 2000 [213]. At low Reynolds' numbers, turbulence is insufficient to transport CO_2 and other nutrients to algae cells; instead, diffusion accounts for nutrient transport. Due to diffusion's high influence on small cells, nutrient transport is not enhanced by motion unless the motion causes the cell to encounter an area of higher nutrient concentration. This is a possible reason that many cells swim in a helical pattern that enables nutrient detection in three dimensions [170].

As the cell swims, most of its boundary layer adheres to it, but the motion helps replenish the boundary layer with nutrients. This boundary layer means that the cell's immediate environment is viscous. Cell suspension is determined by the combination of the behaviour of the phytoplankton relative to its immediate water packet and to the water as transported within the mixed layer [213]. Swimming is more essential for nutrient supply for larger cells. Algae from 1-10 μm diameter obtain far more nutrients (up to 100x more) from diffusion than from movement [170].

8.2. Reactor Planning and Construction

Many PBR designs are available, and each has its own strengths and weaknesses. Flat-plate reactors are very efficient but difficult to scale-up. Fermenters are easy to scale-up but light-limited. An internally illuminated 230 L PBR was devised to integrate several of the advantages of these two reactor types. Internally illuminated bioreactors can show increased productivities due to decreased dark zones, and they may be heat-sterilized [21].

The 230 L PBR was specifically devised to allow several culturing parameters to be altered between trials. The PBR is composed of a single large PBR with up to 5 light boxes that can be hung internally; these parts are composed of poly(methyl-methacrylate), which allows 98% of light to be transmitted from the light box to the water. The removable light boxes allow alteration of the light path. Inside each light box is an internal hanger to hold up to four individually controlled fluorescent tubes. Altering the number of fluorescent tubes allows light intensities to be altered between trials. The light holders are set to hold fluorescent aquarium lights, which are available in a range of wavelength spectra. Gas flow is supplied using three hard plastic tubes with 1 mm holes drilled every 10 mm. Each gas flow tube was prepared to run along the bottom of the tank between each pair of light boxes. The tubes were weighted to maintain their location, but can be easily moved to alter flow patterns. In addition, three removable baffles were prepared to switch between directed media flow like a series of airlift reactors and undirected flow similar to a series of bubble columns. With the baffles in place, the tubing runs between them to form a riser region with the areas between the baffle walls and light box acting as downcomer regions. This continual circulation should greatly reduce cell settling and adherence to the light box walls. This design also ensures that cells are continually carried into the light region of the PBR. When the baffles are removed, height can be a reactor variable because the PBR is 90 cm tall. With all of these arrangement possibilities, the PBR can be used for systematic study of a wide variety of culturing conditions.

8.3. Bubbles and Mixing Dynamics from Various Tubing Setups and Flow Rates

Several bubbling arrangements were tested to visualize effects on flow patterns. Each arrangement was tested in a light box, which is a clear acrylic box with internal dimensions of 3.6 cm long, 30 cm wide, and 85 cm deep. Photographs were taken for each arrangement to examine differences in bubble size and to identify flow patterns. The arrangements tested are shown in Table 30, and those that provided insufficient gas flow and extremely turbulent flow are marked.

Table 30: Tubing arrangements tested for mixing effects using several gas flow rates

Tubing: 12 mm OD, 9 mm ID Tube Wall Thickness: 2.5 mm			Tubing: 11 mm OD, 6 mm ID Tube Wall Thickness: 3 mm			Tubing: 8 mm OD, 5 mm ID Tube Wall Thickness: 1.5 mm		
Hole Size (mm)	**Hole Spacing (mm)**	**Flow Rate (L min^{-1})**	**Hole Size (mm)**	**Hole Spacing (mm)**	**Flow Rate (L min^{-1})**	**Hole Size (mm)**	**Hole Spacing (mm)**	**Flow Rate (L min^{-1})**
1	10	5	1	10	5	1	10	5
1	10	10	1	10	10	1	10	10
1	10	15	1	10	15	1	10	15
1	10	20	1	10	20	1	10	20
1	20	5	1	20	5	1	20	5
1	20	10	1	20	10	1	20	10
1	20	15	1	20	15	1	20	15
1	20	20	1	20	20	1	30	5
2	20	5	1	30	5	1	30	10
2	20	10	1	30	10	1	30	15
2	20	15	1	30	15	2	10	5
2	20	20	1	30	20	2	10	10
2	30	5	2	10	5	2	10	15
2	30	10	2	10	10	2	10	20
2	30	15	2	10	15	2	20	5
2	30	20	2	10	20	2	20	10
3	20	5	2	20	5	2	20	15
3	20	10	2	20	10	2	20	20
3	20	15	2	20	15	2	30	5
3	20	20	2	20	20	2	30	10
3	30	5	2	30	5	2	30	15
3	30	10	2	30	10	2	30	20
3	30	15	2	30	15	3	20	5
3	30	20	2	30	20	3	20	10
4	30	5	3	20	5	3	20	15
4	30	10	3	20	10	3	20	20
4	30	15	3	20	15	3	30	5
4	30	20	3	20	20	3	30	10
4	30	25	3	30	5	3	30	15
			3	30	10	3	30	20
			3	30	15			
			3	30	20			

*Pink blocks indicate arrangements providing insufficient airflow for all holes to be used. Blue blocks specify arrangements producing an extremely turbulent water surface.

As shown in Figure 68, several of the gas flow rates tested produced insufficient air to utilize all tubing holes. Other air flow rates produced extremely turbulent water surfaces that would inhibit algae growth. The uncoloured boxes indicate tubing arrangements that are within an operating envelope.

A. 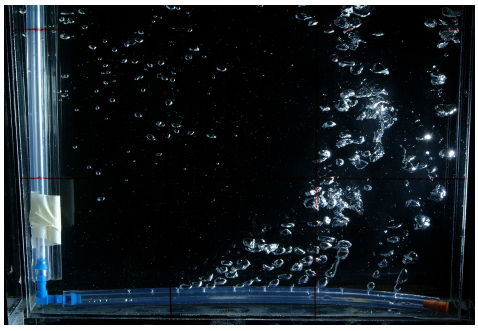 B. 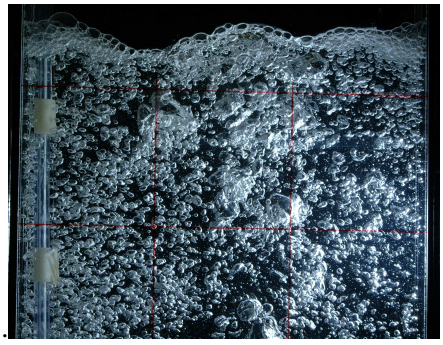

Figure 68. Turbulent bubble flow and insufficient gas flow rate
This figure shows flow through 11 mm OD, 6 mm ID tubing with 10 mm holes spaced 20 mm apart. At 5 L min^{-1} (A), holes are not fully utilized, and at 15 L min^{-1} (B), the water surface is very turbulent.

ImageJ was used to analyse bubbling photos, but the light box depth and resulting bubble overlap made it unreliable to estimate bubble sizes using ImageJ. In addition, the larger bubbles had significant highlights from the light shining on them. Instead, visual observations were used to determine the best tubing arrangements for algae growth. As shown in Figure 69, the bubbling generated distinctive flow patterns in the solution. Several large, amorphous bubbles are visible. Large bubbles break into small bubbles and provide greater mixing, and small bubbles provide greater surface area for mass transfer. However, lots of small bubbles makes the water cloudier and reduces light transmission.

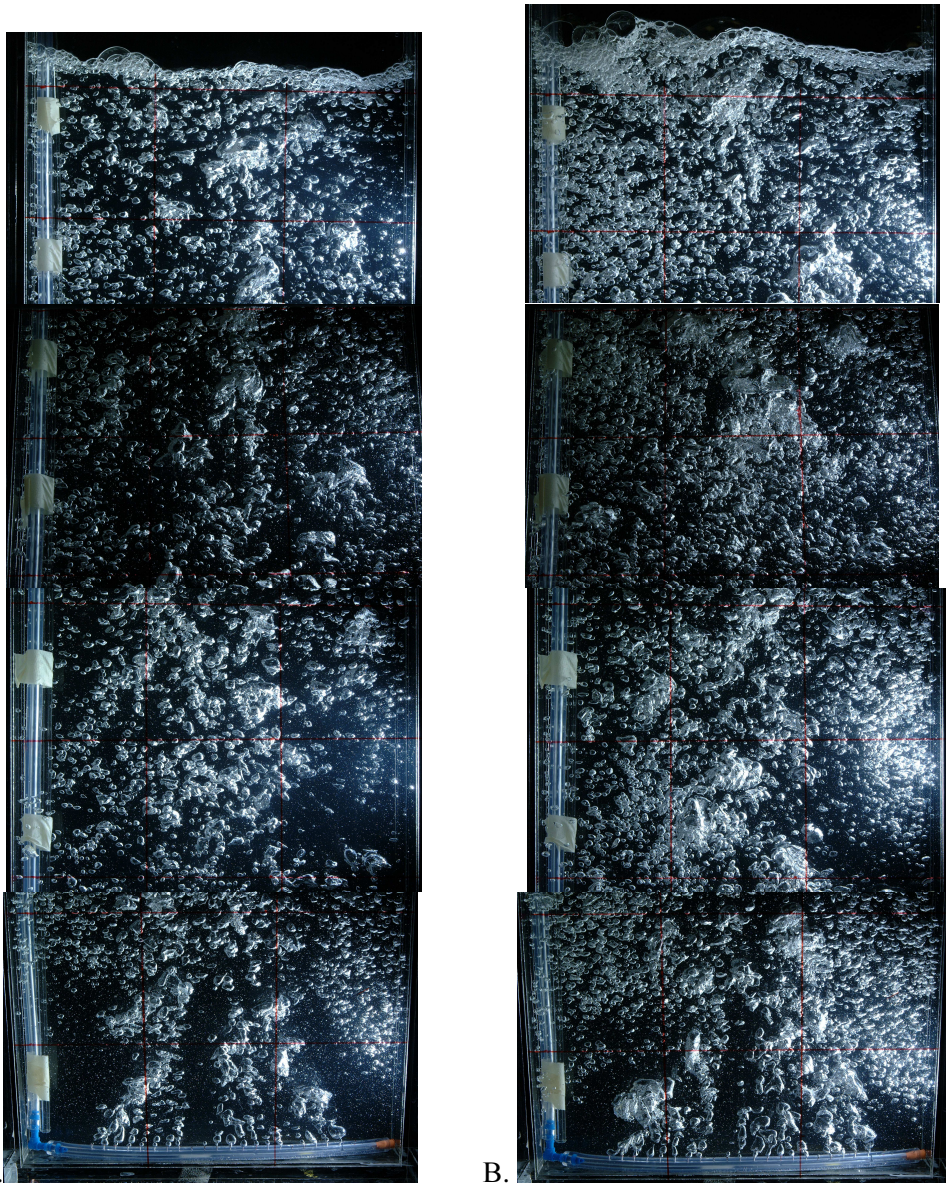

Figure 69. Fluid patterns observed while testing tubing arrangements
This figure shows flow through 11 mm OD, 6 mm ID tubing with 10 mm holes spaced 10 mm apart. Flow patterns are clearly available at 10 L min^{-1} (A) and 15 L min^{-1} (B).

8.4. Fluid Movement within the PBR

Fluid movement within the PBR without baffles was studied at 15, 20, and 25 L min^{-1}. Fluid flow was tracked by inserting red dye into the top of one end of the PBR and taking samples every few seconds until the absorbance was stable. These trials indicated that the reactor was well-mixed because it took >3 minutes for the dye to become completely distributed at all flow rates. This mixing time is many times shorter than typical cell division times. Increased gas flow rates reduced mixing times as shown in Figure 70. When baffles were used at a 20 L min^{-1} air flow, the mixing time increased slightly. These

experiments were performed in tap water. In addition, an experiment was performed using baffles, saltwater and 20 L min^{-1} air. It took longer for the dye to become completely mixed in the saltwater experiment than in any tap water experiments .

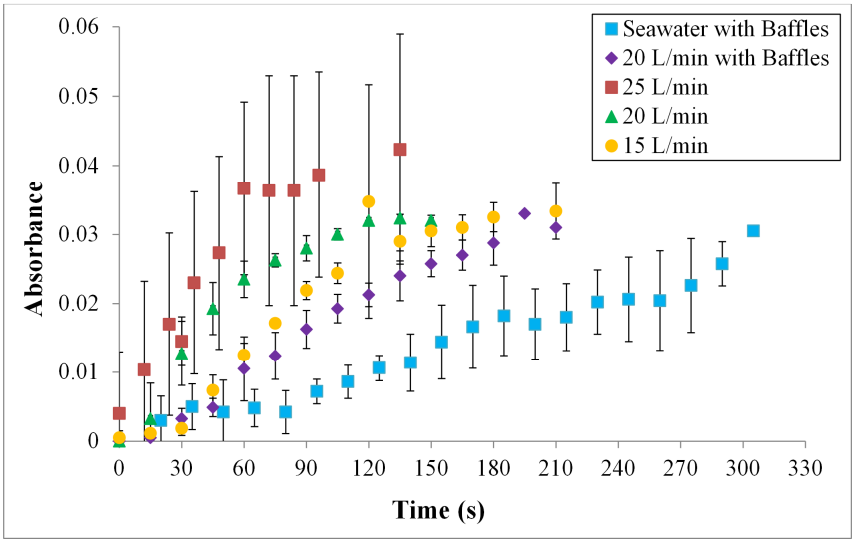

Figure 70. Fluid movement in the photobioreactor
This graph shows the standard deviations of four trials for the 15 L min^{-1}, 20 L min^{-1}, and 20 L min^{-1} with baffles experiments. The graph indicates standard deviations of five trials from the 25 L min^{-1} and seawater with baffles experiments.

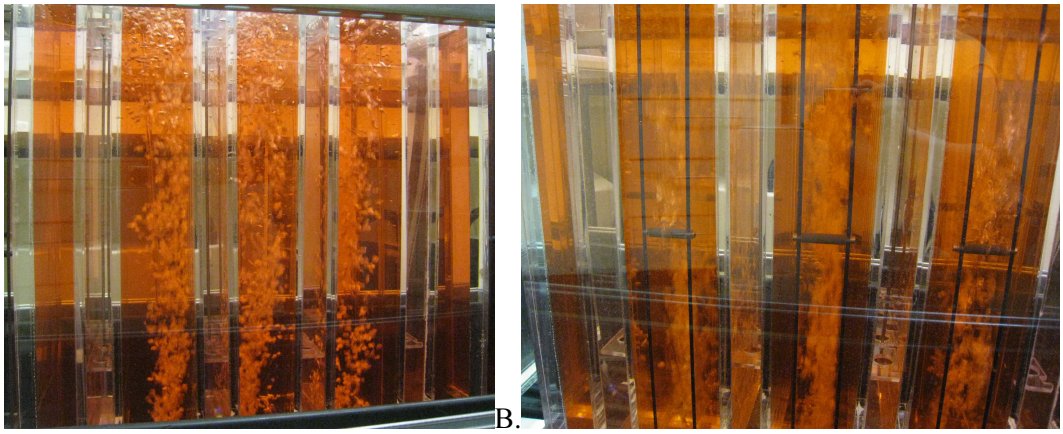

Figure 71. Water flow in the photobioreactor without (A) and with baffles (B)

With baffles, the PBR becomes a three-phase internal-loop airlift reactor with gas (air), liquid (culture media), and solid (algae cells) components. This occurs because the baffles delineate a clear cyclic pattern of media flow with defined riser and downcomer regions as opposed to the undefined liquid path in a bubble column reactor. The gas phase provides the dual purpose of mixing the reactor components and providing mass transfer as CO_2 is added to the culture media and O_2 is stripped from the culture media. As Figure 71 shows,

air is pumped into the bottom of the reactor, and the bubbles rise up between the baffles in the riser section, where flow of culture media and bubbles is primarily upward. As water flows over the baffle walls and into the downcomer region, some air bubbles are trapped with the water, where they influence the reactor's fluid dynamics. Flow in the downcomer region is predominantly downward for both liquid and bubbles. Since the riser section has a much higher gas component than the downcomer section, the mean density of the riser section is significantly lower than the mean density in the downcomer section. This density difference creates a driving force for circulation between the two sections by providing a pressure gradient to push the fluid around the system. Along with the advantages of directed water flow, airlift PBRs have very clean surfaces because of the liquid scrubbing action in the downcomer region. As shown in Figure 72, bubbling in saltwater produced more small bubbles. These bubbles stayed entrained in the PBR for longer. This effect is due to the salts inhibiting bubble coalescence.

A. B.

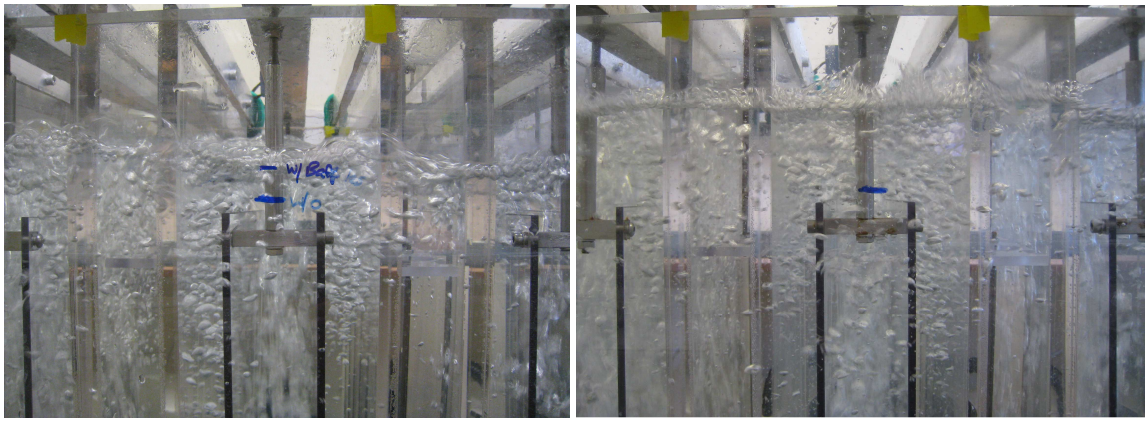

Figure 72. Saltwater and tap water photobioreactor characterization experiments

8.5. Discussion

Relatively large bubbles (≥0.006 m) are recommended for bubble columns [22]. Large bubbles are good for mixing. Small bubbles move more slowly through the media. Small bubbles are made at the cost of friction from the bubble leaving the pore, so coalescence is the enemy. Due to reflectance, a large number of bubbles can reduce light transmission

through a PBR. This reduced light transmission is clearly visible in the 15 L min^{-1} aerated photo as compared to the 10 L min^{-1} aerated photo in Figure 69. Generally, the effects of aeration on internal light transmission reduce as the gas flow rate is reduced [22]. Increased aeration rates lead to increased gas holdup, which provides more reflecting and shading surfaces within the reactor. Even at very low superficial gas velocities of 0.0025 m s^{-1} with less than 1% gas holdup, light transmission may be reduced up to 15% compared to gas-free operation [22].

Using saltwater with baffles produced noticeably more small bubbles and rounder bubbles than using tap water with baffles. This has been noted previously and said to account for increased light transmission in saltwater [22]. In saltwater, the small bubble size increases bubble residence time enough to cause bubbles to build up if aeration is continued. When gas holdup in saltwater is increased above 13%, the gas-liquid dispersion is very cloudy [22]. In fact, very small bubbles remain suspended after bubbling stops. Fine bubbles have been noted to remain suspended for several hours after gas flow ends [22]. Along with increased residence time, fine bubbles may aid in removing O_2. When microbubbles were used to grow algae, they stripped O_2 to ambient levels; this O_2 was postulated to be more important than CO_2 dissolving [314].

8.6. Conclusions

A new 230 L PBR was devised for use in algae scale-up experiments, so it is significantly larger than most lab scale experiments. This PBR is especially useful because it was built to easily change a wide variety of variables. The variables that can easily be changed include light intensity, light source, optical path, gas flow rate, and CO_2 supplementation level. This PBR was characterized to gain an understanding of fluid movement with and without baffles, and suitable operating conditions were identified. Saltwater showed significantly more entrainment of small bubbles. The characterization performed here indicated that the PBR was ready for growth experiments.

Chapter 9. *Tetraselmis* Growth in PBR and SGR Model Testing

This chapter uses *T. impellucida* growth experiments to test a *Tetraselmis* SGR model. This real-world validation test was performed in addition to the statistical validation tests discussed in Chapter 5. This is important because the *Tetraselmis* SGR, MLC and VLP models described in Chapter 6 have many potential applications. They can be used to identify optimal conditions for *Tetraselmis* growth. This is useful because *Tetraselmis* is a vital species for aquaculture, and it has promise for biodiesel production. Also, algae fuels are being studied around the world, especially in the US and China [19]. In addition, the PBR detailed in Chapter 8 allows the model testing to be performed above bench-scale volumes. These experiments are discussed in Section 9.1, and they include a trial to assess growth in the PBR, improving the PBR setup, and a trial to verify the SGR model. Section 9.2 is a discussion of the items noted in the validation trial. Next, the model results are compared with experimental values in Section 9.3. Finally, Section 9.4 discusses future work possibilities.

9.1. *Tetraselmis* Experiments in 230 L Photobioreactor

T. impellucida was grown to assess the effectiveness of the internally illuminated PBR discussed in Chapter 8. Two trials were performed. First, *T. impellucida* was grown with the PBR filled to a working volume of 140 L. During Trial 1, methods of improving the PBR setup were identified, so a second trial was performed using 40 L working volume.

9.1.1. Trial 1: *Tetraselmis impellucida* Photobioreactor Growth at 140 L Photobioreactor

The aim of this trial was to test the PBR setup, gather the first algae growth data in the PBR, and identify potential problems. *T. impellucida* growth was measured in an internally illuminated 230 L PBR. The PBR setup included baffles and tubing described in Section 8.2, so the working volume is 140 L. This setup is displayed in Figure 73. The media was composed of artificial saltwater (made from DI water and Instant Ocean Sea Salt) with 1400 mL of f2 media concentrate added. The culture was mixed using 9.1-10 L

min^{-1} filtered air. Sampling was performed by taking 8 samples of well-mixed culture from different areas of the PBR and averaging them. Biomass was measured by spectrometric analysis at 420 nm. Algae biomass was measured in g L^{-1} with measurements adjusted to account for variations in culture volume on each sampling day.

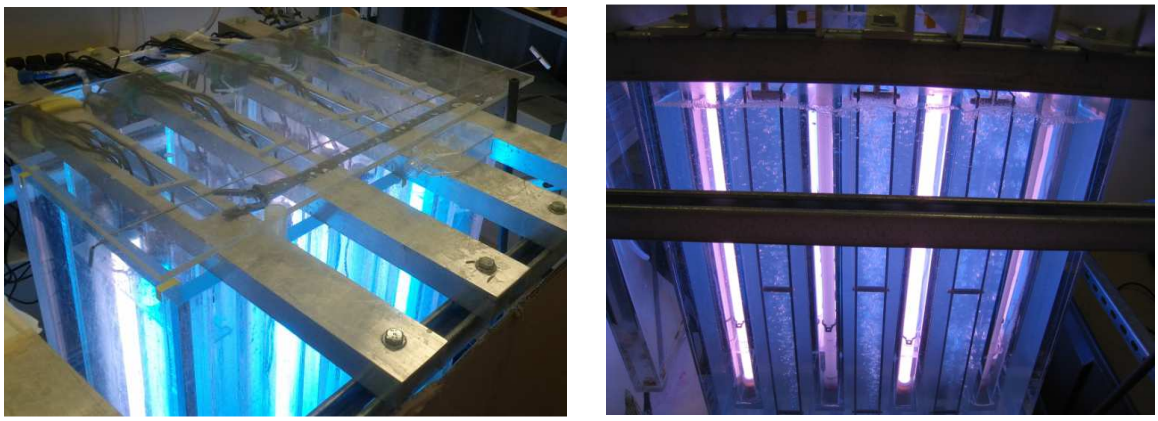

Figure 73. Photobioreactor filled to 140 L working volume

Trial 1 was begun using sixteen 25 W lights alternating between Arcadia Marine Blue Actinic (blue) and Arcadia Original Tropical (white). This setup ensured that the culture would be exposed to all wavelengths necessary for efficient growth as they were circulated around the reactor. The large number of lights caused the culture temperature to increase to 37.4 °C, so the 16 lights were reduced to 12 and then to 7 as shown by the first two arrows in Figure 74. For the remainder of the trial, 7 lights were used with the exception of the third arrow, when the lights were increased to 11 for approximately 6 hours before being reduced back to 7 lights. Trial 1 was inoculated with 4 L of concentrated *T. impellucida* culture, but the high temperatures achieved at the start of the trial made it likely that the lack of growth was due to the initial inoculant having crashed. On Day 5, a second inoculant was added consisting of approximately 3.5 L of concentrated *T. impellucida* culture. After Day 5, the temperature ranged from 28.9 °C to 32.6 °C throughout the trial with an average temperature of 30.0 °C.

No nutrient additions were made, but nutrients were monitored throughout the trial to ensure that they were not limiting. In addition, pH measurements were taken periodically

and showed little change during the trial. Along with biomass measurements, salinity was measured, and then fresh DI water was added to overcome evaporation losses. This caused salinity to fluctuate slightly as shown in Figure 75. Salts crusted the inner walls of the PBR just above the water line. However, the salt crust formed within the first couple of days and did not appear to accumulate significantly later.

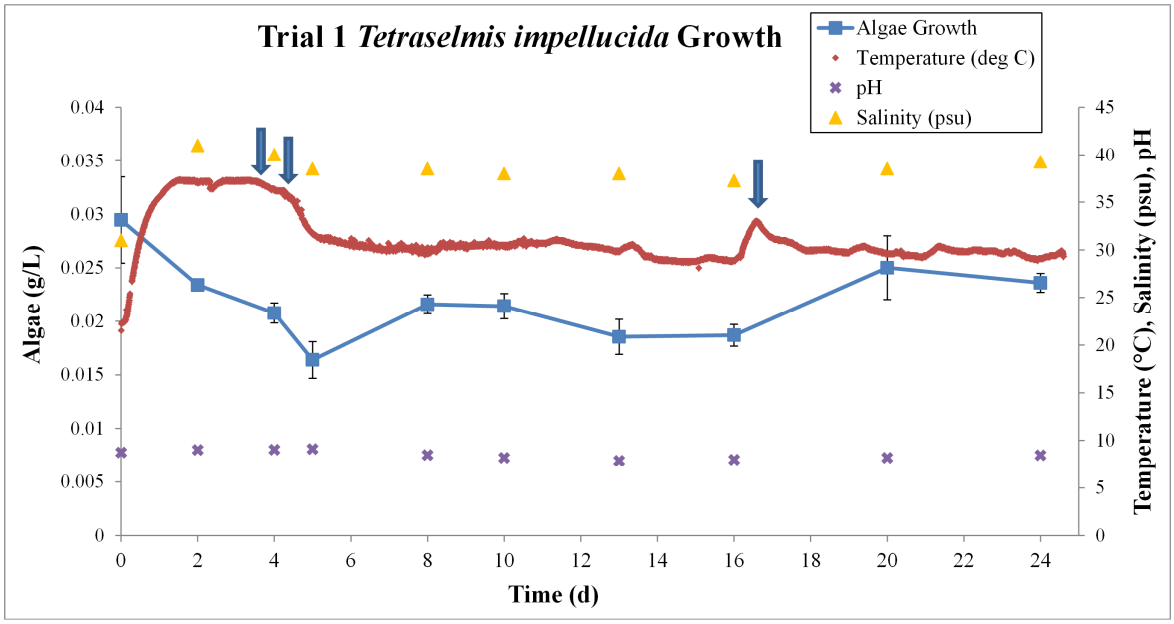

Figure 74. *T. impellucida* growth in an internally illuminated photobioreactor 140 L culture *T. impellucida* growth was measured using 8 samples taken from throughout the PBR, and error bars indicate standard deviation. Temperature was measured continuously. The first two arrows indicate where the 16 fluorescent tubes were reduced to 12 and then to 7. The third arrow indicates a 6 hour increase to 11 tubes before returning back to 7.

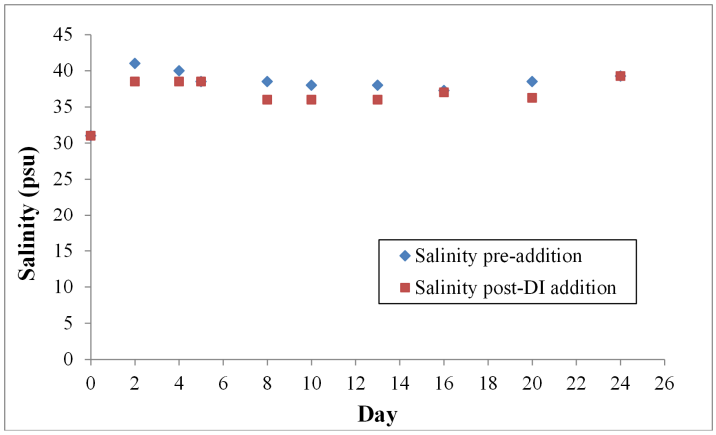

Figure 75. Photobioreactor Trial 1 salinity measurements before and after water addition

Trial 1 produced some growth, but exponential growth was not reached. Several potential problems were identified. A significant lag phase may have been necessary for

the cells to adapt to the conditions within the PBR, or the inoculation level may have been insufficient. The temperature was too high with all lights, and even with reduced lights the temperature averaged 30 °C. Moreover, the cells tended to settle.

9.1.2. Improving Photobioreactor Experimental Setup

Several modifications were made to the PBR experimental setup before a second trial was performed. The working volume was reduced from 140 L to 40 L. This shortened the expected experiment run time and increased the % inoculation. Since the baffles were built to be used with the PBR full, they were removed for the 40 L trial. Accordingly, the gas flow rate was reduced to 7 L min^{-1}. In addition, additional tubing and flow rate meters were added to allow CO_2 supplementation at various rates. Furthermore, in Trial 1 the salinity aim was 32 ppt, so the media was prepared to a specific gravity of 1.025. However, the increased temperatures during Trial 1 caused the salinity to increase up to 38 ppt. In Trial 2, the lights were turned on while the saltwater was made to achieve a more appropriate salinity.

9.1.3. Trial 2: *Tetraselmis impellucida* Photobioreactor Growth at 40 L

A second PBR trial was performed using 40.5 L of artificial saltwater with 400 mL of media concentrate added to prepare f2 media. 3 L of concentrated *T. impellucida* culture was added to give 7.4% inoculate.

The 40 L PBR culture was allowed to grow until it had progressed through all growth phases from lag phase to stationary phase. The culture was aerated by filtered air at a flow rate of 7 L min^{-1}. At the end of Day 9, CO_2 was added at a flow rate of 400 cm^3 min^{-1} to produce a concentration of 3.6%. The CO_2 flow varied slightly as shown in Figure 76 but remained approximately 3%. Addition of CO_2 reduced the pH slightly from an average of 8.67 in Days 0 to 9 to an average of 7.21 for the remainder of the experiment. The stability of pH during exponential growth is likely due to the CO_2 supplementation begun on Day 9. *T. impellucida* growth increased with time, although growth measurements near

the end of exponential and in stationary growth showed increased standard deviations compared to other measurements.

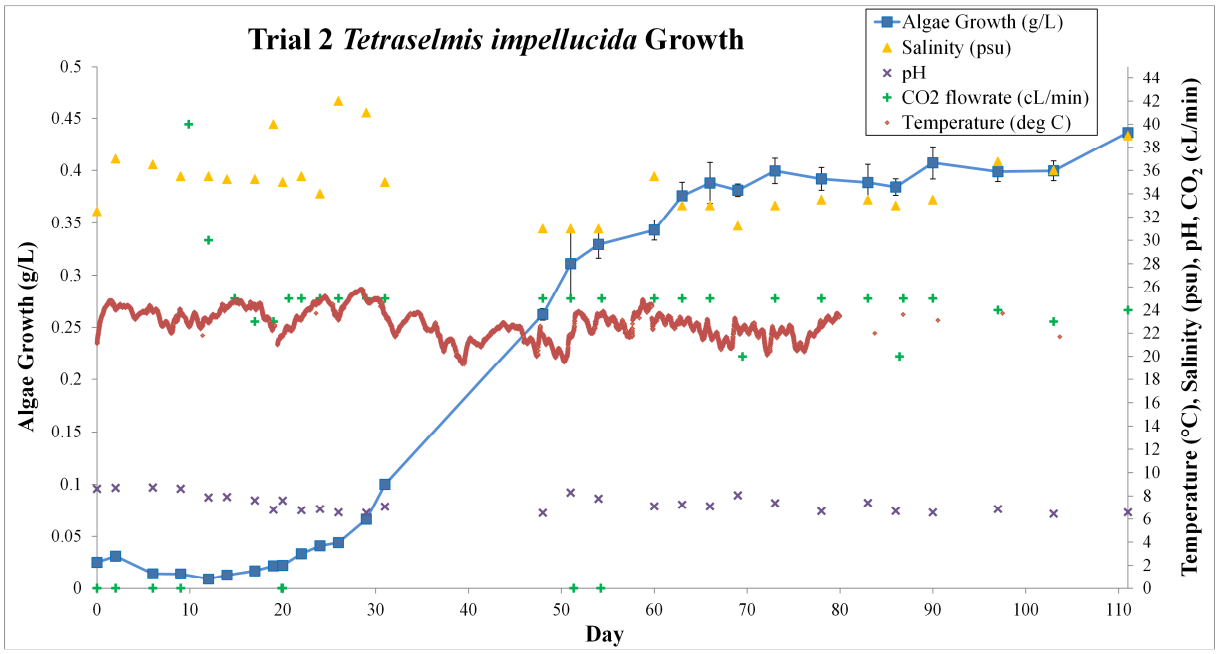

Figure 76. *T. impellucida* growth in an internally illuminated photobioreactor 40 L culture
T. impellucida growth was measured for 8 replicate samples taken from throughout the PBR. Error bars indicate standard deviation of growth samples. Temperature was measured continuously. CO_2 supplementation began on Day 9.

As Figure 76 shows, the *T. impellucida* culture grew well after a significant lag phase of approximately 20 days. The culture increased from 0.066 g L^{-1} to 0.33 g L^{-1} over 25 days. This lag phase is greater than the lengths of the bottle experiments and nearly as long as PBR Trial 1. However, after the lag phase, growth increased quickly. The lag phase existed for approximately 12 days, and the acceleration phase lasted from Day 12 through Day 26. The exponential growth phase lasted to about Day 63 and was followed by a stationary phase lasting to around Day 86.

Figure 76 shows the tank temperature, which ranged from 19.3 °C to 25.8 °C throughout the experiment with an average temperature of 22.8 °C. Nitrate and phosphate concentrations were measured regularly and remained steadily high until exponential growth was achieved. By Day 54, the concentrations were significantly reduced to 5 mg L^{-1} nitrate and 0.03 ppm phosphate. The concentrations continued to decrease slowly until

they were 0 by Day 90. On each day that biomass measurements were taken, salinity measurements were also taken, and then fresh DI water was added to overcome the water lost to evaporation. This caused slight fluctuations in salinity as shown in Figure 77. Note that, in Figure 77, the Day 19 to 31 post-DI water addition salinity measurements were assumed from water added on each sampling day. The salt concentration decreased slightly as cell growth increased, which is likely due to salts being incorporated into new cells. Within the first few days of the trial, a salt crust formed just above the water line inside the PBR and did not appear to accumulate significantly during the trial.

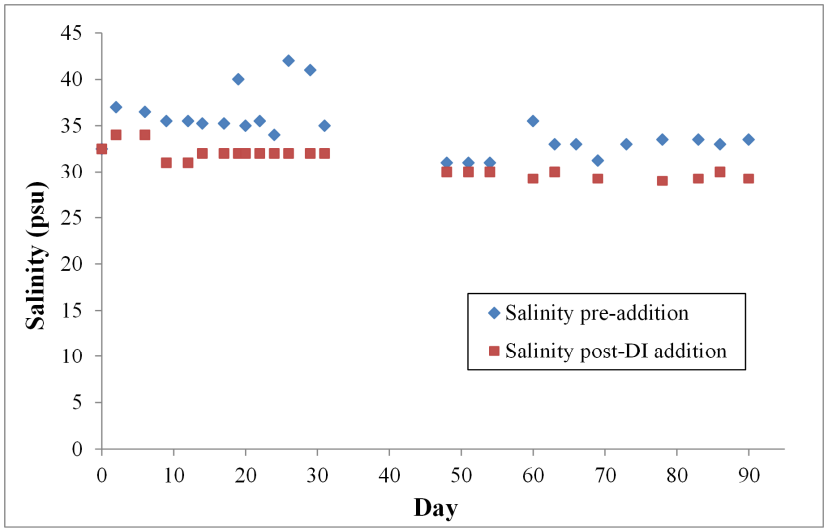

Figure 77. Photobioreactor Trial 2 salinity measurements before and after water addition

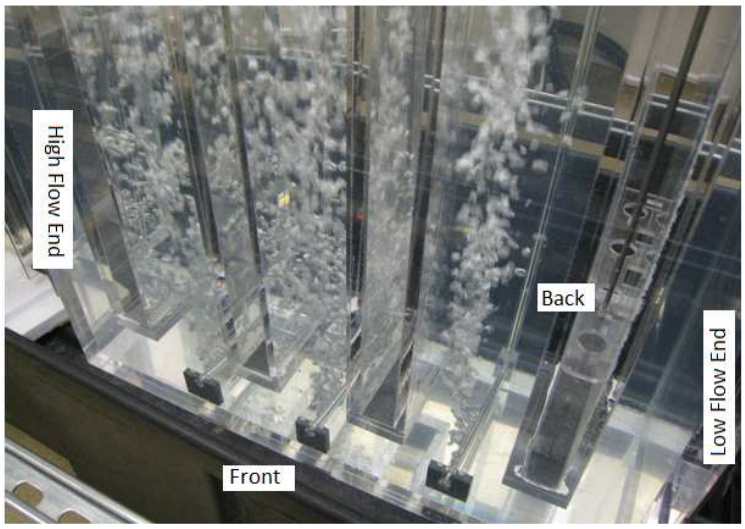

Figure 78. Photobioreactor layout
The PBR experienced differential air flow such that one end of the tank had slightly more gas flow than the other end.

Figure 78 shows the PBR orientation. Figure 79 shows the PBR front view and illustrates that the gas flow is greatest in the left tube, lower in the middle tube and least in the right tube. The culture was well-mixed before every sample was taken, so cells did not build-up significantly in the tank region with reduced bubbling.

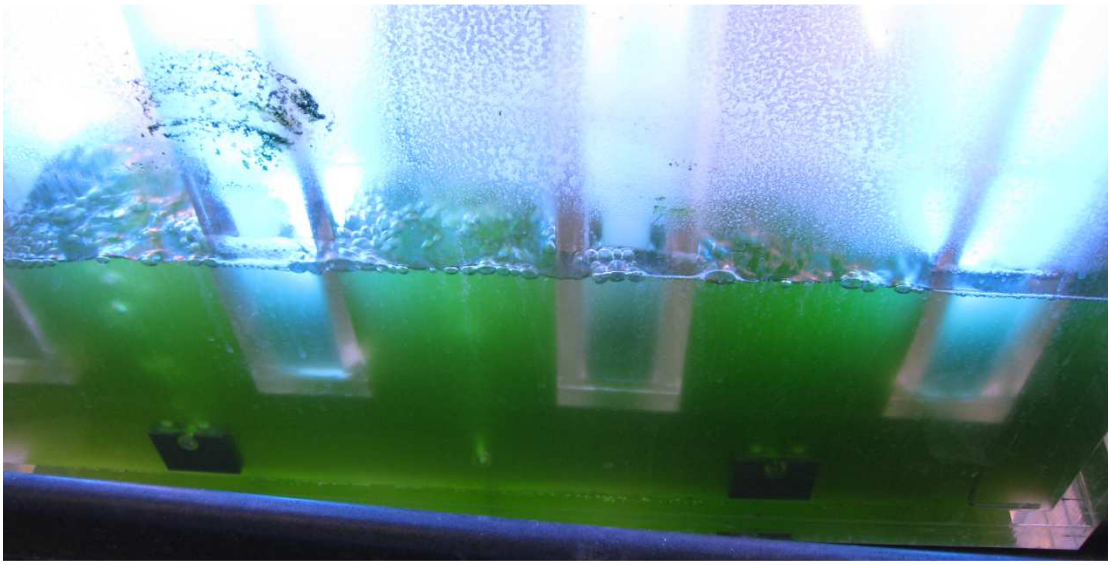

Figure 79. Bubbling differences in the photobioreactor on Day 60 of growth
The slightly higher gas flow rate in the left side of the tank may have caused a slight build-up of algae at the right end. However, the PBR was well mixed before sampling.

The PBR was well mixed before each sample was taken. As the culture reached exponential growth, it began to build up on the walls in a particular pattern. This build up was well mixed when each sample was taken but appeared again. As shown in

Figure 80, algae built up first on the edges of the PBR low flow end and, over several days, it crept towards the middle of the low flow end wall. As the culture aged, algae began to build up on the PBR's back wall nearest the low flow end as shown in greater detail in Figure 81. Over time, the build-up crept along the back wall until it reached the high flow end. It also began to build up on the front wall near the low flow end.

Day 2

Day 9

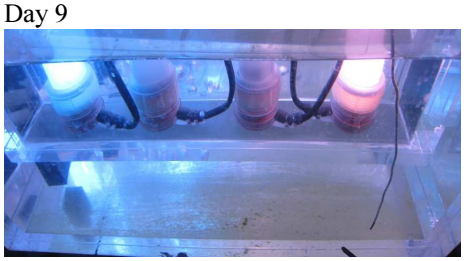

Day 12

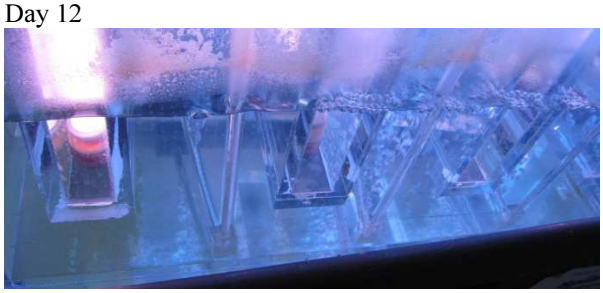

Day 14

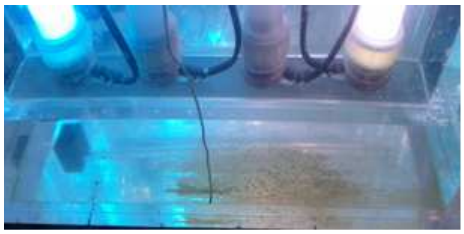

Day 48

Day 48

Day 54

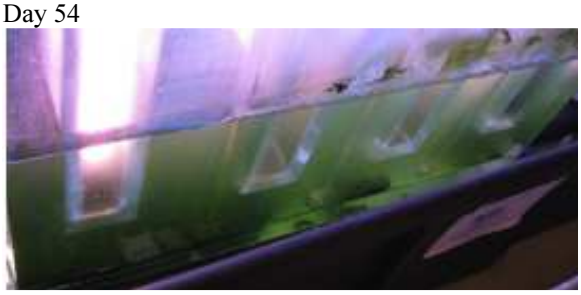

Day 54

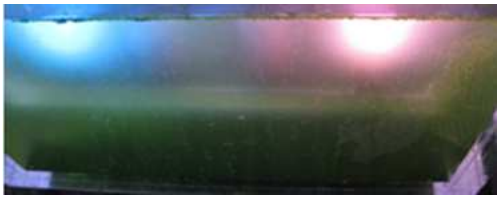

Day 60

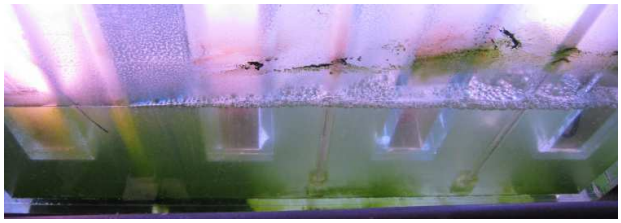

Day 63

Day 73

Day 78

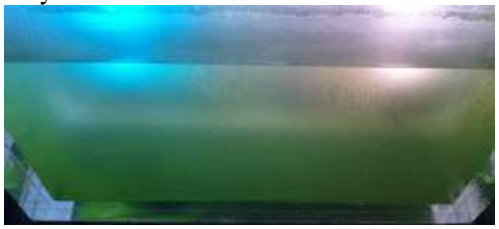

Day 83

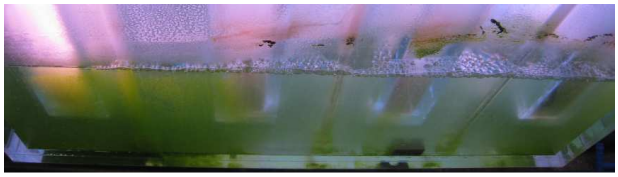

Day 83

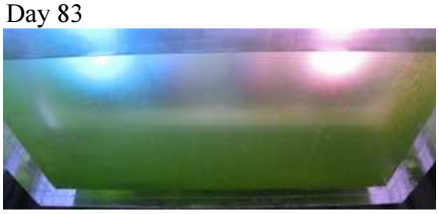

Day 90

Day 90

Figure 80. 40 L *T. impellucida* culture throughout the experiment growth showing the back view and lower flow end

Figure 81. *T. impellucida* build up on Day 86 photobioreactor back wall

The well mixed culture colour changed from nearly clear on Day 0 to pale green to bright green as shown in Figure 82.

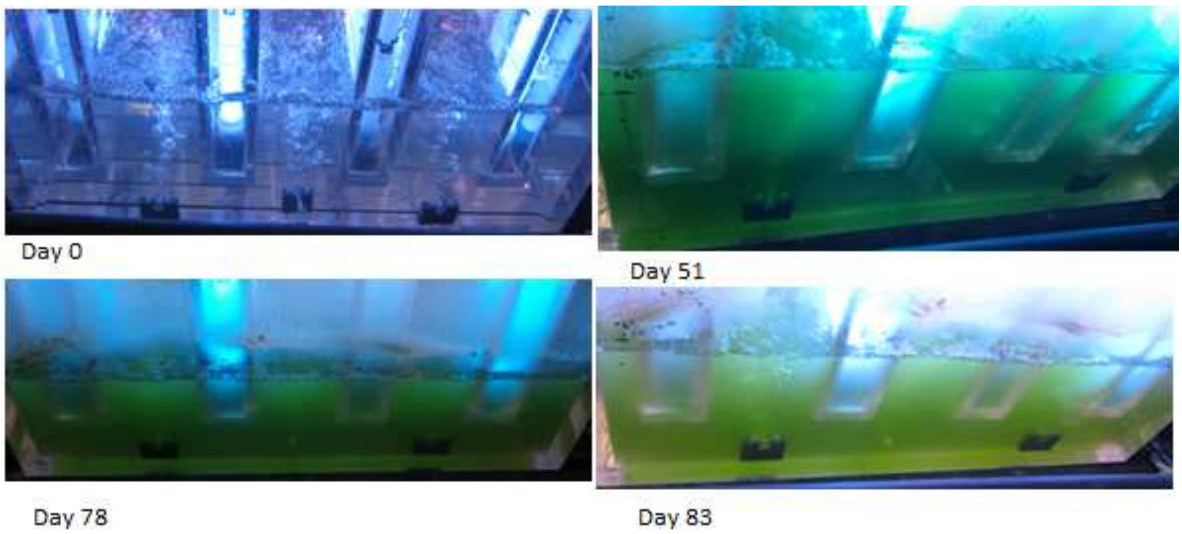

Figure 82. Well mixed 40 L *T. impellucida* culture in the photobioreactor

On Day 54, visual examination of culture samples showed possible contamination by other algae species; these cells are visible alongside *T. impellucida* cells in Figure 83. One dense clump of rectangular cells was identified, although occasional short chains shown in the remainder of Figure 83 were seen as well. These cells represented only a small fraction of total cells, with the remaining cells being clearly *T. impellucida* as shown in Figure 85. These observations match others that show PBRs are effective at reducing contamination over open ponds but not at completely eliminating contamination [315]. Along with being a closed PBR, contamination is reduced by the culture being grown in saltwater and the experiments taking place indoors.


Figure 83. Possible algal contamination in 40 L culture Day 54 at 400X magnification


Figure 84. Sheaths and debris found in 40 L culture Day 60 at 400X magnification

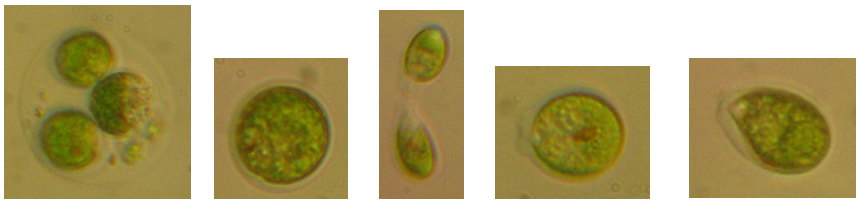
Figure 85. *T. impellucida* cells at 400X from the 40 L photobioreactor on Day 60

Additional examples are shown in Figure 86; one image shows a cell inside a sheath piece, which is a factor seen during multiple observations. As shown in Figure 86, *T. impellucida* accumulates lipid droplets. The cells also accumulate hematochrome in a reddish-pigmented region in the cell posterior.

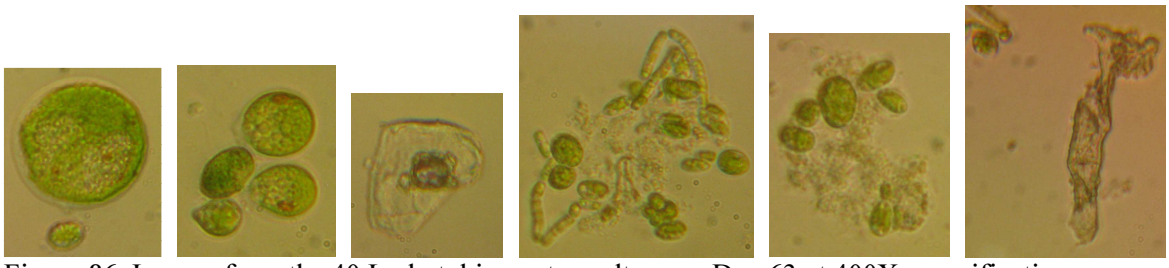
Figure 86. Images from the 40 L photobioreactor culture on Day 63 at 400X magnification

9.2. Discussion of *Tetraselmis* PBR Experiments

T. impellucida growth reached exponential growth during Trial 2. However, two potential issues were identified. These were a long lag phase and cell settling.

9.2.1. Growth Cycle

It took approximately 63 days for the culture to complete a growth cycle from inoculation to stationary phase. Algae growth cycles vary by species. Piorreck and Pohl

[77] grew four algae species under identical conditions of nutrient media, 800 lux, 22 °C, and continuous aeration; they observed growth cycles from 22 days for *Anacystis nidulans* and *Scenedesmus obliquus* to 28 days for *Chlorella vulgaris* up to 46 days for *Microcystis aeruginosa*. The 63 day growth cycle found in Trial 2 is longer because it experienced a significant lag phase of around 12 days. Lag phases are common in larger cultures. During two years of consecutive *Isochrysis galbana* growth in outdoor horizontal PBRs, only one-third showed immediate growth after inoculation [304]. The remaining cultures showed a lag phase or a culture collapse [304].

The duration of a lag phase can vary. Fabregas *et al* [200] grew *Tetraselmis suecica* under a variety of nitrate concentrations and found that the cells experienced a lag phase of 1-2 days followed by exponential growth of 2-6 days. In another experiment, *T. suecica* cultures showed a lag phase of 6-7 days [196]. Similar results have been obtained for other species. *Nannochloropsis salina* cultures repeatedly showed lag phases of 3-5 days in continuously aerated 0.25 L bottles [316].

There are several possible reasons for a lag phase. It is possible that the lag phase within Trial 2 was due to the light intensity used. When considering two years of *Isochrysis galbana* 400 L PBR growth data, a critical value of 1.5 was determined for the ratio of incident solar radiation to cell density [304]. All cultures with values >1.5 had a lag phase or collapse, and this was independent of the initial cell density [304]. However, this light intensity to cell density ratio did not account for all culture lag phases and collapses [304]. Another factor that may have an effect on culture lag phase is the nearest neighbour phenomena. Pane *et al* [196] grew *T. suecica* in free media and immobilized in 3 mm alginate beads. They found that the free cultures had a lag phase of 6-7 days and a stationary phase from day 12-21. Meanwhile, the alginate beads showed a short lag phase of 1-2 days and no stationary phase. However, the immobilized algae had a lower growth

rate than the free algae cultures [196]. The reduced lag phase noted for cultures grown in alginate beads may be due to the confined areas of the beads producing a higher apparent cell concentration.

Many other factors have been noted to affect the length of a culture's lag phase. These include changes in nutrient concentrations, the presence of toxins, the inoculation culture's growth phase and the salinity of marine media. For example, Joseph and Nair [257] found that *T. gracilis* had a prominent lag phase when inoculated into cultures with a high phosphate concentration. They also found that culture phase was important in inoculating new cultures. Stationary phase inoculates produced lag phases that were comparatively longer than when using log phase inoculates [257]. When growing *T. suecica* in the presence of crude oil, Fabregas *et al* [317] found that concentrations above 40 ppm of oil increased the culture's lag phase with higher oil contents resulting in increased lag phases and lower cell density within the stationary phase. Jiang and Chen [199] grew three strains of *Crypthecodinium cohnii* and found that all three strains showed longer lag phases as the salinity of the media increased.

In future experiments, the lag phase may be reduced by preparing a growth curve to ensure that inoculate are added to the PBR while in the log phase of growth, and the initial light intensity may be decreased until the cells reach exponential growth. In addition, the PBR culture salinity will still be monitored to ensure it does not increase significantly.

9.2.2. *Tetraselmis* Motility and Cell Settling

Another issue found during Trial 2 was significant cell settling. Some *Tetraselmis* and *Scherffeila* species regularly shed flagella as part of their cell cycle prior to the onset of cell division [195]. Other green algae flagellates either retain flagella throughout the cell cycle or retract them into the cell body prior to division [195]. *Tetraselmis* species may exhibit a wide variety of cell stages as shown in Figure 87. *Tetraselmis* have three stages

in their cell cycle; these are a flagellate stage, a non-motile vegetative stage and a thick-walled non-flagellate cyst stage [193].

A. B.

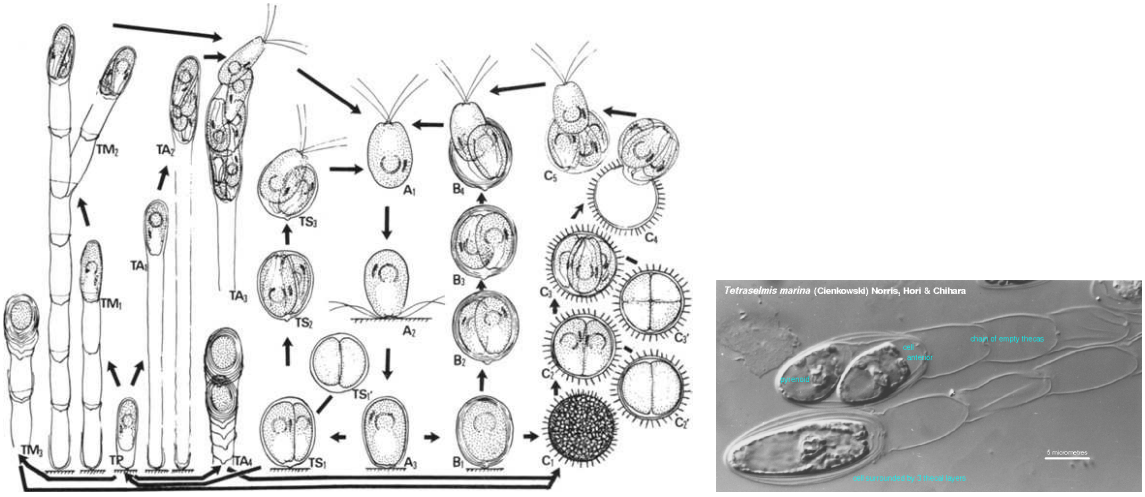

Figure 87. Life cycle of *Tetraselmis* species diagram and photo of *Tetraselmis* forming vegetative stalks
Diagram A shows the *Tetraselmis* cell cycle as drawn by Norris [193]. The vegetative cells may form stalks as in the "TM" drawings in Diagram A, or the non-motile dividing stage can accumulate concentric castoff cells as shown in the "B" drawings in Diagram A. The photograph shows *Tetraselmis marina* cells dividing to form concentric cell sheaths and vegetative stalks [318].

Flagellated green algae have also been seen to shed their flagella under adverse environmental conditions. These have been suggested as being nutrient poor [193], but the optimal environmental conditions for maintaining flagellate cells have not been identified. Not all *Tetraselmis* species undergo vegetative states, and *T. impellucida* has not been well studied previously. However, these experiments indicate that *T. impellucida* goes through a vegetative state.

Under certain environmental conditions, *Tetraselmis* species may remain in a non-motile stage for a very long time, and, during this time, new walls develop with old ones accumulating as either concentric rings around the cell or polarized to one side forming a stalk [193]. If *Tetraselmis* cells are in an unfavourable environment, such as one with depleted nutrients, a dividing cell may form a concentric layer of successive cast-off walls that are either broken or gelatinized around the daughter cells [193]. At any stage,

daughter cells can become motile and swim away from the cast-off walls. Flagellate cells are identical to non-motile cells except flagellates have accumulated several wall layers.

If a flagellate has shed its flagella, it can regenerate them. Reize and Melkonian [195] used either pH shock or mechanical shearing to amputate the flagella of *T. striata* and found that 95% of the cells were able to regrow all four of their flagella to 80-90% of their original length. *Tetraselmis* flagella regrowth occurred at a linear velocity of 50 nm min^{-1} [195], but flagella regeneration varies by algae species. *T. striata* flagellar regeneration takes 2.3 times longer than in *Chlamydomonas reinhardtii*, but it has a higher synthesis rate because four 8 μm flagella are being generated rather than two 10 μm flagella [195].

In Trial 2, some visual observations showed pieces of cell sheaths as seen in Figure 84 that indicate that *T. impellucida* may go form a vegetative stalk as shown in the "TM" drawings in Figure 87's diagram. In the stalk, the cells divide and erupt through the posterior end. It is possible that mixing within the PBR broke up the stalks such that they were not seen in Trial 2. Additionally, some cells were observed to have thick cell membranes encasing multiple cells similar to those in the "B" drawings of Figure 87.

Even when *T. impellucida* goes through a non-flagellate state, it continues to divide well as indicated by Figure 76. This result matches studies on other *Tetraselmis* species [193],[258], which indicate that they continue to divide while in the non-flagellate state and form groupings of cells that eventually burst to release several independent cells. *Tetraselmis* species, including *T. impellucida*, have a rigid cell wall [319]. A similar green flagellate algae, *Scherffelia dubia*, has a rigid cell wall that prevents cell division in its flagellate state because of the lack of expandability [259]. As a result, *S. dubia* sheds its flagella prior to cell division [259]. *Tetraselmis* also has a rigid cell wall, which may explain why *Tetraselmis* divides while non-motile.

Light intensity is a possible reason for flagella loss. When looking at cell motility, *Tetraselmis subcordiformis* cells moved to areas with 100-150 W m^{-2} light intensity [305]. A slightly lower light saturation range of 80-100 W m^{-2} has been suggested for *Tetraselmis* sp [97]. Under higher light intensities (250 W m^{-2}), especially with added ultraviolet light, *T. subcordiformis* spiral swimming disappeared completely and some cells sank [305]. This was due to a combination of flagellar damage and decreased photosynthetic efficiency [305]. As such, light intensity can affect cell settling within a PBR. Very low light intensities may also reduce growth. Dim lighting around 10-30 μE m^{-2} s^{-1} is commonly used in to maintain cultures in a stationary phase for extended periods [6]. Slightly higher light intensities of 50 W m^{-2} were found suboptimal for growing *T. subcordiformis* even though photosynthetic efficiency was not affected [305]. Light intensities may increase cell settling within a reactor. In Trial 2, the light intensity was approximately 52 W m^{-2}, so it may have been slightly low. Future experiments using higher culture volumes will have higher light intensities because more of the light tubes will be utilized.

Another reason for loss of flagella could be the mixing rate within the PBR. Hu et al [224] found that the dinoflagellate *Crypthecodinium cohnii* lost its flagella when pumped through a microfluidic channel at a rate of 50 mL min^{-1}, which had an estimated energy dissipation rate of $1.6x10^{7}$ W m^{-3}. They reported that dinoflagellates may float on the surface of calm seas but, in strong waves, undergo deflagellation and sink into deeper, calmer waters until their flagella are regenerated [224]. Loss of flagella changes the reactor designs optimal for *T. impellucida* growth because the cells need to be well mixed by the reactor design. It may also affect the gas flow rate needed. For example, low liquid velocities allow diatom sedimentation periodically in a bubble column [61]. In addition, there is a potential for cells adhering at least moderately to the reactor.

As Trial 2 wore on, *T. impellucida* cells were observed to attach to the reactor walls. The amount of wall growth will depend greatly upon the algal species grown. However, several methods have been identified for controlling wall growth: using intermittent slugs of air to scour tube walls internal surfaces, circulating close-fitting balls within the tubes, using highly turbulent flow, adding suspended sand or grit to abrade clinging biomass, and flushing the system with enzymes [3].

9.2.3. Continuous Lighting

All of the *Tetraselmis* growth experiments in Chapters 7 and 9 were performed under continuous lighting. Continuous lighting is commonly used in algae growth experiments as shown in Figure 6. In the database discussed in Chapter 3, continuous lighting produced SGRs from 0.07-1.25 d^{-1} for 100 mL-200 L *Tetraselmis* cultures. 12/12 hour light:dark illumination produced SGRs from 0.06-0.68 d^{-1} for 40 mL-10 L *Tetraselmis* cultures. The increased SGRs under continuous illumination matches a direct comparison of continuous lighting to 12/12 illumination for *Nannochloropsis salina*, which showed SGRs of 0.42 d^{-1} and 0.26 d^{-1} respectively [316]. Also, *Tetraselmis* is a flagellate, so it is important to note that flagellar regeneration kinetics are the same whether regeneration occurs in the light or dark [195]. Continuous lighting may allow the same illumination flux using lower light levels. This is important because high light intensities can cause reversible swimming inhibition in *Tetraselmis* [305]. However, as the 12/12 illumination only provided half of the light as continuous lighting, the cells were more efficient during the day than under continuous light [316]. Considering this, 12/12 illumination may be used in future experiments.

9.2.4. Temperature, Salinity and pH

Temperature can affect both algae growth rates and evaporation rates. Evaporation is a common problem in large-scale algae culturing, and affecting evaporation also affects culture salinity. This is important because culture salinity changes can cause osmotic

stress to cells. As such, salinity can influence algae biomass and oil production. However, it is a species specific effect [203]. When looking at oil yields from ten species, increased salinity generally reduced oil yield; however some exceptions were *Chlorella vulgaris*, *Tetraselmis* sp, and *T. chuii* [203].

In Trial 2, the temperature ranged from 19.3 °C to 25.8 °C with an average temperature of 22.8 °C. This was a combination of the heat from the lights and the fact that the PBR was located in a non-temperature controlled room. Meanwhile the Trial 2 salinity ranged from 29-42 ppt with an average of 33 ppt. *Tetraselmis* growth and lipid production can occur at a range of productivities, and these compare favourably with other optimums for *Tetraselmis*. Comparing three *Tetraselmis* species, *T. tetrathele* showed the greatest oil productivity. The highest oil productivities occurred at salinities of 25 g L^{-1} for *T. tetrathele* and 35 g L^{-1} for *T. chuii* and *Tetraselmis* sp [203].

Before CO_2 supplementation began on Day 9, the Trial 2 PBR pH levels ranged from 8.62-8.73. With CO_2 supplementation, the pH levels ranged from 6.5-8.3 with an average pH of 7.14. *T. suecica* growth over many pH levels showed decreased growth rates as pH increased [122]. Considering this, CO_2 should be added to maintain pH levels between 7.5-7.8 for maximum *T. suecica* yields [122].

Abu-Rezq et al [99] tested *Tetraselmis* growth under several environmental parameters including salinities from 5% to 40%, three temperature ranges (19-21 °C, 24-26 °C, and 29-31 °C), and use/absence of CO_2 injection to maintain pH between 6.75-7.25. They determined that the optimum growth conditions for *Tetraselmis* were 20-35% salinity, 19-21 °C, and no CO_2 supplementation [99]. Another study found that *Tetraselmis suecica* productivity was not significantly affected over a temperature range of 17.8-22.0 °C when illumination intensity and pH were constant [122]. Salinity and temperature may be less important than other factors. *T. suecica* % lipids and proteins was affected more by

nitrogen depletion and growth stage than by salinities from 10-35% and temperatures from 18-25 °C [171].

In addition to temperature, a culture's evaporation rate depends on the reactor design, gas flow rate, and the relative humidity where the culture is grown. For example, open ponds have much higher evaporation rates than closed PBRs. Cultures in open outdoor ponds have evaporation rates up to 10 L m^{-2} d^{-1} compared to rates of 1-2 L m^{-2} d^{-1} in horizontal tubular reactors with temperatures controlled to 33-35 °C [43]. With such high evaporation rates in open ponds, DI water addition is necessary to account for evaporation because adding fresh media would greatly increase salt concentration [43]. To prevent increased salinity, DI water was used to account for evaporation in Trial 2.

9.3. *Tetraselmis* Specific Growth Rate Model Test

Tetraselmis growth is potentially important for biodiesel production. Rodolfi et al [4] screened 30 species of algae and found that *Nannochloropsis* and *Tetraselmis* were promising for lipid productivity. Also, Lim et al [320] grew four species and found that *Tetraselmis* had the highest biomass productivity and highest lipid productivity (compared to *Nannochloropsis*, *Isochrysis*, and *Rhodomonas*). This occurred even though *Tetraselmis* showed the lowest SGR of the four cultures because of the large size of *Tetraselmis* cells compared to the other four species [320]. Future *Tetraselmis* production can be enhanced using models to determine culture conditions for improving growth rates.

A multiple regression model for *Tetraselmis* SGRs was prepared using the database and methods detailed in Chapter 6. As discussed in Section 6.6, few *Tetraselmis* models have been prepared previously. In Chapter 6, several models were produced for SGR, MLC, and VLP, and these models were statistically tested for robustness. In addition, results from Trial 2 can be used to validate one *Tetraselmis* SGR model.

As shown in Table 31, Model *Tetraselmis* SGR_{Exp} predicts 93% of the variation in SGRs for 3 *Tetraselmis* species from 5 publications. This model includes data from 800

mL-10.5 L cultures using gas flow rates from 0.007-5.5 L L^{-1} min^{-1}. The cultures used light intensities from 80-230.8 μE m^{-2} s^{-1} and 12 or 24 hour illumination schedules. Culture volume alone accounted for 41% of the variability in *Tetraselmis* SGRs, and illumination schedule accounts for 32.6% of the variability.

Table 31. *Tetraselmis* specific growth rate model for experimental testing

Model Name	Dependent Variable	Regression Equation							
Tetraselmis SGR_{Exp}	Log SGR	y = -0.812(**Log Vol**) – 0.085(SQRT GFR) – 0.832(**Log LI**) + 0.067(**IS**) + 2.955							
		N	pr^2	R	R^2	R_{Adj}	SE	F	$F_{Critical}$
		49	0.150	0.964	0.930	0.924	0.11	146.29	2.58

By inserting the parameters from Trial 2 into Model *Tetraselmis* SGR_{Exp}, an SGR of 0.0643 d^{-1} was predicted. This validity test required a few assumptions. Seven lights were used in Trial 2. Actual light intensity measurements within the culture were not possible with the available equipment, so the light intensity was calculated as 1/6 of each light based on the portion of the light box in the water. All light was assumed to have been transmitted to the algae. There were some cell fluctuations at the beginning of the trial, so Trial 2's SGR was calculated using biomass data from the beginning and end of the exponential growth phase on Day 26 and Day 29 respectively. The results indicate that the model is very useful in predicting *Tetraselmis* growth using given culture conditions. In fact, the model prediction was only 0.43% different than the 0.064 d^{-1} achieved in Trial 2.

Model *Tetraselmis* SGR_{Exp} includes light intensity, which is important for the growth of many algae. *Tetraselmis* phototaxis has been shown to be very sensitive to light stimulus [214], [305]. Light intensity can also affect *Tetraselmis* composition. *Tetraselmis* sp grown at light intensities from 352-530 W m^{-2} showed increased production of polyunsaturated fatty acids, such as EPA, at lower light intensities [156]. The 0.064 d^{-1} SGR for *T. impellucida* achieved in Trial 2 is lower than the maximum SGR for

Tetraselmis sp grown under similar light intensity. However, *Tetraselmis* sp cultures that reached an SGR of 0.059 hr^{-1} under 50 W m^{-2} light intensity were only 1 L in volume [97], while Trial 2 was for a 40 L culture.

9.4. Future Work

In Trial 2, the PBR experienced significant cell settling and a long lag phase. Cell settling may be reduced when the PBR is used with baffles at 140 L working volume. If the baffles are insufficient, one way to reduce cell settling would be to change the bubbling setup. Instead of using tubes and baffles, the reactor could incorporate a fluidic oscillator to produce microbubbles using a setup similar to that proposed by Zimmerman [314].

In addition, the PBR can be used to grow other species. *T. impellucida* was predominately in its non-motile form during Trial 2, so it is not the optimal species for a PBR of this design. Other flagellates that do not attach to reactors or form stalks would be preferable. Alternatively, additional work could be done to establish the culturing parameters that tend to maintain *T. impellucida* in its flagellate stage.

Furthermore, heterotrophic or mixotrophic growth may be used for *Tetraselmis* growth. When 20 strains were screened for heterotrophic growth, *T. suecica* showed promise for industrial cultivation as a mollusc feed [205]. The PBR could be used as a fermenter for future experiments by removing the light boxes but keeping the baffles in place.

9.5. Conclusions

This chapter shows that the PBR discussed in Chapter 8 is useful in algae growth experiments. A 40 L growth trial was used to validate a *Tetraselmis* SGR model produced using multiple regression on published data. The validation experiment showed that the model is very useful in predicting growth under given conditions. This model can also be used to determine optimum growth conditions. This model has many potential uses in biodiesel and aquaculture production.

Chapter 10. Conclusions

This thesis aimed to increase the understanding of how culturing variables affect algae growth rates and lipid production. Six objectives were chosen. Objective 1 was to develop an extensive database of published algae research, and this database included algae growth, lipid content, and lipid productivity information and the environmental parameters used to generate them. Preparing this database made it clear that, even though there is a substantial dataset available in published literature, comparing studies is often difficult. This occurs because a wide variety of data formats are commonly used, and many experimental setup parameters are often under-reported. The usability of data from future studies can be improved by agreeing upon widely accepted standards for data reporting. To this end, a recommended set of culturing parameters and formats has been provided in Chapter 3.

Using the newly prepared database, Objective 2 was to identify key trends in algae research. Several key trends were identified based on 116 publications covering 132 microalgae species. For example, a wide range of light intensities (11.6-2,100 μE m^{-2} s^{-1}) produced SGRs over 1.0 d^{-1} for all light sources except sunlight. A smaller light intensity range (25-277 μE m^{-2} s^{-1}) produced optimal lipid contents. Algae cultures grew well at all temperatures from 10-44 °C. However, the highest SGRs occurred in small cultures around 22 °C, and the highest MLCs generally occurred from 20-30 °C. Culture volume has a major impact on SGR for a wide variety of algae species. All of the SGRs ≥2.3 d^{-1} occurred in PBRs and lab experiments. Raceway and open ponds were the only reactors to reach culture volumes >240 L, and these reactors had lower SGRs (≤0.6 d^{-1}).

When examining aspects concerning lipids, additional trends were identified using data from 131 publications on 128 microalgae species. For instance, the most common nutrient replete lipid content range is 10-20% dw among the 75 marine and 31 freshwater species in this dataset. For many species, nitrogen limitation increased lipid contents, but some

species did not follow this trend. Several high lipid productivities (>150 mg L^{-1} d^{-1}) were produced in small-scale cultures grown under fluorescent lamps from 115-460 μE m^{-2} s^{-1}. Light intensities >2,000 μE m^{-2} s^{-1} reduced lipids to an average of 53.8 mg L^{-1} d^{-1}. The largest cultures (>300 L) produced an average of 24.8 mg L^{-1} d^{-1} lipids but with a wide dispersion. Most of the cultures with MLCs >35% dw had biomass productivities <0.93 g L^{-1} d^{-1}, although a few cultures defied this trend. MLC was not a reliable indicator of SGR, lipid productivity, or biomass productivity. Moreover, the top biomass producers were not necessarily the top lipid producers.

At the same time, trends were identified for motility and cell size. The highest flagellate SGRs occurred for low light intensities with 14 hour illumination. In addition, cell lengths were provided for 146 species. Most of the species in this dataset are unicellular with median cell lengths of 7 μm for freshwater and 9 μm for marine species.

The trends provide valuable information on maximum and typical values for SGRs and MLCs grown using several culturing parameters. In addition, new algae researchers can benefit from the graphs in Chapters 3 and 4, where they can see the commonly used ranges for each culturing parameter and previously obtained results under those conditions.

With this extensive database, it was also possible to accomplish Objective 3, which was to quantify the impacts of several key parameters for algae growth and lipid production. Several models were developed using linear multiple regression analysis to assess the significance of predictor variables on SGRs, MLCs, and VLPs. The predictor variables studied include light intensity, light source, illumination schedule, gas flow rate, CO_2 concentration, culture volume, salinity, and temperature. Each of model was assessed using several statistical validation checks.

A range of non-species specific models was developed depending on the data available. Using only four environmental parameters, over 40% of the variation in SGRs was

predicted for 48 algae species, and 35% of variability in MLCs was predicted from 31 species. Nearly 49% of variation in VLPs for 44 species was accounted for by five environmental parameters. Together, these models help identify variables that should be concentrated on during algae production facility design, biomass life cycle analyses, and carbon capture estimations. These models are especially useful because they are composed of variables that are obtainable with limited specialized equipment.

In addition, Objective 4 was accomplished by preparing genus specific models for *Chlorella*, *Isochrysis*, *Tetraselmis*, *Nannochloropsis*, and *Phaeodactylum*. These models are useful in identifying the impacts of various culturing parameters on SGRs, MLCs, and VLPs. These models make it possible to compare the predictive capabilities of general algae models with genus specific ones. Comparisons between genera are also possible. Moreover, these models greatly extend the range of previous species-specific multiple regression models from literature.

A new 230 L photobioreactor was devised and built to consider scale-up issues as covered in Objective 5. This volume was chosen because the majority of algae studies are performed on <10 L cultures. To prepare for the photobioreactor experiments, several <1 L bottle experiments were performed to develop experimental procedures. These included examinations of the effects of light source, light intensity, mixing type, and mixing speed on the growth rate of *Tetraselmis impellucida*.

A three-month *Tetraselmis* growth experiment was performed to reach Objective 6 and have a real-world test of one *Tetraselmis* SGR model. This 40 L *T. impellucida* culture verified the model's usefulness as the SGR achieved was only 0.43% different than the predicted value. While the other genus specific models were not tested with growth experiments, this result suggests that the models developed here have many potential uses in biodiesel and aquaculture production.

References

1. IEA, *Biofuels for Transport: An International Perspective*. 2004, Paris: International Energy Agency/OCED. 210.
2. Andrews, J. and N. Jelley, *Energy Science: Principles, Technologies, and Impacts*. 2007, New York: Oxford University Press Inc.
3. Chisti, Y., *Biodiesel from microalgae.* Biotechnology Advances, 2007. **25**(3): p. 294-306.
4. Rodolfi, L., et al., *Microalgae for oil: strain selection, induction of lipid synthesis and outdoor mass cultivation in a low-cost photobioreactor.* Biotechnol Bioeng, 2009. **102**(1): p. 100-12.
5. Hu, Q., et al., *Microalgal triacylglycerols as feedstocks for biofuel production: perspectives and advances.* The Plant Journal, 2008. **54**: p. 621-639.
6. Andersen, R.A., *Algal Culturing Techniques*. 2005: Elsevier/Academic Press. 578.
7. Lee, R.E., *Phycology*. 3rd ed. 1999, Cambridge: Cambridge University Press. 614.
8. Carvalho, A.P., L.A. Meireles, and F.X. Malcata, *Microalgal reactors: A review of enclosed system designs and performances.* Biotechnology Progress, 2006. **22**(6): p. 1490-1506.
9. Singh, S.C., R.P. Sinha, and D.P. Hader, *Role of lipids and fatty acids in stress tolerance in cyanobacteria.* ACTA PROTOZOOLOGICA, 2002. **41**(4): p. 297-308.
10. Lynch, D.V. and G.A. Thompson, *Low temperature-induced alterations in the chloroplast and microsomal membranes of Dunaliella salina.* Plant Physiology, 1982. **69**(6): p. 1369-1375.
11. Lebeau, T. and J.M. Robert, *Diatom cultivation and biotechnologically relevant products. Part I: Cultivation at various scales.* Applied Microbiology and Biotechnology, 2003. **60**(6): p. 612-623.
12. Olofsson, M., et al., *Seasonal Variation of Lipids and Fatty Acids of the Microalgae Nannochloropsis oculata Grown in Outdoor Large-Scale Photobioreactors.* Energies, 2012. **5**(5): p. 1577-1592.
13. Coulson, J.M., J.F. Richardson, and D. Peacock, eds. *Chemical Engineering: Chemical & Biochemical Reactors & Process Control*. 3rd ed. Vol. 3. 1994, Pergamon. 778.
14. Moheimani, N.R., *The culture of Coccolithophorid Algae for carbon dioxide bioremediation.* , in *School of Biological Sciences and Biotechnology*. 2005, Murdoch University: Perth.
15. Resurreccion, E.P., et al., *Comparison of algae cultivation methods for bioenergy production using a combined life cycle assessment and life cycle costing approach.* Bioresource Technology, 2012. **126**: p. 298-306.
16. Singh, S., B.N. Kate, and U.C. Banecjee, *Bioactive compounds from cyanobacteria and microalgae: An overview.* Critical Reviews in Biotechnology, 2005. **25**(3): p. 73-95.
17. Sheehan, J., et al., *A Look Back at the U.S. Department of Energy's Aquatic Species Program: Biodiesel from Algae*. 1998, National Renewable Energy Laboratory: Golden, Colorado. p. 328.
18. Pulz, O., *Photobioreactors: Production systems for phototrophic microorganisms.* Applied Microbiology and Biotechnology, 2001. **57**(3): p. 287-293.
19. Chisti, Y. and J. Yan, *Energy from algae: Current status and future trends: Algal biofuels–A status report.* Applied Energy, 2011. **88**(11): p. 3277-3279.
20. Borowitzka, M.A., *Commercial production of microalgae: ponds, tanks, tubes and fermenters.* Journal of Biotechnology, 1999. **70**(1-3): p. 313-321.
21. Ugwu, C.U., H. Aoyagi, and H. Uchiyama, *Photobioreactors for mass cultivation of algae.* Bioresource Technology, 2008. **99**(10): p. 4021-4028.
22. Sanchez Miron, A., et al., *Comparative evaluation of compact photobioreactors for large-scale monoculture of microalgae.* Journal of Biotechnology, 1999. **70**: p. 249-270.
23. Degen, J., et al., *A novel airlift photobioreactor with baffles for improved light utilization through the flashing light effect.* Journal of Biotechnology, 2001. **92**(2): p. 89-94.

24. Rossignol, N., et al., *Comparison of two membrane - Photobioreactors, with free or immobilized cells, for the production of pigments by a marine diatom.* Bioprocess Engineering, 2000. **23**(5): p. 495-501.
25. Sánchez Mirón, A., et al., *Shear Stress Tolerance and Biochemical Characterization of Phaeodactylum tricornutum in Quasi Steady-State Continuous Culture in Outdoor Photobioreactors.* Biochemical Engineering Journal, 2003. **16**(3): p. 287-297.
26. Lee, C.G. and B.O. Palsson, *High-density algal photobioreactors using light-emitting diodes.* Biotechnology and Bioengineering, 1994. **44**(10): p. 1161-1167.
27. Oncel, S.S. and O. Akpolat, *An integrated photobioreactor system for the production of Spirulina platensis.* Biotechnology, 2006. **5**(3): p. 365-372.
28. Sukenik, A., O. Zmora, and Y. Carmeli, *Biochemical quality of marine unicellular algae with special emphasis on lipid composition. II. Nannochloropsis sp.* Aquaculture, 1993. **117**: p. 313-326.
29. Sierra, E., et al., *Characterization of a flat plate photobioreactor for the production of microalgae.* Chemical Engineering Journal, 2008. **138**(1-3): p. 136-147.
30. Renaud, S.M., et al., *Effect of light intensity on the proximate biochemical and fatty acid composition of Isochrysis sp. and Nannochloropsis oculata for use in tropical aquaculture.* J Appl Phycol, 1991. **3**: p. 43-53.
31. Liang, Y., et al., *Effect of light intensity on the total lipid and fatty acid composition of six strains of marine diatoms.* Chinese Journal of Oceanology and Limnology, 2001. **19**(3): p. 249-254.
32. Chen, C.Y. and J.S. Chang, *Enhancing phototropic hydrogen production by solid-carrier assisted fermentation and internal optical-fiber illumination.* Process Biochemistry, 2006. **41**(9): p. 2041-2049.
33. Geider, R.J. and B. Osborne, A., *Algal Photosynthesis*. 1992: Chapman and Hall. 256.
34. Kim, Z.H., et al., *Enhanced production of astaxanthin by flashing light using Haematococcus pluvialis.* Enzyme and Microbial Technology, 2006. **39**(3): p. 414-419.
35. FAO. *Aquatic Biofuels*. 2013 14/06/2013]; Available from: http://www.fao.org/bioenergy/aquaticbiofuels/knowledge/en/.
36. Goldman, J.C., *Outdoor algal mass cultures - I. Applications.* Water Research, 1979. **13**: p. 1-19.
37. Olaizola, M., *Commercial development of microalgal biotechnology: from the test tube to the marketplace.* Biomolecular Engineering, 2003. **20**: p. 459-466.
38. Fisher, T., J. Minnaard, and Z. Dubinsky, *Photoacclimation in the marine alga Nannochloropsis sp. (Eustigmatophyte): a kinetic study.* Journal of Plankton Research, 1996. **18**(10): p. 1797-1818.
39. Kim, S.-K., ed. *Handbook of Marine Macroalgae: Biotechnology and Applied Phycology*. 2012, Wiley-Blackwell: UK. 567.
40. Levetin, E. and K. McMahon, eds. *Plants & Society*. Vol. 6th Edition. 2012, McGraw-Hill. 544.
41. FAO, *Algae-based biofuels: Applications and co-products*, A.B.W. Group, Editor. 2010, Food and Agricultural Organization. p. 107.
42. Rosenberg, J.N., et al., *A green light for engineered algae: redirecting metabolism to fuel a biotechnology revolution.* Current Opinion in Biotechnology, 2008. **19**(5): p. 430-436.
43. Becker, E.W., *Microalgae: Biotechnology and Microbiology*. 1994: Cambridge University Press. 293.
44. Harun, R., M.K. Danquah, and G.M. Forde, *Microalgal biomass as a fermentation feedstock for bioethanol production.* Journal of Chemical Technology & Biotechnology, 2010. **85**: p. 199-203.
45. Rawat, I., et al., *Dual role of microalgae: Phycoremediation of domestic wastewater and biomass production for sustainable biofuels production.* Applied Energy, 2011. **88**: p. 3411-3424.
46. Elmoraghy, M. and I.H. Farag, *Bio-jet Fuel from Microalgae: Reducing Water and Energy Requirements for Algae Growth.* International Journal of Engineering and Science, 2012. **1**(2): p. 22-30.

47. Lee, J.W., ed. *Advanced Biofuels and Bioproducts*. 2013, Springer. 1122.
48. Mercer, P. and R.E. Armenta, *Developments in oil extraction from microalgae.* European Journal of Lipid Science and Technology, 2011. **113**: p. 539-547.
49. Haas, M.J. and K.M. Scott, *Moisture removal substantially improves the efficiency of in situ biodiesel production from soybeans.* JAOCS, Journal of the American Oil Chemists' Society, 2007. **84**(2): p. 197-204.
50. Aresta, M., et al., *Production of biodiesel from macroalgae by supercritical CO_2 extraction and thermochemical liquefaction.* Environmental Chemistry Letters, 2005. **3**(3): p. 136-139.
51. Sharma, A., S.K. Khare, and M.N. Gupta, *Enzyme-assisted aqueous extraction of peanut oil.* Journal of the American Oil Chemists' Society, 2002. **79**(3): p. 215-218.
52. Cao, P., et al., *Effect of Membrane Pore Size on the Performance of a Membrane Reactor for Biodiesel Production.* Industrial & Engineering Chemistry Research, 2007. **46**(1): p. 52-58.
53. He, H.Y., X. Guo, and S.L. Zhu, *Comparison of membrane extraction with traditional extraction methods for biodiesel production.* JAOCS, Journal of the American Oil Chemists' Society, 2006. **83**(5): p. 457-460.
54. Gouveia, L. and A.C. Oliveira, *Microalgae as a raw material for biofuels production.* J Ind Microbiol Biotechnol, 2009. **36**(2): p. 269-274.
55. Dubé, M.A., A.Y. Tremblay, and J. Liu, *Biodiesel production using a membrane reactor.* Bioresource Technology, 2007. **98**(3): p. 639-647.
56. Han, J., et al., *Organic Geochemical Studies II. A Preliminary Report on the Distribution of Aliphatic Hydrocarbons in Algae, in Bacteria, and in a Recent Lake Sediment.* Proceedings of National Academy of Sciences of the USA, 1968. **59**(1): p. 29-33.
57. Leung, D.Y.C., B.C.P. Koo, and Y. Guo, *Degradation of biodiesel under different storage conditions.* Bioresource Technology, 2006. **97**(2): p. 250-256.
58. Xu, H., X. Miao, and Q. Wu, *High quality biodiesel production from a microalga Chlorella protothecoides by heterotrophic growth in fermenters.* Journal of Biotechnology, 2006. **126**(4): p. 499-507.
59. Miao, X. and Q. Wu, *Biodiesel production from heterotrophic microalgal oil.* Bioresource Technology, 2006. **97**(6): p. 841-846.
60. Mallick, N., et al., *Green microalga Chlorella vulgaris as a potential feedstock for biodiesel.* Journal of Chemical Technology and Biotechnology, 2011. **87**(1): p. 137-145.
61. Krichnavaruk, S., S. Powtongsook, and P. Pavasant, *Enhanced productivity of Chaetoceros calcitrans in airlift photobioreactors.* Bioresource Technology, 2007. **98**(11): p. 2123-2130.
62. Jones, C.S. and S.P. Mayfield, *Algae biofuels: versatility for the future of bioenergy.* Current Opinion in Biotechnology, 2012. **23**: p. 346-351.
63. Gerd_Klock. *The Microalgae Industry Directory*. 2010 [cited 2013 17/06/2013]; Available from: http://www.hs-bremen.de/internet/de/studium/stg/istab/forschung/bvt/proj/directory/.
64. Jha, A., *UK announces world's largest algal biofuel project*, in *The Guardian*. 2008: guardian.co.uk.
65. EPA. *Renewable Fuel Standards*. 2013 [cited 2013 June 16]; Available from: http://www.epa.gov/otaq/fuels/renewablefuels/index.htm.
66. REN21, *Renewables Global Futures Report*. 2013, Renewable Energy Policy Network for the 21st Century: Paris.
67. Stephenson, A.L., et al., *Life-cycle assessment of potential algal biodiesel production in the United Kingdom: A comparison of raceways and air-lift tubular bioreactors.* Energy Fuels, 2010. **24**: p. 4062-4077.
68. Harto, C., R. Meyers, and E. Williams, *Life cycle water use of low-carbon transport fuels.* Energy Policy, 2010. **38**: p. 4933-4944.
69. Posten, C., *Design principles of photo-bioreactors for cultivation of microalgae.* Engineering in Life Sciences, 2009. **9**(3): p. 165-177.

70. Quinn, J., L. de Winter, and T. Bradley, *Microalgae bulk growth model with application to industrial scale systems.* Bioresource Technology, 2011. **102**(8): p. 5083-5092.
71. Yang, J., et al., *Life-cycle analysis on biodiesel production from microalgae: Water footprint and nutrients balance.* Bioresource Technology, 2011. **102**: p. 159-165.
72. Chiu, Y.-W., B. Walseth, and S. Suh, *Water Embodied in Bioethanol in the United States.* Environ. Sci. Technology, 2009. **43**: p. 2688-2692.
73. Guiry, M.D., *How Many Species of Algae Are There?* Journal of Phycology, 2012. **48**(5): p. 1529-8817.
74. Seckbach, J., ed. *Algae and Cyanobacteria in Extreme Environments*. 2007, Springer: Dordrecht, Netherlands. 811.
75. Roessler, P.G., *Environmental control of glycerolipid metabolism in microalgae: Commercial implications and future research directions.* Journal of Phycology, 1990. **26**: p. 393-399.
76. Metzger, P. and C. Largeau, *Botryococcus braunii: a rich source for hydrocarbons and related ether lipids.* Applied Microbiology and Biotechnology, 2005. **66**(5): p. 486-496.
77. Piorreck, M. and P. Pohl, *Formation of biomass, total protein, chlorophylls, lipids and fatty acids in green and blue-green algae during one growth phase.* Phytochemistry, 1984. **23**(2): p. 217-223.
78. Liang, Y., K.-s. Mai, and S.-c. Sun, *Effects of harvest stage on the total lipid and fatty acid composition of four Cylindrotheca strains.* Chinese Journal of Oceanology and Limnology, 2002. **20**(2): p. 157-161.
79. Coutteau, P., et al., *Manual on the Production and Use of Live Food for Aquaculture*, P. Lavens and P. Sorgeloos, Editors. 1996, Food and Agricultural Organization: Rome.
80. Gibson, R., M. Barnes, and R. Atkinson, eds. *Oceanography and Marine Biology: an annual review*. Vol. 40. 2002, CRC Press. 640.
81. Li, Y., et al., *Photosynthetic carbon partitioning and lipid production in the oleaginous microalga Pseudochlorococcum sp. (Chlorophyceae) under nitrogen-limited conditions.* Bioresource Technology, 2011. **102**(1): p. 123-129.
82. Suen, Y., et al., *Total lipid production of the green alga Nannochloropsis sp QII under different nitrogen regimes.* Journal of Phycology, 1987. **23**: p. 289-296.
83. Dunahay, T.G., et al. *Manipulation of Microalgal Lipid Production Using Genetic Engineering*. in *Seventeenth Symposium on Biotechnology for Fuels and Chemicals*. 1996. Humana Press.
84. Specht, E., S. Miyake-Stoner, and S. Mayfield, *Micro-algae come of age as a platform for recombinant protein production.* Biotechnology Letters, 2010. **32**(10): p. 1373-1383.
85. Griffiths, M.J. and S.T. Harrison, *Lipid productivity as a key characteristic for choosing algal species for biodiesel production.* J Appl Phycol, 2009. **21**: p. 493-507.
86. Danesi, E.D.G., et al., *Growth and content of Spirulina platensis biomass chlorophyll cultivated at different values of light intensity and temperature using different nitrogen sources.* Brazilian Journal of Microbiology, 2011. **42**: p. 362-373.
87. Baker, J.W., et al., *Growth and Toxicity of Prymnesium parvum (Haptophyta) as a Function of Salinity, Light, and Temperature.* Journal of Phycology, 2007. **43**(2): p. 219-227.
88. Cho, S.H., et al., *Optimum temperature and salinity conditions for growth of green algae Chlorella ellipsoidea and Nannochloris oculata.* Fisheries Science, 2007. **73**(5): p. 1050-1056.
89. Raghavan, G., C.K. Haridevi, and C.P. Gopinathan, *Growth and proximate composition of the Chaetoceros calcitrans f. pumilus under different temperature, salinity and carbon dioxide levels.* Aquaculture Research, 2008. **39**(10): p. 1053-1058.
90. Carvalho, A.P. and F.X. Malcata, *Optimization of w-3 fatty acid production by microalgae: Crossover effects of CO_2 and light intensity under batch and continuous cultivation modes.* Marine Biotechnology, 2005. **7**(4): p. 381-388.
91. Gouveia, L., et al., *Neochloris oleabundans UTEX #1185: a suitable renewable lipid source for biofuel production.* J Ind Microbiol Biotechnol, 2009. **36**(6): p. 821-826.

92. Hu, H. and K. Gao, *Optimization of growth and fatty acid composition of a unicellular marine picoplankton, Nannochloropsis sp., with enriched carbon sources.* Biotechnology Letters, 2003. **25**(5): p. 421-425.
93. https://ccmp@bigelow.org, *The Provasoli-Guillard National Center for Culture of Marine Phytoplankton*, in *Photograph from Online Database*. Accessed on 05/07/2011, CCMP Bigelow Laboratory for Ocean Sciences.
94. www.sbs.utexas.edu, *UTEX The Culture Collection of Algae*. Accessed 05/07/2011, University of Texas.
95. Jameson, I. *Light - Notes on physical and subjective units of measure*. 2006 27/06/2011; 1/07/2006:[Available from: http://www.marine.csiro.au/microalgae/methods/.
96. Lee, C.-G. and B.Ø. Palsson, *High-density algal photobioreactors using light-emitting diodes.* Biotechnology and Bioengineering, 1994. **44**(10): p. 1161-1167.
97. Molina Grima, E., et al., *Biochemical productivity and fatty acid profiles of Isochrysis galbana Parke and Tetraselmis sp. as a function of incident light intensity.* Process Biochemistry, 1994. **29**(2): p. 119-126.
98. Ishida, Y., et al., *A highly CO_2-tolerant diatom, Thalassiosira weissflogii H1, enriched from coastal sea, and its fatty acid composition.* Fisheries Science, 2000. **66**: p. 655-659.
99. Abu-Rezq, T.S., et al., *Optimum production conditions for different high-quality marine algae.* Hydrobiologia, 1999. **403**: p. 97-107.
100. Aidar, E., et al., *Effects of light quality on growth, biochemical composition and photo synthetic production in Cyclotella caspia Grunow and Tetraselmis gracilis (Kylin) Butcher.* Journal of Experimental Marine Biology and Ecology, 1994. **180**(2): p. 175-187.
101. Banerjee, S., et al., *Growth and proximate composition of tropical marine Chaetoceros calcitrans and Nannochloropsis oculata cultured outdoors and under laboratory conditions.* African Journal of Biotechnology, 2011. **10**(8): p. 1375-1383.
102. Benider, A., et al. *Interaction des facteurs héliothermiques sur la croissance de trois espèces du genre Scenedesmus*. 2001. Cambridge Univ Press.
103. Boussiba, S., et al., *Outdoor cultivation of the marine microalga Isochrysis galbana in open reactors.* Aquaculture, 1988. **72**(3): p. 247-253.
104. Boussiba, S., et al., *Lipid and biomass production by the halotolerant microalga Nannochloropsis salina.* Biomass, 1987. **12**: p. 37-47.
105. Chiu, S.-Y., et al., *Reduction of CO_2 by a high-density culture of Chlorella sp. in a semicontinuous photobioreactor.* Bioresource Technology, 2008. **99**(9): p. 3389-3396.
106. Chiu, S.-Y., et al., *Lipid accumulation and CO_2 utilization of Nannochloropsis oculata in response to CO_2 aeration.* Bioresource Technology, 2009. **100**: p. 833-838.
107. Chiu, S.-Y., et al., *The air-lift photobioreactors with flow patterning for high-density cultures of microalgae and carbon dioxide removal.* Engineering in Life Sciences, 2009. **9**(3): p. 254-260.
108. Converti, A., et al., *Effect of temperature and nitrogen concentration on the growth and lipid content of Nannochloropsis oculata and Chlorella vulgaris for biodiesel production.* Chemical Engineering and Processing: Process Intensification, 2009. **48**(6): p. 1146-1151.
109. Cuaresma, M., et al., *Productivity of Chlorella sorokiniana in a short light-path (SLP) panel photobioreactor under high irradiance.* Biotechnology and Bioengineering, 2009. **104**(2): p. 352-359.
110. Dauta, A., et al., *Growth rate of four freshwater algae in relation to light and temperature.* Hydrobiologia, 1990. **207**(1): p. 221-226.
111. Dempster, T.A. and M.R. Sommerfeld, *Effects of Environmental Conditions on Growth and Lipid Accumulation in Nitzschia Communis (Bacillariophyceae).* Journal of Phycology, 1998. **34**: p. 712-721.
112. Emdadi, D. and B. Berland, *Variation in lipid class composition during batch growth of Nannochloropsis salina and Pavlova lutheri.* Marine Chemistry, 1989. **26**(3): p. 215-225.
113. Exley, C., et al., *Silicon, aluminium and the biological availability of phosphorus in algae.* Proceedings: Biological Sciences, 1993. **253**(1336): p. 93-99.

114. Fabregas, J., et al., *Growth of the marine microalga Tetraselmis suecica in batch cultures with different salinities and nutrient concentrations.* Aquaculture, 1984. **42**(3-4): p. 207-215.
115. Fernandez-Reiriz, et al., *Biomass production and variation in the biochemical profile (Total protein, carbohydrates, RNA, lipids and fatty acids) of seven species of marine microalgae.* Aquaculture, 1989. **83**: p. 17-37.
116. Fuentes-Grünewald, C., et al., *Use of the dinoflagellate Karlodinium veneficum as a sustainable source of biodiesel production.* Journal of Industrial Microbiology and Biotechnology, 2009. **36**(9): p. 1215-1224.
117. Goksan, T., A. Zekeriyaoglu, and A. Ilknur, *The growth of Spirulina platensis in different culture systems under greenhouse condition.* Turkish Journal of Biology, 2007. **31**: p. 47-52.
118. Griffiths, M.J., R.P. van Hille, and S.T.L. Harrison, *Lipid productivity, settling potential and fatty acid profile of 11 microalgal species grown under nitrogen replete and limited conditions.* Journal of Applied Phycology, 2011: p. 1-13.
119. Huerlimann, R., R. De Nys, and K. Heimann, *Growth, lipid content, productivity, and fatty acid composition of tropical microalgae for scale-up production.* Biotechnology and Bioengineering, 2010. **107**(2): p. 245-257.
120. Illman, A., A. Scragg, and S. Shales, *Increase in Chlorella strains calorific values when grown in low nitrogen medium.* Enzyme and Microbial Technology, 2000. **27**(8): p. 631-635.
121. Kratz, W.A. and J. Myers, *Nutrition and growth of several blue-green algae.* American Journal of Botany, 1955: p. 282-287.
122. Laing, I. and M. Helm, *Factors affecting the semi-continuous production of Tetraselmis suecica (Kylin) Butch. in 200-l vessels.* Aquaculture, 1981. **22**: p. 137-148.
123. Lee, C.-G. and B.Ø. Palsson, *Light emitting diode-based algal photobioreactor with external gas exchange.* Journal of fermentation and bioengineering, 1995. **79**(3): p. 257-263.
124. Li, Y. and J.G. Qin, *Comparison of growth and lipid content in three Botrycoccus braunii strains.* Journal of Applied Phycology, 2005. **17**: p. 551-556.
125. Liang, Y., K. Mai, and S. Sun, *Differences in growth, total lipid content and fatty acid composition among 60 clones of Cylindrotheca fusiformis.* Journal of Applied Phycology, 2005. **17**(1): p. 61-65.
126. Lopes da Silva, T., et al., *Oil Production Towards Biofuel from Autotrophic Microalgae Semicontinuous Cultivations Monitorized by Flow Cytometry.* Applied Biochemistry and Biotechnology, 2009. **159**(2): p. 568-578.
127. Maddux, W.S. and R.F. Jones, *Some Interactions of Temperature, Light Intensity, and Nutrient Concetration During the Continuous Culture of Nitzschia closterium and Tetraselmis sp.* Limnology and Oceanography, 1964. **9**(1): p. 79-86.
128. Mansour, M.P., et al., *Lipid and fatty acid yield of nine stationary-phase microalgae: Applications and unusual C_{24}-C_{28} polyunsaturated fatty acids.* Journal of Applied Phycology, 2005. **17**: p. 287-300.
129. Molina, E., et al., *Growth and Biochemical Composition with Emphasis on the Fatty Acids of Tetraselmis sp.* Applied Microbiology and Biotechnology, 1991. **36**: p. 21-25.
130. Molina Grima, E., et al., *A study on simultaneous photolimitation and photoinhibition in dense microalgal cultures taking into account incident and averaged irradiances.* Journal of Biotechnology, 1996. **45**(1): p. 59-69.
131. Nedbal, L., et al., *A photobioreactor system for precision cultivation of photoautotrophic microorganisms and for high-content analysis of suspension dynamics.* Biotechnology and Bioengineering, 2008. **100**(5): p. 902-910.
132. Ogbonna, J.C., et al., *A novel internally illuminated stirred tank photobioreactor for large-scale cultivation of photosynthetic cells.* Journal of Fermentation and Bioengineering, 1996. **82**(1): p. 61-67.

133. Ong, S.-C., et al., *Characterization of the thermal-tolerant mutants of Chlorella sp. with high growth rate and application in outdoor photobioreactor cultivation.* Bioresource Technology, 2010. **101**(8): p. 2880-2883.
134. Órpez, R., et al., *Growth of the microalga Botryococcus braunii in secondarily treated sewage.* Desalination, 2009. **246**(1): p. 625-630.
135. Østgaard, K. and A. Jensen, *Diurnal and circadian rhythms in the turbidity of growing Skeletonema costatum cultures.* Marine Biology, 1982. **66**(3): p. 261-268.
136. Qiang, H., H. Guterman, and A. Richmond, *Physiological Characterisitcs of Spirulina platensis (Cyanobacteria) Cultured at Ultrahigh Cell Densities.* Journal of Phycology, 1996. **32**(6): p. 1066-1073.
137. Renaud, S. and D. Parry, *Microalgae for use in tropical aquaculture II: Effect of salinity on growth, gross chemical composition and fatty acid composition of three species of marine microalgae.* Journal of Applied Phycology, 1994. **6**(3): p. 347-356.
138. Renaud, S.M., L.-V. Thinh, and D.L. Parry, *The gross chemical composition and fatty acid composition of 18 species of tropical Australian microalgae for possible use in mariculture.* Aquaculture, 1999. **170**(2): p. 147-159.
139. Renaud, S.M., et al., *Effect of temperature on growth, chemical composition and fatty acid composition of tropical Australian microalgae grown in batch cultures.* Aquaculture, 2002. **211**(1-4): p. 195-214.
140. Sorokin, C. and R.W. Krauss, *Effects of Temperature & Illuminance on Chlorella Growth Uncoupled From Cell Division.* Plant Physiology, 1961. **37**(1): p. 37.
141. Suh, I.S. and S.B. Lee, *Cultivation of a cyanobacterium in an internally radiating air-lift photobioreactor.* Journal of Applied Phycology, 2001. **13**(4): p. 381-388.
142. Thomas, W.H., *Effects of Temperature and Illuminance on Cell Division Rates of Three Species of Tropical Oceanic Phytoplankton.* Journal of Phycology, 1966. **11**: p. 17-22.
143. Thomas, W., et al., *Yields, photosynthetic efficiencies and proximate composition of dense marine microalgal cultures. I. Introduction and Phaeodactylum tricornutum experiments.* Biomass, 1984. **5**(3): p. 181-209.
144. Thomas, W., et al., *Yields, photosynthetic efficiencies and proximate composition of dense marine microalgal cultures. II. Dunaliella primolecta and Tetraselmis suecica experiments.* Biomass, 1984. **5**(3): p. 211-225.
145. Tomaselli, L., G. Boldrini, and M. Margheri, *Physiological behaviour of Arthrospira (Spirulina) maxima during acclimation to changes in irradiance.* Journal of Applied Phycology, 1997. **9**(1): p. 37-43.
146. Tredici, M.R. and G.C. Zittelli, *Efficiency of sunlight utilization: tubular versus flat photobioreactors.* Biotechnology and Bioengineering, 1998. **57**(2): p. 187-197.
147. Tzovenis, I., et al., *Screening for marine nanoplanktic microalgae from Greek coastal lagoons (Ionian Sea) for use in mariculture.* J Appl Phycol, 2009. **21**: p. 457-469.
148. Vieira Costa, J.A., et al., *Modelling of Spirulina platensis growth in fresh water using response surface methodology.* World Journal of Microbiology and Biotechnology, 2002. **18**(7): p. 603-607.
149. Wahal, S. and S. Viamajala, *Maximizing algal growth in batch reactors using sequential change in light intensity.* Applied Biochemistry and Biotechnology, 2010. **161**(1): p. 511-522.
150. Wang, C.-Y., C.-C. Fu, and Y.-C. Liu, *Effects of using light-emitting diodes on the cultivation of Spirulina platensis.* Biochemical Engineering Journal, 2007. **37**(1): p. 21-25.
151. Weiss, V., Gromet-Elhanan, and M. Halmann, *Batch and continuous culture experiments on nutrient limitations and temperature effects in the marine alga Tetraselmis suecica.* Water Resources, 1985. **19**(2): p. 185-190.
152. Wynne, D. and G. Rhee, *Effects of light intensity and quality on the relative N and P requirement (the optimum N: P ratio) of marine planktonic algae.* Journal of Plankton Research, 1986. **8**(1): p. 91-103.
153. Zheng, Y., et al., *Optimization of carbon dioxide fixation and starch accumulation by Tetraselmis subcordiformis in a rectangular airlift photobioreactor.* African Journal of Biotechnology, 2011. **10**(10): p. 1888-1901.

154. Beardall, J. and I. Morris, *The concept of light intensity adaptation in marine phytoplankton: some experiments with Phaeodactylum tricornutum.* Marine Biology, 1976. **37**(4): p. 377-387.
155. Chu, W.-L., S.-M. Phang, and S.-H. Goh, *Environmental effects on growth and biochemical composition of Nitzschia inconspicua Grunow.* Journal of Applied Phycology, 1996. **8**(4): p. 389-396.
156. Molina Grima, E., et al., *Outdoor turbidostat culture of the marine microalga Tetraselmis sp.* Aquaculture and Fisheries Management, 1994. **25**: p. 547-555.
157. Fabregas, J., et al., *The marine microalga Chlorella stigmatophora as a potential source of single cell protein: Enhancement of the protein content in response to nutrient enrichment.* Journal of Industrial Microbiology & Biotechnology, 1986. **1**(4): p. 251-257.
158. Lourenço, S., et al., *Changes in biochemical profile of Tetraselmis gracilis I. Comparison of two culture media.* Aquaculture, 1997. **148**(2-3): p. 153-168.
159. Meseck, S.L., J.H. Alix, and G.H. Wikfors, *Photoperiod and light intensity effects on growth and utilization of nutrients by the aquaculture feed microalga, Tetraselmis chui (PLY429).* Aquaculture, 2005. **246**(1): p. 393-404.
160. Sorokin, C. and R.W. Krauss, *The effects of light intensity on the growth rates of green algae.* Plant Physiology, 1957. **33**(2): p. 109-113.
161. Adam, M., *Metabolic response of the halotolerant green alga Dunaliella bardawil to Nitrogen:Phosphorus ratios in batch culture.* Folia microbiologica, 1997. **42**(4): p. 357-360.
162. Ben-Amotz, A., T.G. Tornabene, and W.H. Thomas, *Chemical profile of selected species of microalgae with emphasis on lipids.* J. Phycol, 1985. **21**(1): p. 72-81.
163. Johansen, J., et al., *Addendum to Microalgae Culture Collection*, S.M.T.R. Group, Editor. 1987, Solar Energy Research Institute: Colorado.
164. Xu, N., et al., *Effects of nitrogen source and concentration on growth rate and fatty acid composition of Ellipsoidion sp.(Eustigmatophyta).* Journal of Applied Phycology, 2001. **13**(6): p. 463-469.
165. Matthijs, H.C.P., et al., *Application of Light-Emitting Diodes in Bioreactors: Flashing Light Effects and Energy Economy in Algal Culture (Chlorella pyrenoidosa).* Biotechnology and Bioengineering, 1996. **50**: p. 98-107.
166. You, T. and S.M. Barnett, *Effect of light quality on production of extracellular polysaccharides and growth rate of Porphyridium cruentum.* Biochemical engineering journal, 2004. **19**(3): p. 251-258.
167. Molina Grima, E., et al., *Photobioreactors: light regime, mass transfer, and scaleup.* Journal of Biotechnology, 1999. **70**: p. 231-247.
168. Ogbonna, J.C., H. Yada, and H. Tanaka, *Light supply coefficient: A new engineering parameter for photobioreactor design.* Journal of fermentation and bioengineering, 1995. **80**(4): p. 369-376.
169. Brody, M. and R. Emerson, *The Effect of Wavelength Intensity of Light on the Proportion of Pigments in Porphyridium cruentum.* American Journal of Botany, 1959. **46**(6): p. 433-440.
170. Barsanti, L. and P. Gualtieri, eds. *Algae: Anatomy, Biochemistry, and Biotechnology*. 2006, CRC Press. 301.
171. Utting, S., *Influence of nitrogen availability on the biochemical composition of three unicellular marine algae of commercial importance.* Aquacultural engineering, 1985. **4**(3): p. 175-190.
172. Widjaja, A., C.-C. Chien, and Y.-H. Ju, *Study of increasing lipid production from fresh water microalgae Chlorella vulgaris.* Journal of the Taiwan Institute of Chemical Engineers, 2009. **40**(1): p. 13-20.
173. Yongmanitchai, W. and O.P. Ward, *Screening of algae for potential alternative sources of eicosapentaenoic acid.* Phytochemistry, 1991. **30**(9): p. 2963-2967.
174. Yoo, C., et al., *Selection of microalgae for lipid production under high levels carbon dioxide.* Bioresource Technology, 2010. **101**(1): p. S71-S74.

175. Siron, R., G. Giusti, and B. Berland, *Changes in the fatty acid composition of Phaeodactylum tricornutum and Dunaliella tertiolecta during growth and under phosphorus deficiency.* Marine Ecology Progress Series, 1989. **55**(1): p. 95-100.
176. Renaud, S., D. Parry, and L.-V. Thinh, *Microalgae for use in tropical aquaculture I: Gross chemical and fatty acid composition of twelve species of microalgae from the Northern Territory, Australia.* Journal of Applied Phycology, 1994. **6**(3): p. 337-345.
177. Burlew, J.S., ed. *Algal Culture from Laboratory to Pilot Plant*. 1953, Carnegie Institution of Washington: Washington, DC. 357.
178. Cerón Garcí, M.C., et al., *Mixotrophic growth of Phaeodactylum tricornutum on glycerol: growth rate and fatty acid profile* Journal of Applied Phycology, 2000. **12**(3-5): p. 239-248.
179. Collyer, D.M. and G.E. Fogg, *Studies on Fat Accumulation by Algae.* Journal of Experimental Botany, 1955. **6**(17): p. 256-275.
180. Gatenby, C.M., et al., *Biochemical composition of three algal species proposed as food for captive freshwater mussels.* Journal of Applied Phycology, 2003. **15**(1): p. 1-11.
181. Hu, H. and K. Gao, *Response of growth and fatty acid compositions of Nannochloropsis sp. to environmental factors under elevated CO_2 concentration.* Biotechnology Letters, 2006. **28**(13): p. 987-992.
182. Li, Y., et al., *Effects of nitrogen sources on cell growth and lipid accumulation of green alga Neochloris oleoabundans.* Appl Microbiol Biotechnol, 2008. **81**(4): p. 629-636.
183. Liang, Y., K.-S. Mai, and S.-c. Sun, *Total lipid and fatty acid composition of eight strains of marine diatoms.* Chinese Journal of Oceanology and Limnology, 2000. **18**(4): p. 345-349.
184. Mourente, G., L.M. Lubian, and J.M. Odriozola, *Total Fatty-Acid Composition as a Taxonomic Index of Some Marine Microalgae Used as Food in Marine Aquaculture.* Hydrobiologia, 1990. **203**(3): p. 147-154.
185. Mutlu, Y., et al., *The effects of nitrogen and phosphorus deficiencies and nitrite addition on the lipid content of Chlorella vulgaris (Chlorophyceae).* African Journal of Biotechnology, 2011. **10**(3): p. 453-456.
186. Parrish, C.C. and P.J. Wangersky, *Particulate and dissolved lipid classes in cultures of Phaeodactylum tricornutum grown in cage culture turbidostats with a range of nitrogen supply rates.* Marine Ecology Progress Series, 1987. **35**(11): p. 119-128.
187. Rao, A.R., et al., *Effect of salinity on growth of green alga Botryococcus braunii and its constituents.* Bioresource Technology, 2007. **98**(3): p. 560-564.
188. Matsunaga, T., et al., *Characterization of marine microalga, Scenedesmus sp. strain JPCC GA0024 toward biofuel production.* Biotechnology Letters, 2009. **31**: p. 1367-1372.
189. Coleman, L.W., B.H. Rosen, and S.D. Schwartzbach, *Environmental Control of Carbohydrate and Lipid Synthesis in Euglena.* Plant Cell Physiology, 1988. **29**(3): p. 423-432.
190. Liu, Z.-Y., G.-C. Wang, and B.-C. Zhou, *Effect of iron on growth and lipid accumulation in Chlorella vulgaris.* Bioresource Technology, 2008. **99**(11): p. 4717-4722.
191. Whyte, J.N.C., *Biochemical composition and energy content of six species of phytoplankton used in mariculture of bivalves.* Aquaculture, 1987. **60**(3-4): p. 231-241.
192. Hu, C., et al., *Variation of lipid and fatty acid compositions of the marine microalga Pavlova viridis (Prymnesiophyceae) under laboratory and outdoor culture conditions.* World Journal of Microbiology and Biotechnology, 2008. **24**: p. 1209-1214.
193. Norris, R.E., T. Hori, and M. Chihara, *Revision of the genus Tetraselmis (Class Prasinophyceae).* Journal of Plant Research, 1980. **93**(4): p. 317-339.
194. Lee, R.E., ed. *Phycology*. 4th ed. 2008, Cambridge University Press: Cambridge. 547.
195. Reize, I. and M. Melkonian, *Flagellar regeneration in the scaly green flagellate Tetraselmis striata (Prasinophyceae): regeneration kinetics and effect of inhibitors.* Helgoland Marine Research, 1987. **41**(2): p. 149-164.
196. Pane, L., et al., *Viability of the marine microalga Tetraselmis suecica grown free and immobilized in alginate beads.* Aquaculture International, 1998. **6**(6): p. 411-420.

197. Patil, V., et al., *Fatty acid composition of 12 microalgae for possible use in aquaculture feed.* Aquaculture International, 2007. **15**(1): p. 1-9.
198. McGinnis, K., T. Dempster, and M. Sommerfeld, *Characterization of the growth and lipid content of the diatom Chaetoceros muelleri.* Journal of Applied Phycology, 1997. **9**: p. 19-24.
199. Jiang, Y. and F. Chen, *Effects of salinity on cell growth and docosahexaenoic acid content of the heterotrophic marine microalga Crypthecodinium cohnii.* Journal of Industrial Microbiology & Biotechnology, 1999. **23**(6): p. 508-513.
200. Fabregas, J., et al., *Mass culture and biochemical variability of the marine microalga Tetraselmis suecica Kylin (Butch) with high nutrient concentrations.* Aquaculture, 1985. **49**(3–4): p. 231-244.
201. Bopp, S.K. and T. Lettieri, *Gene regulation in the marine diatom Thalassiosira pseudonana upon exposure to polycyclic aromatic hydrocarbons (PAHs).* Gene, 2007. **396**(2): p. 293-302.
202. Liu, Z.Y., G.C. Wang, and B.C. Zhou, *Effect of iron on growth and lipid accumulation in Chlorella vulgaris.* Bioresource Technology, 2008. **99**(11): p. 4717-4722.
203. Araujo, G.S., et al., *Bioprospecting for oil producing microalgal strains: evaluation of oil and biomass production for ten microalgal strains.* Bioresource Technology, 2011.
204. Richmond, A. and Z. Cheng-Wu, *Optimization of a flat plate glass reactor for mass production of Nannochloropsis sp. outdoors.* Journal of Biotechnology, 2001. **85**(3): p. 259-269.
205. Day, J., A. Edwards, and G. Rodgers, *Development of an industrial-scale process for the heterotrophic production of a micro-algal mollusc feed.* Bioresource Technology, 1991. **38**(2): p. 245-249.
206. Barbosa, M.J., Hadiyanto, and R.H. Wijffels, *Overcoming shear stress of microalgae cultures in sparged photobioreactors.* Biotechnol Bioeng, 2004. **85**(1): p. 78-85.
207. Boney, A.D., *A Biology of Marine Algae*. 1966: Hutchinson Educational. 216.
208. Open_University, *Seawater: Its Composition, Properties and Behaviour*. 2 ed, ed. Butterworth-Heinemann. 1995: Elsevier Science. 166.
209. Eriksen, N.T., T. Geest, and J.J.L. Iversen, *Phototrophic growth in the lumostat: a photo-bioreactor with on-line optimization of light intensity.* J Appl Phycol, 1996. **8**: p. 345-352.
210. Del Campo, J.A., M. Garcia-Gonzalez, and M.G. Guerrero, *Outdoor cultivation of microalgae for carotenoid production: current state and perspectives.* Applied Microbiology and Biotechnology, 2007. **74**: p. 1163-1174.
211. Apt, K.E. and P.W. Behrens, *Commercial Developments in Microalgal Biotechnology.* Journal of Phycology, 1999. **35**: p. 215-226.
212. Mutanda, T., et al., *Bioprospecting for hyper-lipid producting microalgal strains for sustainable biofuel production.* Bioresource Technology, 2011. **102**: p. 57-70.
213. Reynolds, C.S., *The Ecology of Phytoplankton*. Ecology, Biodiversity and Conservation. 2006, Cambridge: Cambridge University Press.
214. Ross, O.N. and J. Sharples, *Swimming for survival: A role of phytoplankton motility in a stratified turbulent environment.* Journal of Marine Systems, 2008. **70**: p. 248-262.
215. Siver, P.A. *Ankistrodesmus Corda*. SilicaSecchiDisk Accessed on 03/07/2011; Available from: http://silicasecchidisk.conncoll.edu/LucidKeys/Carolina_Key/html/Ankistrodesmus.
216. NIES, *Algae Resource Database of National Bio Resource Project*. Accessed 23/07/2011, National Institute for Environmental Studies.
217. John, D.M., B.A. Whitton, and A.J. Brook, eds. *The Freshwater Algal Flora of the British Isles: An Identification Guide to Freshwater and Terrestrial Algae*. British Phycological Society, Natural History Museum. 2002, Cambridge University Press.
218. www.ccap.ac.uk, *Culture Collection of Algae and Protozoa*. 2007, Scottish Marine institute.
219. CAUP, *The Charles University in Prague (CAUP) image database of algae*. Accessed on 21/06/2012.

220. Privoznik, K.G., K.J. Daniel, and F.P. Incropera, *Absorption, extinction and phase function measurements for algal suspensions of Chlorella pyrenoidosa.* J Quant Spectrosc Radiative Transfer, 1978. **20**: p. 345-352.
221. Oliver, R.L., A.J. Kinnear, and G.G. Ganf, *Measurements of Cell Density of Three Freshwater Phytoplankters by Density Gradient Centrifugation.* Limnology and Oceanography, 1981. **26**(2): p. 285-294.
222. Toppo, K. and M.R. Suseela, *Cosmarium Diversity of Mani Pokhar Pond of Jashpur District in Chhattisgarh State, India.* Annals of Forestry, 2009. **17**(1): p. 117-124.
223. Garric, R.K., *The Cryoflora of the Pacific Northwest.* American Journal of Botany, 1965. **52**(1): p. 1-8.
224. Hu, W., et al., *The sensitivity of the dinoflagellate Crypthecodinium cohnii to transient hydrodynamic forces and cell-bubble interactions.* Biotechnol. Prog., 2007. **23**(1355-1362): p. 1355.
225. http://www.csiro.au, *Australian National Algae Culture Collection*. 2010. Accessed on 12/07/2011.
226. Montresor, M. and U. Sacchi, *Stazione Zoologica Anton Dohrn of Naples*. Accessed on 02/07/2011: Napoli, Italy.
227. Makoto, Y. *Gonyaulacales Images*. *Alexandrium insuetum* Photograph; *Alexandrium minutum* Photograph Accessed 02/07/2011; photographs and sizes]. Available from: http://dinos.anesc.u-tokyo.ac.jp/atlas_verl_5/main/gonyaulacales.html.
228. Tang, H., et al., *Culture of Microalgae Chlorella minutissima for Biodiesel Feedstock Production.* Biotechnology and Bioengineering, 2011. **108**(10): p. 2280-2287.
229. Adolf, J.E., T. Bachvaroff, and A.R. Place, *Can cryptophyte abundance trigger toxic Karlodinium veneficum blooms in eutrophic estuaries?* Harmful Algae, 2008. **8**(1): p. 119-128.
230. JGI. *Cyanothece sp. PCC 8802*. Accessed on 22/06/2012; Available from: http://genome.jgi-psf.org/cya_2/cya_2.home.html.
231. Sanchez Rueda, P., *Stomach content analysis of Mugil cephalus and Mugil curema (Mugiliformes: Mugilidae) with emphasis on diatoms in the Tamiahua lagoon, Mexico.* Rev Biol Trop, 2002. **50**(1): p. 245-252.
232. Bollmann, J., C. Klaas, and L.E. Brand, *Morpological and Physiological Characteristics of Gephyrocapsa oceanica var. typica Kamptner 1943 in Culture Experiments: Evidence for Genotypic Variability.* Protist, 2010. **161**(1): p. 78-90.
233. Naik, R., R. Chitari, and A. Anil, *Karlodinium veneficum in India: effect of fixatives on morphology and allelopathy in relation to Skeletonema costatum.* Current Science, 2010. **99**(8): p. 1112.
234. Zingone, A., D. Sarno, and G. Forlani, *Seasonal dynamics in the abundance of Micromonas pusilla (Prasinophyceae) and its viruses in the Gulf of Naples (Mediterranean Sea).* Journal of Plankton Research, 1999. **21**(11): p. 2143-2159.
235. KMMCC, *Korea Marine Microalgae Culture Center*. Accessed on 08/07/2011.
236. Kociolek, P., *Nitzschia reversa*, in *In Diatoms of the United States*. 2011.
237. Kelly, M.G., et al., *Common freshwater diatoms of Britain and Ireland: an interactive key.* 2005, Environment Agency, Bristol.
238. Green, J.C., *Notes on the flagellar apparatus and taxonomy of Pavlova mesolychnon van der veer, and on the status of Pavlova butcher and related genera within the haptophyceae.* Journal of the Marine Biological Association of the UK, 1976. **56**: p. 595-602.
239. Amato, A., et al., *Life cycle, size reduction patterns, and ultrastructure of the pennate planktonic diatom Pseudo-Nitzschia delicatissima (Bacillariophyceae).* Journal of Phycology, 2005. **41**: p. 542-556.
240. Kiorboe, T., F. Mohlenberg, and K. Hamburger, *Bioenergetics of the planktonic copepod Acartia tonsa: relation between feeding, egg production and respiration, and composition of specific dynamic action.* Marine Ecology Progress Series, 1985. **26**: p. 85-97.
241. Tsukii, Y., *Cyanophyceae: Anabaena cylindrica*. Accessed on 02/07/2011, Protist Information Sever.

242. Dicks, B.L. and D.J. Patterson, *Chroococcus Image*, in *Encyclopedia of Life*. Accessed on 05/07/2011.
243. Olenina, I. and S. Olenin, *DAISIE European Invasive Alien Species Gateway*. 2006.
244. Bhakta, S., et al., *Phyco-diversity Assessment of Bahuda River Mouth Areas of East Coast of Odisha, India.* Recent Research in Science and Technology, 2011. **2**(4): p. 80-89.
245. Celekli, A., O. Obali, and O. Kulkoyluoglu, *The Phytoplankton Community (except Bacillariophyceae) of Lake Abant (Bolu, Turkey).* Turkish Journal of Botany, 2007. **31**: p. 109-124.
246. CCALA, *Culture Collection of Autotrophic Organisms (CCALA)*. Accessed 25/06/2012, Trebon Department of the Institute of Botany of the Academy of Science of the Czech Republic.
247. Gunma, T., et al., *Selenastrum*, in *Protist Information Server*. Accessed on 25/06/2012.
248. Tsukii, Y., *Tribonema sp.* 2001, Protist Information Server.
249. Moore, J., *Seasonal Changes in the Proximate and Fatty Acid Composition of Some Naturally Grown Freshwater Chlorophytes.* Journal of Phycology, 1975. **11**(2): p. 205-211.
250. Hossain, A.S., et al., *Biodiesel Fuel Production from Algae as Renwable Energy.* American Journal of Biochemistry and Biotechnology, 2008. **4**(3): p. 250-254.
251. Zhu, C. and Y. Lee, *Determination of biomass dry weight of marine microalgae.* Journal of Applied Phycology, 1997. **9**(2): p. 189-194.
252. Coombs, J., et al., *Studies on the biochemistry and fine structure of silica shell formation in diatoms. Chemical composition of Navicula pelliculosa during silicon-starvation synchrony.* Plant Physiology, 1967. **42**: p. 1601-1606.
253. Meyers, R.A., *Molecular Biology and Biotechnology*. 1995: Wiley-VCH.
254. Borowitzka, M.A. and L.J. Borowitzka, eds. *Micro-Algal Biotechnology*. 1988, Cambridge University Press: Cambridge. 477.
255. Lembi, C.A., J.R. Waaland, and P.S.o. America, *Algae and Human Affairs*. 1988: Cambridge University Press. 590.
256. Matsumoto, M., et al., *Marine Diatom, Navicula sp. Strain JPCC DA0580 and Marine Green Alga, Chlorella sp. Strain NKG400014 as Potential Sources for Biodiesel Production.* Appl Biochem Biotechnol, 2009.
257. Joseph, K.J. and P.V.R. Nair, *Growth characteristics of certain estuarine phytoplankters.* Bulletin of the Depatrment of Marine Sciences, CUSAT, 1975. **7**(1): p. 151-159.
258. Melkonian, M., *An ultrastructural study of the flagellate Tetraselmis cordiformis stein (Chlorophyceae) with emphasis on the flagellar apparatus.* Protoplasma, 1979. **98**(1): p. 139-151.
259. Wustman, B.A., M. Melkonian, and B. Becker, *A study of cell wall and flagella formation during cell division in the scaly green alga, Scherffelia dubia (Chlorophyta).* Journal of Phycology, 2004. **40**(5): p. 895-910.
260. Dermoun, D., et al., *Modelling of growth of Porphyridium cruentum in connection with two interdependent factors: Light and temperature.* Bioresource Technology, 1992. **42**(2): p. 113-117.
261. Barbosa, M.J., et al., *Microalgae cultivation in air-lift reactors: Modeling biomass yield and growth rate as a function of mixing frequency.* Biotechnology and Bioengineering, 2003. **82**(2): p. 170-179.
262. Tevatia, R., Y. Demirel, and P. Blum, *Kinetic modeling of photoautotropic growth and neutral lipid accumulation in terms of ammonium concentration in Chlamydomonas reinhardtii.* Bioresource Technology, 2012. **119**(0): p. 419-424.
263. Perez, E.B., I.C. Pina, and L.P. Rodriguez, *Kinetic model for growth of Phaeodactylum tricornutum in intensive culture photobioreactor.* Biochemical Engineering Journal, 2008. **40**: p. 520-525.
264. James, S.C. and V. Boriah, *Modeling Algae Growth in an Open-Channel Raceway.* Journal of Computational Biology, 2010. **17**(7): p. 895-906.

265. Li, J., N.S. Xu, and W.W. Su, *Online estimation of stirred-tank microalgal photobioreactor cultures based on dissolved oxygen measurement.* Biochemical Engineering Journal, 2003. **14**(1): p. 51-65.
266. Molina Grima, E., et al., *A mathematical model of microalgal growth in light-limited chemostat culture.* Journal of Chemical Technology & Biotechnology, 1994. **61**(2): p. 167-173.
267. Eilers, P.H.C. and J.C.H. Peeters, *A model for the relationship between light intensity and the rate of photosynthesis in phytoplankton.* Ecological Modelling, 1988. **42**(3–4): p. 199-215.
268. Packer, A., et al., *Growth and neutral lipid synthesis in green microalgae: A mathematical model.* Bioresource Technology, 2011. **102**(1): p. 111-117.
269. Pruvost, J., et al., *Simulation of microalgae growth in limiting light conditions: Flow effect.* AIChE Journal, 2002. **48**(5): p. 1109-1120.
270. Ogbonna, J.C., H. Yada, and H. Tanaka, *Kinetic study on light-limited batch cultivation of photosynthetic cells.* Journal of fermentation and bioengineering, 1995. **80**(3): p. 259-264.
271. Suh, I.S. and S. Lee, *A light distribution model for an internally radiating photobioreactor.* Biotechnology and Bioengineering, 2003. **82**(2): p. 180-189.
272. Csőgör, Z., et al., *Light distribution in a novel photobioreactor – modelling for optimization.* Journal of Applied Phycology, 2001. **13**(4): p. 325-333.
273. Cornet, J.-F. and C.-G. Dussap, *A Simple and reliable formula for assessment of maximum volumetric productivities in photobioreactors.* Biotechnology Progress, 2009. **25**(2): p. 424-435.
274. Çamdevýren, H., et al., *Use of principal component scores in multiple linear regression models for prediction of Chlorophyll-a in reservoirs.* Ecological Modelling, 2005. **181**(4): p. 581-589.
275. Cho, K.H., et al., *Determination of the optimal parameters in regression models for the prediction of chlorophyll-a: A case study of the Yeongsan Reservoir, Korea.* Science of the Total Environment, 2009. **407**(8): p. 2536-2545.
276. Li, F., et al., *Relationships between stream macroinvertebrates and environmental variables at multiple spatial scales.* Freshwater Biology, 2012. **57**: p. 2107-2124.
277. Sun, X., et al., *Large-scale field evidence on the enhancement of small-sized cladocerans by Microcystis blooms in Lake Taihu, China.* Journal of Plankton Research, 2012. **34**(10): p. 853-863.
278. Villarroel, M.J., et al., *Caloric content of Daphnia magna as reflect of propanil stress during a short-term exposure and its relationship to long-term responses.* Environmental Toxicology and Pharmacology, 2013. **35**: p. 465-472.
279. Moreira, S.M., L. Guilhermino, and R. Ribeiro, *An in situ assay with the microalga Phaeodactylum tricornutum for sediment-overlying water toxicity evaluations in estuaries.* Environmental Toxicology and Chemistry, 2006. **25**(9): p. 2272-2279.
280. Moreira-Santos, M., A.M.V.M. Soares, and R. Ribeiro, *A Phytoplankton Growth Assay for Routine in situ Environmental Assessments.* Environmental Toxicology and Chemistry, 2004. **23**(6): p. 1549-1560.
281. Cheng, S.-H., et al., *Competition between the rotifer Brachionus rotundiformis and the ciliate Euplotes vannus fed on two different algae.* Aquaculture, 2004. **241**: p. 331-343.
282. Anjos, M., et al., *Optimization of CO_2 bio-mitigation by Chlorella vulgaris.* Bioresource Technology, 2013. **139**: p. 149-154.
283. Bi, R., C. Arndt, and U. Sommer, *Stoichiometric responses of phytoplankton species to the interactive effect of nutrient supply ratios and growth rates.* Journal of Phycology, 2012. **48**: p. 539-549.
284. Bunsom, C. and A. Prathep, *Effects of salinity, light intensity and sediment on growth, pigments, agar production and reproduction in Gracilaria tenuistipitata from Songkhla Lagoon in Thailand.* Phylogical Research, 2012. **60**: p. 169-178.
285. Xie, T., et al., *Optimization of heterotrophic cultivation of Chlorella sp. for oil production.* Bioresource Technology, 2012. **118**: p. 235-242.

286. Green, K.H. and A. Emerson, *Data Analysis Through Modeling: Thinking and Writing in Context*. 2008.
287. Tabachnick, B.G. and L.S. Fidell, *Using Multivariate Statistics*. 6th ed. 2012, Boston, USA: Pearson Education, Limited. 983.
288. Schafer, J.L. and M.K. Olsen, *Multiple imputation for multivariate missing-data problems: a data analyst's perspective*. 1998, The Pennsylvania State University.
289. Warner, R.M., ed. *Applied Statistics: From Bivariate Through Multivariate Techniques*. 2nd ed. 2013, SAGE: Los Angeles, USA.
290. Johnson, R., *Miller and Freund's Probability and Statistics for Engineers*. 8th International Edition ed. 2011: Pearson Education, Inc. 544.
291. Green, S.B., *How Many Subjects Does It Take To Do a Regression Analysis?* Multivariate Behavioral Research, 1991. **26**(3): p. 499-510.
292. Piloto-Rodríguez, R., et al., *Prediction of the cetane number of biodiesel using artificial neural networks and multiple linear regression.* Energy Conversion and Management, 2013. **65**: p. 255-261.
293. Al-Momani, E.S., et al., *Modeling Blanking Process Using Multiple Regression Analysis and Artificial Neural Networks.* Journal of Materials Engineering and Performance, 2012. **21**(8): p. 1611-1619.
294. Jahandideh, S., et al., *The use of artificial neural networks and multiple linear regression to predict rate of medical waste generation.* Waste management, 2009. **29**(11): p. 2874-2879.
295. Jung, S.-K. and S.B. Lee, *In Situ Monitoring of Cell Concentration in a Photobioreactor Using Image Analysis: Comparison of Uniform Light Distribution Model and Artificial Neural Networks.* Biotechnology Progress, 2006. **22**(5): p. 1443-1450.
296. Bosma, R., et al., *Prediction of volumetric productivity of an outdoor photobioreactor.* Biotechnology and Bioengineering, 2007. **97**(5): p. 1108-1120.
297. Wang, G.C.S. and C.L. Jain, *Regression Analysis: Modeling & Forecasting*. 2003, New York: Graceway Publishing Company, Inc. 295.
298. Merchuk, J.C. and X. Wu, *Modeling of photobioreactors: Application to bubble column simulation.* Journal of Applied Phycology, 2003. **15**(2): p. 163-169.
299. Faramarzi, F., H. Mansouri, and M.A.E. Farsangi, *A rock engineering systems based model to predict rock fragmentation by blasting.* International Journal of Rock Mechanics & Mining, 2013. **60**: p. 82-94.
300. Baptist, G., D. Meritt, and D. Webster, *Growing Microalgae to Feed Bivalve Larvae*. 1993, Northeastern Regional Aquaculture Center, University of Massachusetts: Dartmouth. p. 8.
301. Spolaore, P., et al., *Optimization of Nannochloropsis oculata growth using the response surface method.* Journal of Chemical Technology & Biotechnology, 2006. **81**: p. 1049-1056.
302. Anand, M.A.S.D., V. Sankar, and D.K. Daniel, *Optimization of Light intensity, Nitrate concentration and Cultivation time for Biomass production by Chlorella minutissima using Response Surface Methodology.* Journal of Applied Sciences Research, 2013. **9**(1): p. 94-99.
303. Cheng, K.-C., M. Ren, and K.L. Ogden, *Statistical optimization of culture media for growth and lipid production of Chlorella protothecoides UTEX 250.* Bioresource Technology, 2013. **128**: p. 44-48.
304. van Bergeijk, S.A., E. Salas-Leiton, and J.P. Canavate, *Low and variable productivity and low efficiency of mass cultures of the haptophyte Isochrysis aff. galbana (T-iso) in outdoor tubular photobioreactors.* Aquacultural Engineering, 2010. **43**: p. 14-23.
305. Ma, Z., et al., *Motility and photosynthetic responses of the green microalga Tetraselmis subcordiformis to visible and UV light levels.* J Appl Phycol, 2012. **24**: p. 1613-1621.
306. Melkonian, M., *Algal Cell Motility*. Vol. Volume 3 of Current phycology. 1992: Chapman and Hall. 236.
307. Bailey, J.E. and D.F. Ollis, eds. *Biochemical Engineering Fundamentals*. 2nd ed. 1986, Mcgraw-hill Book Company: New York. 928.

308. Sathyendranath, S., L. Lazzara, and L. Prieur, *Variations in the spectral values of specific absorption of phytoplankton.* Limnology and Oceanography, 1987. **32**(2): p. 403-415.
309. Zapata, M., F. Rodríguez, and J.L. Garrido, *Separation of chlorophylls and carotenoids from marine phytoplankton: a new HPLC method using a reversed phase C8 column and pyridine-containing mobile phases.* Marine Ecology Progress Series, 2000. **195**: p. 29-45.
310. Mao, Z., et al., *Effects of phytoplankton species composition on absorption spectra and modeled hyperspectral reflectance.* Ecological Informatics, 2010. **5**(5): p. 359-366.
311. Arcadia. *Lamp Product Information*. July 28, 2011]; Available from: http://www.arcadia-uk.info/product.php?pid=13&mid=11&lan=en&sub=&id=4.
312. Marcus, N.H. and J.A. Wilcox, *A Guide to the Meso-scale Production of the Copepod Acartia Tonsa*. 2007, Sea Grant Florida; University of Florida; NOAA. p. 26.
313. Thomas, W.H. and C.H. Gibson, *Effects of small-scale turbulence on microalgae.* J Appl Phycol, 1990. **2**: p. 71-77.
314. Zimmerman, W.B., et al., *Design of an airlift loop bioreactor and pilot scales studies with fluidic oscillator induced microbubbles for growth of a microalgae Dunaliella salina.* Applied Energy, 2011. **88**(10): p. 3357-3369.
315. Richmond, A., *Handbook of Microalgal Culture: Biotechnology and Applied Phycology*. 2008: John Wiley & Sons.
316. Sforza, E., et al., *Photobioreactors for microalgal growth and oil production with Nannochloropsis salina: From lab-scale experiments to large-scale design.* Chemical Engineering Research and Design, 2012. **90**(9): p. 1151-1158.
317. Fabregas, J., C. Herrero, and M. Veiga, *Effect of oil and dispersant on growth and chlorophyll a content of the marine microalga Tetraselmis suecica.* Applied and Environmental Microbiology, 1984. **47**(2): p. 445-447.
318. O'Kelly, C.J., *Tetraselmis*, in *Protist Image Data (PID) Online Database*. 2004.
319. Domozych, D.S., K.D. Stewart, and K.R. Mattox, *Development of the cell wall in Tetraselmis: Role of the golgi apparatus and extracellular wall assembly.* J Cell Science, 1981. **52**: p. 351-371.
320. Lim, D.K.Y., et al., *The race for highly productive microalgae strains.* Biofuels, 2010. **1**(6): p. 835-837.